

MODELLING AND ANALYSING RISK IN PRECIOUS METALS



Knowledge Chinhamu

(2009056991)

January 2018

**MODELLING AND ANALYSING RISK IN
PRECIOUS METALS**

by

KNOWLEDGE CHINHAMU
(2009056991)

THESIS

Submitted in fulfilment of the requirements for the degree of

PHILOSOPHIAE DOCTOR

in

**STATISTICS
(APPLIED)**

in the

FACULTY OF NATURAL AND AGRICULTURAL SCIENCES

DEPARTMENT OF MATHEMATICAL SCIENCES AND ACTUARIAL SCIENCE

at the

UNIVERSITY OF THE FREE STATE

BLOEMFONTEIN: JANUARY 2018

Thesis promoter: Dr Delson Chikobvu



UNIVERSITY OF THE FREE STATE

FACULTY OF NATURAL AND AGRICULTURAL SCIENCES

DEPARTMENT OF MATHEMATICAL STATISTICS AND ACTUARIAL SCIENCE

BLOEMFONTEIN, SOUTH AFRICA

Declaration

I, Knowledge Chinhamu, declare that

1. The thesis is hereby submitted for the qualification of Doctor of Philosophy in Statistics at the University of the Free State.
2. The research reported in this thesis, except where otherwise indicated, is my original research.
3. This thesis has not been submitted for any degree or examination at any other University/Faculty.
4. This thesis does not contain other persons' writing, unless specifically acknowledged as being sourced from other researchers. Where other written sources have been quoted, then
 - (a) their words have been re-written but the general information attributed to them has been referenced, or
 - (b) where their exact words have been used, then their writing has been placed in italics and referenced.
5. I cede copyright of the thesis to the University of the Free State.

Knowledge Chinhamu

Date

Copyright © University of the Free State

All right reserved

Disclaimer

This document describes work undertaken as a PhD programme of study at the University of the Free State. All views and opinions expressed therein remain the sole responsibility of the author, and do not necessarily represent those of the institution.

Dedication

*To my wife Chipu and my three sons Nokutenda Knowledge (jnr),
Nomufaro Kelvin & Kupakwashe Nathaniel.*

Do not go where the path may lead, go instead where there is no path and leave a trail.

Ralph Waldo Emerson

Abstract

The prices of precious metals are volatile and financial market participants are interested in knowing the downside of holding precious metals in their portfolios. Risk management tools such as Value-at-Risk (VaR) are highly dependent on the underlying distributional assumption. Identifying a distribution that may best capture all the aspects of the given financial data can provide immense advantages to both investors and risk managers. In the analysis and modelling of financial returns, there are stylised facts that are observed. These include volatility clustering, heavy-tails, asymmetry, conditional heavy tails and long range dependence (long memory). In this study, we investigated the stylised facts of gold, platinum and silver returns. We thus propose models that are able to capture their empirical features. The models capture extreme tails of profit and loss distributions and improve the estimation of Value-at-Risk (VaR) of precious metal prices returns. Firstly, we evaluate the performance of existing heavy-tailed and flexible distributions in modelling extreme risk for precious metal returns. The heavy-tailed and flexible distributions used are: Generalised Hyperbolic Distributions (GHDs), Generalised Lambda Distribution (GLD), Stable Distribution (SD), Generalised Pareto Distribution (GPD), Generalised Extreme Value Distribution (GEVD), Pearson type-IV Distribution (PIVD), Symmetrical Student-t Distribution (STD) and Skewed Student-t Distribution (SSTD). Secondly, we couple ARMA-GARCH models and ARMA-APARCH models with heavy-tailed and flexible distributions. We fit the models to precious metal returns and evaluate their relative performance in estimating Value-at-Risk (VaR) using a number of conditional assumptions. The proposed models

performed favourably when compared with the APARCH models with a Student-t distribution and the APARCH models with a skewed Student-t distribution usually used in the literature. This provides financial analysts with an alternative distributional scheme to be used in economic modelling. Thirdly, because all daily precious metal price returns exhibit volatility clustering, heavy tails, asymmetry and long range dependence, we fit the long-memory GARCH models under the GHDs, the GPD, the GEVD, the SD, the STD, the SSTD, the GLD and the PIVD assumptions to our price return data. The Anderson-Darling test is used to check for model adequacy. Kupiec likelihood ratio tests and Christoffersen conditional coverage tests are also used in this study to evaluate objectively whether VaR model is adequate. The backtesting results confirm that the long-memory GARCH-heavy-tailed models are adequate for improving risk management assessments and hedging strategies in the highly volatile metal markets. ARFIMA-HYGARCH, ARFIMA-FIGARCH and ARFIMA-FIAPARCH models with PIVD, Normal-Inverse Gaussian Distribution (NIGD), full GHD, FMKL GLD and Generalised Hyperbolic Student-t Distribution (GHStD) innovations are found to be suitable for VaR estimation of precious metals, thereby providing a good alternative candidate for modelling financial returns.

Key Words: APARCH, ARFIRMA, Extreme Value Theory, FIAPARCH, FIGARCH, HYGARCH, Generalised Hyperbolic, Generalised Lambda, Pearson type-IV, Precious metals, Stable, Value-at-Risk.

Acknowledgements

I deeply acknowledge the debt I owe to numerous people who generously shared their time and expertise in preparing this thesis. In particular, special thanks to my promoter Dr Delson Chikobvu for his guidance and valuable support. His inspiration, ideas and suggestions were very valuable in the production of this thesis. I am indebted to Chun-Kai Huang of the Department of Statistical Sciences at University of Cape Town for co-authoring two papers. I am extremely thankful to Dr Edmore Ranganai of the Department of Statistics at the University of South Africa for co-authoring a paper. I would also like to express my sincere gratitude to Professor John P. Nolan of the American University for his help and support with the STABLE package in R. I would also like express my gratitude to Ms Danielle Roberts for assisting me in typing the thesis. Last but not least, I express my sincere appreciation to my friends Retius Chifurira, Andrew Makandwa and Jahvaid Hammujuddy and my wife Chipu for moral support during the course of producing this piece of work.

Contents

	Page
List of Figures	xiv
List of Tables	xix
Abbreviations	xx
Research Output	xxii
Conference Presentations	xxiii
Chapter 1: Introduction	1
1.1 Background	1
1.2 Related Literature on Precious Metals	6
1.3 Stylized facts of financial asset returns	10
1.4 Research Problem, Aim and Objectives	12
1.5 Significance of the study	14
1.6 Scientific Contributions of the Study	14
1.7 Thesis Structure	15
Chapter 2: Methodology	17
2.1 Introduction	17
2.2 Testing for Normality	17
2.3 Testing for Autocorrelation and Model Adequacy	18

2.4	Testing for ARCH effects	23
2.5	Goodness-of fit-test	24
2.6	Unit Root and Stationary tests	25
2.7	Stationary Time Series models	30
2.8	Non-stationary Time Series Models	32
2.9	Long memory and Fractional Integration	36
2.10	Summary	43
Chapter 3: Precious metal data		44
3.1	Introduction	44
3.2	Data Analysis	44
3.3	Summary	53
3.4	Statistical software packages	54
Chapter 4: Risk Analysis		56
4.1	Introduction	56
4.2	Risk Measures	56
4.3	Backtesting models	62
4.4	Summary	64
Chapter 5: Evaluating risk in precious metals with Generalised Extreme Value, Generalised Pareto and Generalised Lambda Distributions		65
5.1	Introduction	65
5.2	Extreme Value Theory (EVT)	66
5.2.1	The Generalised Extreme Value Distribution (GEVD)	66
5.2.2	The Generalised Pareto Distribution (GPD)	69
5.3	Generalised Lambda Distribution	73
5.4	Empirical Results	84
5.5	Summary	96

5.6	Statistical software packages	96
5.7	Appendix	97
Chapter 6: Evaluating risk in precious metals with Generalised Hyperbolic, Stable and Pearson type-IV Distributions		99
6.1	Introduction	99
6.2	Generalised Hyperbolic Distribution and its Subclasses	100
6.3	Stable Distribution	107
6.4	Pearson type-IV Distribution	115
6.5	The Skewed Student-t Distribution	119
6.6	Empirical Results	122
6.7	Summary	129
6.8	Statistical software packages	130
6.9	Appendix	130
Chapter 7: Value-at-Risk estimation of precious metals with GARCH-type models		134
7.1	Introduction	134
7.2	The models	135
7.3	Combining Volatility models with Heavy-tailed Distributions	141
7.4	Empirical Results	141
7.5	Summary	163
7.6	Statistical software packages	163
7.7	Appendix	164
Chapter 8: Value-at-Risk estimation of precious metal returns: A long memory GARCH-heavy-tailed approach		174
8.1	Introduction	174
8.2	The GARCH-Type Models	174
8.3	Combining long-memory-GARCH models with heavy-tailed distributions	184

8.4 Empirical Results	184
8.5 Summary	204
8.6 Statistical software packages	205
8.7 Appendix	205
Chapter 9: Conclusion	220
References	226

List of Figures

Figure 3.1	Time series plot of gold prices (left) and one-day returns (right)	45
Figure 3.2	Time series plot of platinum prices (left) and one-day returns (right)	45
Figure 3.3	Time series plot of silver prices (left) and one-day returns (right)	45
Figure 3.4	Sample ACF and PACF of daily gold returns, squared gold returns and absolute gold returns.	48
Figure 3.5	Normal Q-Q plot and Box plot for the daily gold returns.	49
Figure 3.6	Sample ACF and PACF of daily platinum returns, squared platinum re- turns, absolute platinum returns.	49
Figure 3.7	Normal Q-Q plot and Box plot for the daily platinum returns.	50
Figure 3.8	Sample ACF and PACF of daily silver returns, squared silver returns and absolute silver returns.	50
Figure 3.9	Normal Q-Q plot and Box plot for the daily silver returns.	51
Figure 5.1	The parameter space of the RS GLD in terms of Regions 1,2,3,4,5 and 6 (Adapted from van Staden (2013))	76
Figure 5.2	The parameter space of the FMKL GLD in the Regions 1,2,3 and 4. (Adapted from van Staden (2013))	79
Figure 5.3	The parameter space of the FMKL GLD in terms of Classes I, II, II', III, IV', IV and V. (Adapted from van Staden (2013))	82
Figure 5.4	Residual and Q-Q plots for negative platinum returns with block size 5, 10 and 21.	85
Figure 5.5	Mean excess function of negative platinum returns	86

Figure 5.6	Diagnostic plots for negative platinum returns fitted with GPD and a threshold of 0.004662, 0.008302 and 0.014279 respectively.	87
Figure 5.7	Histogram and Q-Q plots for GLD on platinum returns.	87
Figure 5.8	Residual and Q-Q plots for negative gold returns with block size 5, 10 and 21.89	
Figure 5.9	Mean excess function of negative gold returns.	90
Figure 5.10	Diagnostic plots for negative gold returns fitted with GPD and a threshold of 0.002980, 0.005544 and 0.010292 respectively.	90
Figure 5.11	Histogram and Q-Q plots for GLD on gold returns.	91
Figure 5.12	Residual and Q-Q plots for negative silver returns with block size 5, 10 and 21.93	
Figure 5.13	Mean excess function of negative silver returns.	93
Figure 5.14	Diagnostic plots for negative silver returns fitted with GPD and a threshold of 0.006320, 0.011273 and 0.019885 respectively.	94
Figure 5.15	Histogram and Q-Q plots for GLD on silver returns.	94
Figure 6.1	The Pearson Curve family	116
Figure 6.2	Comparison of fit between the different members of the GHD for gold returns (left), platinum returns (center) and silver returns (right).	122
Figure 6.3	Data density and fitted density for gold (left), platinum (center) and silver (right)	128
Figure 6.4	P-P and Q-Q plot for gold returns.	128
Figure 6.5	P-P and Q-Q plot for platinum return.	128
Figure 6.6	P-P and Q-Q plot for silver return.	129
Figure 7.1	Mean excess plot of gold (a) positive (b) negative standardised residuals . .	164
Figure 7.2	Pareto quantile plot of gold (a) positive (b) negative standardised residuals	164
Figure 7.3	Mean excess plot of platinum (a) positive (b) negative standardised residuals	164
Figure 7.4	Pareto quantile plot of platinum (a) positive (b) negative standardised residuals	165
Figure 7.5	Mean excess plot of silver (a) positive (b) negative standardised residuals .	165
Figure 7.6	Pareto quantile plot of silver (a) positive (b) negative standardised residuals	165

Figure 7.7	Mean excess plot of gold (a) positive (b) negative standardised residuals . .	166
Figure 7.8	Pareto quantile plot of gold (a) positive (b) negative standardised residuals	166
Figure 7.9	Mean excess plot of platinum (a) positive (b) negative standardised residuals	166
Figure 7.10	Pareto quantile plot of platinum (a) positive (b) negative standardised residuals	166
Figure 7.11	Mean excess plot of platinum (a) positive (b) negative standardised residuals	167
Figure 7.12	Pareto quantile plot of silver (a) positive (b) negative standardised residuals	167
Figure 7.13	GPD Diagnostic plot of positive standardised residuals (gold)	167
Figure 7.14	GPD Diagnostic plot of negative standardised residuals (gold)	168
Figure 7.15	GPD Diagnostic plot of positive standardised residuals (platinum)	168
Figure 7.16	GPD Diagnostic plot of negative standardised residuals (platinum)	169
Figure 7.17	GPD Diagnostic plot of positive standardised residuals (silver)	169
Figure 7.18	GPD Diagnostic plot of negative standardised residuals (silver)	170
Figure 7.19	GPD Diagnostic plot of positive standardised residuals (gold)	170
Figure 7.20	GPD Diagnostic plot of negative standardised residuals (gold)	171
Figure 7.21	GPD Diagnostic plot of positive standardised residuals (platinum)	171
Figure 7.22	GPD Diagnostic plot of negative standardised residuals (platinum)	172
Figure 7.23	GPD Diagnostic plot of positive standardised residuals (silver)	172
Figure 7.24	GPD Diagnostic plot of negative standardised residuals (silver)	173
Figure 8.1	Q-Q plot of standardised residuals ARFIMA-FIGARCH model (gold returns)	192
Figure 8.2	Q-Q plot of standardised residuals ARFIMA-FIGARCH model (platinum returns)	192
Figure 8.3	Q-Q plot of standardised residuals from ARFIMA-FIGARCH model (silver returns)	192
Figure 8.4	Mean excess plot of gold (a) positive (b) negative standardised residuals . .	206
Figure 8.5	Pareto quantile plot of gold (a) positive (b) negative standardised residuals	206
Figure 8.6	Mean excess plot of platinum (a) positive (b) negative standardised residuals	206

Figure 8.7 Pareto quantile plot of platinum (a) positive (b) negative standardised residuals	206
Figure 8.8 Mean excess plot of silver (a) positive (b) negative standardised residuals	207
Figure 8.9 Pareto quantile plot of silver (a) positive (b) negative standardised residuals	207
Figure 8.10 Mean excess plot of gold (a) positive (b) negative standardised residuals	207
Figure 8.11 Pareto quantile plot of gold (a) positive (b) negative standardised residuals	207
Figure 8.12 Mean excess plot of platinum (a) positive (b) negative standardised residuals	208
Figure 8.13 Pareto quantile plot of platinum (a) positive (b) negative standardised residuals	208
Figure 8.14 Mean excess plot of silver (a) positive (b) negative standardised residuals	208
Figure 8.15 Pareto quantile plot of silver (a) positive (b) negative standardised residuals	208
Figure 8.16 Mean excess plot of gold (a) positive (b) negative standardised residuals	209
Figure 8.17 Pareto quantile plot of gold (a) positive (b) negative standardised residuals	209
Figure 8.18 Mean excess plot of platinum (a) positive (b) negative standardised residuals	209
Figure 8.19 Pareto quantile plot of platinum (a) positive (b) negative standardised residuals	209
Figure 8.20 Mean excess plot of silver (a) positive (b) negative standardised residuals	210
Figure 8.21 Pareto quantile plot of silver (a) positive (b) negative standardised residuals	210
Figure 8.22 Diagnostic plots of GPD fit to positive standardised residuals (gold)	211
Figure 8.23 Diagnostic plots of GPD fit to negative standardised residuals (gold)	211
Figure 8.24 Diagnostic plots of GPD fit to positive standardised residuals (platinum)	212
Figure 8.25 Diagnostic plots of GPD fit to negative standardised residuals (platinum)	212
Figure 8.26 Diagnostic plots of GPD fit to positive standardised residuals (silver)	213
Figure 8.27 Diagnostic plots of GPD fit to negative standardised residuals (silver)	213
Figure 8.28 Diagnostic plots of GPD fit to positive standardised residuals (gold)	214
Figure 8.29 Diagnostic plots of GPD fit to negative standardised residuals (gold)	214
Figure 8.30 Diagnostic plots of GPD fit to positive standardised residuals (platinum)	215
Figure 8.31 Diagnostic plots of GPD fit to negative standardised residuals (platinum)	215
Figure 8.32 Diagnostic plots of GPD fit to positive standardised residuals (silver)	216

Figure 8.33 Diagnostic plots of GPD fit to negative standardised residuals (silver) . . . 216

Figure 8.34 Diagnostic plots of GPD fit to positive standardised residuals (gold) 217

Figure 8.35 Diagnostic plots of GPD fit to negative standardised residuals (gold) 217

Figure 8.36 Diagnostic plots of GPD fit to positive standardised residuals (platinum) . . 218

Figure 8.37 Diagnostic plots of GPD fit to negative standardised residuals (platinum) . 218

Figure 8.38 Diagnostic plots of GPD fit to positive standardised residuals (silver) 219

Figure 8.39 Diagnostic plots of GPD fit to negative standardised residuals (silver) . . . 219

List of Tables

Table 1.1	Previous research about modelling and analysing risk in metal	8
Table 2.1	Box Cox transformation	33
Table 3.1	Descriptive statistics and unit root tests of precious metal price returns . . .	47
Table 3.2	long memory tests R/S method	51
Table 3.3	GPH long memory test for returns	52
Table 3.4	GPH long memory test for Squared returns	52
Table 3.5	Lo's R/S test for precious metal returns and squared returns	53
Table 5.1	Parameter space and support of the RS GLD distribution in terms of regions 1,2,3,4,5 and 6	77
Table 5.2	Parameter space and support of the FMKL GLD distribution in terms of regions 1,2,3, and 4.	79
Table 5.3	Parameter space of the FMKL in terms of Classes I, II, II', III, IV', IV and V. .	81
Table 5.4	Limiting cases of the FMKL GLD	81
Table 5.5	Parameter estimates using GEVD for platinum returns	84
Table 5.6	GPD parameter estimates for platinum negative returns	86
Table 5.7	GLD parameter estimates of platinum returns	87
Table 5.8	VaR and ES estimates for platinum returns using heavy-tailed distributions .	88
Table 5.9	VaR and ES Backtesting for platinum returns versus heavy-tailed distributions	88
Table 5.10	Parameter estimates using GEVD	89
Table 5.11	GPD parameter estimates for negative gold returns.	89

Table 5.12	GLD parameter estimates of gold returns.	90
Table 5.13	VaR and ES estimates for gold returns using heavy-tailed distributions	91
Table 5.14	VaR and ES Backtesting for gold returns versus heavy-tailed distributions . .	92
Table 5.15	Parameter estimates using GEVD for silver returns	92
Table 5.16	GPD parameter estimates for negative silver returns.	93
Table 5.17	GLD parameter estimates of silver returns.	94
Table 5.18	VaR and ES estimates for silver returns using heavy-tailed distributions . . .	95
Table 5.19	VaR and ES Backtesting for silver returns versus heavy-tailed distributions .	95
Table 6.1	Limiting cases of GHDs	106
Table 6.2	Family of distribution for the Pearson System	116
Table 6.3	ML parameter estimates of the GHDs	123
Table 6.4	ML parameter estimates of the Stable Distribution	124
Table 6.5	ML parameter estimates of the Pearson type-IV distribution	124
Table 6.6	Goodness of-fit tests and model selection criteria for precious metal returns.	124
Table 6.7	VaR Estimates for precious metal returns	126
Table 6.8	VaR Backtesting for precious metal returns.	127
Table 7.1	ML parameter estimates for the ARMA(1,1)-GARCH(1,1) model with Gaus- sian Innovations	142
Table 7.2	Standardised residuals test for ARMA(1,1)-GARCH(1,1) model with Gaus- sian Innovations	143
Table 7.3	ML parameter estimates of precious metal returns	144
Table 7.4	Anderson Darling Goodness of-fit tests for precious metal returns.	144
Table 7.5	ML parameter estimates of the FMKL GLD for the ARMA (1,1)-GARCH(1,1)- GLD model.	145
Table 7.6	ML parameter estimates of the Pearson type-IV distribution for the ARMA(1,1)- GARCH(1,1)-PIVD model.	145
Table 7.7	ML parameter estimates of GEVD for the ARMA(1,1)-GARCH(1,1)-GEVD model.	146
Table 7.8	ML parameter estimates of GPD for the ARMA(1,1)-GARCH(1,1)-GPD model	147

Table 7.9	VaR Estimates for precious metal returns.	148
Table 7.10	VaR Backtesting for precious metal returns.	149
Table 7.11	Parameter estimates for the ARMA (1,1)-APARCH (1,1) model with Gaussian Innovations	153
Table 7.12	Descriptive Statistics of Standardised residuals of the ARMA(1,1)-APARCH (1,1) model with Gaussian Innovations	154
Table 7.13	ML parameter estimates of the Pearson type-IV distribution for the ARMA(1,1)-APARCH (1,1)-Pearson type-IV model	154
Table 7.14	ML parameter estimates of the full GHD for the ARMA(1,1)-APARCH (1,1)-GHDs model	155
Table 7.15	Anderson Darling Goodness of-fit tests for precious metal returns	155
Table 7.16	ML parameter estimates of the FMKL GLD for the ARMA(1,1)-APARCH(1,1)-GLD model.	156
Table 7.17	ML parameter estimates of the Stable distribution for the ARMA (1, 1)-APARCH(1,1)-SD model.	157
Table 7.18	ML parameter estimates of GEVD for the ARMA(1,1)-APARCH(1,1)-GEVD model	157
Table 7.19	ML parameter estimates of GPD for the ARMA(1,1)-APARCH(1,1)-GPD model	158
Table 7.20	VaR estimates for the ARMA(1,1)-APARCH (1,1) model combined with different distributions	160
Table 7.21	VaR Backtesting for precious metal returns	161
Table 8.1	ARFIMA-FIGARCH parameter estimation with different error distributions and Diagnostic tests (Gold returns)	186
Table 8.2	ARFIMA-FIGARCH parameter estimation with different error distributions and Diagnostic tests (Platinum returns)	187
Table 8.3	ARFIMA-FIGARCH parameter estimation with different error distributions and Diagnostic tests (Silver returns)	187
Table 8.4	ARFIMA-HYGARCH parameter estimation with different error distributions and Diagnostic tests (Gold returns)	188

Table 8.5	ARFIMA-HYGARCH parameter estimation with different error distributions and Diagnostic tests (Platinum returns)	188
Table 8.6	ARFIMA-HYGARCH parameter estimation with different error distributions and Diagnostic tests (Silver returns)	189
Table 8.7	ARFIMA-FIAPARCH parameter estimation with different error distributions and Diagnostic tests (Gold returns)	189
Table 8.8	ARFIMA-FIAPARCH parameter estimation with different error distributions and Diagnostic tests (Platinum returns)	190
Table 8.9	ARFIMA-FIAPARCH parameter estimation with different error distributions and Diagnostic tests (Silver returns)	190
Table 8.10	Descriptive Statistics of standardised residuals of the ARFIMA-FIGARCH, ARFIMA-HYGARCH and ARFIMA-FIAPARCH models.	191
Table 8.11	ML parameter estimates of the Pearson type-IV distribution for the ARFIMA-FIGARCH-PIVD model	194
Table 8.12	ML parameter estimates of the GHDs for the ARFIMA-FIGARCH -GHDs model	195
Table 8.13	ML parameter estimates of the Pearson type-IV distribution for the ARFIMA-HYGARCH-PIVD model	195
Table 8.14	ML parameter estimates of the FMKL GLD for the ARFIMA-FIGARCH-GLD model.	195
Table 8.15	ML parameter estimates of the Stable distribution for the ARFIMA-FIGARCH-SD model	195
Table 8.16	ML parameter estimates of GEVD for the ARFIMA-FIGARCH-GEVD model.	196
Table 8.17	ML parameter estimates of GPD for the ARFIMA-FIGARCH-GPD model. . .	196
Table 8.18	ML parameter estimates of the GHDs for the ARFIMA-HYGARCH -GHDs model	196
Table 8.19	ML parameter estimates of the Pearson type-IV distribution for the ARFIMA-FIAPARCH-PIVD model	197

Table 8.20 ML parameter estimates of the FMKL GLD for the ARFIMA-HYGARCH-GLD model.	197
Table 8.21 ML parameter estimates of the Stable distribution for the ARFIMA-HYGARCH-SD model.	197
Table 8.22 ML parameter estimates of GEVD for the ARFIMA-HYGARCH-GEVD model	197
Table 8.23 ML parameter estimates of GPD for the ARFIMA-HYGARCH-GPD model. .	198
Table 8.24 ML parameter estimates of the GHDs for the ARFIMA-FIAPARCH -GHDs model	198
Table 8.25 ML parameter estimates of the FMKL GLD for the ARFIMA-FIAPARCH-GLD model.	198
Table 8.26 ML parameter estimates of the Stable distribution for the ARFIMA-FIAPARCH-SD model.	199
Table 8.27 ML parameter estimates of GEVD for the ARFIMA-FIAPARCH-GEVD model	199
Table 8.28 ML parameter estimates of GPD for the ARFIMA-FIAPARCH-GPD model. .	199
Table 8.29 In-Sample VaR Backtesting: ARFIMA-FIAPARCH models	201
Table 8.30 In-Sample VaR Backtesting: ARFIMA-HYGARCH models	202
Table 8.31 In-Sample VaR Backtesting : ARFIMA-FIAPARCH models	203
Table 9.1 The most appropriate models for precious metals.	224

Abbreviations

ACF	Autocorrelation Function
AD	Anderson-Darling
ADF	Augmented Dickey-Fuller
AIC	Akaike Information Criterion
APARCH	Asymmetric Power Autoregressive Conditional Heteroscedasticity
AR	Autoregressive
ARCH	Autoregressive Conditional Heteroscedasticity
ARIMA	Autoregressive Integrated Moving Average
ARMA	Autoregressive Moving Average
CGARCH	Component Generalised Autoregressive Conditional Heteroscedasticity
DPOT	Duration-based peaks-over threshold
EGARCH	Exponential Generalised Autoregressive Conditional Heteroscedasticity
ES	Expected shortfall
EVT	Extreme Value Theory
FIAPARCH	Fractional Integrated Power Autoregressive Conditional Heteroscedasticity
FIGARCH	Fractional Integrated Generalised Autoregressive Conditional Heteroscedasticity
GARCH	Generalised Autoregressive Conditional Heteroscedasticity.
GEVD	Generalised Extreme Value Distribution
GHD	Generalised Hyperbolic Distribution
GHS_tD	Generalised Hyperbolic Skew Student-t Distribution
GLD	Generalised Lambda Distribution
GPD	Generalised Pareto Distribution
GPH	Geweke Porter-Hudak
HYGARCH	Hyperbolic GARCH
iid	Independent and identically distributed
JB	Jacque Bera
KPSS	Kwiatkowski Phillips Schmidt Shin
KS	Kolmogorov Smirnov
LMT	Lagrange Multiplier
ML	Maximum Likelihood
MLE	Maximum Likelihood Estimation
NARCH	Nonlinear Autoregressive Conditional Heteroskedasticity
NIGD	Normal-Inverse Gaussian Distribution
NRIG	Normal Reciprocal Inverse Gaussian Distribution

OLS	Ordinary Least Squares
PACF	Partial Autocorrelation function
PIVD	Pearson Type-IV Distribution
PORT	Peaks-over Random Threshold
POT	Peaks-over-threshold
PP	Phillips Perron
Q-Q	Quantile to Quantile
SBI	Schwarz Bayesian information Criterion
SSTD	Skewed Student-t Distribution
STD	Student-t Distribution
VaR	Value-at-Risk
VGD	Variance-Gamma Distribution

Research Output

A list of publications from this thesis is given below.

Peer-reviewed Journal Publications

1. **K. Chinghamu**, C-K. Huang, C-S. Huang and D. Chikobvu (2015). Extreme Risk, Value-at-Risk and Expected Shortfall in the Gold Market. *International Business and Economics Research Journal*, 14(1), 107-122.
2. **K. Chinghamu**, C-K. Huang and D. Chikobvu (2015). Evaluating Risk in Gold Prices with Generalised Hyperbolic and Stable Distributions. *South African Statistical Journal Proceedings: Proceedings of the 57th Annual Conference of the South African Statistical Association*, 17-24.
3. **K. Chinghamu**, C-K. Huang and D. Chikobvu (2017). Evaluating risk in precious metals with generalised lambda, generalised Pareto and generalised extreme value distributions. *South African Statistical Journal*, 51(1), 159-182.
4. **K. Chinghamu** and D. Chikobvu (2017). Value-at-Risk estimation of gold market with Stable and Generalised Hyperbolic Distributions. *The Journal of Economic and Financial Sciences*, 10(3), 508-521.
5. **K. Chinghamu** and D. Chikobvu (2017). Estimation of Value-at Risk and Backtesting of precious metals with ARMA-APARCH-Pearson type-IV and ARMA-APARCH-GHD models. (*Under review South African Journal of Economic & Management Sciences*).
6. **K. Chinghamu**, E. Ranganai and D. Chikobvu (2017). Value-at-Risk estimation of precious metal returns: A long-memory GARCH-heavy-tailed approach. (*Under Review South African Statistical Journal*).

Conference Presentations

1. **K. Chinhamu** and D. Chikobvu. Extreme risk, extreme economic value-at-risk and expected shortfall: empirical evidence from precious metals. 33rd Southern Africa Mathematical Sciences Association Annual Conference, 24 – 28 November 2014, Victoria Falls, Zimbabwe.
2. **K. Chinhamu**, C-K. Huang and D. Chikobvu. Risk Management with Generalised Hyperbolic Distributions: Application to Precious Metals. 56th Annual Conference of the South African Statistical Association, 28 – 30 October 2014, Rhodes University, Grahamstown, South Africa.
3. **K. Chinhamu**, C-K. Huang and D. Chikobvu. Evaluating Risk in Gold Prices with Generalised Hyperbolic and Stable, Distributions . 57th Annual Conference of the South African Statistical Association, 29 November – 2 December 2015, University of Pretoria, Pretoria, South Africa.

Chapter 1

Introduction

This introductory chapter outlines the background to the study, related literature on precious metals, stylised facts of financial returns, research problem, aim and objectives and the significance of the study. The chapter also provides information on the research contributions of the study and thesis layout.

1.1 Background

Risk measures are used primarily to quantify a financial position against severe losses. To successfully model such tail-related risks, we need to find suitable techniques to measure and capture these extreme events. Despite certain drawbacks, Value-at-Risk (VaR) and Expected Shortfall (ES) remain popular measures of financial risk among practitioners. Therefore, there is a need for the development of more robust methods to estimate VaR and ES. This study, in particular, aims to improve current assumptions of appropriate underlying distributions in capturing extreme tails, which results in the improvement of the estimation of VaR and ES.

The implementation of VaR to identify appropriate regulatory capital requirement suffers from many setbacks such as its inability to capture “tail loss”. Such drawbacks have recently been highlighted by the Basel Committee on Banking Supervision. The committee has also recommended a shift of focus to the alternative ES

measure to address the drawbacks of VaR. Although many operational challenges have been identified by the committee when moving to ES, it is believed that the benefits outweigh the disadvantages. The use of ES has been proposed for the internal model-based approach and to be utilised in determining risk weights for the standardised approach (Basel, 2012). In this study, both VaR and ES were implemented under the assumption of heavy-tailed and volatility of precious metal returns. In addition, backtesting procedures were also conducted to analyse model adequacy.

VaR can be described as the maximum loss of a portfolio such that the likelihood of experiencing a loss exceeding that amount, over a specified risk horizon, is equal to a pre-specified tolerance level. ES measures the mean of losses that are equal to or greater than a corresponding VaR value. In order to capture the effect of market behavior under extreme events, Extreme Value Theory (EVT) has been widely adopted in VaR estimation in recent years. Since EVT is derived from sound statistical theory and provides a parametric form for the tails of a distribution, its methodologies are attractive for risk assessments.

There is substantial research on EVT for risk measures in areas where extreme observations are of interest such as Finance, Insurance, Hydrology, Climatology and Engineering. Numerous studies in finance and commodity markets have been conducted using EVT, including studies by Embrechts *minimising* (1997), Gencay and Selcuk (2004) and Gilli and K ellezi (2006). Bystr om (2005) applied EVT to the case of extremely high electricity prices and declared a good fit with the Generalised Pareto Distribution (GPD). Bali (2003) determined the type of asymptotic distribution for modelling the extreme changes in US treasury yields. Bali (2003) also found that the thin-tailed Gumbel and Exponential distributions perform worse than the heavy-tailed Frechet and Pareto distributions. Marohn (2005) studied the tail index in the case of generalised order statistics and went on to determine the asymptotic properties of the Frechet distribution.

The Generalised Lambda Distribution (GLD) has been used differently in a financial context. Lee (2003) showed that GLD is adequate for modelling spot exchange rates. Chalabi *et al.* (2010) proposed GLD as an alternative to Stable distributions and the Student- t distribution in modelling equities from NASDAQ-100 index. Beena and Kumaran (2010) modelled the personal income data of a population with the GLD. Corrado (2001) used the GLD to model security price distributions. Other studies focusing on the theory and applications of the GLD were undertaken by Su (2007), Corlu and Corlu (2015) and Corlu *et al.* (2016).

Barndorff-Nielsen (1977) introduced a family of continuous distributions in order to capture excess kurtosis, namely the Generalised Hyperbolic Distributions (GHDs), in which the logarithm of its probability density function is a hyperbola. These distributions proved to fit financial returns more adequately than other distributions such as the Normal and Student t distributions. Eberlein and Keller (1995) using a data set consisting of daily prices of the 30 DAX (German Stock Exchange) over a period of three years, were able to show that GHDs presented the best fit when modelling high frequency data. Similar research was carried out by Bibby and Sørensen (1996) and Prause (1999). Huang *et al.* (2014) also applied GHDs to model the South African Mining Index and to estimate its corresponding VaR values. Hansen (1994) and Azzalini and Capitanio (2003), among other researchers, proposed the generalised skew t -type distributions for financial modelling. However, these models do not handle substantial skewness. GHDs cater for asymmetry, heavy and semi-heavy tail and are, therefore, more useful for modelling a variety of data sources.

Over time, several distributions were identified to describe the stock market data. It is notable, however, that no known popular distribution that perfectly fits the data has been established. Stable distributions are amongst some of the distributions used. These are a four parameter family of models that generalise the Normal model, and thus allows for both skewness and heavy tails (Nolan, 2014). McCulloch (1997) investigated the suitability of Stable distributions using data from the stock

market known as the Center for Research in Security Prices (CRSP). The data were analysed from January 1953 to December 1992. The Maximum likelihood (ML) estimates as well as the quantile estimates were calculated and the goodness-of-fit was studied using graphical methods by observing the P-P plots and the stable density plots. The diagnostics confirmed a close fit. Weron (2004) analysed the Dow Jones Industrial Average (DJIA) index from 2 January 1985 to 30 November 1992. The stability analysis was based on the Anderson-Darling (AD) criterion and the weighted Kolmogorov criterion. The parameters of the Stable distribution were estimated by the regression method proposed by Koutrouvelis (1980). Koutrouvelis (1980) stated that the DJIA characteristics correspond perfectly to the Stable distribution. Hoekstoetter *et al.* (2005) analysed the returns of stocks comprising the German stock index (DAX) in relation to the α -Stable distribution. They applied nonparametric estimation methods such as the Hill estimator as well as the parametric estimation methods conditional on the α -Stable distribution. Their results showed that the α -Stable hypothesis cannot be rejected for the return data distribution for both non-parametric and parametric estimation methods.

Kreżłek (2012) used Stable distributions to measure the investment risk of precious non-ferrous metals and their results confirmed the validity of the use of Stable distributions to assess the risk on the precious non-ferrous metals market. Brooks and Persaud (2003) highlighted the significance of asymmetry in the VaR framework and recommended its integration in the volatility specification models. Mittnik and Paolella (2000) and Mittnik *et al.* (2000) recommended extended structures useful in enhancing a VaR forecast in terms of the distribution and the volatility operation. Giot and Laurent (2003a, 2003b) proposed that for VaR forecast, either long or short trading positions, the use of an APARCH model with a skewed Student t -distribution is the best. This was reinforced by Huang and Lin (2004) who added that at a lower confidence level, the Student t -distribution gives better and preferred results. Degiannakis (2004) introduced a fractional integrated APARCH model with the skewed Student- t -distribution for predicting VaR and volatility. Stavroyiannis

(2016) tested the efficiency of the APARCH model with residual after standardising the Pearson type-IV distribution. The daily returns of three oil companies in the US were used in the modelling. It was discovered that the APARCH model alongside the standardised Pearson type-IV distribution provided greater accuracy. Thus, the performance of the VaR model depends on the quality of the distributional assumptions.

An accurate description of the dynamics of stock requires a mix of a time-varying volatility structure and an asymmetric and heavy-tailed distribution. Youssef *et al.* (2015) adopted three long-memory models, namely, FIGARCH, HYGARCH and FI-APARCH to forecast Europe Brent crude oil (Brent) and Cushing West Intermediate crude oil (WTI) volatility by capturing some volatility stylised facts such as long-range memory, heteroscedasticity, asymmetry and heavy-tails. Their findings confirmed that taking into account long-range memory, asymmetry and heavy-tails in the behavior of the commodity (crude oil) prices returns combined with a filtering process such as EVT are important in improving risk management assessments and hedging strategies in the highly volatile energy market. Tang and Shieh (2006) used FIGARCH and HYGARCH models with Normal, Student-t and skewed Student-t distributions on S&P500 and Nasdaq100 and Dow Jones daily prices. They calculated VaR using the estimated models. The HYGARCH models with skewed Student-t distribution perform better based on the Kupiec LR tests for S&P500 and Nasdaq100 future prices. Mabrouk and Saadi (2012) evaluated the performance of several volatility models in estimating one-day ahead VaR of seven stock market indices using many distributional assumptions. They concluded that the AR-FIAPARCH model, under the skewed Student-t distribution outperforms all the models including the widely used GARCH (1,1) and HYGARCH.

1.2 Related Literature on Precious Metals

Precious metal prices respond to both short-term and long-term factors. Gold is a primary form of reserve asset held by central banks around the world and influences other precious metal prices. Sari *et al.* (2010) states: “Among the major precious metal class, an increase in gold price seems to lead to parallel movements in the prices of other precious metals which are also considered investment assets as well as industrial commodities”. This statement suggests that a model that adequately explains gold prices could also contribute to models used in predicting the prices of other precious metals. Hence, many economists consider gold as a leading indicator in the precious metal pack.

Silver is primarily obtained as a by-product of gold mining since two-thirds of the total world silver supply comes from this source. As a result, the price of silver is strongly related to that of gold (Hiller *et al.*, 2006). Platinum is also jointly extracted with other metals such as palladium, rhodium, nickel and chrome. Demand for platinum comes mainly from industry for the conduction of catalytic converters for automobiles. Platinum is not held by central banks in the form of reserves. Therefore, the market for this metal is not directly sensitive to central banks’ actions (Hiller *et al.*, 2006).

There has been a growing interest in precious metal markets by agents that incorporate metals in production processes where metals such as gold, platinum and silver are clearly dominant. These include many metallurgic companies and the jewellery industry. Most research conducted focused on the analysis of the gold market with particular focus on the role of this precious metal as a hedge against inflation. Little research has been carried out on other precious metals (for example, silver, platinum, palladium, etc.). Hiller *et al.* (2006) concluded that financial portfolios that contain precious metals perform significantly better than standard equity portfolios.

They also found that precious metals exhibit some hedging capability during periods of abnormal volatility. Sari *et al.* (2010) examined the co-movements and information transmission among the spot prices of four precious metals, namely, gold, silver, platinum and palladium, plus oil price and the US Dollar/Euro exchange rate. They found evidence of a weak long-run equilibrium relationship and strong feedbacks in the short run.

Hammoudeh *et al.* (2011) examined volatility and correlation dynamics in the price returns of gold, silver, platinum and palladium and explored the corresponding risk management implications for market risk and hedging. They used RiskMetrics and GARCH models and concluded that the GARCH-*t* model should be used to calculate VaR in precious metals. Chaithep *et al.* (2012) used the Generalised Extreme Value Distribution (GEVD) for risk evaluation of gold price returns and the tail distribution of extreme events in gold price returns. According to Chkili *et al.* (2014) the FIAPARCH model is best suited for estimating VaR forecasts of commodity prices. They used daily spot and three-month futures of WTI, Henry Hub natural gas, gold and silver values from January 1997 to March 2011. Chen and Giles (2014) analysed the risk of investment in gold, silver and platinum by applying EVT to historical data for the changes in their prices. VaR and ES (or Conditional VaR - CVaR) estimates were obtained by fitting the Generalised Pareto Distribution (GPD), using the Peaks Over Threshold (POT) method, to the extreme daily price changes. Chinhamu *et al.* (2015) evaluated risk in daily gold returns using Generalised Hyperbolic Distributions (GHDs) and the Stable distribution. They found that the performances of GHDs and the Stable distribution, in terms of VaR estimation, are comparable for gold price returns. Extensive work was conducted on modelling and analysing risk in metals. Data, methodology used and the key findings are shown in Table 1.1 on the next page.

Table 1.1: Previous research about modelling and analysing risk in metal

Studies	Data	Methodology	Main Findings
Tulley and Lucey (2007)	Monthly observations of gold and a set of macroeconomic variables from 1984 to 2003	APGARCH	An APGARCH is applicable to the data set in question, taking into account GARCH, leverage and power effects.
Hammoudeh and Yuan (2008)	Daily time series for closing three-month futures prices of oil, gold, silver and copper, and for the US three-month Treasury bills rates from 2 January 1990 to May 2006	GARCH CGARCH EGARCH	EGARCH results suggest the leverage effect is present and significant in copper only.
Hammoudeh <i>et al.</i> (2011)	Daily return based on spot prices for four precious metals (gold, silver, palladium and platinum) from 4 January 1995 to 12 November 2009.	RiskMetrics GARCH-t GARCH-FHS	GARCH-t should be used to calculate VaR for precious metals as it will yield fewer violations.
Chaithep <i>et al.</i> (2012)	Daily gold price from 1 January 1995 to 31 August 2011	EVT Generalised Extreme Value Distributions (GEVD model)	GEVD is suitable for modelling daily gold prices.
Cochran <i>et al.</i> (2012)	Daily returns of four metals (copper, gold, platinum and silver) from 4 January 1999 to 10 March 2009.	FIGARCH	FIGARCH (1,d,1) appropriately describes the volatility processes of metal returns.
Kreżłek (2012)	Daily log returns of prices of gold, silver, platinum and palladium from January 2000 to June 2011.	Stable distribution	The results confirm the validity of Stable distribution to assess the risk on the precious non-ferrous metal markets.
Chkili <i>et al.</i> (2014)	Daily spot and three-month futures of WTI, Henry Hub, natural gas, gold and silver from 7 January 1997 to 31 March 2011.	GARCH IGARCH Riskmetrics FIGARCH FIAPARCH HYGARCH	The FIAPARCH model is best suited for estimating VaR estimates.
Chen and Giles (2014)	Daily gold, silver and platinum prices.	EVT, Generalised Pareto Distribution (GPD model)	Silver is the most risky metal amongst the three. For negative daily returns, platinum is riskier than gold and the converse is true for positive returns.
Bentes (2015)	Daily gold price returns from 2 August 1976 to 6 February 2015.	GARCH IGARCH FIGARCH	FIGARCH(1,d,1) appropriately describes the volatility process and is the best model to forecast volatility in gold returns.

LM GARCH models have been applied to modelling precious metal returns. Extensive work on the application of nonlinear GARCH models (LM models) in modelling precious metals were carried out by Arouri *et al.* (2012), Cochran *et al.* (2012), Chkili *et al.* (2014), Bentes (2015), and Ranganai and Khubeka (2016), among others. According to Chkili *et al.* (2014), the FIGARCH model is best suited for estimating Value-at-Risk (VaR) forecasts of commodity prices which included daily spot and three-month futures of gold and silver. Cochran *et al.* (2012) found that the FIGARCH (1, d ,1) appropriately describes the volatility processes of metal returns over a long period of time. They used daily log returns of the prices of gold, silver, platinum and palladium from January 2000 to June 2011.

Bentes (2015) compared the relative performances of GARCH, IGARCH and FIGARCH on the daily gold price returns. Her results using the daily price returns from 2 August 1976 to 6 February 2015 were similar to that of Cochran *et al.* (2012). Demiralay and Ulusoy (2014) investigated the VaR predictions of four major precious metals (gold, silver, platinum and palladium) with long memory volatility models, namely, FIGARCG, FIAPARCH and HYGARCH under Normal and Student-t innovations distributions. They considered both long and short trading positions in their analyses. They found that the FIAPARCH model with the Student-t Distribution, which jointly captures LM and asymmetry, as well as heavy-tails outperforms other models in VaR forecasts.

LM has been observed in both the mean and the volatility of precious metal returns, that is, the dual LM phenomenon. Arouri *et al.* (2012), Diaz (2016) and Ranganai and Khubeka (2016) have significantly contributed to research on the dual LM phenomenon. The LM in the mean is handled by the autoregressive fractional integrated moving average (ARFIMA) models and the LM inherent in volatility by nonlinear GARCH models. Arouri *et al.* (2012) confirmed that ARFIMA-FIGARCH is the best model for describing daily spot and 3-month future prices of gold, silver, platinum and palladium. However, they did not address the issue of heavy-tailed error distributions. Diaz (2016) addressed the issue of dual LM and asymmetry phe-

nomena. Ranganai and Khubeka (2016) addressed the issue of structural breaks and heavy-tailed error distributions. Their results suggest that platinum returns are mean reverting while its volatility exhibited strong LM. They also found in the case of platinum returns, that the ARFIMA-FIEGARCH model under the Skewed Student- t Distribution (SSTD) and ARFIMA-HYGARCH under the Normal Distribution were able to capture the ARCH-effect. The best model for platinum return was the AFRIMA-FIAPARCH under the Student- t Distribution (STD) based on the Akaike information criterion (AIC).

It is noted to the best of our knowledge, however, that there have been limited discussions on the application of EVT, GLD, PIVD, GHDs and Stable distribution and GARCH-type models with PIVD and GHDs innovations to the metal market which represent crucial commodities to the world economy. In the analysis and modelling of financial returns, there are stylised facts that must be addressed. Thus, in the following section, we will discuss these phenomena further.

1.3 Stylized facts of financial asset returns

In financial market studies and econometrics, stylised facts refer to the presentation of some empirical findings in a study. These findings are then summarised. The main issue with such generalisations is that they may have inaccuracies and some spurious information. A simple way to explain stylised facts is by taking the common denominator among properties observed in studies of different markets and instruments and generalise it as a rule (Cont, 2001).

There are no fundamental theories that can suggest a distributional model for financial returns and as a result the problem remains largely a statistical one. Nevertheless, the extensive body of empirical research carried out since the 1950s leads to the following stylised facts summarised from Cont (2001):

- **Absence of autocorrelations:** Autocorrelations of asset returns are often insignificant.

- **Heavy tails:** The distribution of returns has a Pareto-like tail with a finite tail index. It means that the probability of extreme profits or losses is much larger than that predicted by the Normal distribution. Tail thickness varies from asset to asset.
- **Volatility Clustering:** Different measures of volatility display a positive autocorrelation over several days which quantifies the fact that highly-volatility events tend to cluster in time. This means that large price changes tend to be followed by large price changes and small price changes tend to be followed by small price changes.
- **Leverage effect:** Most measures of volatility of an asset are negatively correlated with the returns of that asset.
- **Conditional heavy tails:** Even after correcting returns for volatility clustering (for example, via GARCH-type models), the residual time series still exhibit heavy tails. However, the tails are less heavy than the unconditional distribution of returns.
- **Aggregational Gaussianity:** As the time scale increases over which returns are calculated, their distribution looks like a Normal distribution. In particular, the shape of the distribution is not the same at different time scales.
- **Gain/loss asymmetry:** One observes large drawdowns in stock prices and stock index values but not equally large upward movements. This property is not true for exchange rates where there is higher symmetry in up/down moves. Otherwise an asymmetry in the upside and downside potential of price changes is observed.
- **Slow decay of autocorrelation in absolute returns:** The autocorrelation function of absolute returns decays slowly as a function of the time lag, roughly as a power law with exponent $\beta \in [0.2, 0.4]$. This is a sign of long-range dependence in the data (Cont, 2001).

- **Autoregressive behavior:** Price changes depend on price changes in the past, for example, positive price changes tend to be followed by positive price changes.
- **Tail thickness varies across frequencies:** High frequency data tends to be more heavy-tailed than lower-frequency data (Stoyanov et. al, 2011).

A methodology for risk measurement can be based on any statistically accepted time series models capable of capturing these stylised facts and an appropriate risk measure.

1.4 Research Problem, Aim and Objectives

Commodity markets have been highly volatile in recent years due to many factors. In this study, we focus on modelling and analysing risk in the metal market because metals are important and have diversified usage in medicine, jewellery, electronics and other industries. Precious metals (gold, silver and platinum) also play an important role in portfolio selection and management. Quantification of the risk in metal price changes is fundamental in designing risk management strategies. Quantitative literature on the characteristics of metal risk is insufficient. Risk management tools such as Value-at-Risk (VaR) are highly dependent on the underlying distributional assumption. The development of more robust approaches in estimating VaR is crucial.

This study investigated and improved estimations of appropriate underlying distributions (models), in order to capture extreme tails of profit and loss distribution thereby improving the estimation of VaR and ES. The models should be able to capture the features of gold, platinum and silver log-returns.

The main aim of the study was to propose a modelling framework which can be used in precious metal market for carrying out accurate risk management or assessment. The prices of precious metals are volatile and financial participants are interested in knowing the downside of holding precious metals in their portfolio. Since risk management tools such as VaR are highly dependent on the underlying distributional

assumption, identifying a distribution that may best capture all aspects of precious metal data can provide immense advantages to both investors and risk managers. It is thus important to model the volatility of precious metal prices and develop more robust approaches in the estimation of VaR. We aim to improve the estimations of appropriate underlying distributions, in order to capture extreme tails of profit and loss distribution and as result, improve the estimation of VaR.

In this study, we utilised existing distributions and models by comparing their performances in characterising precious metals log-returns and improved the models for modelling extreme risk for platinum, gold and silver log-returns.

The objectives of the study are as follows:

- To evaluate the performance of heavy-tailed distributions in modelling extreme risk for platinum, gold and silver log-returns.
- To improve and extend models by coupling GARCH-type models and heavy-tailed distributions. The new models should be able to capture the features of precious metal returns e.g. heavy-tailed, asymmetry, volatility clustering, leverage effect and long memory.
- To improve existing models in order to accurately measure VaR in the precious metal market.
- To model tail behaviour of precious metal returns using different GARCH-type models with heavy-tailed distribution innovations.
- To validate results by comparing existing and improved models.
- To check for model adequacy using the Anderson-Darling Test.
- To estimate VaR and ES (CVaR) using proposed models.
- To check for model adequacy and select the best models using the Anderson Darling test, the Kupiec LR test and the Christoffersen test.
- To provide recommendations for future studies.

1.5 Significance of the study

Precious metals such as gold, platinum and silver emerged as natural desirable classes eligible for portfolio diversification. A robust estimate of extreme loss and gain is vital, especially for mining companies, to mitigate risk and uncertainty in metal price fluctuations. Investigating the price dynamics of precious metals is of great interest to investors, traders and policy makers. The development of a more robust approach in estimating VaR is crucial, since regulators accept it as a basis for setting capital required for market risk exposure. Modelling precious metal price returns is important in improving risk management assessments and in the hedging of strategies in highly volatile metal markets. The results and recommendations of this research will be of interest to statisticians, researchers, econometricians, risk managers, industry, government decision makers and other interested stakeholders such as investors in precious metals, in terms of modelling and predicting precious metal prices.

1.6 Scientific Contributions of the Study

The major contribution of this thesis is that it applies statistical techniques in modelling and analysing the risk of gold, platinum and silver prices. The contributions are as follows:

- Extension and improvement of existing models for precious metals.
- Application of Generalised lambda distribution in modelling daily precious metal returns.
- Application of Generalised Pareto distribution and Generalised extreme value distribution in modelling daily and monthly precious metal returns.
- Application of Generalised Hyperbolic Distribution and its subclasses (HD, NIGD, VGD, GHStD) in modelling daily precious metal returns.

- Application of Stable Distribution and PIVD in modelling daily precious metal returns.
- Coupling of ARMA-GARCH-type models with heavy-tailed distributions (Stable, GHD, NIGD, GHStD, VGD, GLD, PIVD) and their application in modelling daily precious metal returns.
- Coupling of ARMA-APARCH models with heavy tailed distributions (PIVD and GHD, NIGD, VGD, GHStD, GLD, SD) and their application in modelling daily precious metal returns.
- Coupling of nonlinear-GARCH-type models (ARFIMA-FIGARCH, ARFIMA-FIAPARCH, ARFIMA-HYGARCH) with heavy-tailed distributions (NIGD, VGD, full GHD, GHStD, GLD, SD, SSTD and PIVD) and their application in modelling daily precious metal returns.

Thus, the key original and innovative contributions of this study are to:

- Extend and improve existing volatility models and distributions by proposing potentially new conditional models for VaR estimation in the metal market. Our research focuses on the modelling of precious metals volatility.
- Extend the work of McNeil and Frey (2000) based on the conditional GPD method and Arouri *et al.* (2012) based on dual long memory models. In particular, ARMA-GARCH, ARMA-APARCH, ARFIMA-FIGARCH, ARFIMA-HYGARCH and ARFIMA-FIAPARCH models are used to describe the precious metal return series, while GLD, PIVD, full GHD, NIGD, VGD and GHStD are proposed as potential candidates for the innovations. Our results have potential implications for portfolio managers and policy makers.

1.7 Thesis Structure

This thesis consists of nine Chapters. Subsequent to this introductory chapter, the second Chapter outlines the methods used in the data analyses. **Chapter 3** presents

the analysis of empirical properties of the daily precious metal data used in this study. In **Chapter 4**, we discuss the theory of the risk measures (Value-at-risk and Expected Shortfall) used in this study and the methods used in backtesting the models used. In **Chapter 5**¹, we evaluate risk in precious metals with Generalised Extreme Value, Generalised Pareto and Generalised Lambda Distributions. In **Chapter 6**², we evaluate risk in precious metals with Generalised Hyperbolic Distributions, Pearson type-IV Distributions, Skewed Student-t Distributions, Student-t Distributions and Stable Distributions. In **Chapter 7**^{3,4}, we utilised GARCH-type models coupled with heavy-tailed distributions to estimate the value-at risk of precious metals. We estimated value-at risk of precious metals using long memory GARCH-type models with innovations having heavy-tailed and flexible distributions in **Chapter 8**⁵. Finally, **Chapter 9** summarises the findings, concludes the study and gives recommendations for further study.

¹Evaluating risk in precious metals with generalised lambda, generalised Pareto and generalised extreme value distributions. *South African Statistical Journal*, 51(1), 159-182.

²Evaluating Risk in Gold Prices with Generalised Hyperbolic and Stable Distributions. *South African Statistical Journal Proceedings: Proceedings of the 57th Annual Conference of the South African Statistical Association*, 17-24.

³ Value-at-Risk estimation of gold market with Stable and Generalised Hyperbolic Distributions. *The Journal of Economic and Financial Sciences*. 10(3), 508-521

⁴Estimation of Value-at Risk and Backtesting of precious metals with ARMA-APARCH-Pearson type-IV and ARMA-APARCH-GHD models. (Under review. *South African Journal of Economic & Management Sciences*).

⁵Value-at-Risk estimation of precious metal returns: A long-memory GARCH-heavy-tailed approach. (Under Review. *South African Statistical Journal*).

Chapter 2

Methodology

2.1 Introduction

In this section, we provide the theory of the methodology used in the data analysis. These methods include tests for normality, unit root, autocorrelation and conditional heteroscedasticity, goodness-of-fit and long memory. We also discuss stationary and non-stationary time series models, long memory and fractional integration.

2.2 Testing for Normality

It is widely accepted that the distribution of financial returns is not Normally distributed. This is true for some return structure, which is why each researcher needs to check this assumption before conducting analysis. To check for normality in the data, i.e. returns and/or standardised residuals, the Q-Q plot, the Jarque-Bera and Shapiro-Wilk tests are used and a description of these tests follow.

The Q-Q plot

The Quantile-Quantile (Q-Q) plot is used to evaluate how well the distribution of a dataset matches a hypothesised distribution. The Q-Q plot displays sample quantiles plotted against the theoretical quantiles of the hypothesised distribution. The Q-Q plot illustrates any heavy tails in the returns. If there are any irregularities in the

tails of the Q-Q plot, this suggests that the distribution of the dataset does not follow the hypothesised distribution. A normal Q-Q plot is used to check for normality of the distribution of the data set.

The Jarque-Bera Test (Jarque and Bera, 1987)

The Jarque-Bera test is a normality test and is also used to test whether a series of observations are random and independent. The Jarque-Bera test assumes the series of observations to be normally distributed. The null hypothesis is the data follows a Normal distribution.

The test statistic is given by:

$$JB = \frac{n - k + 1}{6} \left[S^2 + \frac{1}{4}(C - 3)^2 \right], \quad (2.1)$$

where n represents the number of observations,

S represents the sample skewness,

C represents the sample kurtosis,

k is the number of regressors.

Under the null hypothesis of normality, the JB is asymptotically distributed as $\chi^2_{(2)}$. The null hypothesis of normality is rejected if the calculated test statistic exceeds a critical value from the χ^2 distribution with 2 degrees of freedom or p -value is less than the given significance level (0.05).

Fitting a statistical distribution usually assumes that the data are independent and identically distributed (i.e. randomness), have no serial correlation and have no heteroscedasticity.

2.3 Testing for Autocorrelation and Model Adequacy

Autocorrelation

Autocorrelation is correlation between members of a series of observations ordered in time.

Autocorrelation Function

For a stationary process X_t with mean $E(X_t) = \mu$ and variance $Var(X_t) = E(X_t - \mu)^2 = \sigma^2$, which are constant, the covariance function X_t and X_{t+k} is defined as

$$\gamma_k = Cov(X_t, X_{t+k}) = E(X_t - \mu)(X_{t+k} - \mu)$$

and the autocorrelation function (ACF) is defined as

$$\rho_k = \frac{Cov(X_t, X_{t+k})}{\sqrt{Var X_t} \sqrt{Var(X_{t+k})}} = \frac{\gamma_k}{\gamma_0} \quad (2.2)$$

where $\gamma_0 = Var X_t = Var(X_{t+k})$, γ_k is the autocovariance function.

Properties of autocovariance and autocorrelation functions

For any stationary process, the autocovariance function γ_k and the autocorrelation function ρ_k have the following properties:

- $\gamma_0 = E(X_t - \mu)^2 = Var(X_t)$

$$\rho_0 = \frac{\gamma_0}{\gamma_0} = 1$$

- $\gamma_k = E(X_t - \mu)(X_{t+k} - \mu)$

$$= E(X_{t-k} - \mu)(X_t - \mu)$$

$$= \gamma_{-k}$$

$$\text{Also, } \rho_k = \frac{\gamma_k}{\gamma_0} = \frac{\gamma_{-k}}{\gamma_0} = \rho_{-k}$$

- $Var(X_t + X_{t+k}) = Var(X_t) + 2Cov(X_t, X_{t+k}) + Var(X_{t+k}) \geq 0$

$$\text{i.e. } 2\sigma^2 + 2\gamma_k \geq 0$$

$$\gamma_k \geq -\sigma^2$$

$$\rho_k \geq -1$$

From $Var(X_t - X_{t+k}) \geq 0$, it follows that $\rho_k \leq 1$.

Therefore, $|\rho_k| \leq 1$ and $|\gamma_k| \leq \gamma_0$.

Partial Autocorrelation Function

We may want to investigate the correlation between X_t and X_{t+k} after mutual linear dependency on the intervening variables X_{t+1}, X_{t+2}, \dots , and X_{t+k-1} has been removed. The conditional correlation $Corr(X_t, X_{t+k} | X_{t+1}, \dots, X_{t+k-1})$ is referred to as the partial autocorrelation in time series analysis denoted by ϕ_{kk} (Wei, 2006).

Consider the auto-regression model, where the dependent variable X_{t+k} from a zero mean stationary process is regressed on k lagged variables, that is

$$X_{t+k} = \phi_{k1}X_{t+k-1} + \phi_{k2}X_{t+k-2} + \dots + \phi_{kk}X_t + e_{t+k}, \quad (2.3)$$

where ϕ_{ki} denotes the i th auto-regression parameter and e_{t+k} is an error term with mean 0 and uncorrelated with X_{t+k-j} , for $i = 1, 2, \dots, k$.

Multiplying X_{t+k-j} on both sides of Equation 2.3 and taking the expectations, we get

$$\gamma_j = \phi_{k1}\gamma_{j-1} + \phi_{k2}\gamma_{j-2} + \dots + \phi_{kk}\gamma_{j-k}. \quad (2.4)$$

Dividing equation 2.4 by γ_0 , we get

$$\rho_j = \phi_{k1}\rho_{j-1} + \phi_{k2}\rho_{j-2} + \dots + \phi_{kk}\rho_{j-k}. \quad (2.5)$$

For $j = 1, 2, \dots, k$, we have the following system of equations:

$$\begin{aligned} \rho_1 &= \phi_{k1}\rho_0 + \phi_{k2}\rho_1 + \dots + \phi_{kk}\rho_{k-1} \\ \rho_2 &= \phi_{k1}\rho_1 + \phi_{k2}\rho_2 + \dots + \phi_{kk}\rho_{k-2} \\ &\vdots \\ \rho_k &= \phi_{k1}\rho_{j-1} + \phi_{k2}\rho_{j-2} + \dots + \phi_{kk}\rho_0 \end{aligned}$$

We use Cramer's rule successively for $k = 1, 2, \dots$, and get

$$\phi_{11} = \rho_1$$

$$\phi_{22} = \frac{\begin{vmatrix} 1 & \rho_1 \\ \rho_1 & \rho_2 \end{vmatrix}}{\begin{vmatrix} 1 & \rho_1 \\ \rho_1 & 1 \end{vmatrix}}$$

$$\phi_{33} = \frac{\begin{vmatrix} 1 & \rho_1 & \rho_1 \\ \rho_1 & 1 & \rho_2 \\ \rho_2 & \rho_1 & \rho_3 \end{vmatrix}}{\begin{vmatrix} 1 & \rho_1 & \rho_2 \\ \rho_1 & 1 & \rho_2 \\ \rho_2 & \rho_1 & 1 \end{vmatrix}}$$

⋮

$$\phi_{kk} = \frac{\begin{vmatrix} 1 & \rho_1 & \rho_2 & \dots & \rho_{k-2} & \rho_1 \\ \rho_1 & 1 & \rho_1 & \dots & \rho_{k-3} & \rho_2 \\ \vdots & \vdots & \vdots & & \vdots & \vdots \\ \rho_{k-1} & \rho_{k-2} & \rho_{k-3} & \dots & \rho_1 & \rho_k \end{vmatrix}}{\begin{vmatrix} 1 & \rho_1 & \rho_2 & \dots & \rho_{k-2} & \rho_{k-1} \\ \rho_1 & 1 & \rho_1 & \dots & \rho_{k-3} & \rho_{k-2} \\ \vdots & \vdots & \vdots & & \vdots & \vdots \\ \rho_{k-1} & \rho_{k-2} & \rho_{k-3} & \dots & \rho_1 & 1 \end{vmatrix}} \quad (2.6)$$

ϕ_{kk} , as a function of k is referred to as the partial autocorrelation function (PACF).

We checked for autocorrelation in the data and model adequacy in the standardised residuals using the Ljung-Box test, a description of this test follows.

The Ljung-Box Test

Ljung and Box (1978) modified the Box and Pierce (1970)'s Portmanteau test for verifying the adequacy of time series regression models. The Ljung-Box test is used to test whether a series of observations over time are random and independent. This test is also used to check for model adequacy. The Ljung-Box test assumes that the data are serially independent. The null hypothesis is the residuals are independently distributed (model is adequate).

The test statistic is given by:

$$Q = n(n + 2) \sum_{k=1}^h \frac{\hat{\rho}_k^2}{n - k}, \quad (2.7)$$

where n represents the sample size

ρ_k represents the sample autocorrelation at lag k .

If the data are white noise then Q statistic will have an asymptotic chi-square distribution with k degrees of freedom. An insignificant Q statistic value with a p -value greater than 0.05 provides evidence of the absence of significant autocorrelations in the data and vice versa. This test is used for both autocorrelation and conditional heteroscedasticity.

In this study, we used the *The Ljung-Box Test* to:

- Test for autocorrelation in returns and squared returns.
- Check for model adequacy for mean and volatility equations.
- Check ARCH effects in squared standardised residuals.

2.4 Testing for ARCH effects

We checked for Auto-Regressive Conditional Heteroscedasticity (ARCH) effects in the data, that is returns and standardised residuals. We used the ARCH LM test and a description of this test follows.

The ARCH LM Test

The ARCH LM test is used to assess for significant ARCH effects (Engle, 1982). The ARCH LM test assumes the data are conditionally heteroscedastic. The null hypothesis is that there is no ARCH effect.

Consider a time series

$$r_t = \mu_t + a_t,$$

where μ_t is the conditional mean of the process, and a_t is an innovation process with mean zero. Suppose the innovations are generated as

$$a_t = \sigma_t e_t,$$

where e_t is an independent and identically distributed process with mean 0 and variance 1. Let H_t denote the history in the process available at time t . The conditional variance of r_t is

$$\text{Var}(r_t|H_{t-1}) = \text{Var}(a_t|H_{t-1}) = E(a_t^2|H_{t-1}) = \sigma_t^2.$$

Thus, conditional heteroscedasticity in the variance is the same as autocorrelation in the squared innovation process. If all autocorrelation in the original series, r_t is accounted for in the conditional mean model, then the residuals are uncorrelated with mean zero. However, the residuals can be serially dependent.

The ARCH LM is based on the linear regression

$$a_t^2 = \alpha_0 + \alpha_1 a_t^2 + \dots + \alpha_m a_{t-m}^2 + e_t,$$

where e_t denote the error term.

$\alpha_1 = \alpha_2 = \dots = \alpha_m = 0$ is the null hypothesis under which there are no ARCH effects and the alternative hypothesis is the presence of ARCH effect.

The ARCH LM test statistic is given as

$$LM = nR^2,$$

where n is the sample size and R^2 is the squared multiple correlation coefficient from the regression equation used in estimating the innovations. The test statistic has an asymptotic chi-square distribution with m degrees of freedom.

Alternatively, we can use the F-statistic for the regression of squared residuals. Under the null hypothesis, the mF statistic is asymptotically a chi-square distribution with m degrees of freedom. We reject the null hypothesis if $mF > \chi_m^2(\alpha)$, where $\chi_m^2(\alpha)$ is the upper $100(1 - \alpha)$ percentile of χ_m^2 or the p -value of mF is less than α , a type I error (Tsay, 2013).

2.5 Goodness-of fit-test

To check for the goodness-of- fit of the fitted distributions, we use the Anderson-Darling statistic. The Anderson-Darling statistic gives more weight to the tails of the distribution (Chalabi, 2012).

The Anderson-Darling Test

The Anderson-Darling (AD) test was introduced by Anderson and Darling (1952). The AD test is a general test to compare the fit of an observed cumulative distribution function to an expected cumulative distribution function. The null hypothesis is that the data follows the specified distribution.

The AD test procedure is a general test to compare the fit of an observed cumulative distribution function to an expected cumulative distribution function.

This test gives more weight to the tails than other tests (e.g. Kolmogorov Smirnov test).

The Anderson-Darling test statistic (D^2) is defined as

$$(D^2) = m - \frac{1}{m} \sum_{i=1}^m (2i - 1) [\ln F(x_i) + \ln (1 - F(x_{m-i+1}))] \quad (2.8)$$

where $X_{(1)} < \dots < X_{(n)}$ is the ordered sample size n , and $F(x)$ is the underlying theoretical cumulative distribution to which the sample is compared.

The null hypothesis is that $X_{(1)} < \dots < X_{(n)}$ comes from the underlying distribution $F(x)$ (i.e. the data follows a specified distribution) is rejected at a chosen level of significance (α), if the test statistic (D^2) is greater than the critical value obtained from a table. In general, critical values of AD test statistic depends on the specific distribution being tested. However, tables of critical values for many distributions are difficult to find. Bootstrap (resampling) methods are utilised to obtain p -values for the Anderson-Darling test (Thas, 2010). The Anderson-Darling test may be used to compare the goodness-of-fit of several distributions (Engmann and Cousineau, 2011).

2.6 Unit Root and Stationary tests

A common assumption in many time series techniques is that the data is stationary. There are basically two types of stationarity, namely strongly stationary (usually referred to as strictly stationary) and weakly stationary (usually referred to as stationary).

A time series $\{x_n, n \in \mathbb{Z}\}$ is said to be strongly or strictly stationary if the joint distributions $x_{t_1}, x_{t_2}, \dots, x_{t_n}$ is the same as the joint distribution of $x_{t_1+k}, x_{t_2+k}, \dots, x_{t_n+k}$, for all choices of t_1, t_2, \dots, t_n and all choices of the time lag k .

A time series $\{x_n, n \in \mathbb{Z}\}$ is said to be weakly stationary or second-order stationary if

- $E(x_n) = \mu \quad \forall n \in \mathbb{Z}$.
- $E(x_n^2) < \infty \quad \forall n \in \mathbb{Z}$.
- $Cov(x_m, x_n) = Cov(x_{m+k}, x_{n+k}) \quad \forall n, m, k \in \mathbb{Z}$.

Thus, for such a process the mean and variance are constant (and finite) and the covariance between x_m and x_n is time invariant. I.e., it depends only on the time lag $n - m$ and not on m or n (Cryer and Chan, 2010). In this study we consider second-order stationarity.

It is advisable to use several unit root tests. So we use the ADF, PP, and KPSS tests to check for stationarity in the daily returns, a description of these tests follow.

The ADF Test

The Augmented Dickey-Fuller (ADF) test is an augmented version of the original Dickey-Fuller Test that was introduced by Dickey and Fuller (1979). The ADF test is used to test for a unit root in a time-series sample. The ADF test assumes the error term to be white noise. The null hypothesis is that returns have a unit root (non-stationary).

The ADF has three cases depending on the nature of the time series data being tested.

Case 1: no constant

The test equation is:

$$\Delta x_t = \gamma x_{t-1} + \delta_1 \Delta x_{t-1} + \dots + \delta_{p-1} \Delta x_{t-p+1} + \epsilon_t, \quad (2.9)$$

where p is the lag order of the autoregressive process, $\delta_1, \dots, \delta_{p-1}$ are coefficients of lagged difference terms, Δx_{t-i} . Δx_{t-i} are used to approximate the ARMA structure of the errors. The equation has no intercept and no time trend.

Case 2: no trend

The test equation is:

$$\Delta x_t = \alpha + \gamma x_{t-1} + \delta_1 \Delta x_{t-1} + \dots + \delta_{p-1} \Delta x_{t-p+1} + \epsilon_t, \quad (2.10)$$

where α is a constant and p is the lag order of the autoregressive process. The equation has an intercept (α) but no time trend.

Case 3: with trend

The test equation is:

$$\Delta x_t = \alpha + \beta t + \gamma x_{t-1} + \delta_1 \Delta x_{t-1} + \dots + \delta_{p-1} \Delta x_{t-p+1} + \epsilon_t, \quad (2.11)$$

where α is a constant, β is the coefficient on a time trend and p is the lag order of the autoregressive process. The test equation has an intercept (α) and time trend (βt).

In all cases ϵ_t is a white noise error term.

The test statistic is given by:

$$ADF_\tau = \frac{\hat{\gamma}}{SE(\hat{\gamma})}, \quad \text{where } \gamma = \phi - 1, \quad (2.12)$$

where ϕ is the coefficient of the lagged term of an AR(1) model. If $\phi = 1$, we have a unit root.

In the ADF test, we test $\gamma = 0$. Once a value of the test statistic is computed, it can be compared to the critical value of the Dickey-Fuller test. The corresponding p -value can be calculated.

The lag order, in addition to a sample size can affect the finite sample behaviour of the ADF test. Proper correction for the lag effect in implementing the ADF test is desirable. The number of augmenting lags (p) is determined by minimising the Schwarz Bayesian Criterion (SBI) or minimising the Akaike Information Criterion (AIC). In this study the SBI is used and the software automatically selects appropriate lag length.

The PP Test

The Phillips-Perron (PP) test was introduced by Phillips and Perron (1988). The PP test is used to test for a unit root in a time-series sample. They proposed the nonparametric test statistics for the unit root null by using consistent estimates of variances.

In its simplest form, there are three cases of PP test equation depending on the nature of the time series being tested.

Case 1: no constant

The test equation is:

$$x_t = \rho x_{t-1} + e_t$$

The equation has no intercept and no time trend.

Case 2: no trend

The test equation is:

$$x_t = \alpha + \rho x_{t-1} + e_t.$$

The equation has an intercept (α) but no time trend.

Case 3: with trend

The test equation is:

$$x_t = \alpha + \beta t + \rho x_{t-1} + e_t.$$

The test equation has an intercept (α) and time trend (βt). In all cases e_t is a white noise error term.

The two test statistics for each case taken from Maddala and Kim (2004) are given by:

Case 1: no constant

$$Z_p = T(\hat{\rho} - 1) - \frac{1}{2} \frac{(s^2 - s_e^2)}{T^{-2} \sum_1^T x_{t-1}^2}$$

$$Z_t = \frac{s_e t \hat{\rho}}{s} - \frac{1}{2} \frac{(s^2 - s_e^2)}{s \left(T^{-2} \sum_1^T x_{t-1}^2 \right)^{1/2}}$$

Case 2: no trend

$$Z_p = T(\hat{\rho} - 1) - \frac{1}{2} \frac{(s^2 - s_e^2)}{T^{-2} \sum_1^T (x_{t-1} - \bar{x}_{-1})^2}$$

$$Z_t = \frac{s_e}{s} t \hat{\rho} - \frac{1}{2} \frac{(s^2 - s_e^2)}{s \left[T^{-2} \sum_1^T (x_{t-1} - \bar{x}_{-1})^2 \right]^{1/2}}$$

where $\bar{x}_{-1} = \sum_1^{T-1} x_t / (T - 1)$

Case 3: with trend

$$Z_p = T(\hat{\rho} - 1) - \frac{T^6}{24D_X} (s^2 - s_e^2)$$

$$Z_t = \frac{s_e}{s} t \hat{\rho} - \frac{T^3 (s^2 - s_e^2)}{4\sqrt{3} D_X^{1/2} s}$$

where $D_X = \det(X'X)$ and the regressors are $X = (1, t, x_{t-1})$,

s^2 is the Newey-West consistent estimator of σ^2 (Newey and West, 1987),

s_e^2 is the consistent estimator of σ_e^2 ,

$$s_e^2 = \frac{1}{T} \sum_{t=1}^T e_t^2 \quad \text{and} \quad s^2 = \frac{1}{T} \sum_{t=1}^T e_t^2 + \frac{2}{T} \sum_{\tau=1}^{\ell} W_{\tau\ell} \sum_{t=\tau+1}^T e_t e_{t-\tau},$$

where $W_{\tau\ell} = 1 - \frac{\tau}{\ell + 1}$ and $e_t e_{t-\tau}$ is the estimator of the covariance between the error terms. The limiting distributions of Z_p and Z_t are identical to those of $K = T(\hat{\rho} - 1)$ and the t-statistics, respectively, with $s^2 = s_e^2$. Thus, the asymptotic critical values of the tests are the same as the asymptotic critical values tabulated by Fuller (1976).

The KPSS Test

The Kwiatkowski-Phillips-Schmidt-Shin (KPSS) test was introduced by Kwiatkowski, Phillips, Schmidt and Shin (1992). The KPSS test is used to test for a stationary root in a time-series sample. The KPSS test assumes the error term to be white noise.

Using the model:

$$x_t = \beta' D_t \epsilon_t + e_t, \tag{2.13}$$

and

$$\varepsilon_t = \varepsilon_{t-1} + v_t, \quad (2.14)$$

$$v_t \sim iid(0, \sigma_v^2). \quad (2.15)$$

where D_t contains the deterministic components (constant or constant plus time trend). The test statistic is given by:

$$KPSS = \frac{1}{T^2} \frac{\sum_{t=1}^T S_t^2}{\hat{\sigma}_\infty^2}, \quad (2.16)$$

where $S_t = \sum_{s=1}^t \hat{e}_s$ represents a partial sum of e_s ,

e_t is the residual of x_t on a constant (case 1) and the time trend (case 2),

$\hat{\sigma}_\infty^2$ represents a heteroscedasticity and autocorrelation consistent estimator of the variance of \hat{e}_t (This is a Lagrange Multiplier test for constant parameters against a random-walk parameter).

For testing the null hypothesis of level stationary instead of trend stationary, the test is constructed the same way except that e_t is obtained as a residual from a regression of x_t on an intercept only.

2.7 Stationary Time Series models

AR(p) model

We define the p th-order autoregressive AR(p) process or model as

$$X_t = \phi_1 X_{t-1} + \phi_2 X_{t-2} \dots + \phi_p X_{t-p} + a_t \quad (2.17)$$

or

$$\phi_p(L)X_t = a_t,$$

where $\phi_p(L) = (1 - \phi_1 L - \phi_2 L^2 - \dots - \phi_p L^p)$, a_t is a zero mean white noise process, $\phi_1, \phi_2, \dots, \phi_p$ are the autoregressive parameters, L is the backshift operator such that $LX_t = X_{t-1}$.

Since, $\sum_{j=1}^p |\phi_j| < \infty$, the process is always invertible. To be stationary, the roots $\phi_p(L) = 0$ must lie outside the unit circle. The AR processes are useful in describing situations in which the present value of the time series depends on the preceding values plus a random shock (Wei, 2006).

MA(q) model

A moving average (MA) process of order q is defined as

$$X_t = a_t - \theta_1 a_{t-1} - \dots - \theta_q a_{t-q} \quad (2.18)$$

or

$$X_t = \theta_q(L) a_t,$$

where $\theta_q(L) = (1 - \theta_1 L - \theta_2 L^2 - \dots - \theta_q L^q)$ and $\theta_1, \theta_2, \dots, \theta_q$ are the moving average parameters.

Because $1 + \theta_1^2 + \theta_2^2 + \dots + \theta_q^2 < \infty$, a finite moving average process is always stationary. The moving average is invertible if the roots of $\theta_q(L) = 0$ lie outside of the unit circle. An MA model suggests that a time series is a moving average of a white noise process while X_t and X_{t-k} remain uncorrelated. Moving average processes are useful in describing phenomena in which events produce an immediate effect that lasts for a short period. An AR(p) process may be identified as an infinite-order of an MA(q) process and vice versa.

ARMA(p,q) model

An Autoregressive Moving Average (ARMA) Model combines AR and MA models. ARMA model is defined as

$$\phi_p(L) X_t = \theta(L) a_t, \quad (2.19)$$

where $\phi_p(L) = (1 - \phi_1 L - \phi_2 L^2 - \dots - \phi_p L^p)$ and

$$\theta_q(L) = (1 - \theta_1 L - \theta_2 L^2 - \dots - \theta_q L^q).$$

For the process to be invertible, we require the roots of $\theta_q(L) = 0$ to lie outside the circle. To be stationary, we require the roots of $\phi_p(L) = 0$ to lie outside the unit circle.

ARMA models are commonly used in the time series analysis because of their flexibility in estimating many stationary processes. ARMA models are linear processes, hence they are not suitable for non-linear time series (Fan and Yao, 2003).

2.8 Non-stationary Time Series Models

Non-stationary time series models are widely used for non-stationary data, such as economic and stock price series.

Autoregressive Integrated Moving Average (ARIMA) Models

Autoregressive Integrated Moving Average (ARIMA) Models are used to describe nonstationary ARMA models. This is done by differencing the nonstationary time series until it becomes stationary. Consider a process X_t which is nonstationary but can be made stationary by differencing it a certain number of times.

X_t can be represented as

$$\phi_p(L)(1 - L)^d X_t = \theta(L)a_t, \quad (2.20)$$

where $d = 1, 2, \dots$ is the order of the difference parameter. This is an autoregressive integrated moving average ARIMA(p, d, q) model. This process can be represented as an ARMA process by letting $W_t = (1 - L)^d X_t$.

The resulting process becomes the usual ARMA process

$$\phi_p(L)W_t = \theta(L)a_t.$$

Variance stabilizing transformation

Differencing a time series is useful when the process is nonstationary in mean. However, this method is not useful when the time series is nonstationary in variance. If a series is non-stationary in the variance other variance stabilizing transformations are needed. The power transformation is only applicable for a positive data value. If some of the values are negative or zero, a positive constant may be added to all the values to ensure that they are all positive before using the power transformation. A variance stabilizing transformation, if needed, should be performed before any other analysis such as differencing. Box and Cox (1964) introduced the following power transformation.

For a given value of the parameter λ , the transformation is

$$T(X_t) = \begin{cases} \frac{X_t^\lambda - 1}{\lambda}, & \text{for } \lambda \neq 0 \\ \ln x, & \text{for } \lambda = 0. \end{cases} \quad (2.21)$$

The table below shows the commonly used values of λ and their associated transformations.

Table 2.1: Box Cox transformation

λ	-1	-0.5	0	0.5	1
Transformation	Reciprocal	Reciprocal of Square root	Logarithmic	Square root	No transformation
	$\frac{1}{X_t}$	$\frac{1}{\sqrt{X_t}}$	$\ln X_t$	$\sqrt{X_t}$	X_t

To see why $\lambda = 0$ corresponds to the logarithmic transformation, we note that

$$\lim_{\lambda \rightarrow 0} T(X_t) = \lim_{\lambda \rightarrow 0} \frac{X_t^\lambda - 1}{\lambda} = \ln X_t. \quad (2.22)$$

One advantage of using the Box Cox transformation is that we can treat λ as a transformation parameter and estimate its value from the data. We should choose the value of λ that gives the minimum residual mean square error. In a preliminary data

analysis, one can use an AR model of approximation to obtain the value of λ through an AR fitting that minimises the residual mean square error. The choice of the optimum value for λ is based on the evaluations of the residual mean square error on a grid of λ values.

Box Jenkins methodology

The aim of this methodology is to find the most appropriate ARIMA(p, d, q) model to use for forecasting. The stages involved in the Box Jenkins methodology are model identification, model estimation, diagnostic checking (validation or residual analysis), model selection (choice of a model) and forecasting.

Stage 1: Model identification

Model identification refers to the methodology in identifying the required transformation such as variance stabilizing transformations, differencing transformations and polynomial orders of AR(p) and MA(q). The steps involved in model identification are:

- Plot the time series data and choose proper transformations.
- Utilise Unit root and stationary tests discussed in chapter 2 to determine the degree of differencing needed.
- Compute and examine the sample ACF and PACF of the properly transformed and differenced series to identify the orders of p and q . If the ACF cuts off after lag q and PACF tails off as exponential decay or damped sine wave, then the process is MA (q). If the ACF tails off as exponential decay or damped sine wave and PACF cuts off after lag p , then the process is AR(p). If the ACF tails off after lag $(p - q)$ and the PACF tails off after lag $(p - q)$, then the process is ARMA (p, q)(Wei, 2006). However, a certain level of experience is required to make interpretations in practice.

Stage 2: Model Estimation

After identifying a tentative model, the next step is to estimate the parameters in the model. Various approaches are utilised in estimating the parameters of ARMA models. These include methods of moments, Maximum likelihood method, linear least squares and non-linear estimation. Check whether parameters are significant.

Stage 3: Model Validation

The Ljung-Box test is widely used to check whether the assumption that residuals are white noise process is met. The standardised residuals of the GARCH-type model are assumed to be independent and identically distributed. Therefore, if the model is adequate, the standardised residuals are expected not to exhibit autocorrelation (serial correlation) and conditional heteroskedasticity (ARCH effect). In this study, we used the Ljung-Box and ARCH tests.

Stage 4: Forecasting

Once the model is adequate, it can be used in forecasting future values of the series. The objective is to produce optimal forecasts that have little or no error. The minimum mean square error (MSE) is normally used in the literature.

Model selection criteria

Model selection criteria are used to select the best model from candidate GARCH-type models to describe the precious metal returns. It is a useful tool for assessing if a fitted model provides an optimal balance between parsimony and goodness-of-fit. It helps to find the best GARCH-type model that is neither too simple or nore too complex for the precious metal returns. The model selection criteria employed in this thesis are: Akaike information criterion (AIC) and Bayesian information criterion or Schwarz Bayesian criterion (SBI).

The Akaike Information Criterion (AIC)

AIC measures how well the evaluated model fits with the data in respect to candidate models. Given GARCH-type models of different structures, each model is fitted

to the precious metal returns using Gaussian quasi Maximum likelihood. The AIC is computed for each model (Akaike, 1974).

$$AIC = -\frac{2}{k} \log(\text{likelihood}) + \frac{2}{k}(p + q), \quad (2.23)$$

where k is the sample size and $p + q$ is the number of parameters in the model. The model with the smallest number of parameters and with the largest likelihood has the minimum AIC. The model with the smallest AIC is regarded as the best model for the data (Tsay, 2013).

The Schwarz Bayesian Information Criterion (SBI)

SBI is concerned with the Bayes factor. The SBI of a model is given as:

$$SBI = -2 \log(\text{likelihood}) + (p + q) \log k, \quad (2.24)$$

where k is the sample size and $p + q$ is the number of parameters in the model. SBI allows for the comparison of multiple models by penalising complex models (model with many parameters) relative to simpler models. The model that has the largest posterior probability has the minimum SBI and is regarded as the best model for the data.

2.9 Long memory and Fractional Integration

The Long memory concept

A stationary process X_t is a long memory process if there exist a real number $0 < H < 1$, such that the ACF, $\rho(k)$ has the following hyperbolic decay

$$\lim_{k \rightarrow \infty} \rho(k) = C^{2H-1}, \quad C > 0, \quad (2.25)$$

where C is a finite constant and H is the Hurst exponent. Such a process has auto-covariance function $\gamma(k)$ which is not summable, i.e.

$$\sum_{\forall k} |\gamma(k)| = \infty. \quad (2.26)$$

The long-range parameter d of a stationary long memory process has the following relationship with the Hurst exponent

$$d = H - \frac{1}{2}. \quad (2.27)$$

Thus, we can deduce the equivalent interval for the Hurst exponent which is

$$\frac{1}{2} < H < 1.$$

Equivalently, in the frequency domain long memory can be defined as a spectrum as,

$$f(\omega) \approx c|\omega|^{-2d} \text{ as } \omega \rightarrow \infty, \quad 0 < d < \frac{1}{2}. \quad (2.28)$$

For $d > 0$, the ACF decays very slowly and the spectrum typically diverges to infinity at frequency $\omega = 0$, i.e., $\lim_{\omega \rightarrow 0} f(\omega) = \infty$ indicating strong long-range dependence.

For $d < 0$, the spectrum of the series is equal to zero at $\omega = 0$ indicating intermediate-range dependence.

Fractional Integration

According to Tsay (2013), there exist some time series whose ACF decays slowly to 0 at a polynomial rate as lag increases. These time series processes are called long memory time series. The fractionally differenced process defined by

$$(1 - L)^d X_t = a_t, \quad -0.5 < d < 0.5, \quad (2.29)$$

where a_t is a white noise series is one such example.

Properties of the model in equation 2.29 were taken from Tsay (2013). The properties are as follows:

- If $d < 0.5$, then X_t is a weakly stationary process and has the infinite MA representation

$$X_t = a_t + \sum_{i=1}^{\infty} \psi_i a_{t-i}, \text{ with}$$

$$\psi_k = \frac{d(1+d)\dots(k-1+d)}{k!} = \frac{(k+d-1)!}{k!(d-1)!}. \quad (2.30)$$

- If $d > -0.5$, then X_t is invertible and has the infinite AR representation

$$X_t = a_t + \sum_{i=1}^{\infty} \pi_i X_{t-i}, \text{ with}$$

$$\pi_k = \frac{-d(1-d)\dots(k-1-d)}{k!} = \frac{(k-d-1)!}{k!(-d-1)!}. \quad (2.31)$$

- For $-0.5 < d < 0.5$, the ACF of X_t is

$$\rho_k = \frac{d(1+d)\dots(k-1+d)}{(1-d)(2-d)\dots(k-d)}, \quad k = 1, 2, \dots$$

In particular, $\rho_1 = \frac{d}{(1-d)}$ and

$$\rho_k \approx \frac{(-d)!}{(d-1)!} k^{2d-1}, \text{ as } k \rightarrow \infty. \quad (2.32)$$

- For $-0.5 < d < 0.5$, the PACF of X_t is $\phi_{k,k} = \frac{d}{(k-d)}$ for $k = 1, 2, \dots$
- For $-0.5 < d < 0.5$, the spectral density function of $f(\omega)$ of X_t , which is the Fourier transform of the ACF of X_t , satisfies

$$f(\omega) \sim \omega^{-2d}, \text{ as } \omega \rightarrow 0, \quad (2.33)$$

where $\omega \in [0, 2\pi]$ denotes the frequency (Tsay, 2013).

The ARFIMA(p, d, q) model

One of the mostly used parametric models in long memory processes is the autoregressive fractionally integrated moving average (ARFIMA) model introduced by Granger and Joyeux (1980), Granger (1980) and Hoskins (1981). The ARFIMA(p, d, q)

model proposes the difference parameter as noninteger and suggest that fractional integration process $I(d)$ in the conditional mean.

Consider an ARFIMA(p, d, q) model of the form

$$\phi(L)(1 - L)^{d_m}(X_t - \mu) = \theta(L)\varepsilon_t, \quad (2.34)$$

where ε_t is a white noise process, μ is the unconditional mean of X_t , d_m is a fractional integration real number parameter. $\phi(L) = \phi_1L + \phi_2L^2 + \dots + \phi_pL^p$ and $\theta(L) = \theta_1L + \theta_2L^2 + \dots + \theta_qL^q$ are the autoregressive (AR) and moving average (MA) polynomials, respectively, assumed to have all roots outside the unit circle. The fractional difference operator $(1 - L)^{d_m}$ is defined in a natural way, by a binomial series (Hoskins, 1981):

$$(1 - L)^{d_m} = \sum_{k=0}^{\infty} \binom{d_m}{k} (-L)^k = 1 - d_mL - \frac{1}{2}d_m(1 - d_m)L^2 - \frac{1}{6}d_m(1 - d_m)(2 - d_m)L^3 - \dots \quad (2.35)$$

This can be expressed as

$$(1 - L)^{d_m} = \sum_{k=0}^{\infty} \frac{(-1)^k \Gamma(k + d_m) L^k}{\Gamma(d_m) \Gamma(k + 1)} \quad (2.36)$$

where $\Gamma(\cdot)$ denotes the gamma (generalised fractional) function.

The X_t process defined by equation 2.34 and for $d \neq 0$ is said to be $I(d)$. The autocorrelation coefficients and the Wold decomposition will all exhibit a very slow rate of hyperbolic decay. The ARFIMA process is said to be stationary when $-0.5 < d_m < 0.5$, where the effect of shocks to ε_t decays at a gradual rate to zero. The process becomes nonstationary when $d_m \geq 0.5$ and is a stationary but noninvertible process when $d_m \leq -0.5$, implying that the data time series is impossible to be modelled by any AR process. The ARFIMA(p, d, q) process has a positive dependence among distant observations (i.e. long memory process) when $0 < d_m < 0.5$. It has an anti-persistent property (an intermediate memory) if $-0.5 < d_m < 0$, but we follow Box *et al.* (2008) and refer to them as long memory processes or negative long

memory (Baum and Wiggin, 2000). The process is mean reverting for $0.5 \leq d_m < 1$. The ARFIMA model nests to ARMA (short memory) when $d_m = 0$ and ARIMA when $d_m = 1$ (i.e. infinite long memory). The ARFIMA model solves the short-run and long-run dynamics by modelling short-run behaviour through the conventional ARMA lag polynomials while long-run characteristic is captured by the differencing parameter.

For an $I(d)$ process, the spectral density is such that $f(0) = 0$ for $d < 0$ and $f(0) = \infty$ for $d > 0$. For small frequencies, ω , an approximation for $d > 0$ is given by $f(\omega) \approx \omega^{-2d}$, while the process has infinite variance for $d > 0.5$.

We can derive the impulse response weights from the ARFIMA(p, d, q) process in equation 2.34. The impulse weights are defined by first differencing X_t to obtain

$$(1 - L)X_t = D(L)\varepsilon_t, \quad (2.37)$$

where $D(L) = (1 - L)^{1-d_m}\phi(L)^{-1}\theta(L)$. The lag polynomial $D(L)$ can be expressed in terms of the hypergeometric function as $D(L) = F(d - 1, 1, 1; L)\phi(L)^{-1}\theta(L)$, and Gradszteyn and Ryzhnik (1980) showed that $F(d - 1, 1, 1; L) = 0$ for $d < 1$. Thus for $d < 1$,

$$D(1) = F(d - 1, 1, 1; L)\phi(1)^{-1}\theta(1) = 0. \quad (2.38)$$

The impact of a unit innovation at time t on a the process X_{t+1} is the given by as $1 + \sum_{j=1,k} D_j$. For a mean reverting process, $D(1) = 0$. For any process $X_t \sim I(d)$ and for $d < 1$, X_t will be mean reverting. Although X_t is not covariance stationary for $0.5 < d_m < 1$, it is mean reverting. Hence, there is no long run impact of an innovation on future values of the process. See Hoskins (1981) and Campbell and Mankiw (1987) for more details.

Long memory tests

Testing for the long memory property is an essential task since any evidence of long memory would support the use of a long memory modelling techniques. In this

study, we considered the most frequently used estimators of long memory parameter d . The first is the rescaled Range estimator (R/S) which estimates the Hurst exponent developed by Hurst (1951) and introduced in finance by Mandel (1971). See a paper by Kale and Butar (2010) on further details on this estimator. The second and third are Lo's modified rescaled range estimator and the Geweke, Porter and Hudak (GPH) estimator respectively. We tested for long memory components in the return generating process and volatility of precious metals using R/S, Lo's R/S and GPH statistics.

The rescaled range or R/S statistic (Baillie, 1996)

The classical R/S, devised by Hurst (1951) and Mandelbrot (1972), is the range of partial sums of deviations of a time series from its mean, rescaled by its standard deviation. For a sample of T values x_1, x_2, \dots, x_T ,

$$Q_T = \frac{1}{s_T} \left[\max_{1 \leq k \leq T} \sum_{j=1}^k (x_j - \bar{x}) - \min_{1 \leq k \leq T} \sum_{j=1}^k (x_j - \bar{x}) \right], \quad (2.39)$$

where s_T is the Maximum likelihood estimator of the standard deviation of x and $\bar{x} = 1/T \sum_{i=1}^T x_i$. The first bracketed term is the maximum of the partial sums of the first k deviations of x_j from the full sample mean, which is nonnegative. The second bracketed term is the corresponding minimum, which is nonnegative, so that $Q_T > 0$. Empirical studies have shown that the R/S statistic has the ability to detect long memory in the data. Like other estimators of long-range dependence, the R/S statistic is not robust to short-range dependence and heteroscedasticity. See Davies and Harte (1987), Aydogan and Booth (1988) and Lo (1991) for more details.

Lo's modified rescaled range estimator

Lo's (1991) modified rescaled range (R/S) test for long-range dependence of a time series. Thus, it is extremely sensitive to short memory features of the data. Lo (1991) modified the R/S statistic to account for the effect of short-range dependence by applying the Newey-West correction to derive a consistent estimate of the long-range

variance of the time series. The Lo (1991) modified R/S statistic is given by:

$$Q_T = \frac{1}{\hat{\sigma}_T(q)} \left[\max_{1 \leq k \leq T} \sum_{j=1}^k (x_j - \bar{x}) - \min_{1 \leq k \leq T} \sum_{j=1}^k (x_j - \bar{x}) \right], \quad (2.40)$$

where $\hat{\sigma}_T(q)$ is the square root of the Newey-West estimate of the long-range variance with bandwidth q .

GPH test

Geweke and Porter-Hudak(1993) proposed a semi-parametric estimator of the fractional differencing estimator, d based on a log-periodogram regression or regression of the ordinates of the log spectral density on trigonometric function. The estimator exploits the theory of linear filters to express the process $(1 - L)^d X_t = u_t$ where $u_t \sim I(0)$ and the spectral density of X_t is given by

$$f(\omega) = |1 - e^{-i\omega}|^{-2d} f(\omega)_u \quad (2.41)$$

where $f(\omega)_u$ is the spectral density of u .

Equation 2.41 can be expressed as

$$\ln[f(\omega_j)] = \ln[f_u(0)] - d \ln \left[4 \sin^2 \left(\frac{\omega_j}{2} \right) \right] + \ln \left[\frac{f_u(\omega_j)}{f_u(0)} \right] \quad (2.42)$$

We define the periodogram of a time series X_t using the Fast Fourier transform (FFT) for the first m ordinates as $I(\omega_j) = \frac{1}{2\pi T} |\sum_{t=1}^T X_t e^{-\omega_j t}|^2$, where $\omega_j = \frac{2\pi j}{T}$, $j = 1, 2, \dots, m$, with $m = [\sqrt{T}]$ Fourier frequencies and $[.]$ denoting the integer part. The estimate d can be derived from the following linear regression based on equation 2.42 and from the periodogram of X_t .

$$\ln[I(\omega_j)] = a + d \ln \left[4 \sin^2 \left(\frac{\omega_j}{2} \right) \right] + \eta_j,$$

where $\eta_j = \ln \left[\frac{f_u(\omega_j)}{f_u(0)} \right]$ is the error term which is negligible for the near zero m harmonic frequencies. See Baillie (1996) for more details about the GPH test.

2.10 Summary

In this chapter, we described the tests used to investigate the empirical properties of precious metal returns. These include tests for autocorrelation, normality, unit roots and stationarity, ARCH effects and long memory. We also outlined the Anderson-Darling goodness-of-fit test for model adequacy which is essential in later chapters where models are fitted to precious metals data. We also discussed stationary and non-stationary time series models, long memory and fractional integration.

Chapter 3

Precious metal data

3.1 Introduction

In this chapter we analyse some empirical properties of precious metal data used in the study. We start by converting daily gold, platinum and silver prices into log-returns. We compute the descriptive statistics of the log-returns and check for features such as stationarity, volatility clustering, heavy-tailedness, asymmetry, long-memory in the metal log-returns.

3.2 Data Analysis

We make use of daily data for three precious metal prices (i.e. gold, silver and platinum) from 2 April 1990 to 18 September 2014. All of the prices are in US dollars per Troy ounce and are internationally regarded as pricing mechanisms for a variety of precious metal transactions and products. We downloaded daily gold, platinum and silver P.M. fixing spot prices from London Bullion Market Association (LBMA) and London Platinum and Palladium Market (LPPM) database quandl.com. The return series for each index are calculated as the first backward-differences of the natural logarithm of the index values. For day t , the daily log return r_t is defined as

$$r_t = \ln(P_t) - \ln(P_{t-1}) \tag{3.1}$$

where P_t is the price at day t .

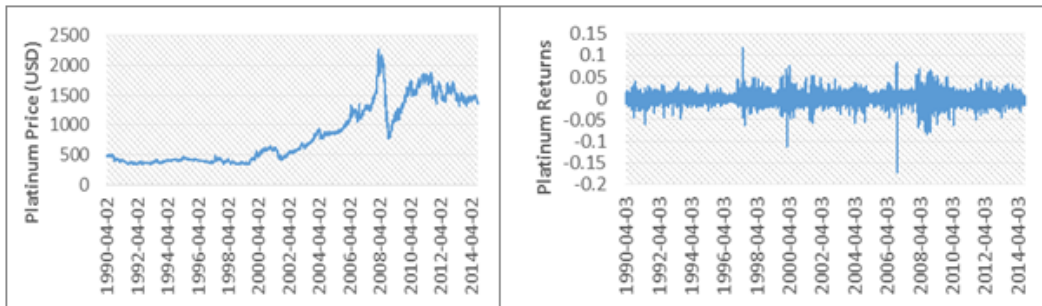


Figure 3.1: Time series plot of gold prices (left) and one-day returns (right)

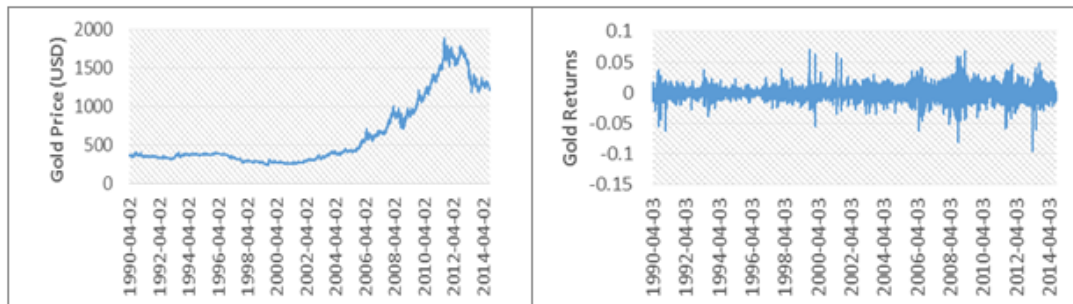


Figure 3.2: Time series plot of platinum prices (left) and one-day returns (right)

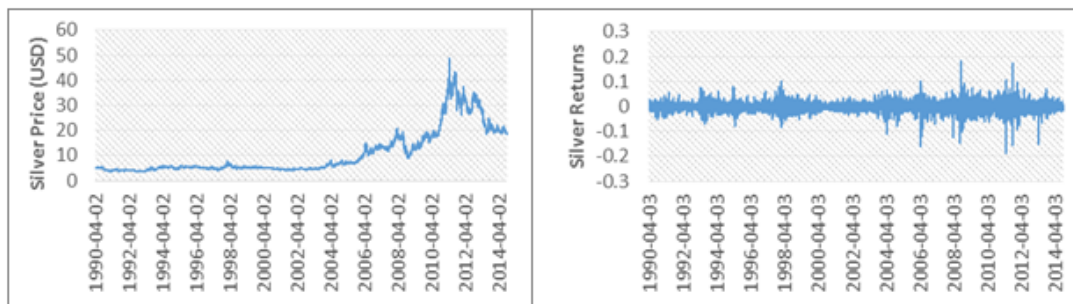


Figure 3.3: Time series plot of silver prices (left) and one-day returns (right)

Figures 3.1, 3.2 and 3.3 provide the time series plot of daily precious metal prices and returns for 25 years. The plots strongly indicate the presence of heteroscedasticity and volatility clustering in all return series. Isolated extreme returns caused by shocks to the financial market can be seen, such as those corresponding to the 2008/9 financial crisis. Descriptive statistics, correlation, normality, heteroscedasticity, unit root and stationary tests are reported in Table 3.1 on the next page.

From Panel A, all returns have a positive mean indicating that the original price series have upward trends over time. We can also see that all precious metal returns are skewed towards the left and they do not correspond to the Normal distribution assumptions. The excess kurtosis value indicates the leptokurtotic behaviour of these return series. This implies that the empirical distribution of the daily precious metal returns has heavier tails compared to the Normal distribution.

From, Panel B, the Anderson-Darling goodness-of-fit (GOF) test for normality and Jarque-Bera test give p -values less than 0.001 for all three precious metals returns rejecting the normality assumption at all levels of significance. The Ljung-Box test, $Q(5)$, $Q(10)$, $Q^2(5)$ and $Q^2(10)$ indicate that autocorrelation is insignificant for gold and platinum returns but highly significant in the squared gold, platinum and silver returns. These results show signs of high degree of persistence in the volatility process of precious metals.

The ARCH-LM test shows the presence of conditional heteroscedasticity in all daily precious metal return series. Therefore, the GARCH-type models seem to be appropriate for modelling and forecasting their time varying conditional volatility. In Panel C, we represent the results of the Augmented Dickey-Fuller Test (1979) and the Philips and Peron (1988) unit root tests and the Kwiatkowski *et al.* (1992) stationarity test.

The ADF and the PP tests reject the hypothesis of unit root for all precious metal return series studied. We can conclude that precious metal price returns are stationary i.e. governed by an $I(0)$ process which have no long-range memory. The KPSS test reveals that we cannot reject the stationarity null hypothesis for all precious metal return time series.

Further analysis was done using the ACF and PACF plots of daily precious metal returns, their squared and absolute returns, Normal Q-Q plots and box plots of returns are reported in Figures 3.4 - 3.9. Figures 3.4, 3.6 and 3.8 show sample ACF and PACF of daily precious metal returns, squared precious metal returns, absolute precious metal returns.

Table 3.1: Descriptive statistics and unit root tests of precious metal price returns

	Gold	Platinum	Silver				
<i>Panel A: Descriptive Statistics</i>							
Minimum	-0.0797200	-0.1728000	-0.1869000				
Maximum	0.0700600	0.1178000	0.1828000				
Mean	0.0002786	0.0002246	0.0003428				
Std.dev	0.01012477	0.01378826	0.01958386				
Moment coefficient of skewness	-0.105173	-0.5253288	-0.3642794				
Moment coefficient of excess kurtosis	6.202978	10.19592	9.671625				
<i>Panel B: Testing for correlation, normality and heteroscedasticity</i>							
	<i>Statistic</i>	<i>p-value</i>	<i>Statistic</i>	<i>p-value</i>	<i>Statistic</i>	<i>p-value</i>	
$Q(5)$	5.4356	0.3651	9.9475	0.07674	42.252	0.0017	
$Q(10)$	12.987	0.2244	10.954	0.3611	47.054	0.0084	
Jarque-Bera test	9670.8	<0.0001	22686	<0.0001	21165	<0.0001	
Anderson Darling test	80.093	<0.0001	67.823	<0.0001	71.102	<0.0001	
$Q^2(5)$	489.95	<0.0001	554.012	<0.0001	721.953	<0.0001	
$Q^2(10)$	796.36	<0.0001	799.762	<0.0001	1055.31	<0.0001	
ARCH LM test	421.56	<0.0001	504.85	<0.0001	607.1	<0.0001	
<i>Panel C: Unit root and stationary tests</i>							
	<i>Statistic</i>	<i>p-value</i>	<i>Statistic</i>	<i>p-value</i>	<i>Statistic</i>	<i>p-value</i>	
<i>ADF</i>	No constant	-71.7637	<0.0001	-70.4528	<0.0001	-78.5207	<0.0001
	No trend	-71.7912	<0.0001	-70.4649	<0.0001	-78.5247	<0.0001
	With trend	-71.7956	<0.0001	-70.4587	<0.0001	-78.5182	<0.0001
<i>PP</i>	No constant	-71.7642	<0.0001	-70.4424	<0.0001	-78.5639	<0.0001
	No trend	-71.7917	<0.0001	-70.4551	<0.0001	-78.5715	<0.0001
	With trend	-71.7952	<0.0001	-70.4488	<0.0001	-78.5652	<0.0001
<i>KPSS</i>	No trend	0.3025	>0.1	0.0823	>0.1	0.1091	>0.1
	With Trend	0.1792	>0.1	0.0790	>0.1	0.0914	>0.1

The ACF and PACF plots suggest that there are no serial correlation in gold and platinum returns. This is confirmed by the Ljung-Box statistics of the log returns which fail to reject the null hypothesis of zero autocorrelation (Panel B, Table 3.1). However, the ACF and PACF of silver returns hint at a slight autocorrelation of first order.

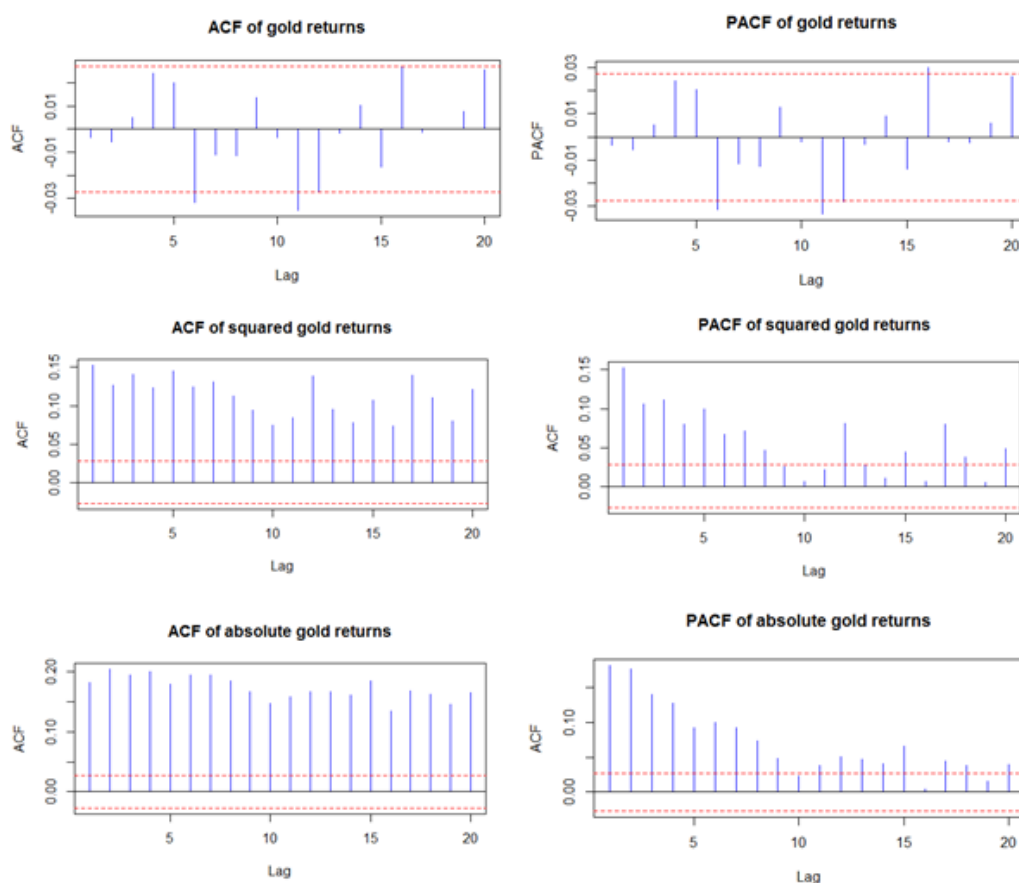


Figure 3.4: Sample ACF and PACF of daily gold returns, squared gold returns and absolute gold returns.

This is confirmed by the Ljung-Box statistics which rejects the null hypothesis of zero autocorrelation for silver returns. Clearly, the squared and absolute returns of daily log-returns of gold, silver and platinum have some serial correlation. Slow decay of autocorrelation in absolute returns indicate long-range dependence in the precious metal returns. i.e. the ACF plots for absolute returns and squared returns suggest the presence of long-memory in the volatility of returns for all precious metal series.

Figures 3.5, 3.7, 3.8 show the Normal Q-Q plots and box plots for gold, platinum and silver returns. The Normal Q-Q plots illustrate that the tails of daily precious metal returns are heavier than the tails of the Normal distribution. It is evident that there is a lack of fit at the extremes for all returns.

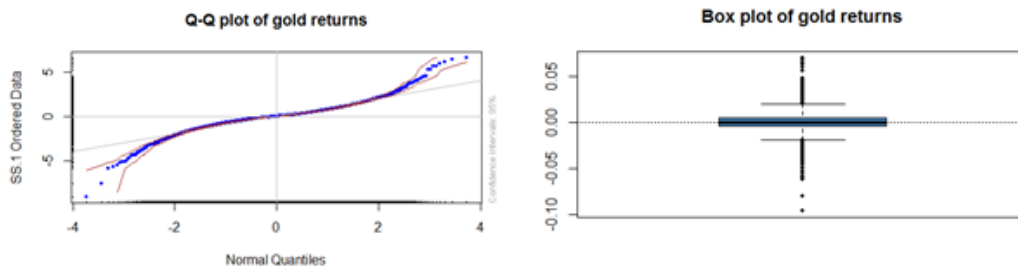


Figure 3.5: Normal Q-Q plot and Box plot for the daily gold returns.

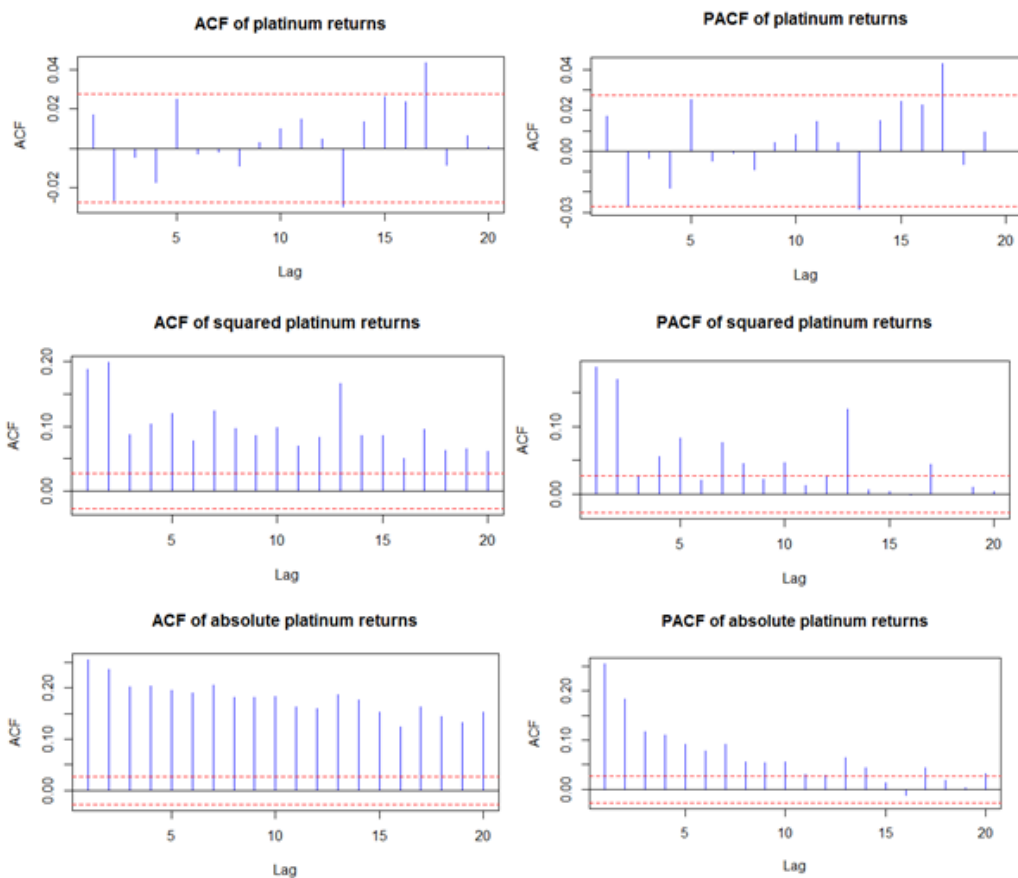


Figure 3.6: Sample ACF and PACF of daily platinum returns, squared platinum returns, absolute platinum returns.

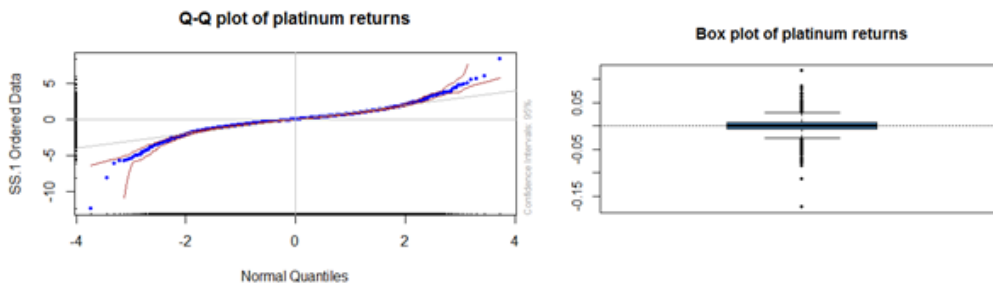


Figure 3.7: Normal Q-Q plot and Box plot for the daily platinum returns.

The negative skew as well as the heavy tails are mirrored from their quantitative values in these graphs. It can be seen from the box plots that daily precious metal returns are skewed to the left and heavy-tails are evident.

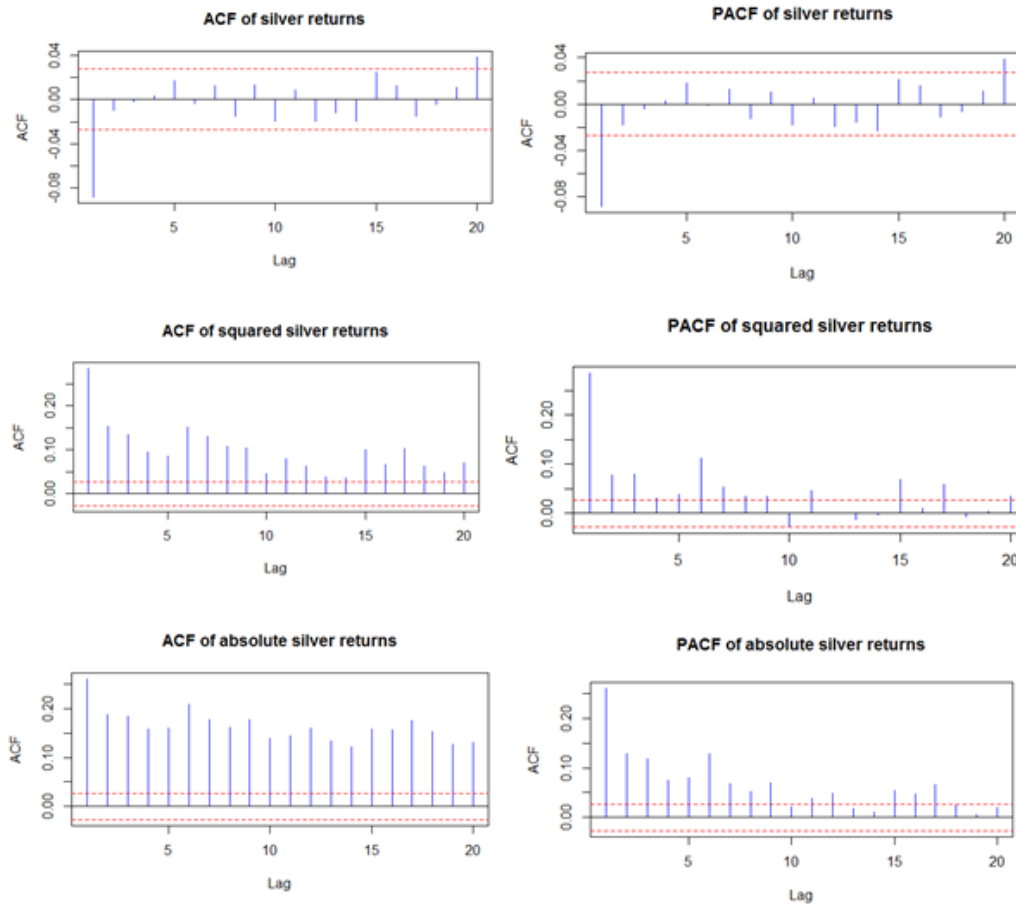


Figure 3.8: Sample ACF and PACF of daily silver returns, squared silver returns and absolute silver returns.

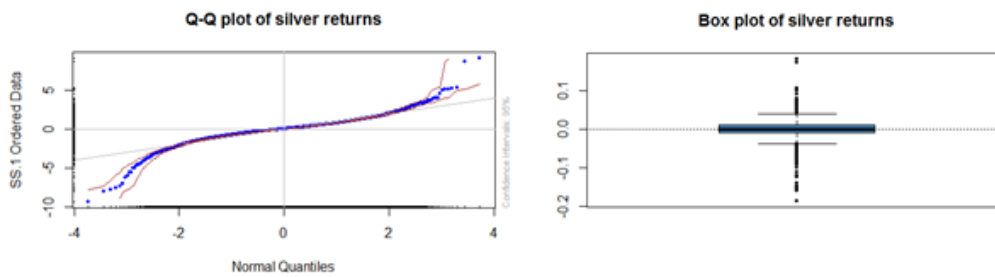


Figure 3.9: Normal Q-Q plot and Box plot for the daily silver returns.

Testing long memory in metal price volatility

In long memory testing, we firstly carried out long memory tests to the squared log returns of gold, platinum and silver returns based on the heuristic estimator. The HURST exponent results of the long memory tests are shown in Table 3.2 for precious metal returns and squared returns.

Table 3.2: long memory tests R/S method

Returns	Hurst	Standard Error	t -value	p -value
Gold returns	0.6246	0.03272	19.0909	< 0.0001
Platinum returns	0.5511	0.02025	27.2105	< 0.0001
Silver returns	0.5435	0.02589	20.9978	< 0.0001
Gold squared returns	0.6340	0.05384	11.7751	< 0.0001
Platinum squared returns	0.7320	0.02785	26.2814	< 0.0001
Silver squared returns	0.7208	0.02594	27.7909	< 0.0001

For all precious metal returns and squared returns, the test suggests long memory and all p -values are less than 0.0001, rejecting the null hypothesis of no persistence. The R/S method indicates strong evidence of long range dependence in the daily conditional return and volatility processes for the precious metals.

Secondly, the Geweke Porter-Hudak (GPH) test was also carried out over the in-sample period and results are shown in Tables 3.3 and 3.4. It is well known that long memory tests are sensitive to selection of bandwidths. We therefore, apply the GPH test with different bandwidths. Based on d -values for $m = T^{0.5}$, $m = T^{0.6}$

and $m = T^{0.7}$, the GPH test confirms the existence of long memory in the squared returns. T is the sample size.

Table 3.3: GPH long memory test for returns

Returns	Bandwidths	d	Standard Error	t -value	p -value
Gold	$m = T^{0.5}$	-0.1345	0.09399	-1.4310	0.157
	$m = T^{0.6}$	-0.1106	0.05246	-2.1087	0.036
	$m = T^{0.7}$	-0.0574	0.03301	-1.7392	0.083
Platinum	$m = T^{0.5}$	0.0360	0.1020	0.3533	0.725
	$m = T^{0.6}$	-0.0151	0.05474	-0.2756	0.783
	$m = T^{0.7}$	-0.0246	0.03164	-0.7764	0.438
Silver	$m = T^{0.5}$	-0.06865	0.08129	-0.8445	0.401
	$m = T^{0.6}$	-0.07558	0.04764	-1.5863	0.115
	$m = T^{0.7}$	-0.003691	0.03059	-0.1207	0.904

Table 3.4: GPH long memory test for Squared returns

Squared Returns	Bandwidths	d	Standard Error	t -value	p -value
Gold	$m = T^{0.5}$	0.5363	0.07892	6.7962	<0.0001
	$m = T^{0.6}$	0.4822	0.05502	8.7654	<0.0001
	$m = T^{0.7}$	0.2747	0.03306	8.3089	0.083
Platinum	$m = T^{0.5}$	0.38583	0.0665	5.8022	<0.0001
	$m = T^{0.6}$	0.3306	0.04266	7.7501	<0.0001
	$m = T^{0.7}$	0.2596	0.02913	8.9111	<0.0001
Silver	$m = T^{0.5}$	0.2291	0.07645	2.9969	0.004
	$m = T^{0.6}$	0.2302	0.05032	4.5748	<0.0001
	$m = T^{0.7}$	0.2371	0.3167	7.4857	<0.0001

We then used the modified Lo's R/S test and Table 3.5 shows long memory test based on Lo's R/S test.

Table 3.5: Lo's R/S test for precious metal returns and squared returns

Returns	Test statistic	Decision
Gold returns	1.84	Fail to reject null hypothesis of not long-range dependent at 1% and 5% levels and reject null hypothesis at 10% level.
Platinum returns	1.38	Fail to reject null hypothesis of not long-range dependent
Silver returns	1.35	Fail to reject null hypothesis of not long-range dependent
Gold squared returns	4.37	Reject null hypothesis of not long-range dependent
Platinum squared returns	2.8	Reject null hypothesis of not long-range dependent.
Silver squared returns	3.34	Reject null hypothesis of not long-range dependent.

Critical values of Lo's modified R/S statistic is 2.098 at 1%, 1.862 at 5% and 1.747 at 10%.

Lo's R/S test does not reject the null hypothesis of no long memory in returns and indicates long memory in squared returns. From Tables 3.3 and 3.5, we clearly notice that the Lo's R/S test and GPH test do not reject the hypothesis of no long-range dependence for the precious metal returns. I.e. the two tests confirm short memory in the returns. For the squared return series, the GPH test provides evidence of long memory as shown in Table 3.4. These results confirm the suitability of GARCH-type models, which capture long memory property in the volatility process.

3.3 Summary

In this chapter, we investigated the empirical properties of daily gold, platinum and silver log returns. The three precious metals return exhibit the following stylised facts:

- Absence of autocorrelation in gold and platinum returns and slight first-order autocorrelation in silver returns.
- The absolute and squared returns of all three precious metals are highly auto-correlated.
- The precious metal returns are characterised by heavy tails, as excess kurtosis is positive. i.e. their distribution is leptokurtic.

- The empirical distribution of all precious metals is skewed to the left. i.e. negative returns are more likely to occur than positive ones
- Volatility clustering (extreme returns were observed closely in time).
- Slow decay of autocorrelation in absolute returns indicating long-range dependence in the precious metal returns. The R/S and the GPH tests confirm the existence of long memory in the squared returns.

Statistically accepted models for the precious metals series should be able to capture these stylised facts. The suggested models are:

- GARCH-type models with heavy tailed innovations.
- Long memory GARCH-type models with heavy tailed innovations.

The suggested distributions for modelling heavy tails are:

- Generalised Extreme Value Distribution (GEVD)
- Generalised Pareto Distribution (GPD)
- Generalised Hyperbolic Distributions and its subclasses Hyperbolic Distribution (HD), Normal-Inverse Gaussian Distribution (NIGD), Generalised Hyperbolic skew Student-t Distribution (GHStD) and Variance-Gamma Distribution (VGD)
- Generalised Lambda Distribution (GLD)
- Pearson type-IV Distribution (PIVD)
- Stable Distribution (SD)

3.4 Statistical software packages

In this chapter, we used the **fbasics** (Wuertz *et al.*, 2014), **tseries** (Trapletti and Hornik, 2017), **TSA** (Chan and Ripley, 2012), **fUnitRoots** (Wuertz *et al.*, 2017) R packages in

data analysis. We used the STATA command `gphudak` (Baum and Wiggins, 2000) to test for the existence of long memory property in precious metal returns and squared returns series using the GPH test. `lomodrs` command in STATA (Baum and Room, 2001) for Hurst-Mandelbrot rescaled range statistic and Lo's modified rescale range test for long range dependence in time series.

Chapter 4

Risk Analysis

4.1 Introduction

Risk management is a core competence of financial institutions like banks, insurance companies, investment funds and others. Techniques for the measurement of risk are central for the process of managing risk. Risk can be measured in terms of probability distributions (Emmer *et al.*, 2015). In this chapter we discuss properties of two risk measures: Value-at-Risk (VaR) and Expected Shortfall (ES). We will also outline the backtesting methods used in this study.

4.2 Risk Measures

The amount of asset risk capital, reserved by financial institutes as per the Basel agreement, is directly associated to the portfolio risk level and two of the most common benchmark measures for evaluating such risk are VaR and ES. VaR is intended to assess the maximum possible loss of a portfolio over a given time period, given a certain risk level and its calculations focus on the tails of a distribution. Whereas, ES evaluates the expected value of losses (or gains) that exceed a corresponding VaR level. Hence, the accuracies of VaR and ES estimation depend on how well a selected model portrays the extreme data observations (McNeil *et al.*, 2005).

Desirable properties of risk measures

In this study, we define a risk measure as providing a risk assessment in the form of a capital amount that serves as some kind of buffer against unexpected future losses (Emmer *et al*, 2015). Artzner *et al* (1999) provide a list of desirable properties that a measure of risk should possess.

Definition 4.1: A risk measure ρ is coherent if it satisfies the following conditions:

- **Homogeneity:** ρ is homogeneous if for all loss variables L and $\alpha \geq 0$, it holds that $\rho(\alpha L) = \alpha\rho(L)$.
- **Subadditivity:** ρ is subadditive if for all loss variables L_a and L_b , it holds that $\rho(L_a + L_b) \leq \rho(L_a) + \rho(L_b)$.
- **Monotonicity:** ρ is monotonic if for all loss variables L_a and L_b , it holds that $L_a \leq L_b \Rightarrow \rho(L_a) \leq \rho(L_b)$.
- **Translation invariance:** ρ is translation invariant if for all loss variables L , it holds that $\rho(L - c) = \rho(L) - c$ for any constant c . This is referred to as risk free condition.

Subadditivity implies that diversification reduces risk.

Definition 4.2: Two real-valued random variables L_a and L_b are said to be comonotonic if there exist a real random variable X (the common risk factor) and non-decreasing functions f_a and f_b such that $L_a = f_a(X)$ and $L_b = f_b(X)$.

A risk measure ρ is **comonotonically additive** if for any comonotonic random variables L_a and L_b it holds that $\rho(L_a + L_b) = \rho(L_a) + \rho(L_b)$.

According to Embrechts *et al* (2002), comonotonicity may be considered the strongest possible dependence of random variables. Thus, if a risk measure is both subadditivity and comonotonically additive, then on one hand it rewards diversification (via subadditivity) but on the other hand does not attribute any diversification benefits to

comonotonic risks (via additivity) (Emmer *et al*, 2015). Risk measures that depend only on the distributions of losses are of special interest because they are estimated from loss observations only i.e. no additional information is needed.

Definition 4.3: A risk measure ρ is **law-invariant** if

$$P(L_a \leq k) = P(L_b \leq k), k \in \mathbb{R} \Rightarrow \rho(L_a) = \rho(L_b).$$

Refer to a paper by Artzner *et al* (1999) and Emmer *et al* (2015) for further details on other properties of risk measures such as elicibility and robustness.

Value-at-Risk

VaR has become a benchmark for evaluating market risks. There are two main approaches to calculating VaR for financial data series; the parametric method and the non-parametric method (Brooks and Persaud, 2000). In this study, we estimate VaR using the proposed distributions (parametric approach for GLD, PIVD, SD, GHDS and semi-parametric approaches for GPD and GEVD).

For a random variable X (usually for modelling the return distribution of some risky financial portfolio) with distribution function F over a specified time period, the VaR (for a given probability p) can be defined as the p -th quantile of F , i.e.

$$\text{VaR}_p = F^{-1}(1 - p), \quad (4.1)$$

where F^{-1} is the quantile function.

VaR sometimes is defined for log-returns of the original series. If $r_t = \ln(P_{t+h}/P_t)$, $t = 1, 2, \dots, n$ are log returns for some h with the marginal cumulative density function F , then VaR can be defined by equation 4.1. If α_h and σ_h denote the mean and standard deviation of the log returns, respectively, then we can write

$$VaR_p = \alpha_h + F^{-1}(1-p)\sigma_h, \quad (4.2)$$

where F^{-1} , the quantile function, denotes the standard form of the log return distribution.

Properties of VaR_p

Pflug (2000) and Jadhav and Ramanathan (2009) established several ordering properties of VaR. Given random variables X , X_1 , X_2 and a constant k some of the ordering properties are:

- VaR_p is translation equivariant, that is $VaR_p(X + k) = VaR_p(X) + k$.
- VaR_p is positively homogeneous, that is $VaR_p(kX) = kVaR_p(X)$ for $k > 0$.
- $VaR_p(X) = -VaR_{1-p}(-X)$.
- VaR_p is monotonic with respect to stochastic dominance of order 1, that is $X_1 \leq X_2 \Rightarrow VaR_p(X_1) \leq VaR_p(X_2)$.
- VaR_p is comonotonic additive, that is if X_1 and X_2 are comonotone then $VaR_p(X_1 + X_2) = VaR_p(X_1) + VaR_p(X_2)$.
- If $X \geq 0$ then $VaR_p(X) \geq 0$.
- VaR_p is monotonic, that is if $X_1 \geq X_2$, then $VaR_p(X_1) \geq VaR_p(X_2)$.

Application of VaR

Application of VaR can be classified as

- **Controlling risk-** setting position limits for traders and business units so they can compare diverse market risky activity.
- **Information reporting-** it measures aggregate risk and corporation risk in a non-technical way of understanding.
- **Managing risk-** reallocating of capital across traders, products, business units and whole institutions.

Other applications of VaR include estimating equity market, foreign exchange rates, measurement of stock index futures market risk and risk management.

Expected Shortfall

Although VaR is often considered as an adequate risk measure, it does not capture all aspects of market risks, such as subadditivity. Hence, Artzner *et al.* (1999) proposed Expected shortfall (ES) or conditional VaR as a better measure of risk, which is sub-additive and also informs one about the likely magnitude of exceedances. ES gives the expected size of return that exceed VaR, i.e., for a probability level p ,

$$ES_p = E(X|X > \text{VaR}_p) \quad (4.3)$$

And, equivalently,

$$ES_p = \text{VaR}_p + E(X - \text{VaR}_p|X > \text{VaR}_p) \quad (4.4)$$

where the second term above represents the mean of the excess distribution $F_{\text{VaR}_p(x)}$ (treating VaR_p as the threshold).

Properties of Conditional VaR ($CVaR_p$)

$CVaR_p$ exhibits the following properties:

- $CVaR_p$ is translation-equivariant, that is $CVaR_p(X + k) = CVaR_p(X) + k$.

- $CVaR_p$ is positively homogeneous, that is $CVaR_p(kX) = kCVaR_p(X)$ for $k > 0$.
- If X has a density,

$$E(X) = (1 - p)CVaR_p(X) - pCVaR_{(1-p)}(-X).$$

- $CVaR_p$ is convex since, for arbitrary (possible) random variables X_1 and X_2 and $0 < \lambda < 1$, $CVaR_p(\lambda X_1 + (1 - \lambda)X_2) \leq \lambda CVaR_p(X_1) + (1 - \lambda)CVaR_p(X_2)$.
- $CVaR_p$ is monotonic with respect to stochastic dominance of order 2, that is $X_1 \leq X_2 \Rightarrow CVaR_p(X_1) \leq CVaR_p(X_2)$.

A risk measure is coherent if it is translation-invariant, convex, positively homogeneous and monotonic with stochastic dominance of order 1. $CVaR_p$ is coherent in this sense. VaR_p is not coherent, since it is not convex but it is comonotone additive.

Relations between VAR and CVaR

VaR and CVaR measure different properties of the distribution in principle. VaR is a quantile and CVaR is a conditional tail expectation. The two values coincide only if the tail is cut off.

Proposition 1

- $CVaR_p(X) \geq VaR_p(X)$
- $VaR_p(X) = \sup\{v : CVaR_p([X]^v) = v\}$.
- If X is nonnegative, then as $n \rightarrow \infty$,

$$\left[\frac{E(X^n) - (1 - p)CVaR_p(X^n)}{p} \right]^{\frac{1}{n}} \rightarrow VaR_p(X).$$

It is well known that VaR, as a risk measure, has some shortcomings and some authors prefer to use the expected shortfall. Since financial institutions must follow the prescriptions of the Basel accord II and III (Basel Committee on Banking Supervision, 2006, 2011) and these are based on VaR, we will use mainly VaR in this study.

4.3 Backtesting models

Financial risk model evaluation or backtesting is a key part of the internal model's approach to market risk management as laid out by the Basel Committee on Banking Supervision (1996). The accuracy of VaR models in predicting future risks is checked by back testing methods (Nieppola, 2009). According to Halulu (2012) and Nieppola (2009), back testing is a statistical procedure where the actual profits and losses are systematically compared to corresponding VaR estimates.

To examine the adequacy and effectiveness of VaR and ES estimates, we utilise various backtesting procedures. In particular, VaR backtesting is performed using the Kupiec likelihood ratio unconditional coverage test (Kupiec, 1995) and Christoffersen conditional coverage test (Christoffersen, 1998). For ES, we follow the backtesting procedure in McNeil and Frey (2000), implemented for both with and without bootstrapping.

The Kupiec Likelihood test

The Kupiec test exploits the fact that an adequate model ought to have its proportion of violations of VaR estimates close to the corresponding tail probability level. The method consists of calculating the number of times x^p the observed returns fall below (for long positions) or above (for short positions) the VaR estimate at level p , i.e., $r_t < \text{VaR}^p$ or $r_t > \text{VaR}^p$, and compare the corresponding failure rates to p .

The null hypothesis is that the expected proportion of violations is equal to p . Under this null hypothesis, the Kupiec statistic, which is given by

$$LR_{UC} = 2 \ln \left(\left(\frac{x^p}{N} \right)^{x^p} \left(1 - \frac{x^p}{N} \right)^{N-x^p} \right) - 2 \ln (\alpha^{x^p} (1-p)^{N-x^p}) \quad (4.5)$$

is asymptotically distributed according to a chi-square distribution with one degree of freedom where x^p is the number of violations, N is the sample size and α is the pre-specified VaR level.

There are two shortcomings of the Kupiec LR test which are:

- the test is statistically weak with small samples (Dowd, 2002, Nyssanov, 2013).
- the test considers only the frequency of losses and not the time which they occur (Halulu, 2012).

The Christoffersen conditional coverage test

The Christoffersen test extends the Kupiec test and accounts for serial independence of violations (i.e., clustering of extremes). It is a joint test that examines both properties of a good VaR model, the correct failure rate and independence of exceptions, thus conditional coverage (Nieppola, 2009).

The Christoffersen test statistic is given by

$$LR_{CC} = LR_{UC} + 2 \ln \frac{[(1 - \pi_0)^{\varphi_{00}} \pi_0^{\varphi_{01}} (1 - \pi_1)^{\varphi_{10}} \pi_1^{\varphi_{11}}]}{\ln[(1 - \pi)^{(\varphi_{00} + \varphi_{10})} \pi^{(\varphi_{01} + \varphi_{11})}]}, \quad (4.6)$$

where φ_{ij} is defined as the number of returns in state i while they have been in state j previously (state 1 indicates that the VaR estimate is violated and state 0 indicates that it is not) and π_i is defined as the probability of having an exception that is conditional on state i the previous day. This statistic is asymptotically chi-square distributed with two degrees of freedom (Nieppola, 2009, Halulu, 2012). The null hypothesis of equal probabilities π_i is rejected if LR_{CC} value is greater than $\chi_{(2)}^2$. According to Nyssanov (2013), one disadvantage of the Christoffersen test is that it is difficult to find the true cause of the model rejection. It could be either violation cluster or inconsistency of the violation proportion with VaR confidence level from Binomial distribution (Nyssanov, 2013).

Bootstrap t-test

The null hypothesis of the ES backtest is that the excess conditional shortfalls (excess of the actual data series when VaR is violated), are iid and has zero mean. The test is a one sided t-test against the alternative that the excess shortfall has a mean greater than zero, and thus the conditional shortfall is systematically underestimated. The

test statistic is given by

$$T = \frac{\bar{r} - \mu_0}{\bar{\sigma}/\sqrt{m}}, \quad (4.7)$$

where \bar{r} and $\bar{\sigma}$ are the mean and standard deviation of “exceedance residuals” $\{r_1, r_2, \dots, r_m\}$, m is the sample size of the exceedance residuals, μ_0 is the mean of the empirical distribution.

The bootstrap techniques can also be utilised to alleviate any bias with respect to assumptions about the underlying distribution of the excess shortfall. For the bootstrap test, we sample $\tilde{r}_1^*, \tilde{r}_2^*, \dots, \tilde{r}_m^*$ without replacement from the shifted residuals $\tilde{r}_i = r_i - \bar{r} + \mu_0$ and compute the test statistic

$$T_j^* = \frac{\tilde{r}^* - \mu_0}{\bar{\sigma}^*/\sqrt{m}} \quad (4.8)$$

for each bootstrap sample j (McNeil and Frey, 2000).

4.4 Summary

In this chapter we discussed the properties of two risk measures VaR and ES. We also outlined the backtesting methods used in this study. In the next chapter we look at evaluating the risk of precious metal prices with Generalised Extreme Value, Generalised Pareto and Generalised Lambda distributions.

Chapter 5

Evaluating risk in precious metals with Generalised Extreme Value, Generalised Pareto and Generalised Lambda Distributions

5.1 Introduction

Distributions with higher tail probabilities compared to a Normal distribution are called heavy-tailed. Heavy-tailed distributions are important models in finance because the distributions of asset returns and other changes in market prices have heavy tails. Heavy-tailed distribution models are required to accurately model the tail behavior and compute probabilities of extreme returns.

In Chapter 3 it was shown that the empirical distribution of precious metal returns is characterised by excess kurtosis and skewness. In order to capture these properties heavy-tailed and asymmetry distributions are required to overcome the drawbacks of the widely used classical normality of distribution assumption. Risk management tools, such as VaR, are highly dependent on the underlying distributional as-

sumption, with particular focus being placed at the extreme tails. In this chapter, we extend the work of Corlu and Corlu (2015) and Chen and Giles (2014). Specifically, we investigate the performances of the Generalised Extreme Value Distribution (GEVD), the Generalised Pareto Distribution (GPD) and the Generalised Lambda Distribution (GLD) in modelling extreme risks for daily platinum, gold and silver log-returns. Our primary goal is to compare GLD against GPD, and GEVD, in the estimation of Value-at-Risk (VaR) and expected shortfall (ES) as per the international Basel regulatory framework. This is done by utilising graphical analyses (such as excess distribution plots, plot of the tail of underlying distribution and scatter plot of residuals) and various backtesting procedures (i.e., Kupiec test, Christoffersen test and bootstrap test) to draw robust conclusions on the adequacy of GLD, GPD and GEVD models for Value-at-Risk (VaR) and expected shortfall (ES) estimates.

5.2 Extreme Value Theory (EVT)

EVT relates to the asymptotic behaviour of extreme observations of a random variable. It provides the fundamentals for the statistical modelling of rare events and is used to assess tail risk measures (Ren and Giles, 2010). The two fundamental methods for identifying extremes in EVT are the block maxima and the Peak Over Threshold (POT) approaches (Coles, 2001; Gilli and Kellezi, 2006). The first method concentrates on the distribution of block maxima, which can be modelled by GEVD (since GEVD asymptotically describes the limiting behaviour of block maxima) (Coles, 2001). The latter method identifies realised large values over a predefined threshold and describes the behaviour of these exceedances by the GPD. This is based on the fact that, given a large enough threshold, the distribution of these exceedances asymptotically tends toward the GPD.

5.2.1 The Generalised Extreme Value Distribution (GEVD)

The GEVD is a family of continuous probability distributions. It includes the Gumbel, Fréchet and Weibull classes of distributions into a single family to allow a con-

tinuous range of possible shapes. Based on the extreme value theorem, GEVD is the limiting distribution of properly normalised maxima of a sequence of independent and identically distributed (*iid*) random variables (Coles, 2001). Thus, GEVD is used to model the maxima of a long (finite) sequence of random variables. The unified GEVD for modelling block maxima is given by

$$G_{\xi,\mu,\sigma}(x) = \begin{cases} \exp \left\{ - \left[1 + \xi \left(\frac{x - \mu}{\sigma} \right) \right]^{-\frac{1}{\xi}} \right\}, & \text{for } \xi \neq 0, \sigma > 0, 1 + \xi \left(\frac{x - \mu}{\sigma} \right) > 0, \\ \exp \left\{ - \exp \left[- \left(\frac{x - \mu}{\sigma} \right) \right] \right\}, & \text{for } \xi = 0, -\infty < x < \infty. \end{cases} \quad (5.1)$$

The probability density function, obtained as the derivative of the distribution function (5.1), is given by:

$$g_{\xi,\mu,\sigma}(x) = \begin{cases} \frac{1}{\sigma} \left[1 + \xi \left(\frac{x - \mu}{\sigma} \right) \right]^{-1-\frac{1}{\xi}} \exp \left\{ - \left[1 + \xi \left(\frac{x - \mu}{\sigma} \right) \right]^{-\frac{1}{\xi}} \right\}, & \xi \neq 0 \\ \frac{1}{\sigma} \exp \left[- \left(\frac{x - \mu}{\sigma} \right) \right] \exp \left\{ \exp \left[- \left(\frac{x - \mu}{\sigma} \right) \right] \right\}, & \xi = 0, \end{cases} \quad (5.2)$$

where μ and σ are the location and scale parameters, respectively. The shape parameter ξ is also known as the extreme value index (EVI). ξ^{-1} is the rate of tail decay of the GEVD distribution. If $\xi > 0$, G belongs to the heavy-tailed Fréchet class of distributions such as the Pareto, Cauchy, Student- t and mixture distributions. If $\xi < 0$, G belongs to the short-tailed Weibull class of distributions such as uniform and beta distributions. If $\xi = 0$, then G belongs to the light-tailed Gumbell class of distributions and includes distributions such as Normal, Exponential, Gamma and Lognormal distributions (Bali, 2003).

Block maxima

The block maxima method is an EVT approach for identifying extremes in a data set and for describing their asymptotic behaviour. It consists of fitting GEVD to a particular set of block maxima chosen in a given sample of data. This method may be summarised as follows.

Given a sample X_1, X_2, \dots, X_N of iid data points drawn from an unknown distribution F :

- (a) We divide the sample into m non-overlapping subsamples of n observations each (n -blocks), for given integers m and n ($0 < m, n < N$), and denote $M_{n,j}$ as the maximum of the j^{th} subsample:
- (b) Assuming that F belongs to the maximum domain of attraction of $G_{\xi, \mu, \sigma}$ for some $\xi, \mu, \sigma \in \mathbb{R}$, with $\sigma > 0$, we fit GEVD to the sequence of block maxima $M_{n,1}, \dots, M_{n,m}$, to determine the parameter estimates $\hat{\xi}$, $\hat{\mu}$ and $\hat{\sigma}$ (by, for example, using Maximum likelihood estimation (MLE)).

Analogous results and methods can be employed to study the asymptotic distribution of minima, taking into account the relation $\min\{X_1, \dots, X_n\} = -\max\{-X_1, \dots, -X_n\}$. In the context of this study, we use block sizes of 5, 10 and 21, corresponding to weekly, fortnightly and monthly maxima. For daily returns, block size 5 and 21 correspond approximately to the number of trading days in a week and in a month, respectively.

Maximum likelihood estimation for GEVD

Under the assumption that X_1, \dots, X_m are independent variables having the GEVD, the log-likelihood for the GEVD parameters, when $\xi \neq 0$ is

$$\ell(\mu, \sigma, \xi) = -m \ln \sigma - \left(1 + \frac{1}{\xi}\right) \sum_{i=1}^m \ln \left[1 + \xi \left(\frac{x^{(i)} - \mu}{\sigma}\right)\right] - \sum_{i=1}^m \ln \left[1 + \xi \left(\frac{x^{(i)} - \mu}{\sigma}\right)\right]^{-1/\xi}, \quad (5.3)$$

provided that $1 + \xi \left(\frac{x^{(i)} - \mu}{\sigma}\right) > 0$ for $i = 1, \dots, m$.

For parameter combinations in which the above condition is violated, i.e. a configuration for which at least one of the observed data points falls beyond an end-point of the distribution, the likelihood is zero and the log-likelihood equals $-\infty$. The case $\xi = 0$ requires separate treatment using the Gumbel limit of GEVD. This leads to the log-likelihood

$$\ell(\mu, \sigma) = -m \ln \sigma - \sum_{i=1}^m \left(\frac{x^{(i)} - \mu}{\sigma}\right) - \sum_{i=1}^m \exp \left\{ - \left(\frac{x^{(i)} - \mu}{\sigma}\right) \right\}. \quad (5.4)$$

Maximization of equations 5.3 and 5.4, with respect to the parameter vector (μ, σ, ξ) , leads to the maximum likelihood estimates for the entire GEVD family (Coles, 2001). MLE offers the advantage of simultaneous estimation of the three parameters.

Model checking for GEVD

After estimating the GEVD parameters, one can check the goodness-of-fit of the model by utilising residual plots, where the residuals are defined as

$$res = \begin{cases} \left(1 + \frac{\xi}{\sigma}(x - \mu)\right)^{-1/\xi} & \text{if } \xi \neq 0 \\ \exp\left[-\exp\left(-\frac{x - \mu}{\sigma}\right)\right] & \text{if } \xi = 0. \end{cases} \quad (5.5)$$

The data points are converted to unit exponentially distributed residuals under the null hypothesis that GEVD provides a good depiction of the data set.

5.2.2 The Generalised Pareto Distribution (GPD)

The two-parameter GPD (with scale parameter β and shape parameter ξ) has the following representation (Tsay, 2013):

$$G_{\xi, \beta}(x) = \begin{cases} 1 - \left(1 + \frac{\xi x}{\beta}\right)^{-1/\xi} & \text{if } \xi \neq 0 \\ 1 - e^{-\left(\frac{x}{\beta}\right)} & \text{if } \xi = 0, \end{cases} \quad (5.6)$$

where $x > 0$ when $\xi \geq 0$, $0 \leq x \leq -\beta/\xi$ when $\xi < 0$, and $\beta > 0$.

Excess Distribution

For a random variable X , the excess distribution function F_u above a certain threshold u is defined as

$$F_u(x) = P(X - u \leq x | X > u), \quad (5.7)$$

where x represents the size of exceedances over u . Furthermore, if we denote F as the distribution function of X , then we can write

$$F_u(x) = \frac{F(x+u) - F(u)}{1 - F(u)}, \quad (5.8)$$

A fundamental theorem in EVT by Balkema and de Haan (1974) and Pickands (1975) identifies the asymptotic behaviour of these exceedances with GPD. Hence, the excess distribution function F_u can be well approximated by the GPD for large enough u .

Peaks-Over-Threshold (POT)

To fit GPD to a data set, we adopt the POT method that focuses on the distribution of exceedances above some high threshold u . For $x - u \geq 0$, we can rewrite the excess distribution function 5.8 as

$$F_u(x - u) = \frac{F(x) - F(u)}{1 - F(u)}, \quad (5.9)$$

and, hence, deduce the following reverse expression

$$F(x) = (1 - F(u))F_u(x - u) + F(u) \quad (5.10)$$

which allows us to apply the POT method.

There are two steps in applying the POT method. Firstly, we need to choose an appropriate threshold. Secondly, we need to fit the GPD function to the data set. Given the choice of a sufficiently high threshold, we may estimate $F(u)$ by $(1 - N_u/n)$, where n is the total sample size and N_u is the amount of observations above the chosen threshold. $F_u(x - u)$ can be estimated by a GPD using Maximum likelihood estimation (Embrechts *et al.*, 1997). We then obtain the following tail estimator (Ren and Giles, 2010),

$$F(x) = 1 - \frac{N_u}{n} \left(1 + \frac{\xi}{\beta}(x - u) \right)^{-\frac{1}{\xi}}. \quad (5.11)$$

Threshold Selection

In this paper, we utilise the empirical mean excess plot for threshold selections. For a random variable X , the mean excess function is defined as

$$e(u) = E(X - u | X > u) \quad (5.12)$$

i.e., the mean of exceedances over a threshold u . If the underlying distribution of $X > u$ follows a GPD, then the corresponding mean excess is

$$e(u) = \frac{\beta + \xi u}{1 - \xi}, \quad \beta + \xi u > 0, \quad (5.13)$$

provided that $\xi < 1$.

From equation 5.13, we can clearly see that the mean excess function must be linear in u . More precisely, $X > u$ follows a GPD if and only if the mean excess function is linear in u (Coles, 2001). This gives us a way of selecting an appropriate threshold.

Given the data set, we define the empirical mean excess function as

$$e_n(u) = \frac{\sum_i^n (X_i - u) I_{\{X_i > u\}}}{\sum_i^n I_{\{X_i > u\}}}, \quad (5.14)$$

where n is the sample size and $I_{\{X_i > u\}}$ is the indicator variable on the event $\{X_i > u\}$ which is defined as

$$I_{\{X_i > u\}} = \begin{cases} 1, & \text{if } X_i > u \\ 0, & \text{otherwise.} \end{cases} \quad (5.15)$$

The empirical excess plot is a graphical representation of the locus of $(u, e_n(u))$ and we can examine this plot to choose the threshold u such that $e_n(u)$ is approximately linear for $X > u$.

Parameter Estimation

There are various techniques for estimating the parameters of the GPD, such as Maximum likelihood estimation (MLE), method of moments and the method of probability-weighted moments. We adopt the MLE method in this study because the Maximum likelihood estimator is asymptotically normal and allows simple approximations for standard errors and confidence intervals (Azzalini, 1996).

Given that we have a sufficiently high threshold u and, assuming there are m observations with $x_i - u \geq 0$, the subsample $x_1 - u, \dots, x_m - u$ has an underlying distribution of GPD, where $x_i - u \geq 0$ for $\xi \geq 0$, $0 \leq x_i - u \leq -\beta/\xi$ for $\xi < 0$,

then the logarithm of the probability density function of x_i can be derived from equation 5.6 as

$$\ln f(x_i - u) = \begin{cases} -\ln(\beta) - \frac{1 + \xi}{\xi} \ln \left(1 + \xi \left(\frac{x_i - u}{\beta} \right) \right) & \text{for } \xi \neq 0 \\ -\ln(\beta) - \frac{1}{\beta}(x_i - u) & \text{for } \xi = 0. \end{cases} \quad (5.16)$$

Hence, the log-likelihood function $L(\xi, \beta | x_i - u)$ for the GPD is the logarithm of the joint density of the m observations, i.e.,

$$L(\xi, \beta | x_i - u) = \begin{cases} -n \ln(\beta) - \frac{1 + \xi}{\xi} \sum_{i=1}^m \ln \left(1 + \xi \left(\frac{x_i - u}{\beta} \right) \right) & \text{for } \xi \neq 0 \\ -n \ln(\beta) - \frac{1}{\beta} \sum_{i=1}^m (x_i - u) & \text{for } \xi = 0. \end{cases} \quad (5.17)$$

Therefore, we obtain the estimates for ξ and β by maximizing the log-likelihood function of the subsample under a suitable threshold u .

Model Validation

We can use quantile plots to assess the adequacy of a fitted generalised Pareto model (Coles, 2001). With a chosen threshold u , the ordered excesses $x_{(1)} \leq \dots \leq x_{(m)}$ and an estimated model \hat{F} with $\hat{\xi} \neq 0$, the quantile (Q-Q) plot consists of the pairs

$$\left\{ \left(\hat{F}^{-1} \left(\frac{i}{m+1} \right), x_{(i)} \right) ; i = 1, \dots, m \right\}, \quad (5.18)$$

where

$$\hat{F}^{-1}(x) = u + \frac{\beta}{\hat{\xi}} \left[x^{-\hat{\xi}} - 1 \right]. \quad (5.19)$$

If GPD is a reasonable fit for the exceedances above u , then the Q-Q plot should depict points that are approximately linear. Furthermore, we may confirm the goodness-of-fit of GPD by utilising the excess distribution plot and plot of the tail of the underlying distribution (McNeil *et al.*, 2005). For a good fit, the exceedances should lie close to the theoretical curves. Lastly, a scatter plot of residuals should not depict any visible pattern, and should show independence of the exceedances.

5.3 Generalised Lambda Distribution

GLD is a family of distributions that can accommodate a wide range of shapes within one distributional form, including heavy-tailedness and asymmetry. Depending on the values of their shape parameters, GLD will exhibit platykurtic, mesokurtic or leptokurtic behaviour. Most continuous probability distributions are defined in terms of their cumulative distribution function (cdf), $F(x)$, or their probability density functions (pdf), $f(x)$. The Tukey's lambda distribution was first introduced by Hastings *et al.* (1947) and Tukey (1960). The Tukey's lambda distribution has a single parameter and is the simplest example of a distribution specified in terms of its quantile-based functions (van Staden, 2013). According to van Staden (2013), various different generations of the Tukey's lambda distribution proposed in the literature are referred to as Generalised lambda distributions (GLDs).

The two types of GLDs are:

- the Ramberg-Schmeiser type (RS GLD) introduced by Ramberg and Schmeiser (1972, 1974),
- the Freimer-Mudholkar-Kollia-Lin type (FMKL GLD) introduced by Freimer *et al* (1988).

The RS GLD and FMKL GLD have become preferred in theoretical development in statistics and practical applications in other fields of research. (King, 1999, van Staden, 2013).

Tukey's Lambda Distribution

Following Bergevin (1993), we define the Tukey's Lambda Distribution in terms of its quantile function, which is simply the inverse of the cumulative distribution function. The quantile function $Q(u)$, of the Tukey's Lambda Distribution is given by

$$Q(u) = F^{-1}(u) = \frac{u^\lambda - (1-u)^\lambda}{\lambda}, \quad (5.20)$$

for $0 \leq u \leq 1$ and $\lambda \neq 0$, or

$$Q(u) = F^{-1}(u) = \log\left(\frac{u}{1-u}\right), \quad (5.21)$$

for $0 \leq u < 1$ and $\lambda = 0$,

where λ represents the shape parameter.

Equation 5.21 is simply the quantile function of the standard logistic distribution, which is the limiting case of Tukey's lambda distribution, attained for $\lambda = 0$ (van Staden, 2013).

According to van Staden (2013) and King (1999), the Tukey's lambda distribution has:

- unimodal bell-shaped distributions with infinite support for $\lambda \leq 0$ and bounded support for $0 < \lambda < 1$.
- the uniform distribution for both $\lambda = 1$ and $\lambda = 2$.
- U-shaped distributions for $1 < \lambda < 2$.
- unimodal truncated distributions for $\lambda > 2$.

See van Staden (2013) for details on the probability density functions of Tukey's lambda distribution for various values of λ .

Equations 5.20 and 5.21 are the standard form of the Tukey's lambda distribution in the literature. According to van Staden (2013), if location and scale parameters are added it results in the more general form,

$$Q(u) = \begin{cases} \alpha + \frac{\beta}{\lambda} (u^\lambda - (1-u)^\lambda), & \lambda \neq 0 \\ \alpha + \beta \log\left(\frac{u}{1-u}\right), & \lambda = 0 \end{cases} \quad (5.22)$$

Accordingly, the quantile density quantile functions of the Tukey's lambda distribution are then

$$q(u) = \beta \left(u^{\lambda-1} + (1-u)^{\lambda-1} \right)$$

and

$$f(u) = \frac{1}{\beta (u^{\lambda-1} + (1-u)^{\lambda-1})} \quad (5.23)$$

respectively (van Staden, 2013).

Ramberg-Schmeiser Type (RS GLD)

The four-parameter Generalised Lambda distribution was first introduced by Ramberg and Schmeiser (1972, 1974) which was then extended by Ramberg *et al* (1979). The RS GLD is flexible and it produces distributions with different shapes (Unimodal, S-shape, Monotone and U-shape). It is a well-known distribution with scale, location and shape parameters that can take different forms of distributions.

The four-parameter Generalised Lambda distribution (RS GLD) is defined by the following quantile function:

$$Q(u) = \lambda_1 + \frac{u^{\lambda_3} - (1-u)^{\lambda_4}}{\lambda_2}, \quad (5.24)$$

where $0 \leq u \leq 1$, are the probabilities; λ_1 is the location parameter, $\lambda_2 \neq 0$ is the scale parameter, λ_3 and λ_4 are the shape parameters. To obtain a Turkey's Lambda Distribution $\lambda_1 = 0$ and $\lambda_2 = \lambda_3 = \lambda_4 = \lambda$.

The following conditions are imposed on the RS GLD:

$$\text{If } \lambda_2 \rightarrow \infty \text{ then } \lambda_3, \lambda_4 \rightarrow -\infty$$

and,

$$\text{If } \lambda_3, \lambda_4 \rightarrow \infty \text{ then } |\lambda_2| > 0.$$

According to van Staden (2013) the quantile density and density quantile functions of the RS GLD are respectively

$$q(u) = \frac{1}{\lambda_2} \left(\lambda_3 u^{\lambda_3-1} + \lambda_4 (1-u)^{\lambda_4-1} \right) \quad (5.25)$$

and

$$f(x) = \frac{\lambda_2}{\lambda_3 u^{\lambda_3-1} + \lambda_4 (1-u)^{\lambda_4-1}}. \quad (5.26)$$

Properties of the RS GLD

Equation 5.24 is not a proper quantile function for all combinations of values of the shape parameters λ_3 and λ_4 (King and MacGillivray, 1999). It can have finite (bounded), half-finite or infinite support depending on the values of λ_3 and λ_4 . Figure 5.1 which is adapted from Van Staden (2013) and also found in Chalabi (2012) and King and MacGillivray (1999), shows the parameter space of the RS GLD. The parameter space based on the two shape parameters λ_3 and λ_4 is divided into six regions. Ramberg *et al.* (1979) identified Region 1,2,3, and 4. Region 5 and 6 were derived by Karian *et al.*(1996). Table 5.1 adapted from van Staden (2013) and also found in Karian and Dudewicz (2000), shows parameter space and support for different values of the shape parameters λ_3 and λ_4 .

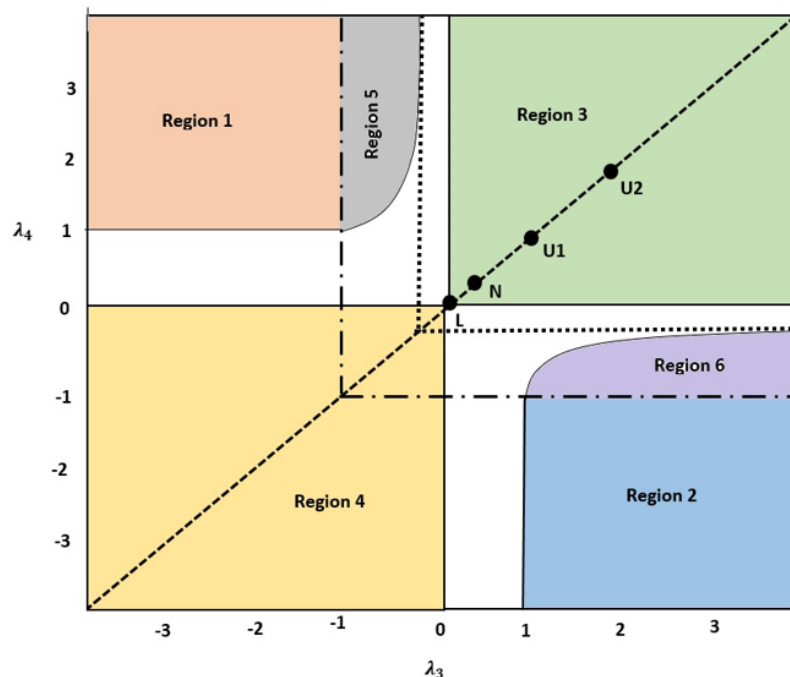


Figure 5.1: The parameter space of the RS GLD in terms of Regions 1,2,3,4,5 and 6 (Adapted from van Staden (2013))

In Figure 5.1 the dotted line at $\lambda_3 = \lambda_4$ represent symmetric distributions. N and L symbolise the approximations of the Normal distribution and logistic distribution by the RS GLD. At $\lambda_3 = \lambda_4 = 1$ and $\lambda_3 = \lambda_4 = 2$, we have uniform distribution denoted by U1 and U2 respectively (van Staden, 2013). For more details on the first four moments and L-moments see van Staden (2013).

Karian and Dudewicz (2000, 2010) performed an in-depth study of the RS GLD. Region 3 of the RS GLD can be divided into sub-regions based on diverse distributional shapes attainable in this region. See van Staden (2013) and King (199) for more details on sub-regions in region 3 of the RS GLD.

Table 5.1: Parameter space and support of the RS GLD distribution in terms of regions 1,2,3,4,5 and 6

Region	Shape parameter values	Support
Region 1	$\lambda_3 < -1, \lambda_4 > 1$	$\left(-\infty, \lambda_1 + \frac{1}{\lambda_2}\right]$
Region 2	$\lambda_3 > 1, \lambda_4 < -1$	$\left[\lambda_1 - \frac{1}{\lambda_2}, \infty\right)$
Region 3	$\lambda_3 = 0, \lambda_4 > 0$	$\left[\lambda_1, \lambda_1 + \frac{1}{\lambda_2}\right]$
	$\lambda_3 > 0, \lambda_4 = 0$	$\left[\lambda_1 - \frac{1}{\lambda_2}, \lambda_1\right]$
	$\lambda_3 > 0, \lambda_4 > 0$	$\left[\lambda_1 - \frac{1}{\lambda_2}, \lambda_1 + \frac{1}{\lambda_2}\right]$
Region 4	$\lambda_3 = 0, \lambda_4 < 0$	$[\lambda_1, \infty)$
	$\lambda_3 < 0, \lambda_4 = 0$	$(-\infty, \lambda_1]$
	$\lambda_3 < 0, \lambda_4 < 0$	$(-\infty, \infty)$
Region 5	$-1 < \lambda_3 < 0, \lambda_4 > 1, a(\lambda_3, \lambda_4) < b(\lambda_3, \lambda_4)$	$\left(-\infty, \lambda_1 + \frac{1}{\lambda_2}\right]$
Region 6	$\lambda_3 > 1, -1 < \lambda_3 < 0, a(\lambda_3, \lambda_4) < b(\lambda_3, \lambda_4)$	$\left[\lambda_1 - \frac{1}{\lambda_2}, \infty\right)$

Source: van Staden (2013)

Note: $a(\lambda_3, \lambda_4) = \frac{(1 - \lambda_i)^{1-\lambda_i} (\lambda_j - 1)^{\lambda_j - 1}}{(\lambda_i - \lambda_j)^{\lambda_i - \lambda_j}}, b(\lambda_3, \lambda_4) = -\frac{\lambda_i}{\lambda_j}$

Source: van Staden (2013)

The Freimer-Muldholar-Kollia-Lin Type (FMKL GLD)

The Freimer-Muldholar-Kollia-Lin Type of the GLD introduced by Freimer *et al.* (1988) denoted by FMKL GLD has a quantile function:

$$Q(u) = \lambda_1 + \frac{1}{\lambda_2} \left(\frac{u^{\lambda_3} - 1}{\lambda_3} - \frac{(1 - u)^{\lambda_4}}{\lambda_4} \right), \quad (5.27)$$

Source: van Staden (2013)

where $0 \leq u \leq 1$; λ_1 is the location parameter, λ_2 is the scale parameter, λ_3 and λ_4 are shape parameters, respectively.

The quantile density and density quantile functions of the FMKL GLD are respectively

$$q(u) = \frac{1}{\lambda_2} \left(u^{\lambda_3 - 1} + (1 - u)^{\lambda_4 - 1} \right)$$

and

$$f(u) = \frac{\lambda_2}{u^{\lambda_3 - 1} + (1 - u)^{\lambda_4 - 1}}$$

Source: van Staden (2013)

For $\lambda_2 > 0$, this Freimer-Mudholkar-Kollia-Lin type of GLD is well defined for all parameter values. Also, for a finite k -th moment of the GLD to exist, we must have $\min(\lambda_3, \lambda_4) > -\frac{1}{k}$.

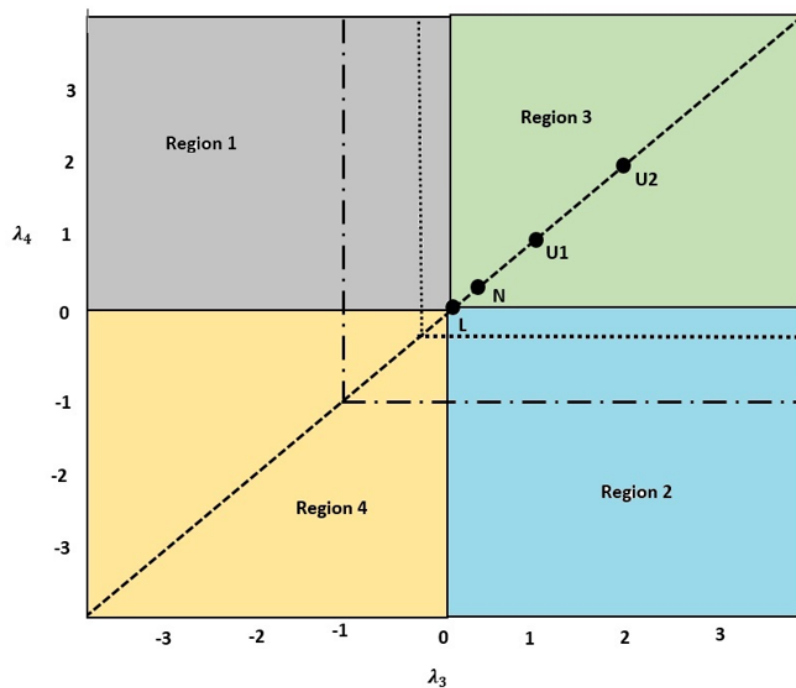
According to Chalabi (2012), and van Staden (2013), the FMKL GLD has three possible type of support namely infinite support, half-infinite and bounded support. Table 5.2 adapted from van Staden(2013) and also found in Chalabi (2012), shows the support obtained by the FMKL GLD for different values of the shape parameters λ_3 and λ_4 . The four regions of the FMKL GLD shown in Table 5.2 are represented graphically in Figure 5.2.

Table 5.2: Parameter space and support of the FMKL GLD distribution in terms of regions 1,2,3, and 4.

Region	Shape parameter values	Support
Region 1	$\lambda_3 \leq 0, \lambda_4 > 0$	$(-\infty, \lambda_1 + \frac{1}{\lambda_2 \lambda_4}]$
Region 2	$\lambda_3 > 0, \lambda_4 \leq 0$	$[\lambda_1 - \frac{1}{\lambda_2 \lambda_3}, \infty)$
Region 3	$\lambda_3 > 0, \lambda_4 > 0$	$[\lambda_1 - \frac{1}{\lambda_2 \lambda_3}, \lambda_1 + \frac{1}{\lambda_2 \lambda_4}]$
Region 4	$\lambda_3 \leq 0, \lambda_4 \leq 0$	$(-\infty, \infty)$

Source: van Staden (2013)

Figure 5.2 displays the parameter space and support region of the FMKL GLD.

**Figure 5.2:** The parameter space of the FMKL GLD in the Regions 1,2,3 and 4. (Adapted from van Staden (2013))

According to Chalabi (2012) the GLD is highly flexible in terms of distributional shape. Freimer *et al.* (1988) classified the shapes return for the FMKL GLD as follows:

- (i) *Class-I family* ($\lambda_3 < 1, \lambda_4 < 1$) represents unimodal distributions with continuous tails. These unimodal members of the FMKL GLD in Class-I are platykurtic leptokurtic or mesokurtic (the approximation of the Normal distribution by the FMKL GLD) (van Staden, 2013).
- (ii) *Class-II family* ($\lambda_3 \geq 1, \lambda_4 \leq 1$) represents monotone decreasing density curves similar to the Exponential distribution. The uniform distribution is obtained when both the shape parameters are equal to one or when one of the shape parameters equals one while the other shape parameter tends to infinity.
- (iii) *Class-III family* ($1 < \lambda_3 \leq 2, 1 < \lambda_4 \leq 2$) represents U-shaped densities with truncated tails. The density curve of the FMKL GLD in Class-III is U-shaped for all pairs of λ_3 and λ_4 . The curve forms a uniform distribution when $(\lambda_3, \lambda_4) = (2, 2)$ (van Staden, 2013).
- (iv) *Class-IV family* ($\lambda_3 > 2, 1 < \lambda_4 < 2$) represents S-shaped pattern of the density curves.
- (v) *Class-V family* ($\lambda_3 \geq 2, \lambda_4 \geq 2, \lambda_3 + \lambda_4 > 4$) represents unimodal truncated density curves.

Two additional classes *Class II'* and *Class IV'* were identified by King (1999). *Class II'* and *Class IV'* contain the reflection of the FMKL GLD from *Class II* and *Class IV* (van Staden, 2013). *Class II'-family* ($\lambda_3 \leq 1, \lambda_4 \geq 1$) represents monotone increasing curves. According to van Staden (2013), the FMKL GLD is negatively skewed in *Class II'*.

Class-IV'-family ($(1 < \lambda_3 < 2, 1 < \lambda_4 > 2)$) represents S-shaped pattern of the density curves. For more information on shape properties of the GLD, see MacGillivray (1982) and van Staden (2013). See King (1999) for picture galleries of probability density functions detailing the behaviour of the FMKL GLD for different values of the shape parameter. The seven classes are listed in Table 5.3 and shown graphically in Figure 5.3.

Table 5.3: Parameter space of the FMKL in terms of Classes I, II, II', III, IV', IV and V.

Class	Shape parameter values
Class I	$\lambda_3 < 1, \lambda_4 < 1$
Class II	$\lambda_3 \geq 1, \lambda_4 \leq 1$
Class II'	$\lambda_3 \leq 1, \lambda_4 \geq 1$
Class III	$1 < \lambda_3 \leq 2, 1 < \lambda_4 \leq 2$
Class IV	$\lambda_3 > 2, 1 < \lambda_4 < 2$
Class IV'	$1 < \lambda_3 < 2, \lambda_4 > 2$
Class V	$\lambda_3 \geq 2, \lambda_4 \geq 2, \lambda_3 + \lambda_4 > 4$

Source: van Staden (2013)

The main difference between parameter spaces of the RS GLD and FMKL GLD is that, the FMKL is a valid distribution for all values of λ_3 and λ_4 unlike the RS GLD. King (1999) gave the quantile functions for the limiting cases of the FMKL GLD. We summarise the limiting distributions of FMKL GLD in Table 5.4.

Table 5.4: Limiting cases of the FMKL GLD

Distribution	Parameter description
Logistic	$\lambda_3 = \lambda_4 = 0$
Exponential	$\lambda_3 \rightarrow \infty$ and $\lambda_4 = 0$
Tukey's lambda	$\lambda_3 = \lambda_4 = \lambda, \lambda_1 = \alpha$ and $\lambda_2 = \frac{1}{\beta}$ (5.21)
Normal	$\lambda_3 = \lambda_4 \approx 0.14$
Uniform	$(\lambda_3, \lambda_4) = (1, 1), (\lambda_3, \lambda_4) = (2, 2), \lambda_3 = 1$ and $\lambda_4 \rightarrow \infty, \lambda_3 \rightarrow \infty$ and $\lambda_4 = 1$

Source: van Staden (2013)

Note: The two pair values $(\lambda_3, \lambda_4) = (1, 1), (\lambda_3, \lambda_4) = (2, 2)$ are similar for RS GLD.

RS GLD and FMKL GLD both reduce to Tukey's lambda when $\lambda_3 = \lambda_4 = \lambda$ (symmetric case). This is the only functional relation between the two distinct types of GLD.

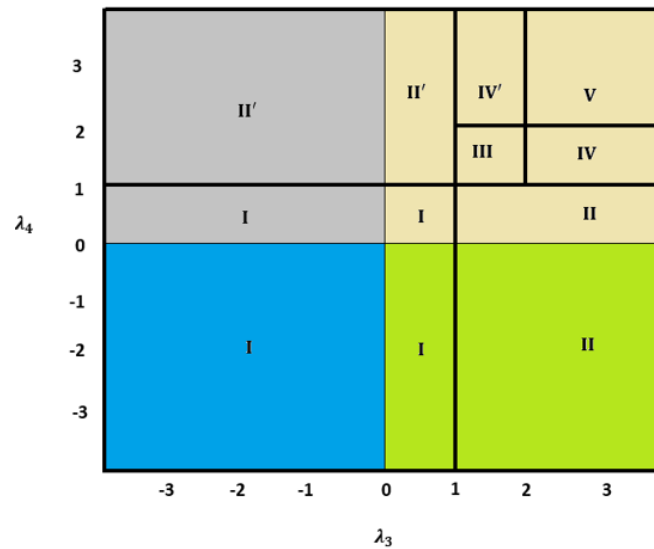


Figure 5.3: The parameter space of the FMKL GLD in terms of Classes I, II, II', III, IV', IV and V. (Adapted from van Staden (2013))

Tail behavior of GLD

The tail behavior plays a major role in modelling stochastic processes (Chalabi, 2012). This is applicable in the case of financial returns which have heavy tail distributions. (Chalabi *et al.* 2012). Certain combinations of the values of the GLD's shape parameters in Region 3 and 4 affect the tails of the GLD. For instance, when $\lambda_3 > 2$ and $\lambda_4 > 2$ in Region 3, a change in the value of λ_4 affects the left tail. In Region 4, for $\lambda_3 < 0$ and $\lambda_4 < 0$, change in values of λ_3 affects the left tail and change in values of λ_4 affects the right tail (van Staden, 2013). See King (1999) and van Staden (2013) for more details on the tail behaviour of GLD.

However, the FMKL GLD is preferable as a result of its ease to use Corlu *et al.* (2016). In this study, we used the FMKL GLD and also the Maximum likelihood estimation method in the GLDEX package of R (Su, 2007).

Parameter Estimation Methods of the FMKL GLD

In the literature, several fitting methods for estimating the parameters of the GLD have been developed. In this study, we discussed the Maximum likelihood estimation method.

Maximum likelihood estimation for the FMKL GLD

Several fitting methods for estimating parameters of the GLD have been proposed due to its flexibility in depicting various distributional shapes (Corlu and Metereliyoz, 2015). In this study we utilise the MLE procedure of Su (2007). The procedure uses the method of moments for the FMKL parameterisation of GLD to find the initial values. These initial values are then used to maximise the numerical log-likelihood to find the parameters of the appropriate GLD.

The algorithm is described below:

- Specify a range of initial values for λ_3, λ_4 and the number of initial values to be selected (λ_3, λ_4 are set by default to a range from -0.25 to 1.5 for the FMKL GLD method of moments (Su, 2007)).
- Evaluate λ_1, λ_2 for each of the initial values of λ_3, λ_4 . Remove all the set initial values that do not: (a) result in a legal parameterisation of GLD (b) span the entire region of the data set.
- Calculate the quantiles μ_i from the initial values. This can be done by solving expression (5.27) numerically.
- Once μ_i is obtained, substitute μ_i into the numerical log-likelihood (5.28). The numerical log-likelihood can be obtained by applying the chain rule to differentiate expression (5.27) to obtain $f(x_i)$ and apply the logarithm on the joint distribution of $f(x_i)$, assuming independence of $f(x_i)$.

$$ML = \sum_{i=1}^n \log \left[\frac{\lambda_2}{\lambda_3 \mu_i^{\lambda_3-1} + \lambda_4 (1 - \mu_i)^{\lambda_4-1}} \right]. \quad (5.28)$$

- The optimal result can be obtained via the Nelder-Mead simplex algorithm, or other suitable numerical optimisation algorithms. It is always desirable to find another set of initial values in the optimisation process to check if the result obtained is a reasonable solution. The final fitting result can be examined using

plots such as a histogram with the fitted line and quantile plot as well as testing the goodness of fit using resample Kolmogorov-Smirnov tests.

5.4 Empirical Results

In this section, we are primarily interested in analysing losses. I.e. negative returns. Results and methods for the GEVD and the GPD can be employed to study the asymptotic distribution of extreme losses, taking into account the relation $\min\{X_1, \dots, X_n\} = -\max\{-X_1, \dots, -X_n\}$. We fitted the GEVD, GPD and the FMKL GLD to each of the three precious metal data sets by using maximum likelihood estimation. The results are presented and discussed in the subsequent sections.

Platinum returns

The block maxima of the negative returns have been fitted to the GEVD with different block sizes (5, 10, and 21). Table 5.5 shows the Maximum likelihood estimates of the parameters with increasing block sizes and their corresponding standard errors.

The shape parameter is positive for all cases. Hence, the extreme negative returns follow a Fréchet family of GEVD for all block sizes considered. The Fréchet type of GEVD confirms that the original series has a negative heavy tail.

Table 5.5: Parameter estimates using GEVD for platinum returns

	No. of Maxima	ξ	SE	σ	SE	μ	SE
GEVD5	1127	0.138586581	0.0181311546	0.007414277	0.0001572313	0.008520950	0.0002394523
GEVD10	564	0.250289053	0.0347814862	0.007295754	0.0002411375	0.012564967	0.0003428281
GEVD21	269	0.22567420	0.0447542623	0.00873558	0.0004230932	0.01772121	0.0005857268

In Figure 5.4, we observe that the residuals are approximately Exponentially distributed, with most points lying on straight lines (recall that the residuals are converted to exponential residuals and the straight line indicates perfectly Exponentially distributed behaviour), indicating that GEVD fits the data set well.

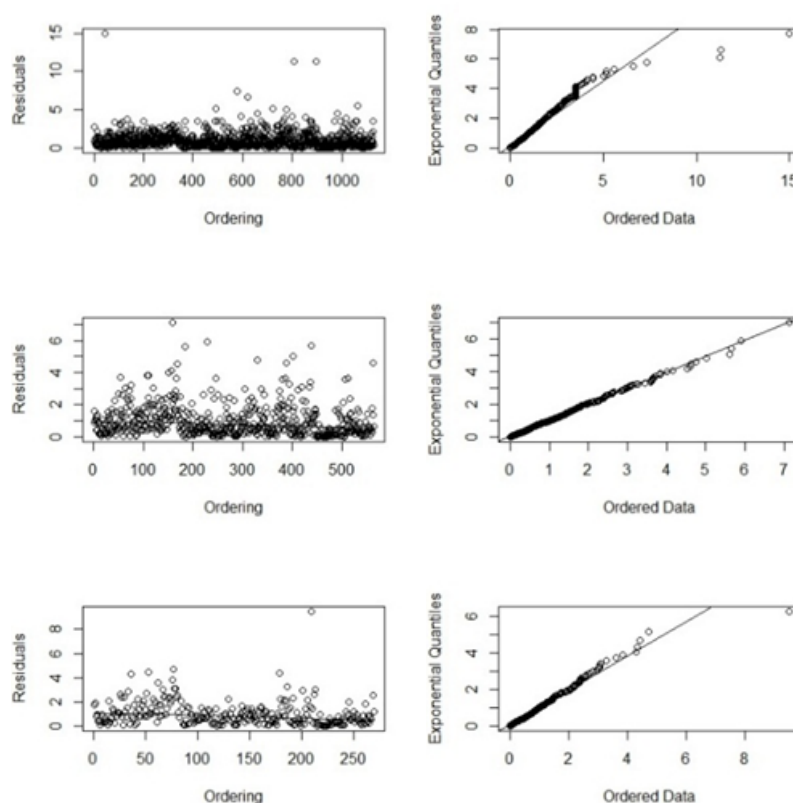


Figure 5.4: Residual and Q-Q plots for negative platinum returns with block size 5, 10 and 21.

The mean excess plots determine a suitable threshold which is necessary for fitting the GPD model. The choice of a threshold should be depicted by linear increases in the excess mean plot. Figure 5.5 presents the mean excess function of negative platinum returns. By observing the mean excess function in Figure 5.5, a threshold of between 0.1% and 2.5% seems to be a reasonable choice.

We selected thresholds at 70th, 80th and 90th percentiles. These provided reasonable choices as they yielded enough data points for analyses and fell within the above range. The GPD parameter estimates for the chosen thresholds are given in Table 5.6.

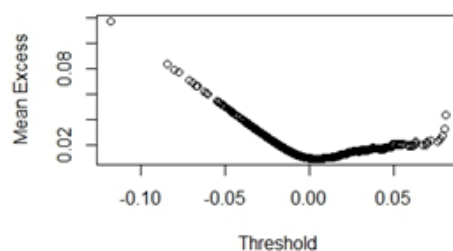


Figure 5.5: Mean excess function of negative platinum returns

Table 5.6: GPD parameter estimates for platinum negative returns

	Threshold	No. of Exceedances	ξ	SE	β	SE
GPD70	0.004662496	1690	0.127558323	0.0249354527	0.008131006	0.0002707504
GPD80	0.008302249	1127	0.185611883	0.0339145722	0.007725041	0.0003314023
GPD90	0.01427866	564	0.266062732	0.054845928	0.007728025	0.000505959

To assess the suitability of the GPD model for our data set, the plot of excess distribution and Q-Q plot of the residuals can be used. Figure 5.6 confirms a good fit of the GPD at all three chosen thresholds. Based on results in Tables 5.7, 5.12 and 5.17, all three precious metals have λ_3 and λ_4 less than 1, i.e., their densities are unimodal with continuous tails, i.e. class-I family of GLD. For all three data sets, the fitted FMKL GLD is leptokurtic with infinite support, since the estimated shape parameters are less than zero. The histogram and Q-Q plots in Figure 5.7 indicate a good fit of FMKL GLD for platinum returns.

Table 5.7: GLD parameter estimates of platinum returns

	λ_1	λ_2	λ_3	λ_4
GLD	-0.00003515827	189.0246	-0.1684266	-0.1938585

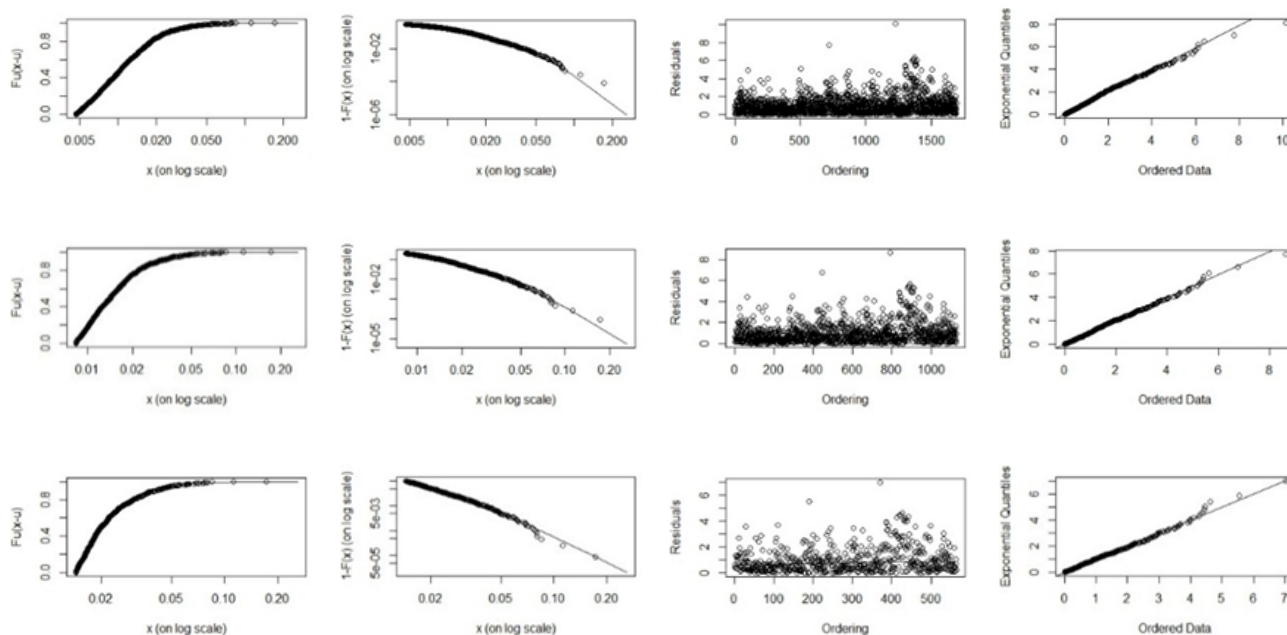


Figure 5.6: Diagnostic plots for negative platinum returns fitted with GPD and a threshold of 0.004662, 0.008302 and 0.014279 respectively.

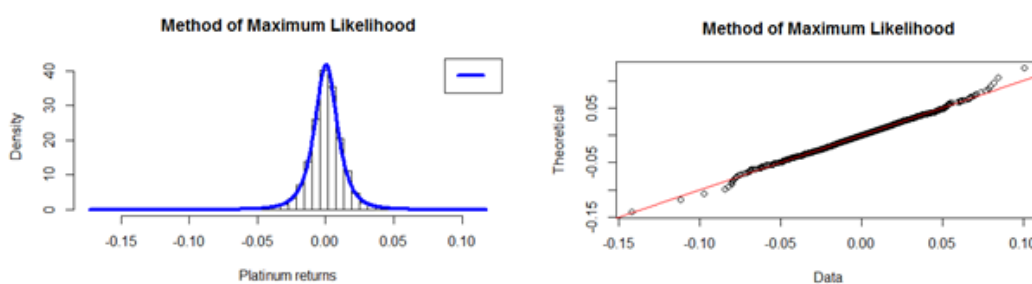


Figure 5.7: Histogram and Q-Q plots for GLD on platinum returns.

Table 5.8: VaR and ES estimates for platinum returns using heavy-tailed distributions

Model	VaR		ES	
	1%	0.1%	1%	0.1%
GEVD5	0.03599667	0.0665049	0.05254638	0.08513325
GEVD10	0.03522065	0.0757051	0.05107759	0.09795668
GEVD21	0.03400134	0.07156585	0.04975126	0.09515629
GPD70	0.03928797	0.07287112	0.05645988	0.09515629
GPD80	0.03926181	0.07796422	0.05645988	0.101456
GPD90	0.03884833	0.08416858	0.05589228	0.1234228
GLD	0.03925881	0.07679914	0.05645988	0.09795668

Table 5.9: VaR and ES Backtesting for platinum returns versus heavy-tailed distributions

Model	No. of violations		Kupiec <i>p</i> -value		Christoffersen <i>p</i> -value		t-test		Bootstrap t-test	
	1%	0.1%	1%	0.1%	1%	0.1%	1%	0.1%	1%	0.1%
GEVD5	74	13	0.0240	0.0081	<0.0001	<0.0001	0.5000	0.5000	0.5547	0.5868
GEVD10	81	7	0.0019	0.5789	<0.0001	0.8498	0.5000	0.5000	0.5303	0.5687
GEVD21	88	8	<0.0001	0.3483	<0.0001	0.6368	0.5000	0.5000	0.5216	0.5602
GPD70	59	8	0.7227	0.3483	<0.0001	0.6368	0.5000	0.5000	0.5318	0.5610
GPD80	59	6	0.7227	0.8783	<0.0001	0.9820	0.5000	0.5000	0.5409	0.5706
GPD90	61	3	0.5372	0.2227	<0.0001	0.4747	0.5000	0.5000	0.5445	0.5368
GLD	59	7	0.7227	0.5789	<0.0001	0.8498	0.5000	0.5000	0.5536	0.5764

Table 5.8 shows VaR and ES estimates for platinum returns using the three heavy-tailed distributions. GPD and GLD give the largest *p*-values at 1% VaR level, GPD gives the highest *p*-values at 0.1% VaR. It is interesting to note that all the distributions were rejected at 1% VaR level using the Christoffersen test. However, at 0.1% all the models were suitable except the GEVD (block size 5) with the best model having been the GPD. With regard to the backtesting of ES, with and without bootstrapping, very suitable ES estimates were obtained for all the three distributions both at 1% and 0.1%.

Gold returns

Parameter estimates of GEVD, GPD and GLD for gold returns were likewise obtained as for platinum returns. The results are presented in Tables 5.10 to 5.12 and Figures 5.8 to 5.11.

Table 5.10: Parameter estimates using GEVD

	No. of Maxima	ξ	SE	σ	SE	μ	SE
GEVD5	1127	0.132949101	0.0191908031	0.005734704	0.0001084900	0.005883060	0.0001839834
GEVD10	564	0.254529125	0.0398705642	0.005818116	0.0001805527	0.008802717	0.0002774462
GEVD21	269	0.178241831	0.0522624337	0.007196091	0.0003462762	0.012848434	0.0005000939

Table 5.11: GPD parameter estimates for negative gold returns.

	Threshold	No. of Exceedances	ξ	SE	β	SE
GPD70	0.002980369	1690	0.121231323	0.0271243494	0.006224234	0.0002103677
GPD80	0.005543627	1127	0.120455789	0.0334280019	0.006556563	0.0002743407
GPD90	0.01029216	564	0.123111999	0.048070092	0.007087633	0.000427269

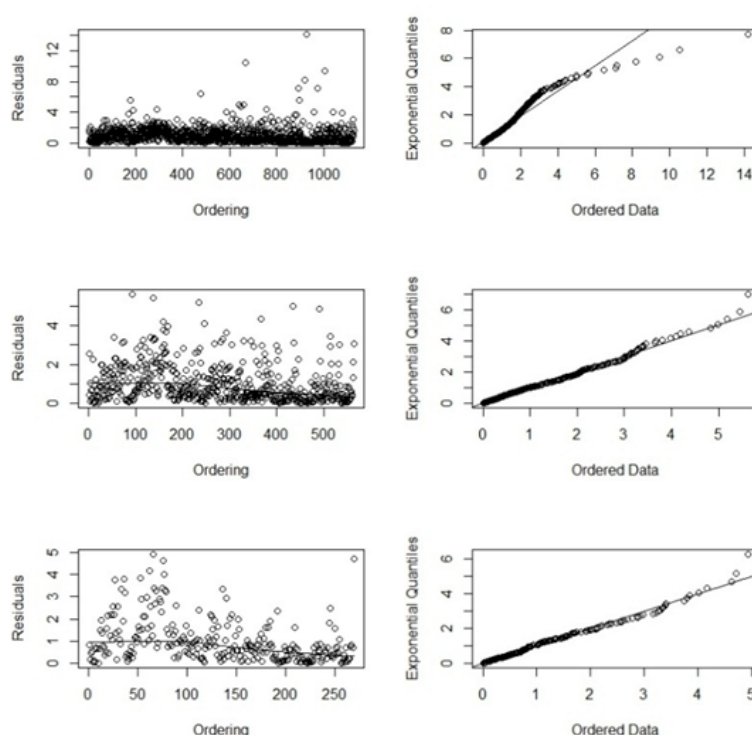
**Figure 5.8:** Residual and Q-Q plots for negative gold returns with block size 5, 10 and 21.

Figure 5.9 presents the mean excess function of negative gold returns. By observing the mean excess function in Figure 5.9, a threshold of between 0.1% and 2% seems to be a reasonable choice for negative platinum returns. Again, we made corresponding selection of threshold as for platinum returns, while conforming to the above range. The GPD parameter estimates for the chosen thresholds are given in Table 5.11.

Table 5.12: GLD parameter estimates of gold returns.

	λ_1	λ_2	λ_3	λ_4
GLD	-0.000267928	301.619722473	-0.258694728	-0.266889288

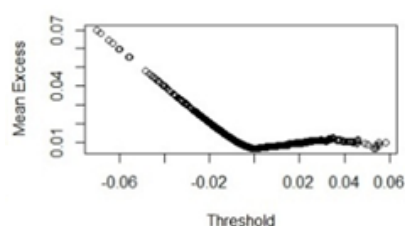


Figure 5.9: Mean excess function of negative gold returns.

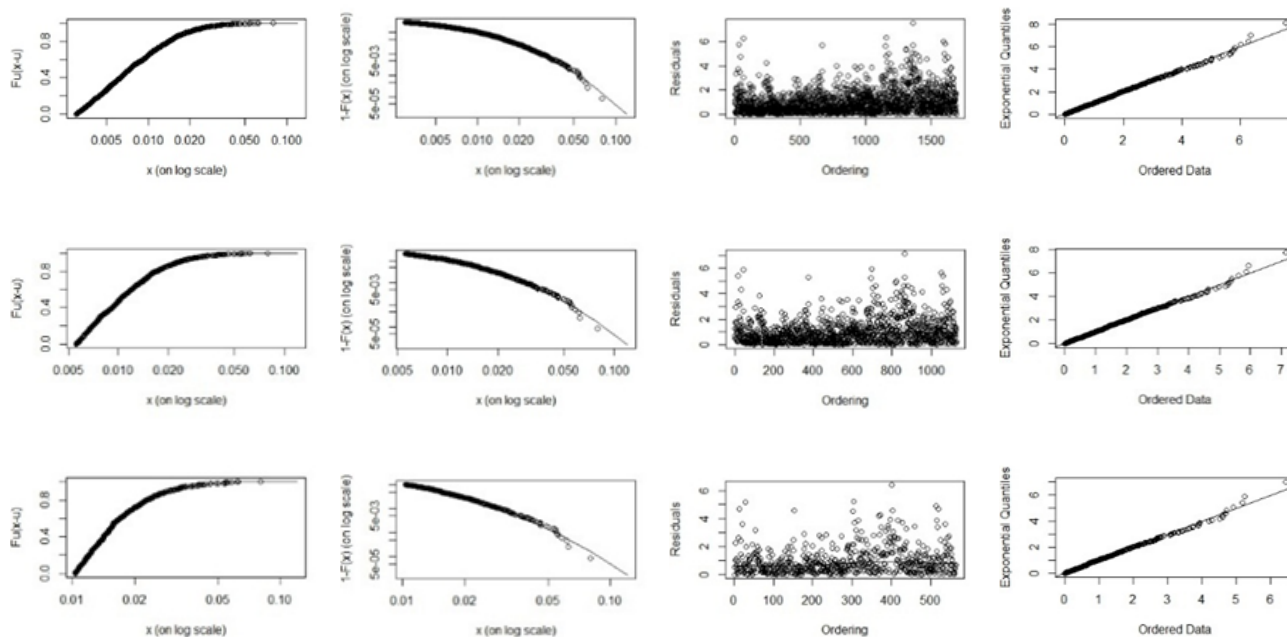


Figure 5.10: Diagnostic plots for negative gold returns fitted with GPD and a threshold of 0.002980, 0.005544 and 0.010292 respectively.

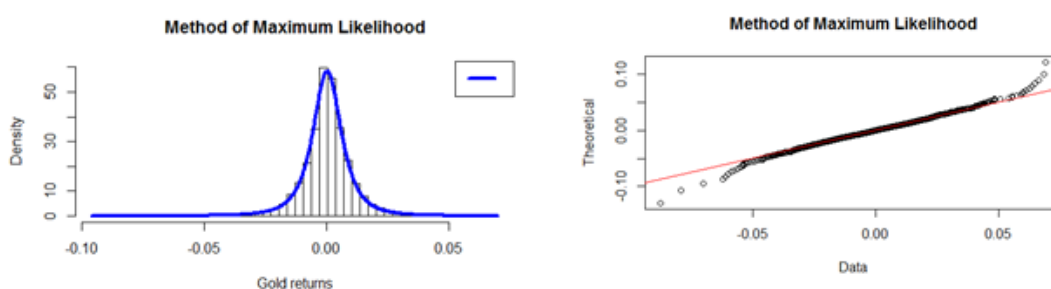


Figure 5.11: Histogram and Q-Q plots for GLD on gold returns.

The model checking plots again indicate good fits for the different models. The only exception is the deviations in GEVD5 and for GLD, suggesting a poor fit on the tails.

Table 5.13 presents the VaR and ES estimates for gold returns using the three heavy-tailed distributions. The GPD, at all the chosen thresholds, is the best model for most of the tests and different VaR levels. In fact, it is the model that stands out in terms of both VaR and ES estimations. Meanwhile, GLD did not perform as well in gold as it did for platinum returns.

Table 5.13: VaR and ES estimates for gold returns using heavy-tailed distributions

Model	VaR		ES	
	1%	0.1%	1%	0.1%
GEVD5	0.02694425	0.04998866	0.03784411	0.05837483
GEVD10	0.03488165	0.07398208	0.04724566	0.07971887
GEVD21	0.04127705	0.07627359	0.0515494	0.07971887
GPD70	0.02918245	0.05415155	0.03988009	0.06829382
GPD80	0.02920024	0.05416033	0.03989458	0.06827302
GPD90	0.02917186	0.05422744	0.03990521	0.06847851
GLD	0.02973696	0.06580758	0.04087007	0.07971887

Table 5.14: VaR and ES Backtesting for gold returns versus heavy-tailed distributions

Model	No. of violations		Kupiec p -value		Christoffersen p -value		t-test		Bootstrap t-test	
	1%	0.1%	1%	0.1%	1%	0.1%	1%	0.1%	1%	0.1%
GEVD5	70	10	0.0778	0.0974	0.0016	0.2486	0.5000	0.5000	0.5108	0.5613
GEVD10	30	1	0.0001	0.0159	0.0005	0.0547	0.5000	0.5000	0.5436	0.5761
GEVD21	20	1	<0.0001	0.0159	<0.0001	0.0547	0.5000	0.5000	0.5350	0.5342
GPD70	58	6	0.8239	0.8783	0.0118	0.9820	0.4993	0.9523	0.5234	0.8915
GPD80	58	6	0.8239	0.8783	0.0118	0.9820	0.5036	0.9518	0.5162	0.8813
GPD90	58	6	0.8239	0.8783	0.0118	0.9820	0.5067	0.9570	0.5228	0.8889
GLD	53	1	0.6524	0.0159	0.0448	0.0547	0.5000	0.5000	0.5272	0.5241

Silver returns

The corresponding results for silver returns are presented in Tables 5.15 to 5.19 and Figures 5.12 to 5.15. Figure 5.12 indicates some tail misfits for GEVD5 while the other two GEVDs seem to provide good general fits. However, this does not necessarily translate into good VaR and ES estimates, as we observed for gold returns.

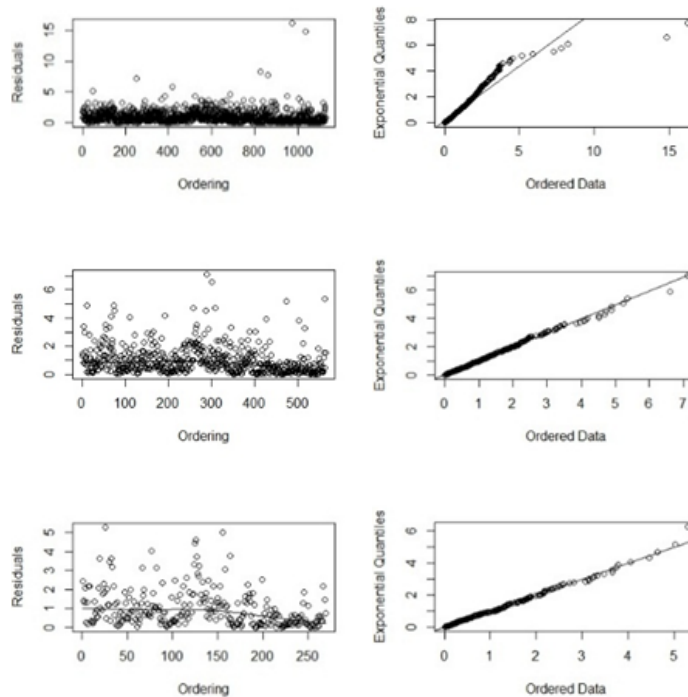
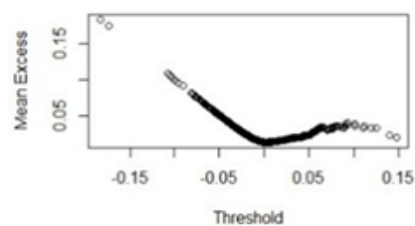
By observing the mean excess function in Figure 5.13, a threshold of between 0.1% and 5% seems to be a reasonable choice for negative silver returns. The GPD parameter estimates for the chosen thresholds are given in Table 5.16. Figure 5.14 illustrates a good fit of the GPD at all the three chosen thresholds.

Table 5.15: Parameter estimates using GEVD for silver returns

	No. of Maxima	ξ	SE	σ	SE	μ	SE
GEVD5	1127	0.14361649	0.0176622739	0.01028936	0.0002348363	0.01216481	0.0003327519
GEVD10	564	0.24768493	0.0343044895	0.01061347	0.0003834909	0.01813485	0.0005023602
GEVD21	269	0.33112549	0.0584081599	0.01162131	0.0006614363	0.02415713	0.0008147953

Table 5.16: GPD parameter estimates for negative silver returns.

	Threshold	No. of Exceedances	ξ	SE	β	SE
GPD70	0.006320252	1690	0.14345273	0.0260461269	0.01135394	0.0003945729
GPD80	0.01127292	1127	0.18153387	0.0340957706	0.01127726	0.0004967514
GPD90	0.01988539	564	0.23889623	0.0535944602	0.01166915	0.0007724233

**Figure 5.12:** Residual and Q-Q plots for negative silver returns with block size 5, 10 and 21.**Figure 5.13:** Mean excess function of negative silver returns.

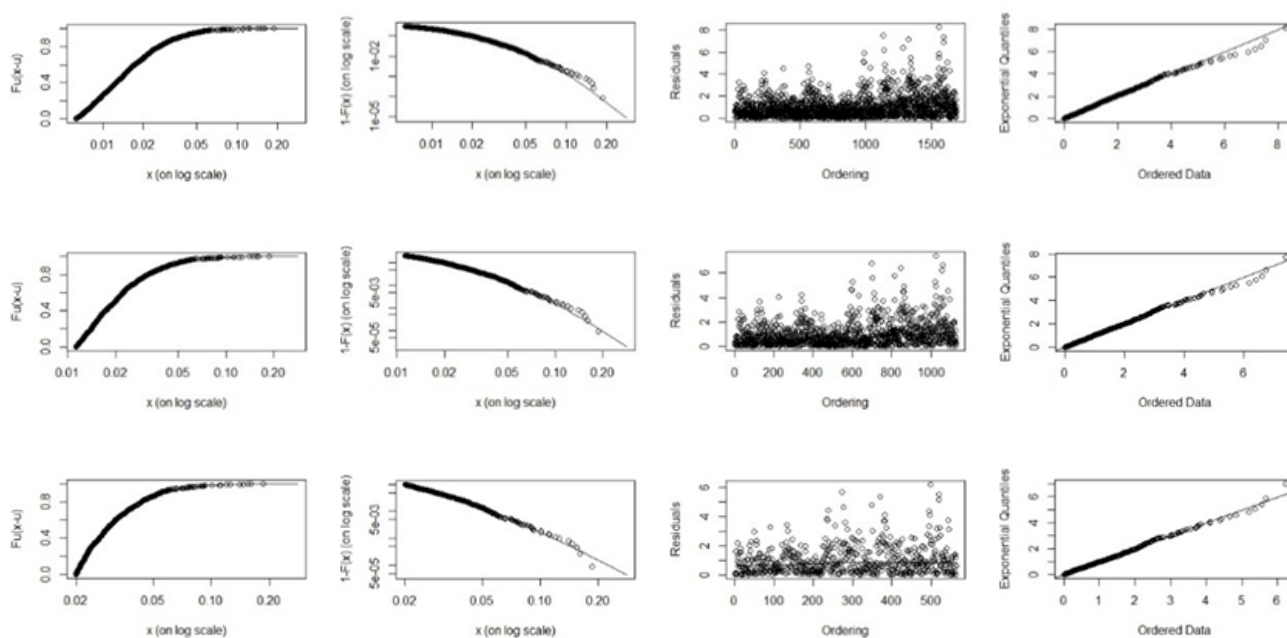


Figure 5.14: Diagnostic plots for negative silver returns fitted with GPD and a threshold of 0.006320, 0.011273 and 0.019885 respectively.

Table 5.17: GLD parameter estimates of silver returns.

	λ_1	λ_2	λ_3	λ_4
GLD	-0.00002282959	141.2906	-0.2018097	-0.214

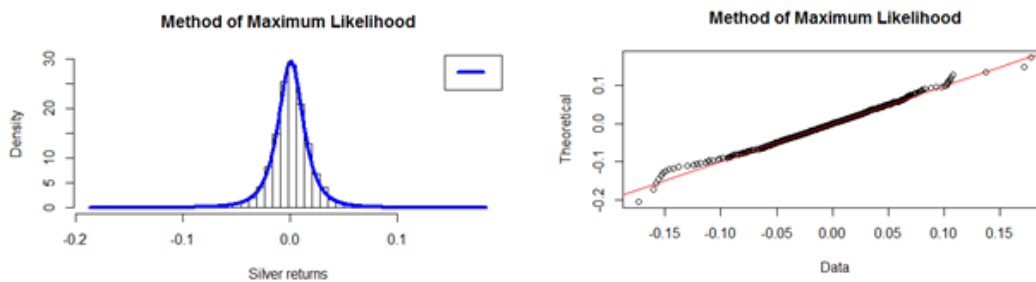


Figure 5.15: Histogram and Q-Q plots for GLD on silver returns.

Figure 5.15 indicates a good fit of GLD for silver returns.

Table 5.18 presents the VaR and ES estimates for silver returns using the three heavy-tailed distributions. For the Kupiec test, GLD provides the largest p-values at 1% VaR level and the GPD (at 90% threshold) gives the highest p-values at 0.1% VaR. It is interesting to note that all the distributions were rejected at 1% VaR level using the Christoffersen test. However, at 0.1% all the models were suitable except the GEVD (block size 5).

As for the backtesting of ES, the results from the test with and without bootstrapping indicate very suitable ES estimates for the three distributions both at 1% and 0.1%. GPD at 90% threshold, however, performs the best at 0.1% level.

Table 5.18: VaR and ES estimates for silver returns using heavy-tailed distributions

Model	VaR		ES	
	1%	0.1%	1%	0.1%
GEVD5	0.05060311	0.09384714	0.07335927	0.1328763
GEVD10	0.05098534	0.1093363	0.07366153	0.1399215
GEVD21	0.04780574	0.1151699	0.07083345	0.1481313
GPD70	0.05609807	0.1065598	0.07769023	0.1366032
GPD80	0.05616838	0.1117015	0.07990462	0.1477549
GPD90	0.05573374	0.1178478	0.08231774	0.1639282
GLD	0.05544103	0.1119322	0.08178319	0.1436126

Table 5.19: VaR and ES Backtesting for silver returns versus heavy-tailed distributions

Model	No. of violations		Kupiec p-value		Christoffersen p-value		t-test		Bootstrap t-test	
	1%	0.1%	1%	0.1%	1%	0.1%	1%	0.1%	1%	0.1%
GEVD5	76	11	0.0124	0.0456	<0.0001	0.0071	0.5000	0.5000	0.5114	0.5169
GEVD10	75	9	0.0173	0.1920	<0.0001	0.0147	0.5000	0.5000	0.5340	0.4987
GEVD21	85	7	0.0003	0.5789	<0.0001	0.0173	0.5000	0.5000	0.5152	0.5240
GPD70	50	9	0.3875	0.1920	0.0002	0.0147	0.0785	0.3480	0.1488	0.3826
GPD80	49	8	0.3154	0.3483	0.0002	0.0173	0.1527	0.6835	0.2301	0.6588
GPD90	52	7	0.5569	0.5789	0.0004	0.0173	0.4561	0.9677	0.4964	0.9158
GLD	54	8	0.7534	0.3483	<0.0001	0.0173	0.5000	0.5000	0.5254	0.5030

5.5 Summary

We have analysed daily log returns of precious metals (platinum, gold and silver) using three distributions namely, GEVD, GPD and GLD. The data sets were for the period 2 April 1994 to 18 September 2014. Our analysis shows that, generally the GPD and the GLD outperform the GEVD for VaR estimation of negative precious metal returns. For gold, GPD stands out as the most suitable model. For platinum, it is between GPD and GLD, especially at 1% level. For silver, GLD is the most suitable at 1% level, whereas GPD is the best model at 0.1%. However, the difference in ES estimation between the three distributions for platinum is minor while GPD stands out for ES estimation at the 0.1% level for both gold and silver.

The purpose of this study was to compare the performance of the two EVT models to a flexible distribution, GLD, for describing daily log returns of precious metals. This study confirms the results by Ren and Giles (2010) that EVT is a reliable method for predicting future potential extreme losses/gains for precious metals. It also shows that GLD competes favourably with EVT for predicting future potential extreme losses/gains for precious metal results, especially for silver and platinum returns. These results do not imply that GPD and GLD will always provide good fits for every financial data set. As further research, we recommend out-of-sample backtests and comparisons with generalised POT models, such as DPOT and PORT and the generalised logistic distribution for block maxima (Nidhin and Chandran, 2013, Balakrishnan, 1992, Johnson *et. al.*, 1995).

5.6 Statistical software packages

The extreme value theory part of the research (GEVD and GPD) was done using the **evd** (Stephenson, 2002, Stephenson and Ferro, 2015), **evir** (Pfaff *et al.*, 2012) and **Ismev** (Heffernan *et al.*, 2012) R packages. We used **laeken** R package (Alfons and Templ, 2013) to estimate suitable threshold and exceedances for GPD. In this study, we used the Maximum likelihood estimation method in the **GLDEX** package of R to

fit FMKL GLD (Su, 2007, 2016). We also used the **gld** (King *et al.*, 2016) R package. For model adequacy, we used the AD test in the **ADGofTest** (Bellosta, 2011) R package. To check for VaR models adequacy, we utilised the Kupiec LR and Christoffesen tests in the **rugarch** R package (Ghalanos, 2015).

5.7 Appendix

VaR and CVaR

GLD is represented with a quantile function (Corlu and Corlu, 2015)

$$\widehat{\text{VaR}}_p = F^{-1}\left(p, \hat{\lambda}_1, \hat{\lambda}_2, \hat{\lambda}_3, \hat{\lambda}_4\right) = \hat{\lambda}_1 + \frac{1}{\hat{\lambda}_2} \left(\frac{p^{\hat{\lambda}_3} - 1}{\hat{\lambda}_3} - \frac{(1-p)^{\hat{\lambda}_4} - 1}{\hat{\lambda}_4} \right). \quad (5.29)$$

We may also use GEVD and GPD to model and approximate this risk measure. For a small upper tail probability p , the GEVD approximation to VaR can be written as

$$\widehat{\text{VaR}}_p = \begin{cases} \hat{\mu} - \frac{\hat{\sigma}}{\hat{\xi}} \left\{ 1 - [-n \ln(1-p)]^{-\hat{\xi}} \right\}, & \hat{\xi} \neq 0 \\ \hat{\mu} - \sigma \ln[-n \ln(1-p)], & \hat{\xi} = 0, \end{cases} \quad (5.30)$$

where n is the length of the subperiod and μ , $\hat{\sigma}$ and $\hat{\xi}$ are the Maximum likelihood estimates of the GEVD parameters, and the GPD approximation to VaR is given by

$$\widehat{\text{VaR}}_p = \begin{cases} u + \frac{\hat{\beta}}{\hat{\xi}} \left\{ \left(\frac{n}{N_u} p \right)^{-\hat{\xi}} - 1 \right\}, & \hat{\xi} \neq 0 \\ u - \hat{\beta} \log \left(\frac{n}{N_u} (1-p) \right), & \hat{\xi} = 0, \end{cases} \quad (5.31)$$

where $\hat{\beta}$ and $\hat{\xi}$ are the estimates of the GPD parameters and N_u is the number of exceedances above the threshold u in a given sample (Tsay, 2013).

Proceeding as before, if the threshold VaR_p is sufficiently large, then $F_{\text{VaR}_p(x)}$ is a

GPD, that is,

$$F_{\text{VaR}_p(x)} = G_{\xi, \beta + \xi(\text{VaR}_p - u)}(x). \quad (5.32)$$

Thus, the mean of the excess distribution $F_{\text{VaR}_p(x)}$ can be calculated as

$$\frac{\beta + \xi(\text{VaR}_p - u)}{1 - \xi}, \quad (5.33)$$

where $\xi < 1$, and substituting into equation 4.4 yields

$$\widehat{ES}_p = \frac{\widehat{\text{VaR}}_p}{1 - \hat{\xi}} + \frac{\hat{\beta} - \hat{\xi}u}{1 - \hat{\xi}}. \quad (5.34)$$

ES for GLD is given by (Corlu and Corlu, 2015)

$$ES(p) = \frac{1}{p} \int_0^p F^{-1}(p, \lambda_1, \lambda_2, \lambda_3, \lambda_4) dy \quad (5.35)$$

$$= \lambda_1 + \frac{1}{p\lambda_2\lambda_3} \left(\frac{p^{\lambda_3+1}}{\lambda_3+1} - p \right) - \frac{1}{p\lambda_2\lambda_4} \left(\frac{1 - (1-p)^{\lambda_4+1}}{\lambda_4+1} - p \right). \quad (5.36)$$

Chapter 6

Evaluating risk in precious metals with Generalised Hyperbolic, Stable and Pearson type-IV Distributions

6.1 Introduction

Various heavy-tailed distributions have been proposed for modelling extreme events. Among them, Generalised Hyperbolic Distributions (GHDs), Stable Distributions (SDs) and the Pearson type-IV Distribution (PIVD) have attractive mathematical properties to be viable alternatives to Normal distributions in trading, optimisation and risk management systems.

Risk management tools such as value-at-risk (VaR) are highly dependent on the underlying distributional assumption. Identifying a distribution that best captures all the aspects of the given financial data may provide advantages to both investors and risk managers. In this chapter, we investigate this possibility by establishing the best generalised hyperbolic distributions to fit precious metal price returns, while

comparisons to Stable distributions are also drawn. There are limited studies with which to compare GHDs to the Stable distribution which is also useful for modelling financial data (Mandelbrot, 1963; Nolan, 2003). Furthermore, Vee *et al* (2012) have suggested that the best models for different financial data may differ. Thus, the primary objective in this study was to examine the performances of GHDs on precious metal price returns and to identify the most appropriate GHD for their respective VaR estimates. Secondly, we contrast these results with estimates from the Stable Distribution, Pearson type-IV Distribution and symmetric and asymmetric Student-t Distributions. The adequacy of these distributions is assessed through the Anderson-Darling test and backtesting of their respective VaR estimates.

6.2 Generalised Hyperbolic Distribution and its Subclasses

GHDs are continuous probability distributions defined as variance-mean mixtures of Generalised Inverse Gaussian Distributions (GIGDs). The class owes its name to the fact that the logarithm of the densities is of the hyperbolic shape, whereas the logarithmic values of the Normal distribution are parabolic. GHDs are five parameter continuous distributions and are useful in modelling a variety of data mainly due to the fact that they cater for asymmetry, heavy and semi-heavy tailed data (Prause, 1999, Aas and Haff, 2006, Eberlein and Keller, 1995).

We follow Prause (1999) for the parameterisation of univariate GHD. Suppose X is a random variable following GHD, then its probability density function (pdf) can be defined as

$$f_{GHD_{full}}(x) = \frac{(\alpha^2 - \beta^2)^{\lambda/2} K_{\lambda-1/2} \left(\alpha \sqrt{\delta^2 + (x - \mu)^2} \right) \exp(\beta(x - \mu))}{\sqrt{2\pi} \alpha^{\lambda-1/2} \delta^\lambda K_\lambda \left(\delta \sqrt{\alpha^2 - \beta^2} \right) \left(\sqrt{\delta^2 + (x - \mu)^2} \right)^{1/2-\lambda}}, \quad x \in \mathbb{R} \quad (6.1)$$

where K_j is the modified Bessel function of the third kind of order j (Abramowitz and Stegun, 1972) and the following conditions apply to the parameters:

$$\delta \geq 0, |\beta| < \alpha, \text{ if } \lambda > 0,$$

$$\begin{aligned} \delta > 0, |\beta| < \alpha, \text{ if } \lambda = 0, \\ \text{and } \delta > 0, |\beta| \leq \alpha, \text{ if } \lambda < 0. \end{aligned} \quad (6.2)$$

In all cases $\mu \in \mathbb{R}$.

The parameters μ and δ determine the location and scale respectively, while α and β control the shape of the density. If $\beta = 0$, the distribution is symmetric. The class of GHDs is closed under affine transformation. Thus, if $X \sim H(\lambda, \alpha, \beta, \delta, \mu)$ and $Y = aX + b$, for some positive a , then we have that:

$$Y \sim H(\lambda, \alpha/a, \beta/a, a\delta, a\mu + b). \quad (6.3)$$

From equation 6.3, we also see that the parameter λ is invariant under affine transformation as a generalised hyperbolic random variable.

The GHD behaves as:

$$f_{GHD_{\text{full}}}(x) \sim \text{const}|x|^{\lambda-1} \exp\{(\mp\alpha + \beta)x\} \quad \text{as } x \rightarrow \pm\infty, \quad (6.4)$$

for all the values of λ . This means that, as long as $\beta \neq \alpha$, the GHD has two semi-heavy tails.

The GHD may be represented as a normal variance-mean mixture with the Generalised Inverse Gaussian (GIG) as a mixing distribution where the GIGD has a density

$$f(z; \lambda, \delta, \gamma) = \left(\frac{\gamma}{\delta}\right)^\lambda \frac{z^{\lambda-1}}{2K_\lambda(\gamma\delta)} \exp\left\{-\frac{1}{2}(\delta^2 z^{-1} + \gamma^2 z)\right\}. \quad (6.5)$$

This means that a generalised hyperbolic variable X can be represented as

$$X = \mu + \beta Z + \sqrt{Z}Y, \quad (6.6)$$

where $Y \sim N(0, 1)$, $Z \sim GIG(\lambda, \delta, \gamma)$ with Z and Y independent.

It follows from equation 6.6 that

$$X|Z = z \sim N(\mu + \beta z, z). \quad (6.7)$$

GHD sub-classes

Sub-classes of the GHDs are obtained via different parameter choices some of which arise as limiting distributions. These special cases used in this study are given below.

The Hyperbolic Distribution (HD)

The Hyperbolic Distribution is a sub-class of GHD when $\lambda = 1$. The hyperbolic distribution is defined as a normal variance-mean mixture where the mixing distribution is the Generalised Inverse Gaussian (GIG) law with parameter $\lambda = 1$; that is, it is conditionally Gaussian. More precisely, a random variable Z has the hyperbolic distribution if

$$(Z|Y) \sim N(\mu + \beta Y, Y), \quad (6.8)$$

where Y is a Generalised Inverse Gaussian $GIG(\lambda = 1, \chi, \psi)$ random variable and $N(m, s^2)$ denotes the Gaussian distribution with mean m and variance s^2 . Relation 6.8 implies that the hyperbolic random variable $Z \sim H(\chi, \psi, \beta, \mu)$ can be represented in the form:

$$Z \sim \mu + \beta Y + \sqrt{Y}N(0, 1), \quad (6.9)$$

with characteristic function

$$\Phi_z(u) = e^{iu\mu} \int_0^\infty e^{i\beta zu - \frac{1}{2}zu^2} dF_Y(z). \quad (6.10)$$

Here, $F_Y(z)$ denotes the distribution function of a Generalised Inverse Gaussian random variable Y with parameter $\lambda = 1$.

Hence, the pdf is given by

$$f_{HD}(x) = \frac{\sqrt{\psi/\chi}}{2\sqrt{\psi + \beta^2}K_1(\sqrt{\psi\chi})} e^{-\sqrt{\psi + \beta^2\chi + (x - \mu)^2} + \beta(x - \mu)}, \quad (6.11)$$

where the normalising constant $K_\lambda(t)$ is a modified Bessel function of the third kind with index λ (here $\lambda = 1$), also known as the MacDonald function (MacDonald, 1899).

If another parameterisation of the Hyperbolic distribution with $\delta = \sqrt{\chi}$ and $\alpha = \sqrt{\psi + \beta^2}$ is used, then the pdf of the hyperbolic $H(\alpha, \beta, \delta, \mu)$ law can be written as

$$f_{HD}(x) = \frac{\sqrt{\alpha^2 - \beta^2}}{2\alpha\delta K_1\left(\delta\sqrt{\alpha^2 - \beta^2}\right)} e^{-\alpha\sqrt{\delta^2 + (x - \mu)^2} + \beta(x - \mu)}, \quad (6.12)$$

where K_1 denotes the Bessel function of the third kind with index 1. The first two of the four parameters, namely α and β with $\alpha > 0$ and $0 \leq |\beta| < \alpha$, determine the shape of the distribution with α representing the gradient and β , the skewness. $\delta > 0$ is a scale parameter and $\mu \in \mathbb{R}$ is a location parameter. The calculation of the pdf is straightforward. However, the cdf has to be numerically integrated from equation 6.12.

With $\xi = \left(1 + \delta\sqrt{\alpha^2 - \beta^2}\right)^{-\frac{1}{2}}$ and $\chi = \xi \frac{\beta}{\alpha}$, one gets a the parameterisation $\text{hyp}(x; \chi, \xi, \mu)$ which has the advantage that ξ and χ are invariant under scale and location transformations. The new invariant shape parameters vary in the triangle $0 \leq |\chi| < \xi < 1$, which was conveniently called the shape triangle by Barndorff-Nielsen *et al.* (1985).

For $\xi \rightarrow 0$, the Normal distribution is obtained as a limiting case; for $\xi \rightarrow 1$, one gets the symmetric and asymmetric Laplace distribution; for $\chi \rightarrow \pm\xi$, it is a Generalised Inverse Gaussian distribution and finally, for $|\chi| \rightarrow 1$, we end up with an Exponential distribution.

The Normal-Inverse Gaussian Distribution (NIGD)

The Normal-Inverse Gaussian Distribution (NIGD) is a subclass of the GHDs with $\lambda = -1/2$. Its pdf is

$$f_{NIGD}(x) = \frac{\alpha\delta}{\pi} e^{\delta\sqrt{\alpha^2 - \beta^2} + \beta(x - \mu)} \frac{K_1\left(\alpha\sqrt{\delta^2 + (x - \mu)^2}\right)}{\sqrt{\delta^2 + (x - \mu)^2}}, \quad (6.13)$$

where $\delta > 0$ and $0 < \beta \leq \alpha$. K_1 denotes the Bessel function of the third kind with index 1.

The tails of NIGD behave as

$$f_{NIGD}(x) \sim \text{const}|x|^{-3/2} \exp(\mp(\alpha + \beta)x) \quad \text{as } x \rightarrow \pm\infty. \quad (6.14)$$

This means that the heaviest tail decays as

$$NIGD(x) \sim \text{const}|x|^{-3/2} \exp(-\alpha x + \beta|x|) \quad \text{when } \begin{cases} \beta < 0 & \text{and } x \rightarrow -\infty, \\ \beta > 0, & \text{and } x \rightarrow +\infty, \end{cases}$$

and the lightest as

$$NIGD(x) \sim \text{const}|x|^{-3/2} \exp(-\alpha x + \beta|x|) \quad \text{when } \begin{cases} \beta < 0 & \text{and } x \rightarrow +\infty, \\ \beta > 0, & \text{and } x \rightarrow -\infty. \end{cases}$$

The two tails of NIGD are semi-heavy and non-identical i.e. behave differently, but are both semi-heavy. This makes the NIGD attractive for financial applications. However, it is only appropriate when the two tails are not too heavy (Aas and Haff, 2006).

The Variance-Gamma Distribution (VGD)

For $\lambda > 0$ and $\delta \rightarrow 0$ in equation 6.1, we obtain the pdf of the variance-gamma distribution (VGD),

$$f_{VGD}(x) = \frac{(\alpha^2 - \beta^2)^\lambda |x - \mu|^{\lambda-1/2} K_{\lambda-1/2}(\alpha|x - \mu|)}{\sqrt{\pi} \Gamma(\lambda) (2\alpha)^{\lambda-1/2}} e^{\beta(x-\mu)}, \quad (6.15)$$

where $K_{\lambda-1/2}$ denotes the Bessel function of the third kind with index $\lambda = -1/2$. The tails of VGD decrease more slowly than that of the Normal distribution, making it a suitable model for phenomena where extreme values are more probable than in the case of the Normal distribution. Returns from financial assets exhibit this phenomenon.

Generalised Hyperbolic Skew Student-t Distribution (GHStD)

Letting $\alpha \rightarrow |\beta|$ in equation 6.1, we obtain the Generalised Hyperbolic skew Student-t Distribution (GHStD)

$$f_{GHStD}(x) = \frac{2^{1/2+\lambda}\delta^{-2\lambda}|\beta|^{1/2-\lambda}K_{1/2-\lambda}\left(\sqrt{\beta^2(\delta^2+(x-\mu)^2)}\right)\exp(\beta(x-\mu))}{\Gamma(-\lambda)\sqrt{\pi}\left(\sqrt{\delta^2+(x-\mu)^2}\right)^{1/2-\lambda}}, \quad (6.16)$$

where $\beta \neq 0$ and $\lambda < 0$.

If $\beta = 0$, we get the non-central (scaled) Student t distribution with -2λ degrees of freedom.

In the tails from equation 6.4, the GHStD density is given by

$$f_{GHStD}(x) \sim \text{const}|x|^{-v/2-1}\exp(-|\beta||x| + \beta x) \quad \text{as } x \rightarrow \pm\infty, \lambda = -v/2.$$

The heaviest tail decays as:

$$f_{GHStD}(x) \sim \text{const}|x|^{-v/2-1} \quad \text{when } \begin{cases} \beta < 0 & \text{and } x \rightarrow -\infty, \\ \beta > 0, & \text{and } x \rightarrow +\infty, \end{cases}$$

and the lightest as

$$f_{GHStD}(x) \sim \text{const}|x|^{-v/2-1} \quad \text{when } \begin{cases} \beta < 0 & \text{and } x \rightarrow +\infty, \\ \beta > 0, & \text{and } x \rightarrow -\infty. \end{cases}$$

Thus, the GHStD has one heavy and one semi-heavy tail. An important property of this distribution is that it has one heavy polynomial tail and one semi-heavy exponential tail. This makes it unique for modelling skewed data with dissimilar tail behaviours which are commonly found in financial returns (Aas and Haff, 2006).

Limiting distributions of GHDs

An important aspect of GHDs is that they cover many special cases such as Normal distribution, Student-t distribution and Cauchy-distribution. The Normal distribution is obtained as a limiting case of the GHD for $\delta \rightarrow \infty$ and $\frac{\delta}{\alpha} \rightarrow \sigma^2$. The Student-t

results from the mixture of Normal and inverse gamma distributions. We have a Student-t as a limit of GHD for $\lambda < 0$ and $\alpha = \beta = \mu = 0$. Cauchy distribution can be obtained from limiting the case of GHDs with $\lambda = -1/2, \alpha = \beta = 0$ and $\delta = 1$. See Barndorff-Nielsen (1978) and Blaesild (1999) for more details. We summarise the limiting distributions of GHDs in Table 6.1.

Table 6.1: Limiting cases of GHDs

Distribution	Parameter Description
Normal(μ, σ^2)	$\delta \rightarrow \infty$ and $\frac{\delta}{\alpha} \rightarrow \sigma^2$.
Student- v	$\lambda < 0$ and $\alpha = \beta = \mu = 0, \lambda = -\frac{v}{2}, \delta = \sqrt{v}$
Cauchy(0,1)	$\lambda = -1/2, \alpha = \beta = 0$ and $\delta = 1$

Maximum likelihood estimation for the GHDs

We utilise the Maximum likelihood estimation (MLE) for parameter estimates of the GHDs.

Assuming the independence of the observations $x_i, i = 1, \dots, n$, we maximise the log-likelihood function

$$L_{GHD}(\lambda, \alpha, \beta, \delta, \mu) = n \log \{a(\lambda, \alpha, \beta, \delta, \mu)\} + \left(\frac{\lambda}{2} - \frac{1}{4}\right) \sum_{i=1}^n \log \{\delta^2 + (x_i - \mu)^2\} + \sum_{i=1}^n \left[\log K_{\lambda - \frac{1}{2}} \left(\alpha \sqrt{\delta^2 + (x_i - \mu)^2} \right) + \beta(x_i - \mu) \right]. \quad (6.17)$$

Taking the first derivatives of the log-likelihood function with respect to the five parameters, we obtain the following expression, in which the log-likelihood function is denoted by L .

$$\frac{d}{d\lambda} L = n \left\{ \frac{1}{2} \ln \left(\frac{\alpha^2 - \beta^2}{\alpha\delta} \right) - \frac{k_\lambda \left(\delta \sqrt{\alpha^2 - \beta^2} \right)}{K_\lambda \left(\delta \sqrt{\alpha^2 - \beta^2} \right)} \right\} + \sum_{i=1}^n \left\{ \frac{1}{2} \ln \{\delta^2 + (x_i - \mu)^2\} + \frac{k_{\lambda - 1/2} \left(\alpha \sqrt{\delta^2 + (x_i - \mu)^2} \right)}{K_{\lambda - 1/2} \left(\alpha \sqrt{\delta^2 + (x_i - \mu)^2} \right)} \right\}, \quad (6.18)$$

$$\begin{aligned} \frac{d}{d\alpha}L &= n \frac{\delta\alpha}{\sqrt{\alpha^2 - \beta^2}} R_\lambda \left(\delta\sqrt{\alpha^2 - \beta^2} \right) \\ &\quad - \sum_{i=1}^n \sqrt{\delta^2 + (x_i - \mu)^2} R_{\lambda-1/2} \left(\alpha\sqrt{\delta^2 + (x_i - \mu)^2} \right), \end{aligned} \quad (6.19)$$

$$\frac{d}{d\beta}L = n \left\{ \frac{\delta\beta}{\sqrt{\alpha^2 - \beta^2}} R_\lambda \left(\delta\sqrt{\alpha^2 - \beta^2} \right) - \mu \right\} + \sum_{i=1}^n x_i, \quad (6.20)$$

$$\begin{aligned} \frac{d}{d\delta}L &= n \left\{ -\frac{2\lambda}{\delta} + \sqrt{\alpha^2 - \beta^2} R_\lambda \left(\delta\sqrt{\alpha^2 - \beta^2} \right) \right\} \\ &\quad + \sum_{i=1}^n \left\{ \frac{(2\lambda - 1)\delta}{\delta^2 + (x_i - \mu)^2} - \frac{\alpha\delta R_\lambda \left(\alpha\sqrt{\delta^2 + (x_i - \mu)^2} \right)}{\sqrt{\delta^2 + (x_i - \mu)^2}} \right\}, \end{aligned} \quad (6.21)$$

$$\begin{aligned} \text{and } \frac{d}{d\mu}L &= -n\beta + \sum_{i=1}^n \frac{x_i - \mu}{\sqrt{\delta^2 + (x_i - \mu)^2}} \\ &\quad \times \left\{ \frac{2\lambda - 1}{\sqrt{\delta^2 + (x_i - \mu)^2}} - \alpha R_{\lambda-1/2} \left(\alpha\sqrt{\delta^2 + (x_i - \mu)^2} \right) \right\}, \end{aligned} \quad (6.22)$$

where

$$\begin{aligned} k_\lambda(x) &= \frac{dK_\lambda(x)}{d\lambda} \\ \text{and } R_\lambda(x) &= \frac{K_{\lambda+1}(x)}{K_\lambda(x)} \end{aligned}$$

Setting the derivatives to zero, we get a complicated system of nonlinear equations. Theoretically, there is a solution to a system with five equations and five unknown parameters. However, in practice, the solution is not easy to obtain. Algorithms without using derivatives are, therefore, utilised to solve the problem of maximizing a function in a five-dimensional space (Prause, 1999).

6.3 Stable Distribution

The Stable Distribution (SD) is a class of probability distributions described by four parameters namely, α an index of stability which is also referred to as the shape

parameter in the literature with $0 < \alpha \leq 2$, β is the skewness parameter with $-1 \leq \beta \leq 1$, $\gamma \geq 0$ the scale parameter, and $\delta \in \mathbb{R}$ a location parameter. These distributions are widely used in practice because they allow for skewness and heavy tails.

The theory of Stable distributions comes from the pioneering work of Levy in the 1930s. Levy (1937) studied the limits arising from normalising sums of independent terms. For this reason, these distributions are sometimes called Levy stable laws.

Definition 6.1 (Nolan, 2003)

- (i) A random variable X is stable if for X_1 and X_2 independent copies of X , and any positive constants a and b ,

$$aX_1 + bX_2 \stackrel{d}{=} cX + d \quad (6.23)$$

for some positive c and some $d \in \mathbb{R}$, where $\stackrel{d}{=}$ denotes equality in distribution.

A random variable X is stable if it satisfies equation 6.23.

- (ii) Any random variable X is symmetrically stable if it is stable and symmetrically distributed around 0, that is $X \stackrel{d}{=} -X$.

- (iii) A random variable X is strictly stable if equation 6.23 holds for $d = 0$.

Three special cases exist which can be expressed in closed-form densities. Stable random variables have probability density functions which are continuous and unimodal but do not have a closed form except for Normal, Cauchy and Levy distributions (Belov, 2005).

Normal Distribution:

$X \sim N(\mu, \sigma^2)$ if it has the probability density

$$f(x) = \frac{1}{\sqrt{2\pi\sigma}} \exp \left[-\frac{(x - \mu)^2}{2\sigma^2} \right], \quad -\infty < x < \infty. \quad (6.24)$$

The Normal distribution is a Stable distribution with parameters $\alpha = 2$, $\beta = 0$, $\gamma = \frac{\sigma}{\sqrt{2}}$, and $\mu = 0$. It is symmetric with finite variance. For Normal distribution all moments exist.

Cauchy Distributions:

$X \sim \text{Cauchy}(\gamma, \delta)$ if it has the density

$$f(x) = \frac{\gamma}{\pi[\gamma^2 + (x - \delta)^2]}, \quad -\infty < x < \infty. \quad (6.25)$$

Cauchy distribution is a Stable distribution with parameters $\alpha = 1$, $\beta = 0$. It is symmetric with infinite variance. For the Cauchy distribution, no moments exist.

Levy Distributions:

$X \sim \text{Levy}(\gamma, \delta)$ if it has the density

$$f(x) = \frac{\sqrt{\gamma}}{\sqrt{2\pi}(x - \delta)^{\frac{3}{2}}} \exp\left[-\frac{\gamma}{2(x - \delta)}\right], \quad \delta < x < \infty. \quad (6.26)$$

Levy distribution is a Stable distribution with parameters $\alpha = 1/2$, $\beta = 1$. It is non-symmetric with infinite variance. Also, for the Levy distribution, no moments exist.

Alternative definitions of stability

Definition 6.2 (Nolan 2014)

Non-degenerate X is stable if and only if $\forall n > 1, \exists$ constants $c_n > 0$ and $d_n \in \mathbb{R}$ such that

$$X_1 + \dots + X_n \stackrel{d}{=} c_n X + d_n, \quad (6.27)$$

where X_1, \dots, X_n are independent and identical copies of X and are strictly stable if and only if $d_n = 0$. Nolan (2014) showed that the only possible choice for the scaling constant is $c_n = n^{1/\alpha}$ for some $\alpha \in (0, 2]$. Equation 6.27 generalises the familiar property of normal random variables: sum of normal terms are normal. Thus, some of the iid stable terms are stable (stability under addition property).

The most accurate way of describing Stable distributions is by a characteristic func-

tion or Fourier transform. For a random variable X with a distribution function $F(x)$, the characteristic function is defined as

$$\phi(t) = E(e^{itX}) = \int_{-\infty}^{\infty} e^{itX} dF(x), \quad (6.28)$$

where the $\phi(t)$ determines the distribution of X and has many mathematical properties, see Nolan (2014).

Definition 6.3 (Nolan 2015)

A random variable X is stable if and only if $X \stackrel{d}{=} aZ + b$, where $0 < \alpha \leq 2$, $-1 \leq \beta \leq 1$, $a \neq 0$, $b \in \mathbb{R}$ and Z is a random variable with characteristic function

$$E(e^{itZ}) = \begin{cases} \exp(-|u|^\alpha [1 - i\beta \tan \frac{\pi\alpha}{2}(\text{sign } t)]), & \alpha \neq 1 \\ \exp(-|u| [1 + i\beta \frac{2}{\pi}(\text{sign } t) \log |t|]), & \alpha = 1 \end{cases}. \quad (6.29)$$

The distributions are symmetric when $\beta = 0$ and $b = 0$. Then, the characteristic function of aZ has the form

$$\phi(t) = e^{-a|t|^\alpha}.$$

In this study, the sign function used in equation 6.29 above is defined as

$$\text{sign } t = \begin{cases} -1 & t < 0 \\ 0 & t = 0 \\ 1 & t > 0. \end{cases}$$

For the $\alpha = 1$ case, $x \log x$ at $x = 0$, is interpreted as $\lim_{x \downarrow 0} x \log x = 0$.

In this thesis, unified notation was used as suggested by Nolan (2015). The notation $S(\alpha, \beta, \gamma, \delta)$ was used to specify a Stable distribution.

The four parameters required to specify stable law are interpreted as:

- α , the tail index or characteristic exponent which describes the power rate at which the tail(s) of the density function decay;

- β , the skewness index which describes how skewed the distribution is. If $\beta > 0$, the distribution is skewed to the right and if $\beta < 0$, the distribution is skewed to the left.
- γ , the scale parameter;
- δ , the location parameter. It denotes the rightward and leftward shift of the distribution. The distribution has a left shift if $\delta < 0$ and conversely, the distribution has a rightward shift if $\delta > 0$.

Parameterisations of Stable distributions

Although many parameterisations can be used to describe the characteristic function of a Stable distribution, it does not have an analytical form in general. Different parameterisations are used in the literature to accommodate different needs of solving problems. While one parameterisation may be better for the analytical properties of the distribution, another may simplify the numerical computations or parameter estimation. There is no one parameterisation that may be best for all the different purposes that might exist. It is thus important to observe what type of parameterisation is used.

Definition 6.4 Nolan's S_0 parameterisation (Nolan, 2015)

A random variable X is $S(\alpha, \beta, \gamma, \delta; 0)$ if

$$X \stackrel{\text{d}}{=} \begin{cases} \gamma (Z - \beta \tan \frac{\pi\alpha}{2}) + \delta, & \alpha \neq 1 \\ \gamma Z + \delta, & \alpha = 1, \end{cases} \quad (6.30)$$

where $Z = Z(\alpha, \beta)$ has a characteristic function 6.29.

In this case, X has a characteristic function

$$E(e^{itX}) = \begin{cases} \exp(-\gamma^\alpha |t|^\alpha [1 + i\beta \tan \frac{\pi\alpha}{2} (\text{sign } t)(|\gamma t|^{1-\alpha} - 1)] + i\delta t), & \alpha \neq 1 \\ \exp(-\gamma |t| [1 + i\beta \frac{2}{\pi} (\text{sign } t) \log(\gamma |t|)] + i\delta t), & \alpha = 1. \end{cases} \quad (6.31)$$

Definition 6.5 Nolan's S_1 parameterisation (Nolan, 2015)

A random variable X is $S(\alpha, \beta, \gamma, \delta; 1)$ if

$$X \stackrel{d}{=} \begin{cases} \gamma Z + \delta, & \alpha \neq 1 \\ \gamma Z + (\delta + \beta \frac{2}{\pi} \gamma \log \gamma), & \alpha = 1, \end{cases} \quad (6.32)$$

where $Z = Z(\alpha, \beta)$ has a characteristic function 6.29. In this case, X has a characteristic function

$$E(e^{itX}) = \begin{cases} \exp(-\gamma^\alpha |t|^\alpha [1 - i\beta (\tan \frac{\pi\alpha}{2}) (\text{sign } t)] + i\delta t), & \alpha \neq 1 \\ \exp\left(-\gamma |t| \left[1 + i\beta \frac{2}{\pi} (\text{sign } t) \log(\gamma |t|)\right] + i\delta t\right), & \alpha = 1. \end{cases} \quad (6.33)$$

Definition 6.6 Zolotarev's A – parameterisation (Zolotarev, 1996)

A random variable X is $S(\alpha, \beta, \gamma, \delta; A)$ if its characteristic function can be represented as follows:

$$E(e^{itX}) = \begin{cases} \exp(\gamma [it\delta - |t|^\alpha + it|t|^{\alpha-1}\beta (\tan \frac{\pi\alpha}{2})]), & \alpha \neq 1 \\ \exp(\gamma [it\delta - |t|^\alpha + i\beta \frac{2}{\pi} t \log |t|]), & \alpha = 1. \end{cases} \quad (6.34)$$

The characteristic function of the stable laws in equation 6.34 is not continuous in the parameters determining the laws. Discontinuities exist at all the points of the form $\alpha = 1$ and $\beta \neq 0$. If we take the limits $\alpha^* \rightarrow 1$ ($\alpha^* \neq 1$), $\beta^* \rightarrow \beta \neq 0$, $\gamma^* \rightarrow \gamma$, and $\delta^* \rightarrow \delta$ it does not yield a stable law with the parameters $\alpha = 1$, β , γ and δ but it does not even yield a proper distribution in the limit.

Definition 6.7 Zolotarev's B – parameterisation (Zolotarev, 1996)

A random variable X is $S(\alpha, \beta, \gamma, \delta; B)$ if its characteristic function can be described as follows:

$$E(e^{itX}) = \begin{cases} \exp(\gamma [it\delta - |t|^\alpha \exp(-i\frac{\pi}{2}\beta K(\alpha)) (\text{sign } t)]), & \alpha \neq 1 \\ \exp(\gamma [it\delta - |t|^\alpha + i\beta \log |t|] (\text{sign } t)), & \alpha = 1, \end{cases} \quad (6.35)$$

where $K(\alpha) = \alpha - 1 + \text{sign}(1 - \alpha)$, and the parameters have the same domain of variation as in the form A.

The B-parameterisation as in A-parameterisation show that stable laws are discontinuous at the point $\alpha = 1$. However, the B-parameterisation has a limit distribution that exists and is a Stable distribution, as $\alpha^* \rightarrow 1_+$, $\beta^* \rightarrow \beta$, $\gamma^* \rightarrow \gamma$, and $\delta^* \rightarrow \delta$, where 1_+ denotes converging to 1 from above.

Definition 6.8 Zolotarev's C– parameterisation (Zolotarev, 1996)

A random variable X is $S(\alpha, \beta, \gamma, \delta; C)$ if its characteristic function can be represented in the form

$$E(e^{itX}) = -\delta|t|^\alpha \exp\left(-i\left(\frac{\pi}{2}\right)\theta_\alpha \text{sign}t\right), \quad (6.36)$$

where the parameters vary within their limits: $0 < \alpha \leq 2$, $|\theta| \leq \theta_\alpha = \min(1, \frac{2}{\alpha} - 1)$.

Definition 6.9 Zolotarev's M– parameterisation (Zolotarev, 1996)

A random variable X is $S(\alpha, \beta, \gamma, \delta; M)$ if its characteristic function can be represented in the form

$$E(e^{itX}) = \begin{cases} \exp\left(\gamma\left[it\delta - |t|^\alpha + it\left(|t|^{\alpha-1} - 1\right)\beta \tan\frac{\pi\alpha}{2}\right]\right), & \alpha \neq 1 \\ \exp\left(\gamma\left[it\delta - |t|^\alpha + i\beta\frac{2}{\pi}t \log|t|\right]\right), & \alpha = 1. \end{cases} \quad (6.37)$$

We should note the similarities between Nolan's S_0 parameterisation and Zolotarev's M –parameterisation, where changes only in γ and δ are made so that they are more compliant with the classical sense of the scale and location parameters. The same relation applies to Nolan's S_1 parameterisation and Zolotarev's A –parameterisation.

In this study, we followed the S_0 parameterisation suggested by Nolan (2014) for numeric and statistical inference and thus advocate the view that a random variable X follows a Stable distribution if its characteristic function is given in equation 6.31.

Stable Parameter Estimation

Nolan (2015) states that many standard parameter estimation procedures fail to work for Stable data since there is a lack of closed-form densities for Stable distribution as discussed earlier.

There are multiple nonstandard techniques for estimating stable parameters, some of which are ingenious. These methods include tail estimators, fractional moments, quantile matching and empirical characteristic functions. In this study, we utilised the numerical Maximum likelihood estimation as summarised in Nolan (2005).

Maximum likelihood estimation

We denote the parameter vector by $\vec{\theta} = (\alpha, \beta, \gamma, \delta)$ and the density function by $f(x|\vec{\theta})$. The parameter space is $\Theta = (0, 2] \times [-1, 1] \times (0, \infty) \times (-\infty, \infty)$. The log-likelihood function for an independent and identically distributed stable sample X_1, \dots, X_n is given by

$$L(\vec{\theta}) = \sum_{i=1}^n \log f(X_i|\vec{\theta}). \quad (6.38)$$

Since there are no closed formulas for general stable densities, there are some difficulties in computing the log likelihood function. The program STABLE (Robust Analysis Inc., 2013) computes stable densities that are reliable for $\alpha > 0.1$ and any β , γ and δ . The McCulloch (1996) quantile method is used initially to approximate the parameters and then a constrained (by the parameter space) quasi-Newton method is used to maximise. DuMouchel (1973) indicated that if $\vec{\theta}_0$ lies in the interior of the parameter space Θ , the Maximum likelihood estimator is consistent and asymptotically Normal with mean $\vec{\theta}_0$ and covariance matrix given by $n^{-1}B$ where $B = (b_{ij})$ is an inverse Fisher information matrix I . Entries in I are given by

$$I_{ij} = \int_{-\infty}^{\infty} \frac{\partial f}{\partial \theta_i} \frac{\partial f}{\partial \theta_j} \partial x. \quad (6.39)$$

The behavior of the estimators is known when $\vec{\theta}$ is near the boundary of the parameter space. The distribution of the estimator gets skewed away from the boundary. When $\alpha = 2$ or $\beta \pm 1$, $\vec{\theta}$ is on the boundary of the parameter space. The Normal distribution for the estimators tends to a degenerate distribution at the boundary point.

6.4 Pearson type-IV Distribution

The Pearson system of the distribution is a generalisation of the differential equation

$$\frac{f'(x)}{f(x)} = \frac{x + a}{b_0 + b_1x + b_2x^2} \quad (6.40)$$

with a solution

$$f(x) = (b_0 + b_1x + b_2x^2)^{-\frac{1}{2}} b_2 \exp \left[\left(\frac{2b_1 - 2ab_2}{\sqrt{4b_0b_2 - b_1^2}} \right) \tan^{-1} \left(\frac{b_1 + 2b_2x}{\sqrt{4b_0b_2 - b_1^2}} \right) \right]. \quad (6.41)$$

Depending on the values of b_i coefficients and $\sqrt{4b_0b_2 - b_1^2}$ in equation 6.40, the Pearson system provides most of the known distributions as shown in Table 6.2 (Stavroyiannis, 2013). If the discriminant of $b_0 + b_1x + b_2x^2$ in equation 6.41 is negative, the roots of the quadratic equation $b_0 + b_1x + b_2x^2$ are complex, i.e. $b_1^2 < 4b_0b_2$, rearranging equation 6.41 resulting in Pearson type-IV distribution given as (Nagahara, 1999; Nagahara, 2007). The Pearson type IV curve is suitable for those distributions which have excess kurtosis and moderate skewness (Bhattacharyya *et al*, 2012).

Table 6.2: Family of distribution for the Pearson System

Distribution	Type
Normal	0
Beta	I
Continuous uniform	II
Gamma, Chi-squared and Exponential	III
Cauchy (or Lorentz, or Breit-Wigner)	IV
Inverse Gamma, Inverse chi-squared	V
F	VI
t-Student	VII
Monotonically decreasing power	VIII

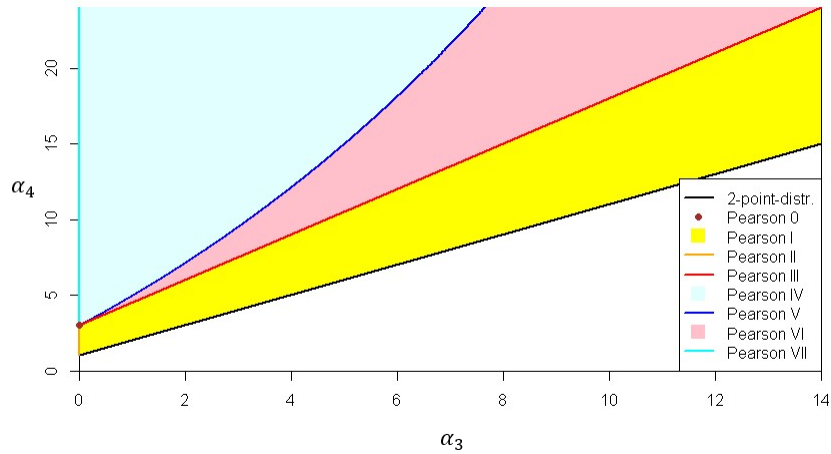
**Figure 6.1:** The Pearson Curve family

Figure 6.1 shows the types of curves to be used for each range of skewness and kurtosis. The x-axis is α_3 for the Pearson's moment coefficient of skewness and the y-axis is α_4 for the Pearson's moment coefficient of kurtosis. The probability density function (pdf) of the Pearson type-IV distribution (PIVD) is given by

$$f_{PIVD}(x) = k \left[1 + \left(\frac{x - \lambda}{a} \right)^2 \right]^{-m} \times \exp \left[-v \tan^{-1} \left(\frac{x - \lambda}{a} \right) \right], \quad (6.42)$$

where $m > \frac{1}{2}$, $v, a > 0$, λ are real valued parameters, $-\infty < x < \infty$ and $k = \frac{[\Gamma(m + \frac{v}{2}i)]^2}{aB(m - \frac{1}{2}, \frac{1}{2})}$ is a normalisation constant that depends on m , v and a .

The pdf of the Pearson type-IV distribution is invariant under simultaneous change (a to $-a$, v to $-v$). We specify $a > 0$ so that the curve is always bell-shaped. λ and a are the location and scale parameters respectively and v is the skewness parameter. When $v > 0$, the PIVD is positively skewed, while it is negatively skewed for $v < 0$. Parameter m controls the tail thickness and can thus be regarded as a kurtosis parameter. If m is decreased, the kurtosis is increased, and for smaller values of m , the tails of Pearson type-IV distribution are much heavier than those of a Gaussian distribution. The Pearson type-IV distribution is essentially an asymmetric version of the Student- t distribution i.e. when $v = 0$ (Nagahara, 2007).

The normalisation constant, k , can be expressed as

$$k = \frac{2^{2m-2} |\Gamma(m - \frac{iv}{2})|^2}{\pi a \Gamma(2m - 1)} = \frac{\Gamma(m)}{\sqrt{\pi} a \Gamma(m - 0.5)} \left| \frac{\Gamma(m - \frac{iv}{2})}{\Gamma(m)} \right|^2, \quad (6.43)$$

where $\Gamma(\cdot)$ is the Gamma function.

Moments of Pearson type-IV distribution

The first four moments in terms of the parameters of the distribution are given below. The mean and variance of Pearson type-IV are given as:

$$\mu = \lambda - \frac{av}{2m - 2}, \quad \text{for } m > 1, \quad (6.44)$$

$$\text{and } \sigma^2 = \frac{a^2}{2m - 3} \left[1 + \frac{v^2}{4(m - 1)^2} \right], \quad \text{for } m > \frac{3}{2}. \quad (6.45)$$

The third and fourth moments are given in equations 6.46 and 6.47 respectively as

$$\alpha_3 = \frac{4a^3 v (r^2 + v^2)}{r^2 (r - 1)(r - 2)}, \quad \text{for } m > 2, \quad (6.46)$$

$$\text{and } \alpha_4 = \frac{3a^3 v (r^2 - v^2) [(r + 6)(r^2 - v^2) - 8r^2]}{r^4 (r - 1)(r - 2)(r - 3)}, \quad \text{for } m > \frac{5}{2} \quad (6.47)$$

where $r = 2(m - 1)$.

The Cumulative density function (cdf) of Pearson type-IV distribution.

The cumulative distribution is defined as

$$F(x) = \int_{-\infty}^x f(t)dt \quad (6.48)$$

Thus, the cdf of Pearson type-IV distribution is given as

$$F(x) = \int_{-\infty}^x k \left(1 + \left(\frac{t-\lambda}{a}\right)^2\right)^{-m} \exp \left[-v \tan^{-1} \left(\frac{t-\lambda}{a}\right)\right] dt. \quad (6.49)$$

According to Heinrich (2004), the cdf of Pearson type-IV distribution that is $F(x)$ in equation 6.49 can be expressed in terms of the hyper-geometric function as

$$F(x) = f(x) \frac{a}{2m-1} \left(i - \frac{x-\lambda}{a}\right) F_1 \left(1, m + \frac{iv}{2}; 2m; \frac{2}{1 - i \left(\frac{x-\lambda}{a}\right)}\right), \quad (6.50)$$

where F_1 is the Gauss hypergeometric function. The cumulative distribution above is needed for the calculation of the constants at the confidence intervals.

Maximum likelihood parameter estimation of the Pearson type-IV distribution

We obtain the parameter estimates of the Pearson type-IV distribution by minimising the negative log likelihood given by

$$-\ln L = m \sum_{i=1}^N \ln \left[1 + \left(\frac{x_i - \lambda}{a}\right)^2\right] + v \sum_{i=1}^N \tan^{-1} \left(\frac{x_i - \lambda}{a}\right) - N \ln k, \quad (6.51)$$

where N is the number of observed data points x_i . The minimising procedure is done numerically.

For more details on the Maximum likelihood estimation (MLE) of the Pearson's family distributions see Johnson *et al.* (1994) and Nagahara (1999). In this study, the Maximum likelihood estimates for the Pearson type-IV distribution were estimated using the R package (PearsonDS).

6.5 The Skewed Student-t Distribution

The SSTD was first introduced by Hansen (1994) as a skewed extension to the Student-t distribution which was used to model financial returns. Since then, there were several proposed extensions of the Student-t distribution for financial and other applications namely, Branco and Dey (2001); Jones and Faddy (2003); Azzalini and Capitanio (2003); Aas and Haff (2006) and Zhu and Galbraith (2010). The SSTD is known as an alternative distribution for modelling skewed and heavy-tailed data as it provides more flexibility and best accommodates long-tailed data than skewed Normal (SN) distributions.

Following the Azzalini and Capitanio (2003) proposition for the multivariate SSTD, we use the transformation

$$X = \xi + V^{-\frac{1}{2}}Z, \quad (6.52)$$

where $Z \sim SN_d(\xi, \Omega, \alpha)$, $\xi = 0$, and $V \sim x_v^2$, where V is independent of Z . An equivalent interpretation of X is to regard it as a scale mixture of SN variates, with mixing scale factor $V^{-\frac{1}{2}}$.

Application of lemma (ii) in Azzalini and Capitanio (2003) to a Gamma $\left(\frac{v}{2}, \frac{v}{2}\right)$ variate and algebra results in the density of X , which is given as

$$f(x; \xi, \Omega, \alpha, v) = \frac{1}{\Omega} t_v \left(\frac{x - \xi}{\Omega} \right) 2 T_{v+1} \left(\alpha \left(\frac{x - \xi}{\Omega} \right) \sqrt{\frac{v+1}{\left(\frac{x - \xi}{\Omega} \right)^2 + v}} \right), \quad (6.53)$$

or,

$$f(x; \xi, \Omega, \alpha, v) = 2 t_v(x) T_{v+1} \left(\alpha^T \omega^{-1} (x - \xi) \left(\frac{v+1}{Q_x + v} \right)^{\frac{1}{2}} \right), \quad (6.54)$$

where for a $d \times d$ covariance matrix $\Omega = (\omega_{rs})$, we define

$$\omega = \text{diag}(\omega_1, \omega_2, \dots, \omega_d) = \text{diag}(\omega_{11}, \omega_{22}, \dots, \omega_{dd})^{\frac{1}{2}}, \quad (6.55)$$

$$Q_x = (x - \xi)^T \Omega^{-1} (x - \xi), \quad (6.56)$$

and

$$t_v(x) = \frac{g_v(Q_x)}{|\Omega|^{\frac{1}{2}}} = \frac{\Gamma\left(\frac{v+1}{2}\right)}{|\Omega|^{\frac{1}{2}}(\pi v)^{\frac{1}{2}}\Gamma\left(\frac{v}{2}\right)} \left(\frac{1+Q_x}{v}\right)^{-\frac{(v+1)}{2}}, \quad (6.57)$$

where

v represents the degrees of freedom and controls the tails of the distribution,

t_v represents the pdf of the standard Student-t distribution with v degrees of freedom, and

T_{v+1} represents the cdf of the standard Student-t distribution with $v + 1$ degrees of freedom.

See Branco and Dey (2001) for more details on the properties of the Skewed Student-t distribution.

Parameter Estimation of the Skewed Student-t Distribution

The Maximum likelihood estimation method

There are several methods that have previously been used to estimate the parameters of the SSTD. However, Azzalini and Capitanio (2003) suggested that the MLE method has a higher chance of being close to the parameters being estimated. For this reason, we have chosen to use the MLE method for the SSTD.

According to Peter (2001), the log-likelihood function of a standardised (zero mean and unit variance) SSTD($x; \xi, \Omega, \alpha, v$) is given by:

$$\begin{aligned} L_{SST} = & \ln \left[\Gamma\left(\frac{v+1}{2}\right) \right] - \ln \left[\Gamma\left(\frac{v}{2}\right) \right] - 0.5 \ln[\pi(v-2)] + \ln \left(\frac{2}{\alpha + \frac{1}{\alpha}} \right) + \ln(s) \\ & - 0.5 \sum_{t=1}^T \left[\ln(\sigma_t^2) + (1+v) \ln \left(1 + \frac{sz_t + m}{v-2} \xi^{-I_t} \right) \right], \end{aligned} \quad (6.58)$$

where ξ is the asymmetry parameter, v is the degrees of freedom of the distribution,

$$I^t = \begin{cases} +1 & \text{if } z_t \geq -\frac{m}{s} \\ -1 & \text{if } z_t < -\frac{m}{s} \end{cases}, \quad (6.59)$$

$$m = \frac{\Gamma\left(\frac{v+1}{2}\right) \sqrt{v-2}}{\sqrt{\pi} \Gamma\left(\frac{v}{2}\right)} \left(\alpha - \frac{1}{\alpha} \right), \quad (6.60)$$

and

$$s = \sqrt{\left(\alpha^2 + \frac{1}{\alpha^2} - 1\right) - m^2}. \quad (6.61)$$

refer to Lambert and Laurent (2001) for more details.

A number of skewed Student-t distributions have been proposed in the literature.

In this study we follow the parametrization used in Azzalini and Capitanio (2003).

A random variable X from the SSTD has a density of the form:

$$f_{SSTD}(x, \delta, v, \mu, \beta) = \frac{1}{\delta} t_v \left(\frac{x - \mu}{\delta} \right) 2 T_{v+1} \left(\beta \left(\frac{x - \mu}{\delta} \right) \sqrt{\frac{v+1}{\left(\frac{x - \mu}{\delta} \right)^2 + v}} \right), \quad (6.62)$$

where,

- μ , δ and β represent the location, scale and shape parameters, respectively.
- t_v represents the density of the standard Student-t distribution with v degrees of freedom.
- T_{v+1} represents the distribution function of the T_{v+1} Student-t distribution with $v + 1$ degrees of freedom.

6.6 Empirical Results

Evaluating risk in precious metals with GHDs, SD, PIVD, STD and SSTD

This section focuses on the parameter estimation and comparison of fits for the subclasses of the GHDs, Stable and Pearson type-IV distributions on precious metal returns. In addition, the Anderson Darling test and Kupiec likelihood test are performed to select an optimal model for the precious metals returns.

We estimate the parameters of the GHDs using the MLE method. Table 6.3 on the next page illustrates the MLE parameter estimates from the gold, platinum and silver returns for different subclasses of the GHDs.

The combined Q-Q plots (Figure 6.2) suggest that all four GHD subclasses fit the gold, platinum and silver returns well on the upper tail. The GH Skew t-distribution provides the best fit for the lower tails for gold, platinum and silver returns.

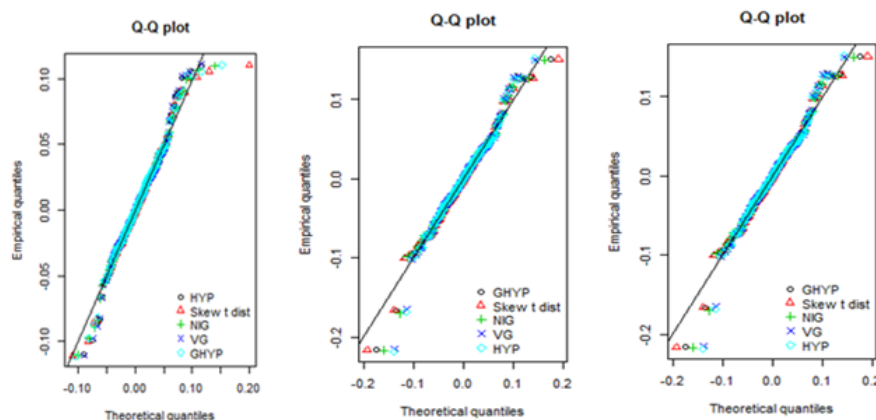


Figure 6.2: Comparison of fit between the different members of the GHD for gold returns (left), platinum returns (center) and silver returns (right).

Table 6.6 presents the results from the Anderson Darling test. We observe that all five models produce high p -values when fitted to precious metal returns. There is strong evidence that we cannot reject the null hypothesis that gold, platinum and silver returns follow the GHD and its subclasses. Based on comparing the results from the AD test, the full GHD, NIGD, GHStD seem most adequate for modelling gold, platinum and silver returns.

We utilise the Maximum likelihood estimation for parameter estimates of the Stable and Pearson type-IV distributions. The goodness-of-fit for these models are compared via the Anderson Darling test (due to its greater emphasis on the tail fits). Tables 6.4 and 6.5 summarise the ML parameter estimates of the Stable and Pearson type-IV respectively. From Table 6.6, the AD test statistics significant for these models (PIVD, SD) for gold, platinum and silver returns. Thus, SD and PIVD are adequate in modelling gold platinum and silver returns.

Figures 6.3, 6.4, 6.5 and 6.6 show the fitted density curves, Q-Q plots and variance stabilised P-P plots of gold, platinum and silver returns for Stable distributions. The plots show a very close stable fit, even far out into the tails. This is also confirmed by the Anderson-Darling goodness-of-fit test in Table 6.6. Nolan (2005) suggested that the Q-Q plot is not satisfactory in evaluating goodness of fit since heavy tailed data is dominated by extreme values. The variance stabilized P-P plot is recommended by Nolan (2005) for Stable distributions.

Table 6.3: ML parameter estimates of the GHDs

Returns	Distribution	alpha	beta	delta	mu	lambda
Gold	GHD _{full}	22.32272	5.606462	0.02564967	-0.0001667632	-1.108093
	NIGD	34.13534	6.011279	0.02037565	-0.0003577191	-0.5
	HD	62.50774	7.249417	0.006912042	-0.0009062716	1
	GHStD	4.953998	4.953998	0.03102517	0.0001285342	-1.716938
	VGD	65.82172	7.604023	0	-0.001122763	1.239731
Platinum	GHD _{full}	14.63196	-0.2300937	0.03951476	0.002119232	-1.313779
	NIGD	25.48649	-0.1195819	0.02982325	0.002030183	-0.5
	HD	45.61431	0.1888852	0.01238619	0.001677815	1
	GHStD	0.1926186	-0.1926186	0.04501745	0.002129134	-1.802714
	VGD	48.94515	0.4684469	0	0.001374926	1.347854
Silver	GHD _{full}	48.00958	6.043766	4.531688e-08	-0.003609232	0.9597865
	NIGD	26.65151	2.980588	0.02313699	-0.001212947	-0.5
	HD	49.22572	5.954825	1.07703e-06	-0.003609959	1
	GHStd	1.596119	1.596119	0.03624158	-9.50005e-05	-1.652204
	VGD	47.38249	6.000306	0	-0.003709994	0.9379813

Table 6.4: ML parameter estimates of the Stable Distribution

Returns	alpha	Beta	gamma	delta
gold	1.642918017	0.298205383	0.013396152	0.001312549
platinum	1.667548615	-0.077521349	0.018785671	0.002299482
silver	1.642400000	0.139000000	0.0002949782	-0.0001157542

Table 6.5: ML parameter estimates of the Pearson type-IV distribution

Returns	\hat{m}	\hat{v}	$\hat{\lambda}$	\hat{a}
Gold	2.184944	-0.4850296	-0.002801191	0.03046648
Platinum	2.300538	0.01108813	0.002130587	0.04497783
Silver	2.09237	-0.2864025	-0.002715397	0.03502179

Table 6.6: Goodness of-fit tests and model selection criteria for precious metal returns.

Distribution	Gold returns		Platinum returns		Silver returns	
	Anderson Darling Test		Anderson Darling Test		Anderson Darling Test	
	Statistic	<i>p</i> -value	Statistic	<i>p</i> -value	Statistic	<i>p</i> -value
GHD _{full}	0.1719	0.9962	0.2123	0.9867	0.59498	0.6526
NIGD	0.1915	0.9926	0.2716	0.9578	0.61323	0.6355
HD	0.2974	0.9401	0.3818	0.8665	0.62918	0.6207
GHStD	0.1764	0.9956	0.1867	0.9936	0.76151	0.5095
VGD	0.3587	0.8885	0.4587	0.7891	0.6724	0.5822
STABLE	0.1783	0.9952	0.1626	0.9974	1.3686	0.2112
STD	0.5107	0.7358	0.1862	0.9937	0.8831	0.4247
SSTD	0.1339	0.9994	0.1859	0.9938	0.5506	0.6957
PIVD	0.1398	0.9992	0.1864	0.9937	0.6368	0.6138

Table 6.7 presents VaR estimates for different models at various VaR levels. We observe that the VaR estimates from GHDs and the SD, PIVD, SSTD and STD are closer to that of the empirical distribution as compared to that of the Normal distribution, at most VaR levels. The Normal distribution provides underestimates for VaR. This phenomenon is well-known in the literature (see Chapter 1). To evaluate objectively whether the VaR model is adequate, the Kupiec LR test is used. The p -values of the Kupiec test for different distributions are summarised in Table 6.8. The VaR estimates from the Normal distribution produced the lowest or joint lowest p -value for the Kupiec test at almost all VaR levels.

The best model for VaR estimation for gold returns differ at different VaR levels. For example, the full GHD, NIGD, SD, GHStD, SSTD, PIVD model produced the highest or joint highest p -value for the Kupiec test at a 1% VaR level. All models are outperformed by the Stable distribution at a 5% VaR level. The full GHD seems to be the best model out of all GHD models. At first glance, this does not seem surprising since it has the highest number of parameters.

However, comparisons with the subclasses are still necessary since some of them arise only as limiting distributions, e.g. GHStD. On the other hand, the Stable distribution is in the top three of the four VaR levels under consideration.

The Normal distribution for the VaR estimates were rejected by the Kupiec test at 5% and 99% VaR levels for gold returns, a 99% VaR level for platinum returns and at 1% and 5% for silver returns. The best GHDs models for VaR estimation differ at different levels for gold, platinum and silver returns. The Stable distribution is the best model at 95% and 99% VaR levels for platinum returns. SSTD is the overall best model for silver returns.

In general, it seems that both GHDs and SD, PIVD and SSTD favourably capture the extreme risk in gold, platinum and silver returns. Their differences in performance, in terms of VaR estimation, is only marginal.

Table 6.7: VaR Estimates for precious metal returns

Returns	Distribution	1%	5%	95%	99%
Gold	Empirical	-0.0567073	-0.03052	0.04333106	0.08835737
	Normal	-0.05501448	-0.03793572	0.04450679	0.061585554
	GHD _{full}	-0.05903795	-0.030309844	0.04383046	0.08103414
	NIGD	-0.05911129	-0.03339242	0.04465826	0.07987971
	HD	-0.05705802	-0.03381565	0.04500804	0.07427349
	GHStD	-0.05886976	-0.03287492	0.04271782	0.08209614
	VGD	-0.05706296	-0.0339911	0.04540735	0.0744847
	STABLE	-0.0620693	-0.03122799	0.04224126	0.09158642
	STD	-0.06799548	-0.03568347	0.03993771	0.07224972
	SSTD	-0.05953214	-0.03214536	0.04344617	0.08014395
	PIVD	-0.05854787	-0.03220016	0.04352644	0.08167587
Platinum	Empirical	-0.09764475	-0.0869032	0.1121076	0.1264497
	Normal	-0.08757139	-0.0789065	0.08268916	0.09135405
	GHD _{full}	-0.113436	-0.09254853	0.09510851	0.1155426
	NIGD	-0.1119001	-0.09287949	0.0961477	0.1150289
	HD	-0.1030705	-0.08786841	0.09212533	0.107501
	GHStD	-0.1168157	-0.09311668	0.09577887	0.1187157
	VGD	-0.1024524	-0.08761425	0.09260786	0.1077287
	STABLE	-0.1052786	-0.0496257	0.05143204	0.1009174
	STD	-0.09252882	-0.05020652	0.05415584	0.09647814
	SSTD	-0.09225646	-0.05008483	0.0542789	0.09676875
	PIVD	-0.09279068	-0.05030653	0.05405553	0.09621017
Silver	Empirical	-0.08123376	-0.0457851	0.5178906	0.0935678
	Normal	-0.6753866	-0.03456233	0.0456908	0.81556098
	GHD _{full}	-0.07243449	-0.04294733	0.05280524	0.09078005
	NIGD	-0.07667083	-0.04308733	0.04941093	0.09041849
	HD	-0.07216776	-0.04300408	0.05223667	0.08941096
	GHStD	-0.07909455	-0.04320854	0.0473261	0.08981113
	VGD	-0.07279265	-0.04309419	0.05280309	0.09111553
	STABLE	-0.1263287	-0.04667956	0.05158978	0.1467801
	STD	-0.08303883	-0.04441655	0.04608608	0.08470836
	SSTD	-0.07566646	-0.04047918	0.05015079	0.09601545
	PIVD	-0.07724361	-0.04173992	0.04895535	0.09392512

Table 6.8: VaR Backtesting for precious metal returns.

Returns	Distribution	p -value of Kupiec Test			
		1%	5%	95%	99%
Gold	Normal	0.7103	0.0354	0.5783	0.0095
	GHD _{full}	0.9503	0.5783	0.8869	0.4345
	NIGD	0.9503	0.4431	0.5783	0.4345
	HD	0.7103	0.4431	0.4431	0.1219
	GHStD	0.9503	0.5783	0.6461	0.4345
	VGD	0.7103	0.2308	0.4431	0.1219
	STABLE	0.9502	0.9517	0.6461	0.5990
	STD	0.5990	0.1559	0.3960	0.1219
	SSTD	0.9503	0.7280	0.9517	0.4345
	PIVD	0.9503	0.7280	0.9517	0.4345
Platinum	Normal	0.1789	0.4345	0.1219	0.0018
	GHD _{full}	0.1707	<0.001	0.1219	0.4085
	NIGD	0.7106	0.5990	0.1219	0.4085
	HD	0.7107	0.9503	0.1219	0.0677
	GHStD	0.7107	0.5990	0.1219	0.4085
	VGD	0.9502	0.1219	0.1219	0.0677
	STABLE	0.1121	0.5124	0.7280	0.4345
	STD	0.5990	0.5125	0.1559	0.1219
	SSTD	0.5990	0.5125	0.1559	0.1219
	PIVD	0.5990	0.5125	0.2308	0.1219
Silver	Normal	0.0157	0.0031	0.8773	0.3691
	GHD _{full}	0.4767	0.4087	0.7984	0.3797
	NIGD	0.5183	0.4087	0.9073	0.3797
	HD	0.1082	0.4087	0.1050	0.3797
	GHStD	0.4767	0.5182	0.1050	0.3797
	VGD	0.1082	0.4087	0.1050	0.3797
	STABLE	0.0325	0.1011	0.8773	0.4678
	STD	0.8267	0.9807	0.1034	0.3599
	SSTD	0.2412	0.4638	0.6169	0.1050
	PIVD	0.2412	0.6169	0.4638	0.1050

Based on the Kupiec likelihood test, Stable distributions can be used for VaR estimation of gold, platinum and silver price returns. Thus, confirming the results by Kręzłek (2012), Stable distributions can be used to assess risk on precious metal markets.

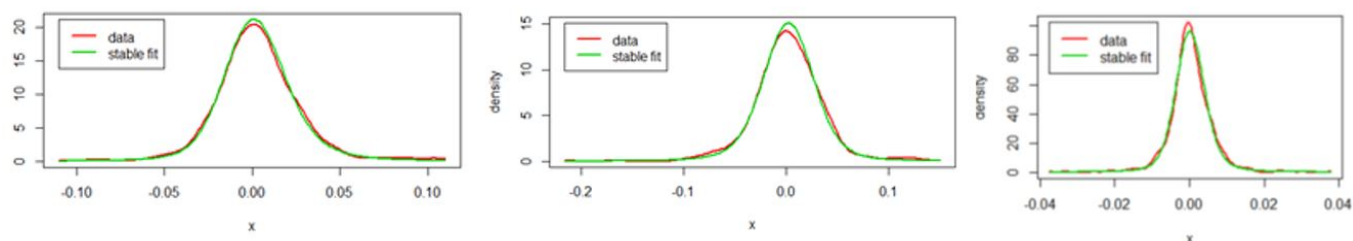


Figure 6.3: Data density and fitted density for gold (left), platinum (center) and silver (right)

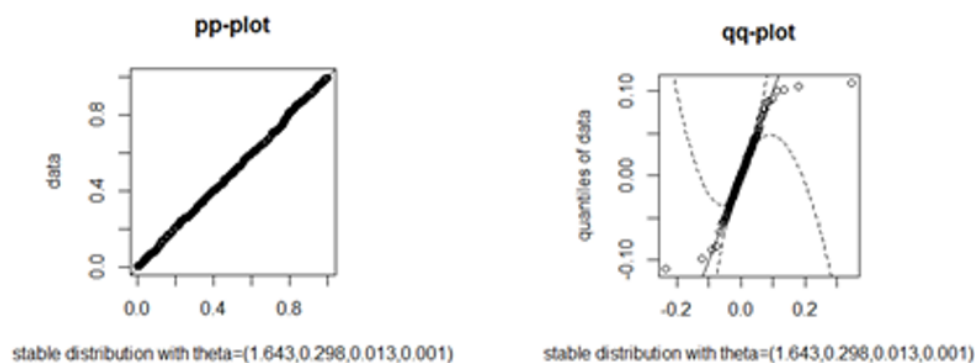


Figure 6.4: P-P and Q-Q plot for gold returns.

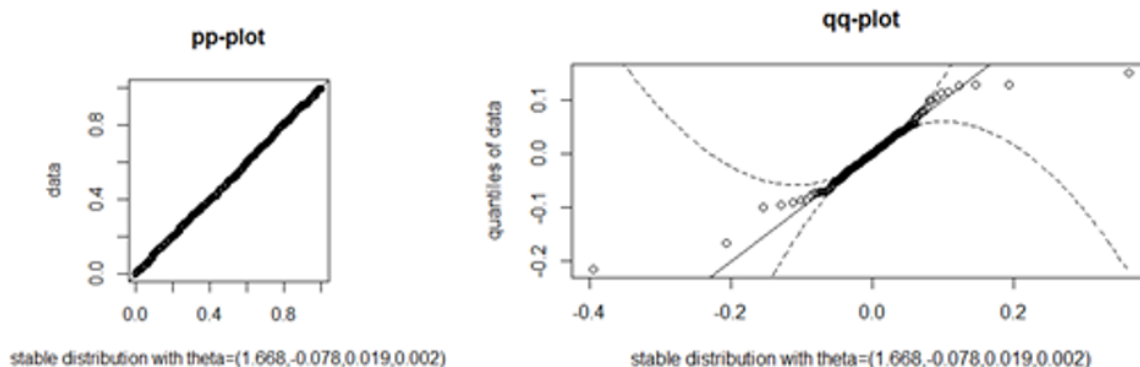


Figure 6.5: P-P and Q-Q plot for platinum return.

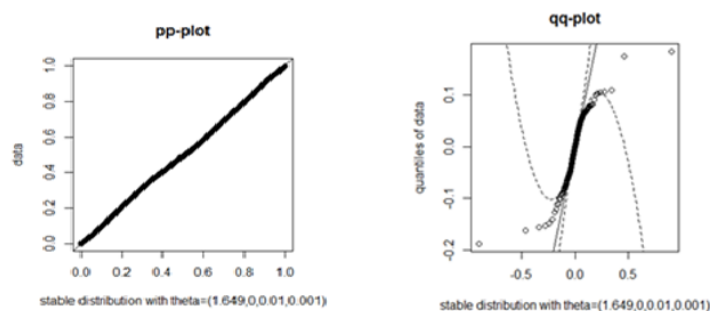


Figure 6.6: P-P and Q-Q plot for silver return.

6.7 Summary

In this chapter, we evaluated the performance of Generalised Hyperbolic distributions, Pearson type-IV distribution, asymmetric and symmetric Student- t distributions and Stable distributions in characterising the gold, platinum and silver returns. In particular, we utilised the full GHD and its subclasses namely the hyperbolic, the Normal-inverse Gaussian, the Variance-Gamma and GH skew Student's t -distributions. These models' ability to capture certain stylised facts such as skewness and both symmetric and asymmetric heavy tails provides a high degree of accuracy when fitted to financial returns data. We conclude that the GHDs outperform the classical normality assumption of financial returns. In addition, the AD goodness-of-fit test failed to reject the null hypotheses at all levels of significance, suggesting minimal error bias. The models' performances in VaR estimation and results from the Kupiec Likelihood test show that the best GHD models for VaR estimation differ at different levels for gold, platinum and silver returns. This is a strong motivation for the possible implementation of stepwise functions and mixture models on these distributions. In addition, the SD, PIVD and SSTD seem to outperform the GHDs in VaR estimation at various VaR levels. In general, performances of GHDs and the SD, PIVD and SSTD, in terms of VaR estimation are comparable for gold, platinum and silver price returns.

6.8 Statistical software packages

We fitted STD and SSTD to returns using the MLE method in the **fGarch** package (Wuertz *et al.*, 2016). We fitted PIVD to returns using MLE in the **PearsonDS** package (Becker and Klöbner, 2017). We fitted the full GHD and its subclasses, HD, NIGD, VGD, GHStD using **gyhp** package (Luethi and Breymann, 2016) and **Generalized-Hyperbolic** package (Scott, 2015). We fitted SD using the **stable** package (Robust Analysis Inc, 2013).

6.9 Appendix

GHD

Bessel Function

We present the Bessel function of the third kind, which forms an integral part of the generalised hyperbolic function.

Let $\lambda \in \mathbb{R}$, the modified Bessel function of the third kind with index λ is defined by the equation

$$K_\lambda(x) = \frac{1}{2} \int_0^\infty u^{\lambda-1} e^{-\frac{1}{2}x(u+u^{-1})} du, \quad x > 0. \quad (6.63)$$

Using the function above, the following results follow:

$$K_{-\lambda}(x) = K_\lambda(x), \quad (6.64)$$

$$K_{\lambda+1}(x) = \frac{2\lambda}{x} K_\lambda(x) + K_{\lambda-1}(x), \quad (6.65)$$

$$\text{and } K'_\lambda(x) = -\frac{\lambda}{x} K_\lambda(x) - K_{\lambda-1}(x). \quad (6.66)$$

Proofs:

$$\begin{aligned}
K_{-\lambda}(x) &= \frac{1}{2} \int_0^\infty u^{-\lambda-1} e^{-\frac{1}{2}x(u+u^{-1})} du \\
&= -\frac{1}{2} \int_0^\infty v^{\lambda+1} e^{-\frac{1}{2}x(v^{-1}+v)} v^{-2} dv, \quad (v = \frac{1}{u}, \quad dv = -\frac{1}{u^2} du) \\
&= \frac{1}{2} \int_0^\infty v^{\lambda-1} e^{-\frac{1}{2}x(v+v^{-1})} dv \\
&= K_\lambda(x).
\end{aligned}$$

Thus, equation 6.64 holds.

$$\begin{aligned}
K_{\lambda+1}(x) - K_{\lambda-1}(x) &= \frac{1}{2} \int_0^\infty (u^\lambda - u^{\lambda-2}) e^{-\frac{1}{2}x(u+u^{-1})} du \\
&= \frac{1}{2} \int_0^\infty u^\lambda (1 - u^{-2}) e^{-\frac{1}{2}x(u+u^{-1})} du.
\end{aligned}$$

Using integration by parts, we obtain

$$\begin{aligned}
K_{\lambda+1}(x) - K_{\lambda-1}(x) &= \frac{1}{2} \left(\left[-\frac{2u^\lambda}{x} e^{-\frac{1}{2}x(u+u^{-1})} \right]_0^\infty + \frac{2\lambda}{x} \int_0^\infty u^{\lambda-1} e^{-\frac{1}{2}x(u+u^{-1})} du \right) \\
&= \frac{2\lambda}{x} \left(\frac{1}{2} \int_0^\infty u^{\lambda-1} e^{-\frac{1}{2}x(u+u^{-1})} du \right) \\
&= \frac{2\lambda}{x} K_\lambda(x).
\end{aligned}$$

Thus, equation 6.65 holds.

$$\begin{aligned}
K'_\lambda(x) &= -\frac{1}{2} \int_0^\infty u^{\lambda-1} \frac{1}{2} (u + u^{-1}) e^{-\frac{1}{2}x(u+u^{-1})} du \\
&= -\frac{1}{4} \int_0^\infty u^\lambda (1 + u^{-2}) e^{-\frac{1}{2}x(u+u^{-1})} du \\
&= -\frac{1}{4} \int_0^\infty u^\lambda e^{-\frac{1}{2}x(u+u^{-1})} du - \frac{1}{4} \int_0^\infty u^{\lambda-2} e^{-\frac{1}{2}x(u+u^{-1})} du \\
&= -\frac{1}{2} K_{\lambda+1}(x) - \frac{1}{2} K_{\lambda-1}(x) \\
&= -\frac{1}{2} \left(2\frac{\lambda}{x} K_\lambda(x) + K_{\lambda-1}(x) \right) - \frac{1}{2} K_{\lambda-1}(x) \text{ from above} \\
&= -\frac{\lambda}{x} K_\lambda(x) - K_{\lambda-1}(x).
\end{aligned}$$

Thus, equation 6.66 holds.

It should also be noted that when $\lambda = n + \frac{1}{2}$, $n = 0, 1, 2, \dots$ we have

$$K_{n+\frac{1}{2}}(x) = \sqrt{\frac{\pi}{2x}} e^{-x} \left\{ 1 + \sum_{i=1}^n \frac{(n+i)!}{(n-i)! i!} (2x)^{-i} \right\}.$$

It should also be noted that if $\lambda > 0$, then for very small values of its argument ($x \downarrow 0$), this function can be approximated by

$$K_\lambda \approx \Gamma(\lambda) 2^{\lambda-1} x^{-\lambda},$$

and for large values of the argument, we have

$$K_\lambda = \sqrt{\frac{\pi}{2x}} e^{-x} \left(1 + \frac{4\lambda^2 - 1}{8x} + \frac{(4\lambda^2 - 1)(4\lambda^2 - 9)}{2!(8x)^2} + \frac{(4\lambda^2 - 1)(4\lambda^2 - 9)(4\lambda^2 - 25)}{3!(8x)^3} + \dots \right).$$

The GHD may be represented as a Normal variance-mean mixture with the Generalised Inverse Gaussian (GIG) as mixing distribution, where the GIGD has a density

$$f(z; \lambda, \delta, \gamma) = \left(\frac{\gamma}{\delta}\right)^\lambda \frac{z^{\lambda-1}}{2K_\lambda(\gamma\delta)} \exp\left\{-\frac{1}{2}(\delta^2 z^{-1} + \gamma^2 z)\right\}.$$

This means that a generalised hyperbolic variable X can be represented as

$$X = \mu + \beta Z + \sqrt{Z} Y, \quad (6.67)$$

where $Y \sim N(0, 1)$, $Z \sim GIG(\lambda, \delta, \gamma)$ with Z and Y independent.

It follows from equation 6.67 that

$$X|Z = z \sim N(\mu + \beta z, z).$$

Proof:

$$X = \mu + \beta Z + \sqrt{Z}Y$$
$$(X|Z = z) = \mu + \beta z + \sqrt{z}Y$$

where μ , β , z are now constants.

Now since $Y \sim N(0, 1)$, then $(X|Z = z)$ follows a Normal distribution with

$$E(X|Z = z) = \mu + \beta z + \sqrt{z}E(Y)$$
$$= \mu + \beta z$$

and

$$\text{Var}(X|Z = z) = \text{Var}(\mu + \beta z + \sqrt{z}Y)$$
$$= z\text{Var}(Y)$$
$$= z$$

Chapter 7

Value-at-Risk estimation of precious metals with GARCH-type models

7.1 Introduction

While academic literature is abundant in models that account for heavy tails, this stylised fact should not be considered in isolation. A realistic model for financial returns should take into account all statistically relevant stylised facts. In this chapter we, therefore, discuss the methods and linear models useful in modelling and forecasting financial time series. The models include stationary and non-stationary time series models. This chapter also gives an overview of the volatility models used in the literature and in this study. Thereafter, the chapter concludes with an application of both linear and volatility models coupled with heavy-tailed distributions to precious metals log-returns.

7.2 The models

The following steps of building a volatility model were taken from Tsay (2013).

These are:

- Specify a mean equation by testing for serial dependence and if necessary, building an ARMA model for the return series to remove any linear dependence.
- Use the residuals of the mean equation to test for ARCH effects.
- Specify volatility model if ARCH effects are statistically significant and perform a joint estimation of the mean and volatility equations.
- Check the fitted model carefully and refine if necessary.

The Mean Model

ARMA models have been identified as mean models. The removal of possible linear dependence in the data is achieved by specifying the mean model; this is the same as removing sample mean from the data.

The Volatility Models

Volatility clustering phenomenon is evident in metal prices. In this study we will use the ARMA-GARCH model to capture time varying volatility which relies on modelling the conditional variance as a linear function of the squared past innovations.

The GARCH(p, q) model

GARCH models are used to explain volatility clustering and heteroscedasticity. Bollerslev (1996) introduced the symmetric GARCH(p, q). For a log return r_t , let $a_t = r_t - \mu_t$ be the innovation at time t . Then a_t follows a GARCH (p, q) model if

$$a_t = \sigma_t \epsilon_t, \quad \sigma_t^2 = \omega + \sum_{i=1}^p \alpha_i a_{t-i}^2 + \sum_{j=1}^q \beta_j \sigma_{t-j}^2, \quad (7.1)$$

where $\{\epsilon_t\}$ is a sequence of iid random variables with mean 0 and variance 1 with $\omega > 0$, $\alpha_i \geq 0$, $\beta_j \geq 0$ and $\sum_{i=1}^{\max(p,q)} (\alpha_i + \beta_i) < 1$.

equation 7.1 can be written as

$$\sigma_t^2 = \omega + \alpha(L)a_t^2 + \beta(L)\sigma_t^2, \quad (7.2)$$

where L denotes the lag or backshift operator $\alpha(L) \equiv \alpha_1 L + \alpha_2 L^2 + \dots + \alpha_q L^q$, and $\beta(L) \equiv \beta_1 L + \beta_2 L^2 + \dots + \beta_p L^p$.

For stability and covariance stationarity of the $\{a_t\}$ process, all the roots of $[1 - \alpha(L) - \beta(L)]$ and $[1 - \beta(L)]$ are constrained to lie outside the unit circle.

The GARCH(p, q) process may be represented as the infinite-order ARCH process,

$$\begin{aligned} \sigma_t^2 &= \omega[1 - \beta(1)]^{-1} + \alpha(L)[1 - \beta(1)]^{-1}a_t^2 \\ &\equiv \omega[1 - \beta(1)]^{-1} + \lambda(L)a_t^2. \end{aligned} \quad (7.3)$$

The stationarity conditions mentioned above imply that the effect of the past squared innovations on the current conditional variance decays exponentially with the lag length.

The GARCH (1,1) model specifically generates volatility forecasts as a weighted average of the constant or average variance, the previous forecasting variance and the previous variance reflecting squared news about the returns.

The GARCH (1,1) model is a parsimonious model in volatility forecasting (Eberlein, 2003). The model provides a simple representation of main statistical characteristics of a return process such as autocorrelation and volatility clustering. The GARCH (1,1) model is the most popular structure for volatility forecasting and therefore it is used to model real financial time series.

We assume that the daily precious log returns is an ARMA (1,1)-GARCH (1,1) process (i.e. the conditional mean follows an ARMA(1,1) model and the conditional variance follows a GARCH(1,1) distribution), which is given by

$$\begin{cases} r_t = \mu_t + \sigma_t \varepsilon_t, \\ \mu_t = \phi r_{t-1} - \theta a_{t-1}, \\ \sigma_t^2 = \omega + \alpha_1 a_{t-1}^2 + \beta_1 \sigma_{t-1}^2, \end{cases}$$

where $0 \leq \alpha_1, \beta_1 \leq 1, 0 < (\alpha_1 + \beta_1) < 1$. σ_t is the volatility of the return on day t , μ_t is the expected return and ε_t are the innovations that are assumed to follow the standard Normal distribution. However, in practice they follow distributions heavier than the Normal distribution.

Extensions of the GARCH model

The GARCH model was unable to detect the leverage effect and capture asymmetry extensions that we introduced.

Asymmetric GARCH Models

In various research studies, it has been shown that the sign of the shock is consequential (Bekaert and Guojun, 2000; Bucevska, 2013). The conclusion of the comprehensive studies show that negative returns have a greater volatility when compared to positive returns of equivalent size. This indicates that bad news increases volatility compared to good news (Angabini and Wasiuzzaman, 2011).

For asymmetry to be captured in return volatility, a new class of models was developed and called asymmetric ARCH models. These are the Exponential GARCH (EGARCH), Threshold GARCH (TGARCH) models, and Asymmetric Power ARCH (APARCH).

The Exponential GARCH Model (EGARCH)

To overcome some weaknesses of the GARCH model, Nelson (1991) proposed the

first extension to GARCH called Exponential GARCH (EGARCH) to model the asymmetric effects of both positive and negative asset returns. The volatility process of the EGARCH(p, q) can be written as

$$\ln(\sigma_t^2) = \omega + \sum_{i=1}^p \alpha_i g(\varepsilon_{t-i}) + \sum_{j=1}^q \beta_j \ln \sigma_{t-i}^2, \quad (7.4)$$

where $g(\varepsilon_t) = \gamma_1 \varepsilon_t + \gamma_2 [|\varepsilon_t| - E(|\varepsilon_t|)]$ is the weighted innovation, $\gamma_1 \varepsilon_t$ is the sign effect and $\gamma_2 [|\varepsilon_t| - E(|\varepsilon_t|)]$ is the magnitude effect, γ_1 and γ_2 are real constants. The conditional variance of the EGARCH model is in logarithmic form that guarantees its non-negativity without the need to force extra non-negativity limitations.

The mean of $[g(\varepsilon_t)]$ is zero since the mean of ε_t and $[|\varepsilon_t| - E(|\varepsilon_t|)]$ are zero. As a result $g(\varepsilon_t)$ permit the conditional variance to respond to asymmetric effects which can be easily seen by rewriting $g(\varepsilon_t)$ as

$$g(\varepsilon_t) = \begin{cases} (\gamma_1 + \gamma_2)\varepsilon_t - \gamma_2 E(|\varepsilon_t|), & \varepsilon_t \geq 0 \\ (\gamma_1 - \gamma_2)\varepsilon_t - \gamma_2 E(|\varepsilon_t|), & \varepsilon_t < 0. \end{cases} \quad (7.5)$$

If $\varepsilon_t \geq 0$, the positive shocks have an impact of $(\gamma_1 + \gamma_2)$ on the conditional variance and if $\varepsilon_t < 0$, the negative shocks have an impact of $(\gamma_1 - \gamma_2)$, on the conditional variance. To ascertain a non-negative conditional variance, no restrictions are required on the parameters which are contrary to GARCH models. As a result, an EGARCH model is able to model asymmetrical effect, volatility persistence and mean reversion. An important feature of using EGARCH over GARCH is that it allows positive and negative shocks to have different impacts on the volatility (Karlsson, 2002).

The parameter estimates from equation 7.4 can be defined as follows:

- α_i represents a magnitude effect or symmetric effect of the model.
- β_j measures the persistence in the conditional volatility irrespective of occurrences in the market.
- γ_i measures asymmetry or leverage effects.

The Threshold GARCH Model (TGARCH)

Glosten *et al.* (1993a) propose another way of modelling the asymmetric effects of positive and negative asset returns called TGARCH or GJR-GARCH. The volatility equation is shown below:

$$\sigma_t^2 = \omega + \sum_{i=1}^m (\alpha_i + \omega_i G_{t-i}) a_{t-i}^2 + \sum_{j=1}^n \beta_j \sigma_{t-j}^2, \quad (7.6)$$

where G_{t-i} is an indicator variable for negative a_{t-i} , given as

$$G_{t-i} = \begin{cases} 1, & a_{t-i} < 0 \\ 0, & a_{t-i} \geq 0. \end{cases}$$

Under the condition that $\omega > 0$, $\alpha_i \geq 0$, $\omega_i \geq 0$, and $\beta_j \geq 0$, we ensure nonnegative conditional variance. From this model, the impact of a_{t-i}^2 on σ_t^2 is dependent on the sign of a_{t-i} which permits the model to accommodate asymmetric effect. As a result, the positive shock has an impact of $\alpha_i a_{t-i}^2$ on the conditional variance while the negative shock has an impact of $(\alpha_i + \omega_i) a_{t-i}^2$ on the conditional variance.

The GJR-GARCH model is fundamentally the same as the EGARCH model, both have the capacity to capture the impact of both positive and negative shocks. As a result, the TGARCH and the EGARCH might both be considered for the same data hence it is important to find a criterion for choosing between the two models (Karls-son, 2002). The TGARCH belongs to the class of asymmetric power autoregressive conditional heteroscedastic (APARCH) models introduced by Ding *et al.* (1993).

Asymmetric Power GARCH models (APARCH)

The APARCH model is an extension of the GARCH model. The APARCH generalised both the ARCH and GARCH models. The structure of the volatility equation APARCH(m,s) is given as (Tsay, 2013)

$$\sigma_t^\delta = \omega + \sum_{i=1}^m \alpha_i (|a_{t-i}| + \gamma_i a_{t-i})^\delta + \sum_{j=1}^s \beta_j \sigma_{t-j}^\delta. \quad (7.7)$$

Under the condition that $\omega > 0$, $\alpha_i \geq 0$, $\beta_j \geq 0$, and $0 \leq \sum_{i=1}^m \alpha_i + \sum_{j=1}^s \beta_j \leq 1$, where α_i and β_j are respectively the ARCH and GARCH coefficients, γ_i is the leverage coefficient such that when γ_i is positive, it implies that the negative shocks have a stronger impact on price volatility than the positive shocks, and δ is the positive real number which functions as the symmetric power transformation of δ_t .

The APARCH model is an asymmetric GARCH model. The structure of APARCH (1,1) model is given as

$$r_t = \mu_t + a_t = \mu_t + \sigma_t \varepsilon_t, \quad \varepsilon_t \sim N(0, 1), \quad (7.8)$$

$$\text{and } \sigma_t^\delta = \omega + \alpha_1(|a_{t-1}| + \gamma_1 a_{t-1})^\delta + \beta_1 \sigma_{t-1}^2, \quad (7.9)$$

where μ_t and σ_t are the conditional mean and variance respectively, α_1 and β_1 are the ARCH and GARCH coefficients. γ_1 is the leverage coefficient, and δ is the Taylor effect regarding the difference in the sample autocorrelations of absolute and squared returns. The APARCH model is a nested model and special cases are:

- When $\delta = 2$, $\beta_j = 0$ and $\gamma_i = 0$, the APARCH model reduces to ARCH.
- When $\delta = 2$ and $\gamma_i = 0$, the APARCH model reduces to standard linear GARCH models.
- When $\delta = 1$ and $\gamma_i = 0$, the APARCH model becomes Taylor-Schwert GARCH (TS-GARCH).
- When $\delta = 2$ and $0 \leq \gamma_i \leq 1$, the APARCH model reduces to GJR-GARCH model of Glosten *et al.* (1993).
- When $\delta = 1$ and $0 \leq \gamma_i \leq 1$, the APARCH model becomes the TARCH model of Zakoian (1994).
- When $\beta_j = 0$ and $\gamma_i = 1$, the APARCH model becomes the NARCH.
- When $\delta \rightarrow 0$ and $\gamma_i = 0$, the APARCH model becomes the log-APARCH model.

In this study we utilise the APARCH model since most extensions of the GARCH are nested in the APARCH model.

For $\mu_t = \phi r_{t-1} - \theta a_{t-1}$, and $\sigma_t^\delta = \omega + \alpha_1(|a_{t-1}| + \gamma_1 a_{t-1})^\delta + \beta_1 \sigma_{t-1}^2$, we have ARMA(1,1)-APARCH(1,1).

The standardised residuals follow the heavy tailed and flexible distributions, i.e. GEVD, GPD, GLD, SD, PIVD, GHDs, STD and SSTD, as defined in chapters 6 and 7.

7.3 Combining Volatility models with Heavy-tailed Distributions

- Step 1 - ARMA-GARCH-type model is fitted to precious metal returns using the Gaussian quasi-Maximum likelihood estimation. That is, the log-likelihood is maximised assuming a Normal distribution innovation.
- Step 2 - Extract the standardised residuals.
- Step 3 - Heavy-tailed distributions are fitted on standardised residuals, i.e. combining ARMA-GARCH models with heavy-tailed distributions to produce improved models for precious metal returns.
- Step 4 - VaR is calculated and then backtesting.
- Repeat the four steps using the ARMA-APARCH model instead of the ARMA-GARCH model.

7.4 Empirical Results

The ARMA-GARCH model

This section focuses on parameter estimation and model comparison for the Stable distribution and GHDs on precious metals returns.

Table 7.1 records the Maximum likelihood (ML) parameter estimates for the ARMA(1,1)-GARCH(1,1) model with Gaussian Innovations. All parameters are statistically significant. The Ljung-Box test statistics for the standardised residuals are given in Table 7.2. The p -values are all greater than 0.05. In addition, the Ljung-Box test statistics of the squared residuals also have p -values greater than 0.05. The ARCH Lagrange Multiplier (ARCH LM) test was used to check for ARCH effects in the standardised residuals. The ARCH test statistics and p -values, presented in Table 7.2 show that there are no ARCH effects in the residuals. Table 7.3 illustrates the ML parameter estimates of the full GHD, GHStD NIGD, VGD, SD fitted to the standardised residuals extracted from the ARMA(1,1)-GARCH(1,1) models. ARMA(1,1)-GARCH(1,1)-STD and ARMA(1,1)-GARCH(1,1)-SSTD were also fitted to the gold, platinum and silver returns.

Table 7.4 presents the results for the AD goodness-of fit test. There is strong evidence that we cannot reject the null hypothesis that gold returns follow these distributions, except for the Normal distribution. The AD test indicated that the ARMA(1,1)-GARCH(1,1)-VGD as the most suitable overall model (highest p -value) for gold returns, ARMA(1,1)-GARCH(1,1)-GHD_{full} for platinum returns and ARMA(1,1)-GARCH(1,1)-GHStD for silver returns.

Table 7.1: ML parameter estimates for the ARMA(1,1)-GARCH(1,1) model with Gaussian Innovations

	Gold returns		Platinum returns		Silver returns	
Mean equation						
	Estimate	p -value	Estimate	p -value	Estimate	p -value
ϕ	-6.96e-01	0.0059	-8.458e-01	<0.0001	-9.295e-02	2.27e-10
θ	6.93e-01	0.0070	8.669e-01	<0.0001	0.0000	-
Variance equation						
	Estimate	p -value	Estimate	p -value	Estimate	p -value
α_0	4.15e-07	0.0002	1.683e-06	0.0265	1.435e-06	0.00052
α_1	7.74e-02	<0.0001	9.415e-02	<0.0001	5.670e-02	<0.0001
β_1	9.26e-01	<0.0001	9.023e-01	<0.0001	9.424e-01	<0.0001

Table 7.2: Standardised residuals test for ARMA(1,1)-GARCH(1,1) model with Gaussian Innovations

Returns		Statistic	<i>p</i> -value
Gold	Q(10)	9.7941	0.4587
	Q(15)	15.1283	0.4422
	Q(20)	31.1144	0.0536
	Q ² (10)	12.0140	0.2841
	Q ² (15)	16.9864	0.3197
	Q ² (20)	21.2297	0.3837
	ARCH LM test	13.9884	0.3014
Platinum	Q(10)	5.9447	0.8199
	Q(15)	9.8965	0.8262
	Q(20)	21.0813	0.3924
	Q ² (10)	12.9619	0.2258
	Q ² (15)	15.3883	0.4238
	Q ² (20)	19.8940	0.4646
	ARCH LM test	14.3855	0.2768
Silver	Q(10)	13.9810	0.1739
	Q(15)	20.2569	0.1623
	Q(20)	27.0635	0.1335
	Q ² (10)	7.5575	0.6720
	Q ² (15)	9.8690	0.8279
	Q ² (20)	12.5046	0.8976
	ARCH LM test	8.1195	0.7757

Table 7.3: ML parameter estimates of precious metal returns

Returns	Model	alpha	beta	Delta	mu	lambda	gamma	sigma
Gold	ARMA(1,1)-GARCH(1,1)-Normal				0.0258			0.9990
	ARMA(1,1)-GARCH(1,1)-Stable	1.7751	4.45e-09	0.0262			0.6017	
	ARMA(1,1)-GARCH(1,1)-GHD _{full}	1.0455	-0.0061	1.0499	0.0343	-0.5104		
	ARMA(1,1)-GARCH(1,1)-NIGD	1.0444	-0.0054	1.0258	0.0311	-0.5000		
	ARMA(1,1)-GARCH(1,1)-GHStD	0.0038	-0.0038	1.6245	0.0295	-2.3122		
	ARMA(1,1)-GARCH(1,1)-VGD	1.7439	-0.0052	0.0000	0.0307	1.4758		
Platinum	ARMA(1,1)-GARCH(1,1)-Normal				0.0247			0.9992
	ARMA(1,1)-GARCH(1,1)-Stable	1.6960	-0.0800	0.0295			0.5955	
	ARMA(1,1)-GARCH(1,1)-GHD _{full}	0.7395	-0.0341	1.6637	0.0562	-1.9291		
	ARMA(1,1)-GARCH(1,1)-NIGD	1.2495	-0.0277	1.2402	0.0525	-0.5000		
	ARMA(1,1)-GARCH(1,1)-GHStD	0.0240	-0.0240	1.9027	0.0488	-2.7962		
	ARMA(1,1)-GARCH(1,1)-VGD	2.0588	-0.0228	0.0000	0.0472	2.0852		
Silver	ARMA(1,1)-GARCH(1,1)-Normal				0.0177			0.9996
	ARMA(1,1)-GARCH(1,1)-Stable	1.7210	-0.0580	0.0216			0.5918	
	ARMA(1,1)-GARCH(1,1)-GHD _{full}	0.3489	-0.0363	1.6819	0.0525	-2.3030		
	ARMA(1,1)-GARCH(1,1)-NIGD	1.1571	-0.0313	1.1335	0.0483	-0.5000		
	ARMA(1,1)-GARCH(1,1)-GHStD	0.0292	-0.0292	1.7410	0.0468	-2.5189		
	ARMA(1,1)-GARCH(1,1)-VGD	1.9428	-0.0200	0.0000	0.0370	1.8272		

Table 7.4: Anderson Darling Goodness of-fit tests for precious metal returns.

Model	Gold returns		Platinum returns		Silver returns	
	AD Test		AD Test		AD Test	
	Statistic	<i>p</i> -value	Statistic	<i>p</i> -value	Statistic	<i>p</i> -value
ARMA(1,1)-GARCH(1,1)-Normal	1936.1020	0.0244	16.433	0.0011	22.533	0.0011
ARMA(1,1)-GARCH(1,1)-Stable	3.0989	0.1232	1.1684	0.2799	0.7518	0.5171
ARMA(1,1)-GARCH(1,1)-GHD _{full}	0.4476	0.8006	0.1666	0.9970	0.1962	0.9914
ARMA(1,1)-GARCH(1,1)-NIGD	0.3315	0.9127	0.2014	0.9900	0.3707	0.8772
ARMA(1,1)-GARCH(1,1)-GHStD	0.8127	0.4720	0.1816	0.9946	0.1855	0.9939
ARMA(1,1)-GARCH(1,1)-VGD	0.2137	0.9862	0.4457	0.8025	0.7999	0.4811
ARMA(1,1)-GARCH(1,1)-STD	0.8172	0.4688	0.2551	0.9676	0.2291	0.9804
ARMA(1,1)-GARCH(1,1)-SSTD	0.4705	0.7771	0.1753	0.9957	0.1989	0.9907

Table 7.5: ML parameter estimates of the FMKL GLD for the ARMA (1,1)-GARCH(1,1)-GLD model.

Returns	$\hat{\lambda}_1$	$\hat{\lambda}_2$	$\hat{\lambda}_3$	$\hat{\lambda}_4$	AD test	
					Statistic	<i>p</i> -value
Gold	0.02701677	2.18902607	-0.0980823	-0.097152	0.4705	0.7771
Platinum	0.03070983	1.99871965	-0.0571853	-0.049388	0.2011	0.9901
Silver	0.02679557	2.09899790	-0.0845292	-0.067889	0.2881	0.9468

Table 7.6: ML parameter estimates of the Pearson type-IV distribution for the ARMA(1,1)-GARCH(1,1)-PIVD model.

Returns	\hat{m}	\hat{v}	$\hat{\lambda}$	\hat{a}	AD test	
					Statistic	<i>p</i> -value
Gold	2.811296	0.03049733	0.03854743	1.623921	0.80698	0.4760
Platinum	3.296612	0.1356774	0.07963036	1.902716	0.16598	0.9970
Silver	3.017391	0.1110931	0.06612122	1.740363	0.18843	0.9932

FMKL GLD was fitted to the standardised residuals extracted from the ARMA(1,1)-GARCH(1,1) models. The ML parameter estimates and AD test results are shown in Table 7.6. The AD test results suggest that the extracted residuals follow FMKL GLD. PIVD was also fitted to the standardised residuals extracted from the ARMA(1,1)-GARCH(1,1) models using the Maximum likelihood procedure. Table 7.7 show the ML parameter estimates of the PIVD fitted to the standardised residuals extracted from the ARMA(1,1)-GARCH(1,1) models with Normal innovations. The PIVD provides a good fit to the standardised residuals extracted from the ARMA(1,1)-GARCH(1,1) model since the AD statistics are significant.

The GEVD is fitted to the positive and negative standardised residuals using MLE. We used the block size of 5 to perform a block maxima method since less accuracy is attached to estimates with larger block sizes in accordance with asymptotic property as noted by Coles (2001). Table 7.7 shows the ML parameter estimates of the GEVD with the corresponding standard errors in brackets. The shape parameter is positive for gold and silver suggesting that the standardised residuals follow a Fréchet distribution.

Table 7.7: ML parameter estimates of GEVD for the ARMA(1,1)-GARCH(1,1)-GEVD model.

Returns	Standardised Residuals	$\hat{\xi}$ (Se)	$\hat{\mu}$ (Se)	$\hat{\sigma}$ (Se)	AD test	
					Statistic	<i>p</i> -value
Gold	Positive	0.0357 (0.0185)	0.7537 (0.0208)	0.6048 (0.0151)	0.4023	0.8464
	Negative	0.02281 (0.0174)	0.7251 (0.0207)	0.6042 (0.0148)	0.4048	0.8443
Platinum	Positive	-0.0799 (0.0098)	0.8109 (0.0028)	0.6897 (0.0148)	5.7195	0.0013
	Negative	0.0047 (0.0202)	0.7699 (0.0207)	0.5998 (0.0149)	0.2399	0.9755
Silver	Positive	0.0226 (0.0192)	0.7850 (0.0201)	0.5848 (0.0144)	1.0382	0.3378
	Negative	0.0458 (0.0186)	0.7541 (0.0202)	0.5885 (0.0147)	0.3978	0.8509

*Se means standard error

For platinum, the shape parameter is negative suggesting that the standardised residuals follow a Weibull distribution. However, for negative standardised residuals, the 95% confidence interval of the shape parameter include zero suggesting a Gumbel distribution. All the AD statistics (except positive standardised residuals for platinum) are significant, confirming that GEVD is a good fit in the upper tail.

The GPD is fitted to the positive and negative standardised residuals extracted from the ARMA-GARCH model with Normal innovations. The suitable threshold must lie where there is a positive gradient change in the mean excess plot. To confirm the threshold the Pareto quantile plot is used. The mean residual life (mean excess) plot and the Pareto quantile plot select the highest possible threshold on the upper tail of the distribution.

Figures 7.1 to 7.6 in the Appendix at the end of this chapter shows the mean residual life plot of the standardised residual of both positive and negative standardised residuals for platinum and silver returns. The suitable threshold must lie where there is a positive gradient in the mean excess. The threshold selected should lie around 2 for both positive and negative standardised residuals. Figure 7.2 shows the Pareto quantile plots for both positive and negative standardised residuals. From Figure 7.2 (a), the threshold is $u = \exp(0.5455) = 1.7255$ for positive standardised residuals (gold). From Figure 7.2 (b) the threshold is $u = \exp(0.7406) = 2.0971$ for negative standardised residuals.

The same method was used to get threshold positive and negative standardised residuals for both platinum and silver. We use the same procedure in subsequent sections in this chapter and chapter 8. Table 7.8 summarises the ML parameter estimates of the GPD for the ARMA(1,1)-GARCH(1,1)-GPD model. Figures 7.13, 7.14, 7.15, 7.16, 7.17 and 7.18 show GPD diagnostics for both positive and negative standardised residuals. It is observed from these figures that both positive and negative standardised residuals seem to follow the GPD. The Q-Q plots and P-P plots do not show any serious deviation from straight lines (except for platinum suggesting a poor fit). The empirical and the return level estimates suggest that the positive and negative standardised residuals follow a GPD in the upper tail.

Table 7.8: ML parameter estimates of GPD for the ARMA(1,1)-GARCH(1,1)-GPD model.

Returns	Standardised Residuals	Threshold	No. of Exceedances	$\hat{\xi}$ (Se)	$\hat{\beta}$ (Se)
Gold	Positive	1.7255	1327	0.1732 (0.0697)	0.5507 (0.0533)
	Negative	2.0971	915	0.1781 (0.0953)	0.5571 (0.0750)
Platinum	Positive	1.6780	1453	0.1270 (0.0807)	0.5780 (0.0605)
	Negative	2.0106	1042	-0.0345 (0.0767)	0.6615 (0.0769)
Silver	Positive	1.9937	1126	-0.0087 (0.1100)	0.7589 (0.1081)
	Negative	1.9945	1064	0.1952 (0.0967)	0.5905 (0.0749)

*Se means standard error

Table 7.9 presents VaR estimates for the different models at various levels. The p -values of the Kupiec and Christoffersen tests for different distributions are summarised in Table 7.10.

Table 7.9: VaR Estimates for precious metal returns.

Returns	Model	1%	5%	95%	99%
Gold	ARMA(1,1)-GARCH(1,1)-Normal	-2.2982	-1.6174	1.6689	2.3497
	ARMA(1,1)-GARCH(1,1)-Stable	-2.6634	-1.4987	1.5511	2.7158
	ARMA(1,1)-GARCH(1,1)-GHD _{full}	-2.6585	-1.5556	1.6190	2.6979
	ARMA(1,1)-GARCH(1,1)-NIGD	-2.6447	-1.5575	1.6038	2.6812
	ARMA(1,1)-GARCH(1,1)-GHStD	-2.6111	-1.5257	1.5742	2.6501
	ARMA(1,1)-GARCH(1,1)-VGD	-2.6041	-1.5865	1.6330	2.6446
	ARMA(1,1)-GARCH(1,1)-STD	-2.6040	-1.5233	1.5765	2.6573
	ARMA(1,1)-GARCH(1,1)-SSTD	-2.6170	-1.5293	1.5705	2.6444
	ARMA(1,1)-GARCH(1,1)-GEVD	-2.5951	-1.5602	1.5970	2.6625
	ARMA(1,1)-GARCH(1,1)-GPD	-2.5354	-1.6549	1.6259	2.6089
	ARMA(1,1)-GARCH(1,1)-GLD	-2.6277	-1.5403	1.5920	2.6756
	ARMA(1,1)-GARCH(1,1)-PIVD	-2.6176	-1.5286	1.5712	2.6438
Platinum	ARMA(1,1)-GARCH(1,1)-Normal	-2.2999	-1.6190	1.6684	2.3494
	ARMA(1,1)-GARCH(1,1)-Stable	-3.1925	-1.5855	1.5633	2.9890
	ARMA(1,1)-GARCH(1,1)-GHD _{full}	-2.5995	-1.5757	1.5971	2.5681
	ARMA(1,1)-GARCH(1,1)-NIGD	-2.6078	-1.5904	1.6193	2.5996
	ARMA(1,1)-GARCH(1,1)-GHStD	-2.5975	-1.5677	1.6011	2.5869
	ARMA(1,1)-GARCH(1,1)-VGD	-2.5602	-1.6064	1.6398	2.5736
	ARMA(1,1)-GARCH(1,1)-STD	-2.5631	-1.5559	1.6131	2.6203
	ARMA(1,1)-GARCH(1,1)-SSTD	-2.6001	-1.5734	1.5955	2.5826
	ARMA(1,1)-GARCH(1,1)-GEVD	-2.5765	-1.5887	1.7001	2.6454
	ARMA(1,1)-GARCH(1,1)-GPD	-2.6195	-1.5595	1.5915	2.6041
	ARMA(1,1)-GARCH(1,1)-GLD	-2.6002	-1.5785	1.6204	2.6128
	ARMA(1,1)-GARCH(1,1)-PIVD	-2.6069	-1.5732	1.5958	2.5774
Silver	ARMA(1,1)-GARCH(1,1)-Normal	-2.3078	-1.6266	1.6619	2.3432
	ARMA(1,1)-GARCH(1,1)-Stable	-2.9910	-1.5472	1.5379	2.8638
	ARMA(1,1)-GARCH(1,1)-GHD _{full}	-2.6371	-1.5615	1.5681	2.5708
	ARMA(1,1)-GARCH(1,1)-NIGD	-2.6385	-1.5838	1.5929	2.6002
	ARMA(1,1)-GARCH(1,1)-GHStD	-2.6274	-1.5536	1.5681	2.5791
	ARMA(1,1)-GARCH(1,1)-VGD	-2.5733	-1.5997	1.6192	2.5735
	ARMA(1,1)-GARCH(1,1)-STD	-2.5802	-1.5375	1.5844	2.6271
	ARMA(1,1)-GARCH(1,1)-SSTD	-2.6083	-1.5508	1.5711	2.5978
	ARMA(1,1)-GARCH(1,1)-GEVD	-2.6407	-1.5805	1.5932	2.5947
	ARMA(1,1)-GARCH(1,1)-GPD	-2.6090	-1.6144	1.4221	2.6427
	ARMA(1,1)-GARCH(1,1)-GLD	-2.6507	-1.5729	1.5850	2.5977
	ARMA(1,1)-GARCH(1,1)-PIVD	-2.6221	-1.5543	1.5677	2.5843

Table 7.10: VaR Backtesting for precious metal returns.

Returns	Model	<i>p</i> -value of Kupiec Test				<i>p</i> -value of Christoffersen Test			
		1%	5%	95%	99%	1%	5%	95%	99%
Gold	ARMA(1,1)-GARCH(1,1)-Normal	0.0059	0.2430	0.3000	0.0018	0.006	0.1685	0.2180	2.74e-05
	ARMA(1,1)-GARCH(1,1)-Stable	0.4574	0.0041	0.4835	0.0241	0.5596	0.0095	0.3074	3.56e-05
	ARMA(1,1)-GARCH(1,1)-GHD _{full}	0.4574	0.6097	0.9488	0.0359	0.5596	0.2952	0.3334	6.23e-05
	ARMA(1,1)-GARCH(1,1)-NIGD	0.4574	0.5239	0.8477	0.0520	0.5596	0.3005	0.3917	0.0001
	ARMA(1,1)-GARCH(1,1)-GHStD	0.8656	0.0774	0.7015	0.1019	0.7988	0.1140	0.4190	0.0003
	ARMA(1,1)-GARCH(1,1)-VGD	0.8656	0.9489	0.6521	0.1018	0.7988	0.3570	0.3392	0.0003
	ARMA(1,1)-GARCH(1,1)-STD	0.8656	0.0676	0.7492	0.0737	0.7988	0.1055	0.4118	0.0002
	ARMA(1,1)-GARCH(1,1)-SSTD	0.8656	0.1293	0.6549	0.1019	0.7988	0.1959	0.4242	0.0003
	ARMA(1,1)-GARCH(1,1)-GEVD	0.3739	0.5660	0.8477	0.0520	0.0018	0.3054	0.3917	0.0001
	ARMA(1,1)-GARCH(1,1)-GPD	0.9776	0.5188	0.6993	0.2362	0.0067	0.2661	0.3640	0.0009
	ARMA(1,1)-GARCH(1,1)-GLD	0.7556	0.3733	0.8477	0.0520	0.7555	0.2932	0.3917	0.0001
ARMA(1,1)-GARCH(1,1)-PIVD	0.8656	0.1143	0.7015	0.1019	0.7987	0.1833	0.4190	0.0003	
Platinum	ARMA(1,1)-GARCH(1,1)-Normal	3.2e-06	0.3998	0.0307	0.0020	4.4e-06	0.0401	0.0892	0.0061
	ARMA(1,1)-GARCH(1,1)-Stable	2.1e-08	0.8505	0.9008	0.0020	2.1e-08	0.0309	0.9558	0.0035
	ARMA(1,1)-GARCH(1,1)-GHD _{full}	0.3654	0.7521	0.3998	0.7187	0.2644	0.0355	0.6958	0.3039
	ARMA(1,1)-GARCH(1,1)-NIGD	0.4412	0.9515	0.2173	0.8245	0.2820	0.0264	0.4458	0.2992
	ARMA(1,1)-GARCH(1,1)-GHStD	0.2986	0.4864	0.3998	0.8245	0.0622	0.0474	0.6958	0.2992
	ARMA(1,1)-GARCH(1,1)-VGD	0.2986	0.6047	0.0582	0.8245	0.0622	0.0396	0.1596	0.2991
	ARMA(1,1)-GARCH(1,1)-STD	0.2985	0.2830	0.2427	0.8426	0.0622	0.0304	0.4865	0.2514
	ARMA(1,1)-GARCH(1,1)-SSTD	0.3654	0.6579	0.4765	0.8245	0.2644	0.0399	0.7742	0.2992
	ARMA(1,1)-GARCH(1,1)-GEVD	0.8245	0.6504	0.0030	0.6288	0.2991	0.9014	0.0110	0.2003
	ARMA(1,1)-GARCH(1,1)-GPD	0.8426	0.8505	0.5175	0.8245	0.2513	0.9536	0.8104	0.2992
	ARMA(1,1)-GARCH(1,1)-GLD	0.3654	0.7521	0.1938	0.9342	0.2644	0.0355	0.4064	0.2884
ARMA(1,1)-GARCH(1,1)-PIVD	0.4412	0.6579	0.4765	0.8245	0.2820	0.0399	0.7742	0.2992	
Silver	ARMA(1,1)-GARCH(1,1)-Normal	0.0006	0.0640	0.0035	0.0051	1.5e-05	0.0123	0.0011	0.0136
	ARMA(1,1)-GARCH(1,1)-Stable	0.0030	0.9238	0.8734	0.0444	0.0010	0.1011	0.0171	0.0001
	ARMA(1,1)-GARCH(1,1)-GHD _{full}	0.9219	0.7734	0.4598	0.7495	0.0064	0.1113	0.0539	0.3456
	ARMA(1,1)-GARCH(1,1)-NIGD	0.9219	0.3505	0.0982	0.8563	0.0064	0.0365	0.0217	0.4142
	ARMA(1,1)-GARCH(1,1)-GHStD	0.9219	0.8731	0.4598	0.7495	0.0064	0.1306	0.0539	0.3465
	ARMA(1,1)-GARCH(1,1)-VGD	0.5531	0.1643	0.0472	0.7495	0.0106	0.0234	0.0153	0.3465
	ARMA(1,1)-GARCH(1,1)-STD	0.6480	0.6795	0.1453	0.9665	0.0101	0.0430	0.0365	<0.0001
	ARMA(1,1)-GARCH(1,1)-SSTD	0.9665	0.9745	0.3505	0.8564	0.0074	0.0883	0.3504	<0.0001
	ARMA(1,1)-GARCH(1,1)-GEVD	0.9219	0.1643	0.0855	0.0745	<0.0001	0.0234	0.0181	<0.0001
	ARMA(1,1)-GARCH(1,1)-GPD	0.8564	0.0472	<0.0001	0.8112	<0.0001	0.0153	<0.0001	<0.0001
	ARMA(1,1)-GARCH(1,1)-GLD	0.9219	0.5001	0.1453	0.8563	0.0064	0.0608	0.0365	<0.0001
ARMA(1,1)-GARCH(1,1)-PIVD	0.9219	0.8731	0.5001	0.7496	0.0064	0.1306	0.0608	<0.0001	

Gold Returns

The VaR estimates from the ARMA(1,1)-GARCH(1,1)-Normal model produced the lowest p -values for both Kupiec and Christoffersen tests at 1% and 99% VaR levels. However, the model is adequate at 5% and 95% VaR levels. It is interesting to note that all models were rejected at 99% using the Christoffersen test. An ARMA(1,1)-GARCH(1,1)-Stable model is suitable at 1% and 95% VaR levels. ARMA(1,1)-GARCH(1,1)-GHD_{full} model, ARMA(1,1)-GARCH(1,1)-NIGD model, ARMA(1,1)-GARCH(1,1)-GHStD model, ARMA(1,1)-GARCH(1,1)-STD, ARMA(1,1)-GARCH(1,1)-SSTD, ARMA(1,1)-GARCH(1,1)-GEVD, ARMA(1,1)-GARCH(1,1)-GPD, ARMA(1,1)-GARCH(1,1)-GLD and ARMA(1,1)-GARCH(1,1)-VGD are good models for gold returns. An ARMA(1,1)-GARCH(1,1)-VGD is the best model for VaR estimation of gold returns at different levels.

Platinum Returns

The VaR estimates from an ARMA(1,1)-GARCH(1,1)-N model produced the lowest p -values for both Kupiec and Christoffersen tests at 1%, 95% and 99% VaR levels. The ARMA(1,1)-GARCH(1,1)-GPD model is suitable at 1%, 5% and 99% VaR levels and is the best model for VaR estimation of platinum returns using Kupiec test. It is also suitable at 1%, 5% and 99% based on the Christoffersen test. The ARMA(1,1)-GARCH(1,1)-Stable is the most suitable at 95% VaR levels using both Kupiec test and Christoffersen test. ARMA(1,1)-GARCH(1,1)-STD, ARMA(1,1)-GARCH(1,1)-SSTD, ARMA(1,1)-GARCH(1,1)-GEVD, ARMA(1,1)-GARCH(1,1)-GPD and ARMA(1,1)-GARCH(1,1)-GLD are suitable models for platinum returns based on the Kupiec and Christoffersen tests.

Silver Returns

The ARMA(1,1)-APARCH(1,1)-N model is not suitable using both tests. Using the Kupiec test, ARMA(1,1)-GARCH(1,1)-GHD_{full}, ARMA(1,1)-GARCH(1,1)-NIGD, ARMA(1,1)-GARCH(1,1)-GHStD, ARMA(1,1)-GARCH(1,1)-VGD models are suitable at all VaR levels. However, they are rejected at 1% using the Christoffersen test.

The ARMA(1,1)-GARCH(1,1)-SD model is suitable at 5% and 95% based on the Kupiec test. The ARMA(1,1)-GARCH(1,1)-VGD, ARMA(1,1)-GARCH(1,1)-STD, ARMA(1,1)-GARCH(1,1)-SSTD, ARMA(1,1)-GARCH(1,1)-GEVD, ARMA(1,1)-GARCH(1,1)-GPD and ARMA(1,1)-GARCH(1,1)-GLD model are not suitable at 1% 99% using the Christoffersen test. Based on the Kupiec test, for silver returns the overall best model is ARMA(1,1)-GARCH(1,1)-SSTD.

We evaluated the performance of ARMA-GARCH-Normal, ARMA-GARCH-Stable and ARMA-GARCH-GHDs in characterising precious metal log-returns. The advantage of the proposed models lies in their ability to capture conditional heteroscedasticity in the returns through the GARCH framework and at the same time model their heavy tail behaviour through the Stable Distribution, GLD, GEVD, GPD, STD, PIVD, SSTD and Generalised Hyperbolic Distributions. We also compared the VaR in-sample backtesting of the twelve models using the Kupiec likelihood ratio test and the Christoffersen test.

An ARMA (1,1)-GARCH-Normal model does not fit gold log returns adequately. VaR estimates were obtained from all fitted models, both the Kupiec test and the Christoffersen test showed that an ARMA (1,1)-GARCH(1,1)-VGD model is the best model for VaR estimation at different levels, for gold returns. Interestingly all models were rejected at 99% using the Christoffersen test. An ARMA (1,1)-GARCH(1,1)-SD is a good model for gold returns at 1% and 95% VaR levels. All ARMA-GARCH models with full GHD and its subclasses are all good models for precious metal returns at all different levels using Kupiec test. Thus ARMA (1,1)-GARCH(1,1)-GHD_{full}, ARMA (1,1)-GARCH(1,1)-NIGD, ARMA (1,1)-GARCH(1,1)-GHStD and ARMA (1,1)-GARCH(1,1)-VGD are good models for precious metal returns. Using Kupiec tests, the ARMA(1,1)-GARCH(1,1)-STD, ARMA(1,1)-GARCH(1,1)-SSTD, ARMA(1,1)-GARCH(1,1)-GEVD, ARMA(1,1)-GARCH(1,1)-GPD and ARMA(1,1)-GARCH(1,1)-GLD model are suitable for precious metal returns. An ARMA (1,1)-GARCH(1,1)-NIGD is the best model for platinum returns. The overall best model for silver returns is ARMA(1,1)-GARCH(1,1)-SSTD based on the Kupiec test.

In general, the performance of the models in terms of VaR estimation is comparable at different levels.

With forecasted volatility, absolute magnitude of returns and quantiles may be predicted for risk management and portfolio management purposes. The volatility of a stock generally exhibits either a positive or negative shock which has different implications for the portfolio manager and risk management. For instance, the declining stock prices tend to increase the firm's leverage (debt-to-equity) ratio making the stock a riskier asset. This results in increased volatility of returns to stockholders and reduced demand for the stock due to investors' risk aversion. Thus, the results of this study provide an impetus for investors and the risk management community to consider a holistic, yet more accurate, measure of stock volatility on gold prices.

The ARMA-APARCH model

In this section, the ARMA APARCH model is used to describe the precious metal return series. While Pearson type-IV (PIVD) and the Generalised Hyperbolic Distributions and its subclasses are proposed as potential candidates for the innovations.

The first step is to fit the ARMA-APARCH model to the returns. Table 7.11 records the parameter estimates for the ARMA-APARCH(1,1) model with Gaussian innovations. All parameters are statistically significant. The Ljung-Box test statistics for standardised residuals all have p -values greater than 0.05. In addition, the Ljung-Box test statistics of the squared residuals also have p -values greater than 0.05. This indicates that ARMA(1,1)-APARCH(1,1) is adequate for gold and platinum returns and AR(1)-APARCH(1,1) for silver returns. AIC and SBI were used to select the best model for each of the returns.

Combining APARCH model with the Pearson type-IV distribution

The standardised residuals were extracted from the ARMA-APARCH models. The descriptive analyses of the standardised residuals in Table 7.12 indicate that they are realised from a heavy-tailed distribution. These findings promote the use of full

GHD, NIGD, VGD, GHStD, GLD, GEVD, SD, GPD and PIVD in modelling the standardised residuals as suggested by McNeil and Frey (2000).

The Pearson type-IV Distribution is fitted to the standardised residuals extracted from the GARCH model with Normal innovations. The parameters are estimated using the method of Maximum likelihood. The Maximum likelihood procedure is carried out using the R package Pearson DS. Table 7.13 shows the ML estimates of the Pearson type-IV distribution fitted to the standardised residuals of the ARMA-APARCH (1,1) model with Normal innovations. Based on the AD test, there is strong evidence that we cannot reject the null hypothesis that the standardised residuals follow the Pearson type-IV distribution.

Table 7.11: Parameter estimates for the ARMA (1,1)-APARCH (1,1) model with Gaussian Innovations

	Gold returns		Platinum Returns		Silver Returns	
Mean equation						
	Estimate	<i>p</i> -value	<i>Estimate</i>	<i>p</i> -value	<i>Estimate</i>	<i>p</i> -value
ϕ	-6.898e-01	0.011497	-8.289e-01	3.33e-15	-9.238e-02	3.46e-10
θ	6.858e-01	0.013593	8.490e-01	<0.001	0.000000	-
Variance equation						
	Estimate	<i>p</i> -value	<i>Estimate</i>	<i>p</i> -value	<i>Estimate</i>	<i>p</i> -value
α_0	2.204e-06	0.000204	2.912e-05	1.03e-05	9.692e-06	0.000505
α_1	8.207e-02	<0.001	1.004e-01	<0.001	6.323e-02	<0.001
γ_1	-1.234e-01	0.000100	-8.631e-02	0.0094	-1.222e-01	0.000480
β_1	9.265e-01	<0.001	9.106e-01	<0.001	9.443e-01	<0.001
δ	1.693	<0.001	1.364e+00	<0.001	1.545e+00	<0.001

Table 7.12: Descriptive Statistics of Standardised residuals of the ARMA(1,1)-APARCH (1,1) model with Gaussian Innovations

Descriptive statistics	Gold	Platinum	Silver
Minimum	-11.374510	-5.451543	-11.147371
Maximum	8.985934	6.269666	6.060636
Mean	0.024892	0.023259	0.015779
Standard deviation	1.001264	1.004506	1.005391
Skewness	-0.058249	0.001335	-0.312938
Excess Kurtosis	6.826097	2.221601	5.369963
Jarque-Bera test (p -value)	<0.001	<0.001	<0.001

Table 7.13: ML parameter estimates of the Pearson type-IV distribution for the ARMA(1,1)-APARCH (1,1)-Pearson type-IV model

Returns	\hat{m}	\hat{v}	$\hat{\lambda}$	\hat{a}	AD test	
					Statistic	p -value
Gold	2.845817	0.05477293	0.0484141	1.64519	0.7712	0.5022
Platinum	3.290102	0.168224	0.09219255	1.908614	0.1875	0.9934
Silver	3.010683	0.1591492	0.08540718	1.742093	0.2042	0.9892

Combining APARCH model with the Generalised Hyperbolic distribution and its subclasses

We fit full GHD, NIGD, VGD and GHStD to the standardised residuals extracted from the ARMA-APARCH model. The ML parameter estimates and the AD goodness-of-fit tests results are shown in Table 7.14 and Table 7.15 respectively. The results for the AD test show that the standardised residuals follow full GHD and subclasses NIGD, VGD and GHStD.

Table 7.14: ML parameter estimates of the full GHD for the ARMA(1,1)-APARCH (1,1)-GHDs model

Returns	Model	alpha	beta	delta	mu	lambda
Gold	GHD _{full}	1.088611	-0.02509541	1.040878	0.0457103	-0.4677474
	NIGD	1.056933	-0.01144674	1.039805	0.03604058	-0.5000
	VGD	1.754253	-0.0095166	0.0000	0.03397757	1.497852
	GHStD	0.2118817	0.2118817	2.271571	-0.2112665	-3.638579
Platinum	GHD _{full}	1.570932	-0.0320112	0.9093495	0.06162931	0.5507648
	NIGD	1.242034	-0.03686325	1.245575	0.06025677	-0.5000
	VGD	2.047528	-0.0323519	0.0000	0.05511616	2.081978
	GHStD	0.03246213	-0.03246213	1.91036	0.05615237	-2.792913
Silver	GHD _{full}	0.1331804	-0.04191774	1.741526	0.05835805	-2.496682
	NIGD	1.149471	-0.04374491	1.13436	0.05885885	-0.5000
	VGD	1.940429	-0.03312781	0.0000	0.0481042	1.835648
	GHStD	0.04117774	-0.04117774	1.74296	0.0572794	-2.512545

Table 7.15: Anderson Darling Goodness of-fit tests for precious metal returns

Model	Gold returns		Platinum returns		Silver returns	
	Statistic	<i>p</i> -value	Statistic	<i>p</i> -value	Statistic	<i>p</i> -value
ARMA(1,1)-APARCH (1,1)-GHD _{full}	1.0073	0.3534	0.4249	0.8238	0.1985	0.9908
ARMA(1,1)-APARCH (1,1)-NIGD	0.34103	0.9045	0.2296	0.9801	0.44237	0.8059
ARMA(1,1)-APARCH (1,1)-VGD	0.24667	0.9721	0.48434	0.7628	0.91699	0.4039
ARMA(1,1)-APARCH(1,1)-GHStD	0.27268	0.9572	0.2019	0.9899	0.19871	0.9908
ARMA(1,1)-APARCH(1,1)-STD	0.79681	0.4833	0.31006	0.9304	0.28556	0.9486
ARMA(1,1)-APARCH(1,1)-SSTD	0.77381	0.5003	0.20161	0.99	0.2205	0.9838

Table 7.16: ML parameter estimates of the FMKL GLD for the ARMA(1,1)-APARCH(1,1)-GLD model.

Returns	$\hat{\lambda}_1$	$\hat{\lambda}_2$	$\hat{\lambda}_3$	$\hat{\lambda}_4$	AD test	
					Statistic	<i>p</i> -value
Gold	0.0281	2.1738	-0.0968	-0.0925	0.46154	0.7862
Platinum	0.0318	1.9904	-0.0601	-0.0475	0.22458	0.9822
Silver	0.0287	2.0960	-0.0891	-0.0658	0.34264	0.9030

Table 7.17: ML parameter estimates of the Stable distribution for the ARMA (1, 1)-APARCH(1,1)-SD model.

Returns	$\hat{\alpha}$	$\hat{\beta}$	$\hat{\gamma}$	$\hat{\delta}$	AD test	
					Statistic	<i>p</i> -value
Gold	1.7781	0.0005	0.6038	0.0264	2.9468	0.02912
Platinum	1.8054	-0.1090	0.6268	0.0377	0.94502	0.3875
Silver	1.7847	-0.0982	0.6070	0.0335	0.63321	0.6172

ARMA-APARCH models

FMKL GLD, SD, GEVD and GPD are fitted to the standardised residuals extracted from the ARMA(1,1)-APARCH(1,1) models. The ML parameter estimates and AD test results of the FMKL GLD are shown in Table 7.17. The AD test results suggest that the extracted residuals follow FMKL GLD. Table 7.18, Table 7.19 and Table 7.20 show the ML estimates of the SD, GEVD and GPD respectively fitted to the standardised residuals extracted from the ARMA(1,1)-APARCH(1,1) models with Normal innovations. The AD test statistics are significant for SD (except for gold returns) and GEVD (except for positive standardised platinum residuals). The GPD diagnostic plots are presented in Figures 7.19, 7.20, 7.21, 7.22 and 7.23. The P-P plot indicate that the standardised residuals follow the GPD. However, for positive gold and negative platinum standardised residuals the Q-Q plots show some deviations from the straight line suggesting a poor GPD fit.

Table 7.18: ML parameter estimates of GEVD for the ARMA(1,1)-APARCH(1,1)-GEVD model

Returns	Standardised Residuals	$\hat{\xi}$ (Se)	$\hat{\mu}$ (Se)	$\hat{\sigma}$ (Se)	AD test	
					Statistic	<i>p</i> -value
Gold	Positive	0.0296(0.0182)	0.7628(0.0209)	0.5507(0.0533)	0.5073	0.7393
	Negative	0.0268(0.0173)	0.7252(0.0206)	0.6029(0.0149)	0.4035	0.8453
Platinum	Positive	-0.0865(0.0095)	0.8200(0.0230)	0.6957(0.0148)	6.3915	0.0006
	Negative	0.0096(0.0202)	0.7703(0.02070)	0.6001(0.0149)	0.2517	0.9695
Silver	Positive	0.0140(0.0182)	0.7944(0.0201)	0.5884(0.0143)	1.2616	0.2452
	Negative	0.0541(0.0189)	0.7539(0.0202)	0.5891(0.0147)	0.4943	0.7526

*Se means standard error

Table 7.19: ML parameter estimates of GPD for the ARMA(1,1)-APARCH(1,1)-GPD model.

Returns	Standardised Residuals	Threshold	No. of Exceedances	$\hat{\xi}$ (Se)	$\hat{\beta}$ (Se)
Gold	Positive	1.7135	1348	0.1631(0.0700)	0.5661(0.0553)
	Negative	1.9059	1069	0.1699(0.0817)	0.5416(0.0622)
Platinum	Positive	1.7759	1357	0.1189(0.0903)	0.5979(0.0694)
	Negative	1.7951	1213	-0.0531(0.0646)	0.7193(0.0710)
Silver	Positive	1.6648	1467	0.1154(0.0833)	0.6010(0.0647)
	Negative	1.8427	1177	0.1626(0.0833)	0.6445(0.0731)

*Se means standard error

VaR estimates and Backtesting

VaR is calculated for each model and tests performed at 1%, 5% for long positions and at 95% and 99% for short positions of trade. These results are vital in the determination of VaR forecasting adequacy of the different models on the metal returns. Table 7.20 presents VaR estimates for the ARMA(1,1)-APARCH(1,1)-Normal, ARMA(1,1)-APARCH(1,1)-STD, ARMA(1,1)-APARCH(1,1)-SSTD, ARMA(1,1)-APARCH(1,1)-PIVD, ARMA(1,1)-APARCH(1,1)-GHD_{full}, ARMA(1,1)-APARCH(1,1)-NIGD, ARMA(1,1)-APARCH(1,1)-VGD, ARMA(1,1)-APARCH(1,1)-GHStD, ARMA(1,1)-APARCH(1,1)-GLD, ARMA(1,1)-APARCH(1,1)-GEVD, ARMA(1,1)-APARCH(1,1)-SD and ARMA(1,1)-APARCH(1,1)-GPD models at different levels of significance. The p -values of the Kupiec and Christoffersen tests, for different distributions are summarised in Table 7.21.

Gold returns

Using Kupiec LR test, the p -values for all fitted models (except ARMA(1,1)-APARCH(1,1)-N at 1% and 99% VaR levels) are greater than 0.05. Thus the null hypothesis of model adequacy is not rejected at all VaR levels under investigation. The best model is selected at different VaR levels using p -values of Kupiec LR and Christoffersen test statistics. The model with the highest p -value is selected as a robust model. We ob-

serve that at 1%, 5%, 95% and 99% VaR levels, the Kupiec LR test indicate the fitted ARMA(1,1)-APARCH(1,1) models with STD, SSTD, GHD_{full} , NIGD, VGD, GHStD, GEVD, GPD and GLD innovations are suitable models. However, all these models were rejected at 99% using the Christoffersen test. The ARMA-APARCH-GLD is the best model based on Christoffersen test statistics.

Platinum returns

ARMA(1,1)-APARCH (1,1) models with STD, SSTD, GHD_{full} , NIGD, VGD, GHStD, GEVD, GPD and GLD innovations are suitable models using the Kupiec LR test. ARMA(1,1)-APARCH (1,1)-GLD model has highest p-values at 5% and 99% VaR levels. Using the Christoffersen test, the best model is ARMA(1,1)-APARCH(1,1)-GPD. It is interesting to note that the ARMA-APARCH (1,1)-GPD is suitable at all VaR levels using both the Kupiec LR and Christoffersen tests.

Silver returns

For the Kupiec test, AR(1)-APARCH (1,1)-GLD provides the largest p -value at 1% VaR and AR(1)-APARCH (1,1)-SD at 95% VaR level. AR(1)-APARCH (1,1)- GHD_{full} performed favourably well using the Christoffersen test. AR(1)-APARCH (1,1)-GEVD and AR(1)-APARCH (1,1)-NIGD are only suitable at 5% and 1% respectively and AR(1)-APARCH(1,1)-VGD are not suitable at all VaR levels based on the Christoffersen test.

For all the three metals based on Kupiec and Christoffersen tests ARMA(1,1)-APARCH (1,1)-STD and ARMA(1,1)-APARCH (1,1)-SSTD are suitable at 1%, 5% and 95%. The proposed models performed favourably well compared with APARCH models with Student-t distribution and APARCH models with skewed Student-distribution usually used in the literature (Laurent, 2003a, 2003b; Degiannakis, 2004).

Table 7.20: VaR estimates for the ARMA(1,1)-APARCH (1,1) model combined with different distributions

Returns	Model	VaR estimates			
		1%	5%	95%	99%
Gold	ARMA(1,1)-APARCH(1,1)- Normal	-2.30417	-1.621881	1.671664	2.353953
	ARMA(1,1)-APARCH(1,1)-STD	-2.600636	-1.526073	1.580221	2.654784
	ARMA(1,1)-APARCH(1,1)-SSTD	-2.62081	-1.535501	1.570769	2.634412
	ARMA(1,1)-APARCH(1,1)-PIVD	-2.624472	-1.53544	1.570867	2.631156
	ARMA(1,1)-APARCH(1,1)-GHD _{full}	-2.65662	-1.570405	1.589533	2.63322
	ARMA(1,1)-APARCH(1,1)-NIGD	-2.650796	-1.563979	1.602656	2.66931
	ARMA(1,1)-APARCH(1,1)-VGD	-2.609919	-1.592015	1.632592	2.639719
	ARMA(1,1)-APARCH(1,1)-GHStD	-2.35549	-1.552049	1.648013	2.704532
	ARMA(1,1)-APARCH(1,1)-GEVD	-2.6027	-1.5607	1.6057	2.6611
	ARMA(1,1)-APARCH(1,1)-GPD	-2.5403	-1.6259	1.6032	2.6120
	ARMA(1,1)-APARCH(1,1)-GLD	-2.636654	-1.546968	1.592352	2.664543
ARMA(1,1)-APARCH(1,1)-SD	-2.658062	-1.501585	1.554464	2.71094	
Platinum	ARMA(1,1)-APARCH(1,1)-Normal	-2.313344	-1.628846	1.675364	2.359863
	ARMA(1,1)-APARCH(1,1)-STD	-2.577053	-1.563667	1.62086	2.634247
	ARMA(1,1)-APARCH(1,1)-SSTD	-2.621893	-1.584987	1.599425	2.58813
	ARMA(1,1)-APARCH(1,1)-PIVD	-2.631561	-1.58532	1.599248	2.580328
	ARMA(1,1)-APARCH(1,1)-GHD _{full}	-2.622574	-1.612667	1.646417	2.619109
	ARMA(1,1)-APARCH(1,1)-NIGD	-2.633994	-1.604376	1.622608	2.602358
	ARMA(1,1)-APARCH(1,1)-VGD	-2.582821	-1.619776	1.642329	2.576642
	ARMA(1,1)-APARCH(1,1)-GHStD	-2.623602	-1.579847	1.604639	2.58819
	ARMA(1,1)-APARCH(1,1)-GEVD	-2.5910	-1.5922	1.7131	2.6533
	ARMA(1,1)-APARCH(1,1)-GPD	-2.6634	-1.5323	1.5862	2.6066
	ARMA(1,1)-APARCH(1,1)-GLD	-2.629018	-1.591606	1.623518	2.613186
ARMA(1,1)-APARCH(1,1)-SD	-2.72514	-1.562463	1.570441	2.587058	
Silver	ARMA(1,1)-APARCH(1,1)-Normal	-2.322882	-1.637781	1.669339	2.35444
	ARMA(1,1)-APARCH(1,1)-STD	-2.58993	-1.54196	1.590047	2.638017
	ARMA(1,1)-APARCH(1,1)-SSTD	-2.63165	-1.561787	1.570115	2.593936
	ARMA(1,1)-APARCH(1,1)-PIVD	-2.650105	-1.566141	1.565909	2.575951
	ARMA(1,1)-APARCH(1,1)-GHD _{full}	-2.653053	-1.564816	1.567598	2.56699
	ARMA(1,1)-APARCH(1,1)-NIGD	-2.66814	-1.597724	1.591743	2.594975
	ARMA(1,1)-APARCH(1,1)-VGD	-2.595314	-1.612823	1.618278	2.568815
	ARMA(1,1)-APARCH(1,1)-GHStD	-2.657109	-1.564782	1.567069	2.570009
	ARMA(1,1)-APARCH(1,1)-GEVD	-2.6661	-1.5857	1.6029	2.5920
	ARMA(1,1)-APARCH(1,1)-GPD	-2.6659	-1.5636	1.5497	2.5891
	ARMA(1,1)-APARCH(1,1)-GLD	-2.682946	-1.584972	1.584034	2.590284
ARMA(1,1)-APARCH(1,1)-SD	-2.740308	-1.531321	1.531941	2.594307	

Table 7.21: VaR Backtesting for precious metal returns

Returns	Model	<i>p</i> -value of Kupiec test				<i>p</i> -value of Christoffersen test			
		1%	5%	95%	99%	1%	5%	95%	99%
Gold	ARMA(1,1)-APARCH(1,1)-Normal	0.0005	0.1181	0.0782	0.0007	0.0003	0.1131	0.1070	0.0581
	ARMA(1,1)-APARCH(1,1)-STD	0.6497	0.0588	0.7015	0.1019	0.2044	0.0971	0.5657	0.0002
	ARMA(1,1)-APARCH(1,1)-SSTD	0.6497	0.0884	0.4449	0.1019	0.2044	0.1226	0.5371	0.0003
	ARMA(1,1)-APARCH(1,1)-PIVD	0.6496	0.0884	0.4449	0.1019	0.2044	0.1226	0.5371	0.0003
	ARMA(1,1)-APARCH(1,1)-GHD _{full}	0.5497	0.7015	0.7492	0.1019	0.1771	0.5570	0.5608	0.0003
	ARMA(1,1)-APARCH(1,1)-NIGD	0.5497	0.5660	0.9489	0.0737	0.1771	0.4206	0.5148	0.0002
	ARMA(1,1)-APARCH(1,1)-VGD	0.6496	0.7971	0.4776	0.1019	0.2044	0.4040	0.3565	0.0003
	ARMA(1,1)-APARCH(1,1)-GHStD	0.0176	0.2051	0.3000	0.0359	0.0132	0.2440	0.3120	<0.0001
	ARMA(1,1)-APARCH(1,1)-GEVD	0.3001	0.4082	0.9489	0.1019	0.0013	0.5233	0.5148	0.0003
	ARMA(1,1)-APARCH(1,1)-GPD	0.9776	0.5188	0.9489	0.1378	0.0006	0.3871	0.5148	0.0004
	ARMA(1,1)-APARCH(1,1)-GLD	0.5497	0.1458	0.8477	0.1019	0.1771	0.1565	0.5428	0.0003
	ARMA(1,1)-APARCH(1,1)-SD	0.5497	0.0086	0.3734	0.0359	0.1771	0.0162	0.5074	<0.0001
Platinum	ARMA(1,1)-APARCH(1,1)-Normal	0.0140	0.2173	0.0182	0.0008	0.0048	0.0016	0.0544	0.0028
	ARMA(1,1)-APARCH(1,1)-STD	0.2986	0.3760	0.3644	0.9342	0.0014	0.0078	0.6551	0.2884
	ARMA(1,1)-APARCH(1,1)-SSTD	0.4412	0.8009	0.6976	0.6187	0.0013	0.0171	0.9049	0.3024
	ARMA(1,1)-APARCH(1,1)-PIVD	0.7188	0.8505	0.6976	0.6188	0.0644	0.0158	0.9049	0.3024
	ARMA(1,1)-APARCH(1,1)-GHD _{full}	0.4412	0.4764	0.0676	0.9342	0.0013	0.0065	0.1821	0.2884
	ARMA(1,1)-APARCH(1,1)-NIGD	0.7188	0.6505	0.3644	0.8245	0.0645	0.0113	0.6551	0.2992
	ARMA(1,1)-APARCH(1,1)-VGD	0.2986	0.2995	0.0901	0.5259	0.0014	0.0029	0.2331	0.2949
	ARMA(1,1)-APARCH(1,1)-GHStD	0.4412	0.6578	0.6505	0.6188	0.0014	0.0106	0.8745	0.3023
	ARMA(1,1)-APARCH(1,1)-GEVD	0.6188	0.8955	0.0012	0.8426	0.3024	0.9177	0.0045	0.2514
	ARMA(1,1)-APARCH(1,1)-GPD	0.8426	0.0897	0.9974	0.8245	0.2514	0.0944	0.9460	0.2992
	ARMA(1,1)-APARCH(1,1)-GLD	0.4412	0.9515	0.3644	0.9342	0.0013	0.0132	0.6551	0.2884
	ARMA(1,1)-APARCH(1,1)-SD	0.2251	0.3431	0.7044	0.6188	0.0100	0.0081	0.7225	0.3024
Silver	ARMA(1,1)-APARCH(1,1)-Normal	0.0010	0.0342	0.0028	0.0074	0.0133	0.0012	0.0008	0.0186
	ARMA(1,1)-APARCH(1,1)-STD	0.2579	0.9238	0.1851	0.9666	0.0109	0.1011	0.0500	NaN
	ARMA(1,1)-APARCH(1,1)-SSTD	0.4661	0.6771	0.3850	0.4661	0.0682	0.0519	0.1275	NaN
	ARMA(1,1)-APARCH(1,1)-PIVD	0.5531	0.6306	0.3850	0.4661	0.0684	0.0465	0.1275	NaN
	ARMA(1,1)-APARCH(1,1)-GHD _{full}	0.6480	0.6306	0.3850	0.3877	0.0671	0.0466	0.1275	NAN
	ARMA(1,1)-APARCH(1,1)-NIGD	0.7496	0.2874	0.1643	0.4661	0.0644	0.0273	0.0428	NaN
	ARMA(1,1)-APARCH(1,1)-VGD	0.3183	0.0982	0.0290	0.3877	0.0112	0.0057	0.0043	NaN
	ARMA(1,1)-APARCH(1,1)-GHStD	0.6480	0.6306	0.3850	0.3877	0.0671	0.0466	0.1275	NaN
	ARMA(1,1)-APARCH(1,1)-GEVD	0.8112	0.2078	0.0741	0.4661	<0.0001	0.0581	0.0150	<0.0001
	ARMA(1,1)-APARCH(1,1)-GPD	0.8117	0.5001	0.7734	0.4661	<0.0001	0.1065	0.1847	<0.0001
	ARMA(1,1)-APARCH(1,1)-GLD	0.9666	0.3850	0.2078	0.4661	0.0558	0.0219	0.0581	<0.0001
	ARMA(1,1)-APARCH(1,1)-SD	0.6006	0.6795	0.7746	0.4661	0.0320	0.1296	0.1191	<0.0001

NAN-means statistics not available

We examined the volatility dynamics of gold, platinum and silver and explored the corresponding risk management implications. The conditional volatility in price returns of gold are modelled using daily data from 2 April 1994 to 18 September 2014. We used the ARMA-APARCH model to take into account major stylised facts such as volatility clustering and asymmetry in gold price returns and PIVD and GHDs to model heavy tail behavior of standardised residuals. We computed VaR estimates for gold, silver and platinum returns using ARMA-APARCH-PIVD, ARMA-APARCH-GHD_{full}, ARMA-APARCH-NIGD, ARMA-APARCH-VGD, ARMA-APARCH-GHStD, ARMA-APARCH-STD, ARMA-APARCH-SSTD, ARMA-GARCH-GLD, ARMA-GARCH-GPD, ARMA-GARCH-GEVD and ARMA-APARCH-N models.

We also compared the VaR in-sample of backtesting of the three models using the Kupiec test and the Christoffersen test. The backtesting results show that ARMA-APARCH with GHDs, PIVD, SD, GLD, GEVD and GPD perform well in characterising metal returns. For gold returns, VaR is best modelled by an ARMA(1,1)-APARCH(1,1)-GLD. VaR is best modelled by an ARMA(1,1)-APARCH(1,1)-GPD for platinum returns. For silver returns, AR(1)-APARCH(1,1)-GHDs and AR(1)-APARCH(1,1)-PIVD are appropriate at all levels using the Kupiec test. However, there is no best model for the silver return series.

Our findings confirm that taking into account volatility clustering, leverage effect and asymmetry as well as heavy tails in the behavior of time series, combined with filtering process such as PIVD, SD, GEVD, GPD, GLD and GHDs are important in improving risk management assessments and hedging strategies in a highly volatile metal market. GLD, GEVD, GPD, SD, PIVD and GHDs are more appropriate to describe the heavy-tails evident in metal returns. Regulators can determine capital requirements by implementing the dynamic VaR model. We thus propose the GHDs, GLD, SD, GEVD, GPD and PIVD in conjunction with ARMA-APARCH model based on superior in-sample VaR prediction. The proposed models are valid and accurate models performing better than ARMA-APARCH with Student-t Distribution and

ARMA-APARCH skewed Student-t Distribution, providing financial analysts with an alternative distributional scheme to be used in econometric modelling.

7.5 Summary

In this Chapter we improved our models used in Chapter 5 in order to capture additional features of volatility and the leverage effect. We coupled linear GARCH models with some heavy-tailed distribution as innovation. The empirical results show that the ARMA-APARCH model with full GHD, NIGD, NGD, GHStD, GLD, GPD, GEVD, SD and PIVD innovations are suitable for depicting precious metal returns and can be used for VaR estimation.

7.6 Statistical software packages

The main R package used is **rugarch** (Ghalanos,2015). **rugarch** provides a large set of methods to fit, forecast and diagnose a wide variety of AFRIMAX-GARCH models (Ghalanos, 2015). We also used the **fGarch** package to fit GARCH-type models (Wuertz *et al.*, 2016). Other R packages used in data analysis are **ADGofTest** (Bellosa, 2011), **evir** (Pfaff *et al.*, 2012), **evd** (Stephenson, 2002, Stephenson and Ferro, 2015), **ismev** (Heffernan *et al.*, 2012), **ghyp** (Luethi and Breymann, 2016), **PearsonDS** (Becker and Klner, 2017), **fGarch** (Wuertz *et al.*, 2016), **stable** (Robust Analysis Inc, 2013) , **laeken** (Alfons and Templ, 2013) and **GLDEX** (Su, 2007, 2016).

7.7 Appendix

ARMA(1,1)-GARCH(1,1)-GPD model

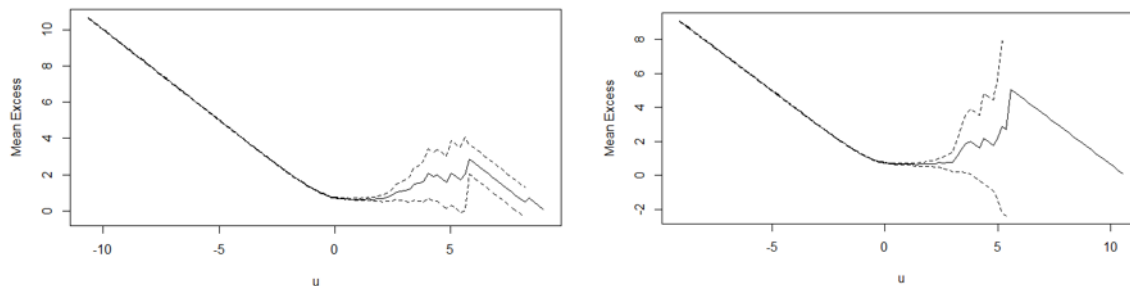


Figure 7.1: Mean excess plot of gold (a) positive (b) negative standardised residuals

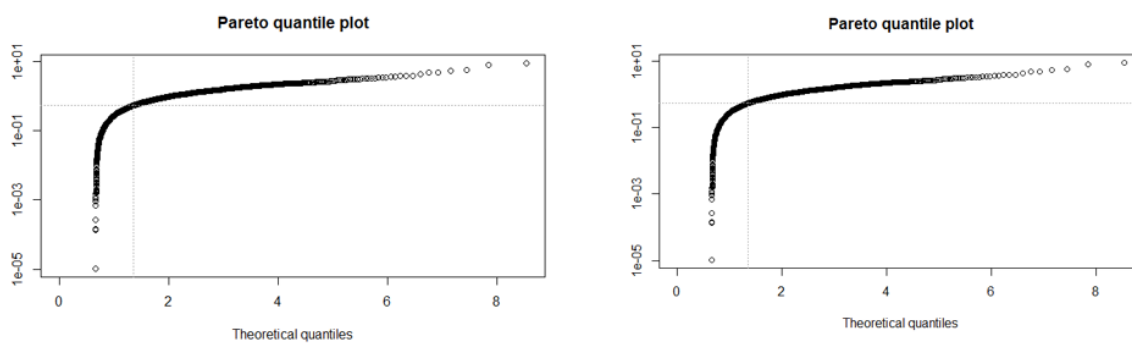


Figure 7.2: Pareto quantile plot of gold (a) positive (b) negative standardised residuals

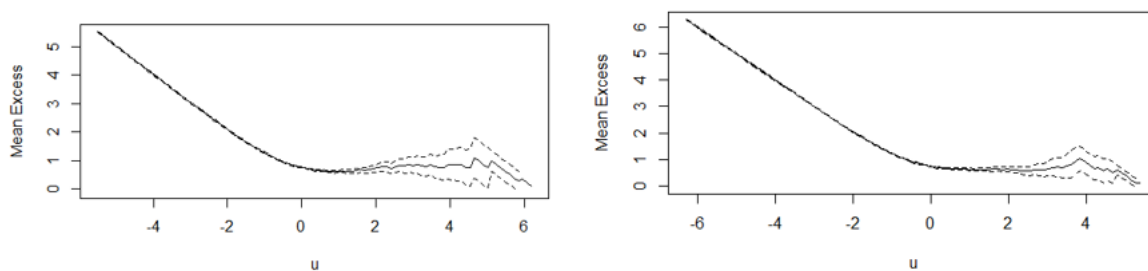


Figure 7.3: Mean excess plot of platinum (a) positive (b) negative standardised residuals

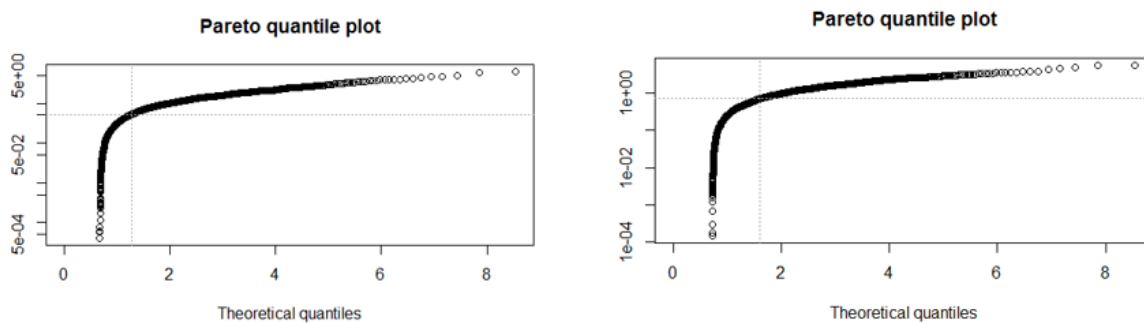


Figure 7.4: Pareto quantile plot of platinum (a) positive (b) negative standardised residuals

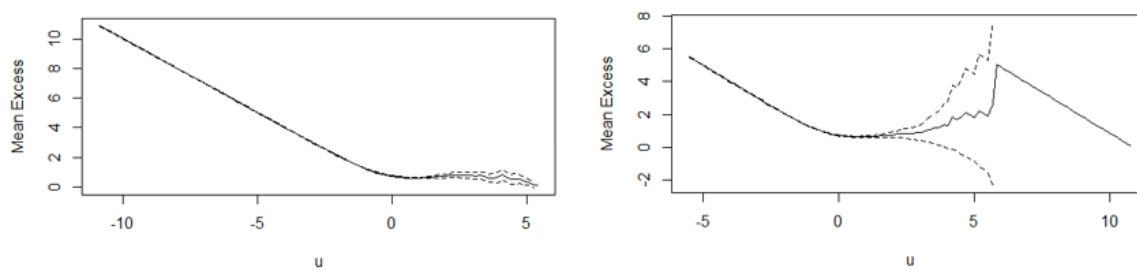


Figure 7.5: Mean excess plot of silver (a) positive (b) negative standardised residuals

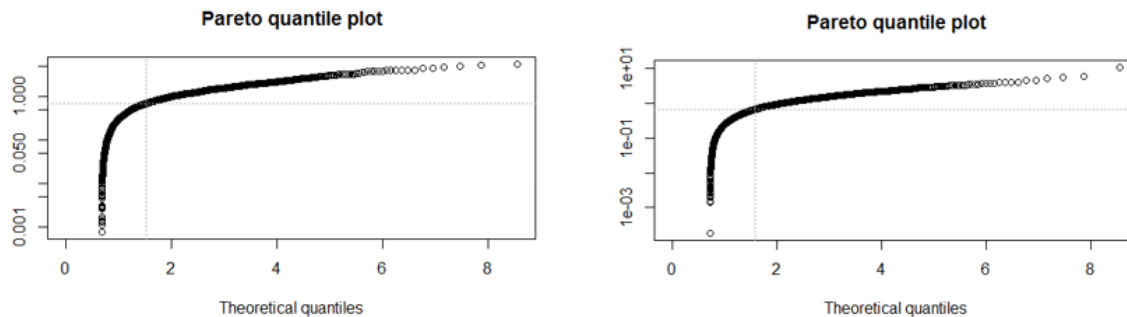


Figure 7.6: Pareto quantile plot of silver (a) positive (b) negative standardised residuals

ARMA(1,1)-APARCH(1,1)-GPD model

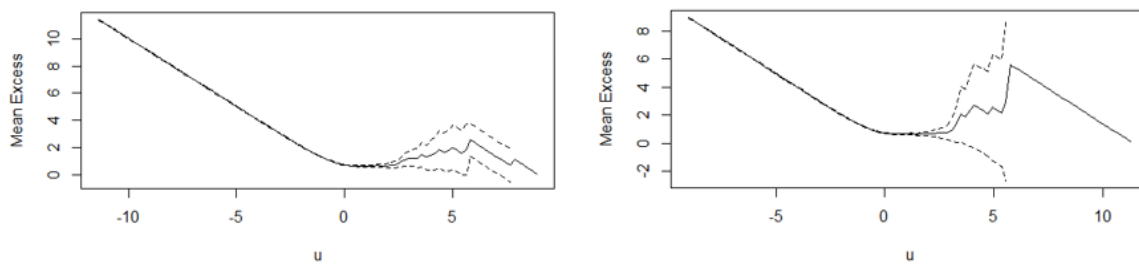


Figure 7.7: Mean excess plot of gold (a) positive (b) negative standardised residuals

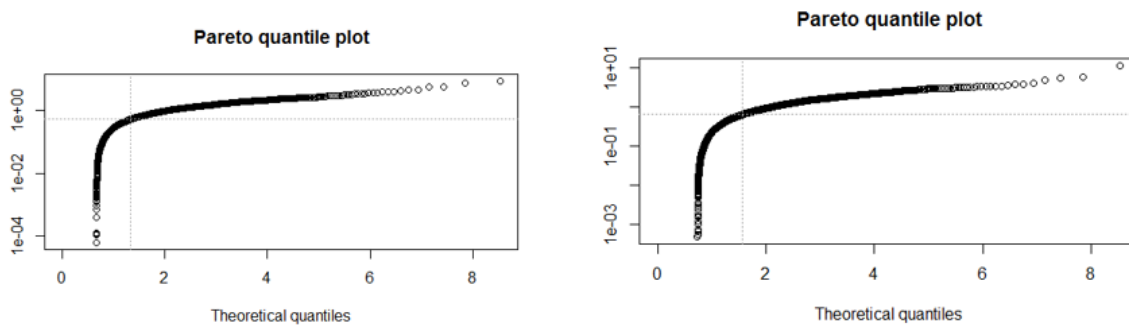


Figure 7.8: Pareto quantile plot of gold (a) positive (b) negative standardised residuals

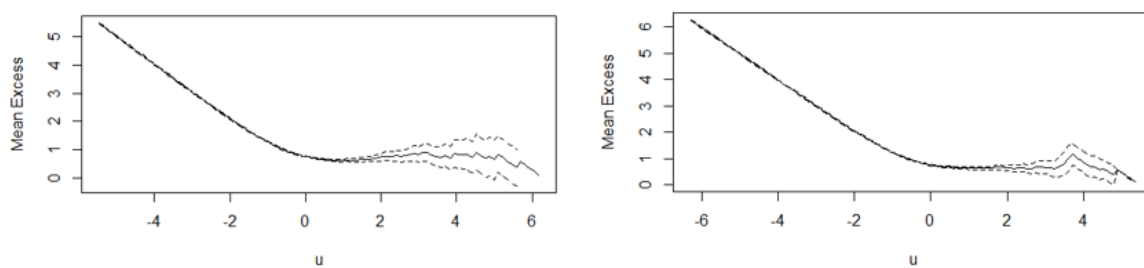


Figure 7.9: Mean excess plot of platinum (a) positive (b) negative standardised residuals

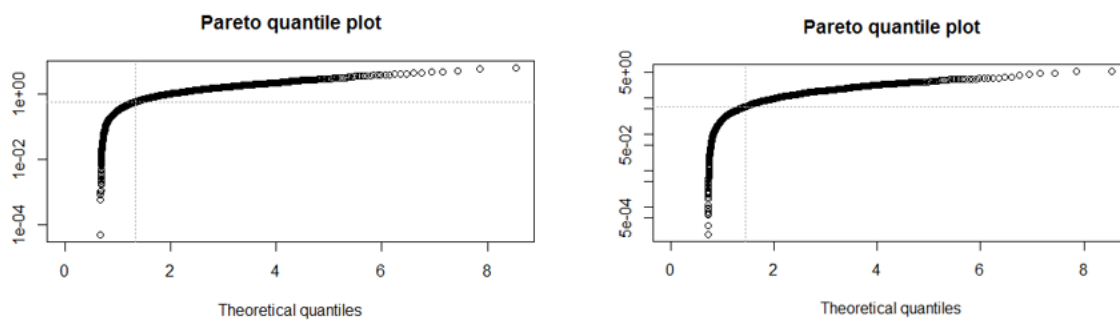


Figure 7.10: Pareto quantile plot of platinum (a) positive (b) negative standardised residuals

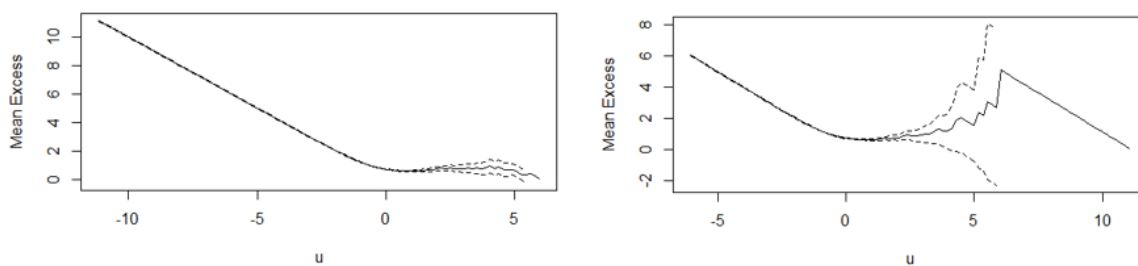


Figure 7.11: Mean excess plot of platinum (a) positive (b) negative standardised residuals

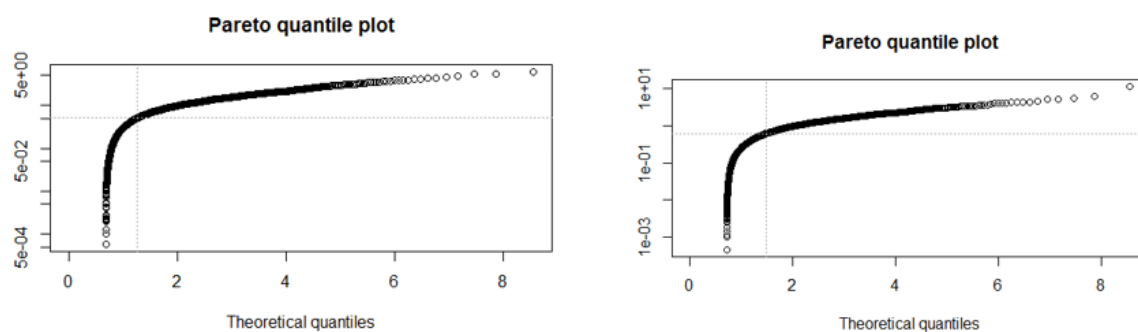


Figure 7.12: Pareto quantile plot of silver (a) positive (b) negative standardised residuals

ARMA(1,1)-GARCH(1,1)-GPD Model

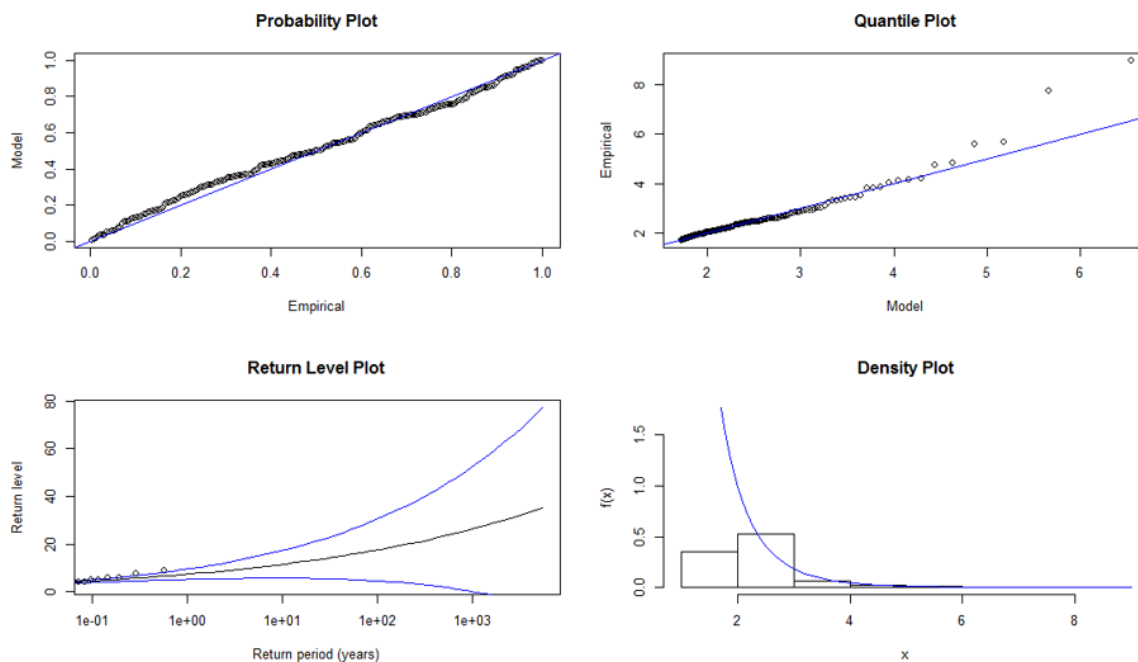


Figure 7.13: GPD Diagnostic plot of positive standardised residuals (gold)

*P-P plot (on the upper left panel), Q-Q Plot (on the upper right panel), Return level plot (on the lower left panel), Density plot (on the lower right panel)

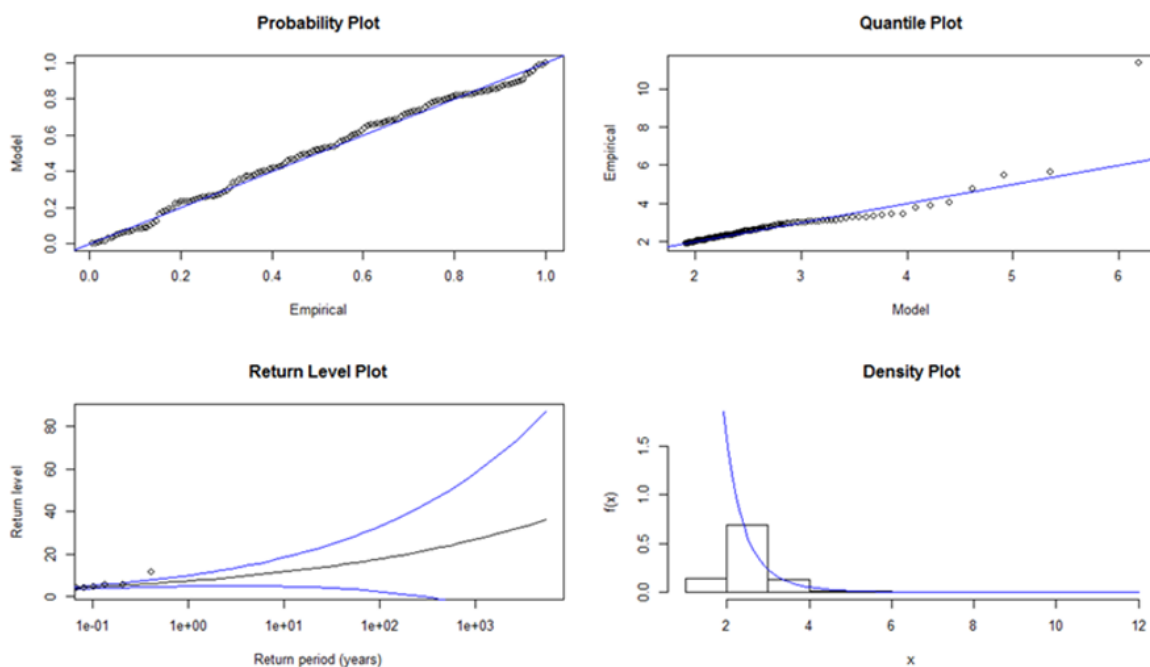


Figure 7.14: GPD Diagnostic plot of negative standardised residuals (gold)

*P-P plot (on the upper left panel), Q-Q Plot (on the upper right panel), Return level plot (on the lower left panel), Density plot (on the lower right panel)

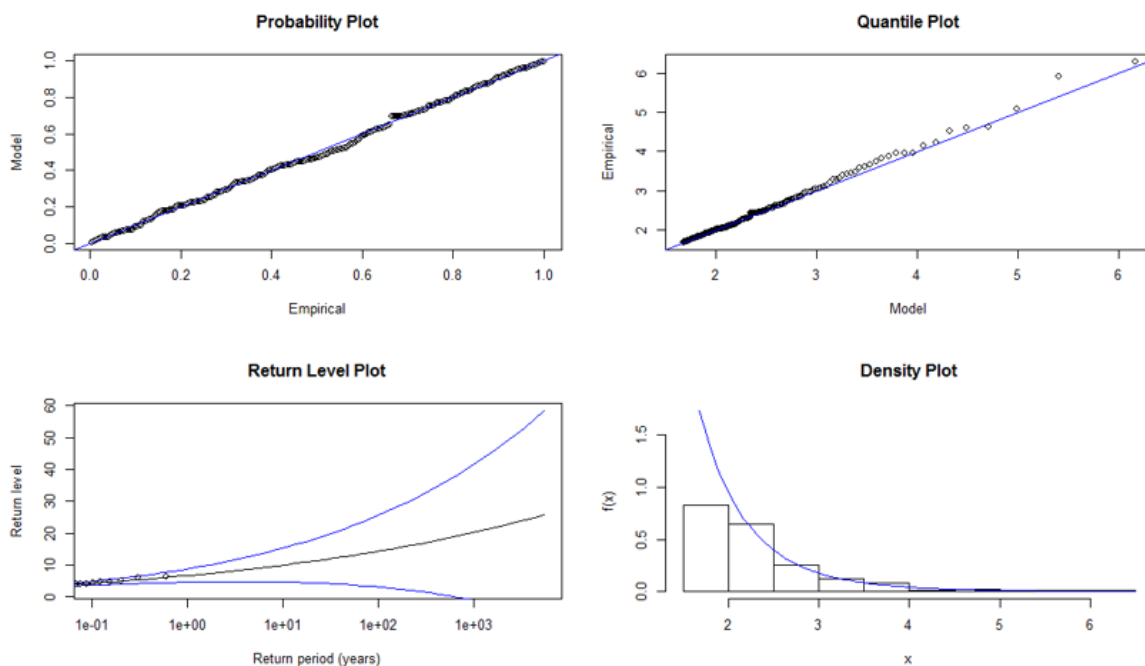


Figure 7.15: GPD Diagnostic plot of positive standardised residuals (platinum)

*P-P plot (on the upper left panel), Q-Q Plot (on the upper right panel), Return level plot (on the lower left panel), Density plot (on the lower right panel)

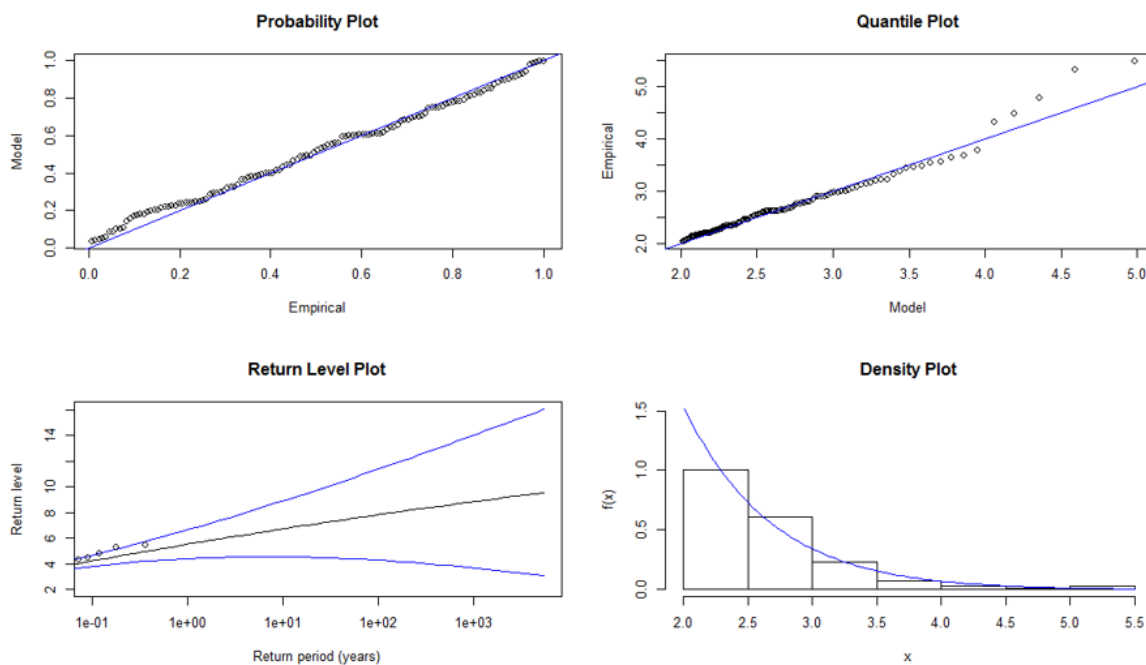


Figure 7.16: GPD Diagnostic plot of negative standardised residuals (platinum)

*P-P plot (on the upper left panel), Q-Q Plot (on the upper right panel), Return level plot (on the lower left panel), Density plot (on the lower right panel)

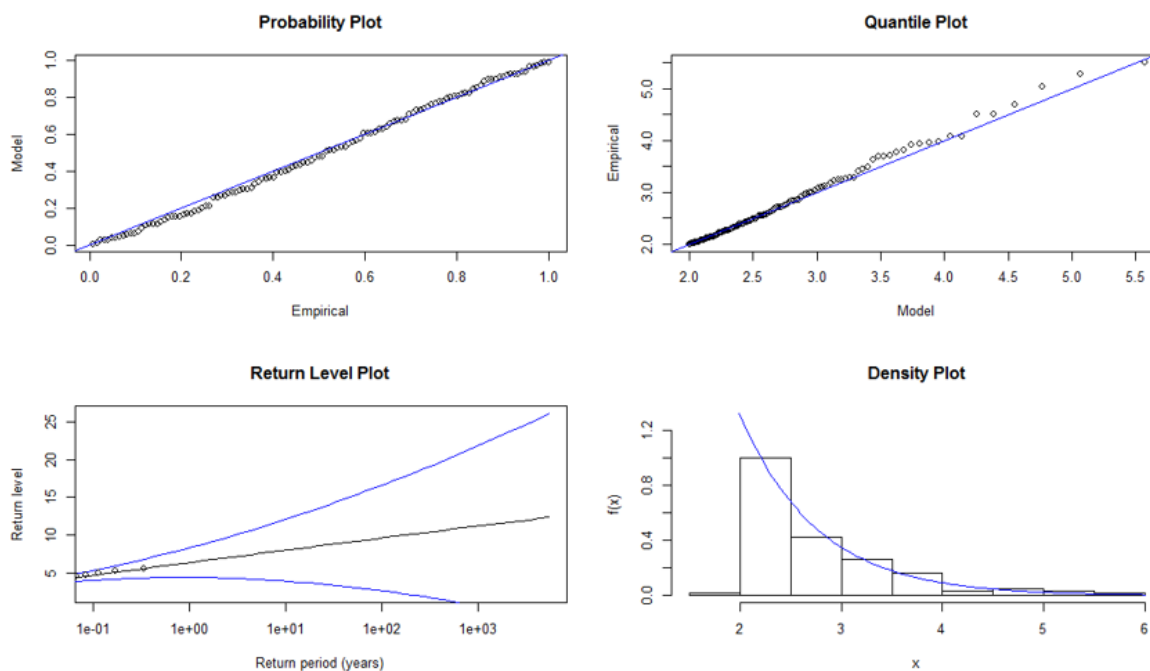


Figure 7.17: GPD Diagnostic plot of positive standardised residuals (silver)

*P-P plot (on the upper left panel), Q-Q Plot (on the upper right panel), Return level plot (on the lower left panel), Density plot (on the lower right panel)

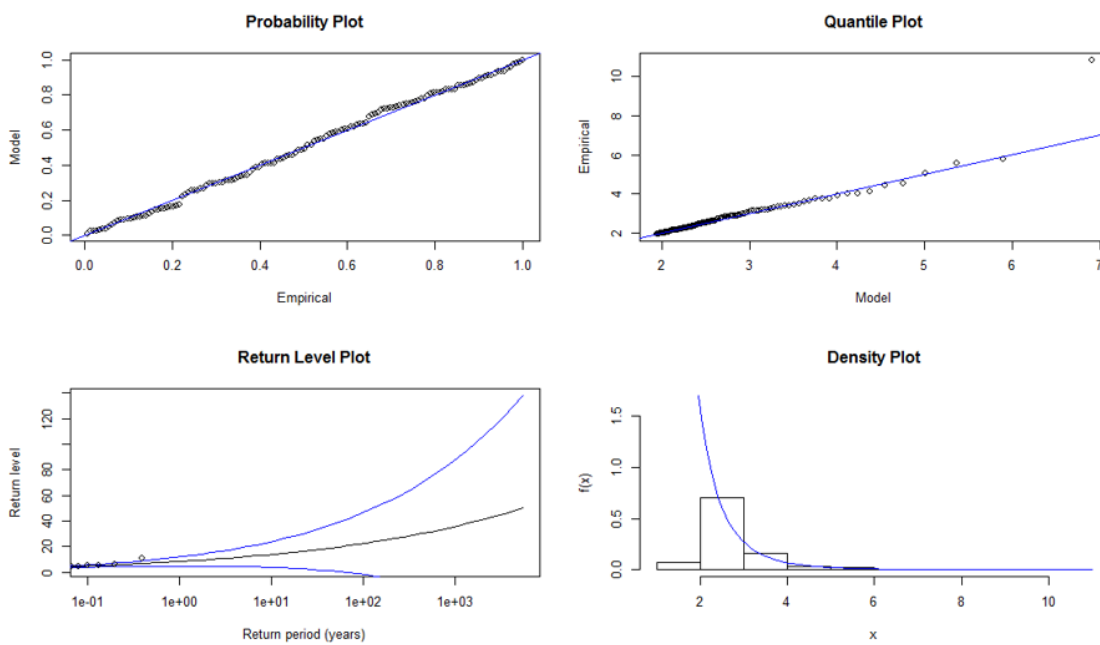


Figure 7.18: GPD Diagnostic plot of negative standardised residuals (silver)

*P-P plot (on the upper left panel), Q-Q Plot (on the upper right panel), Return level plot (on the lower left panel), Density plot (on the lower right panel)

ARMA(1,1)-APARCH(1,1)-GPD Model

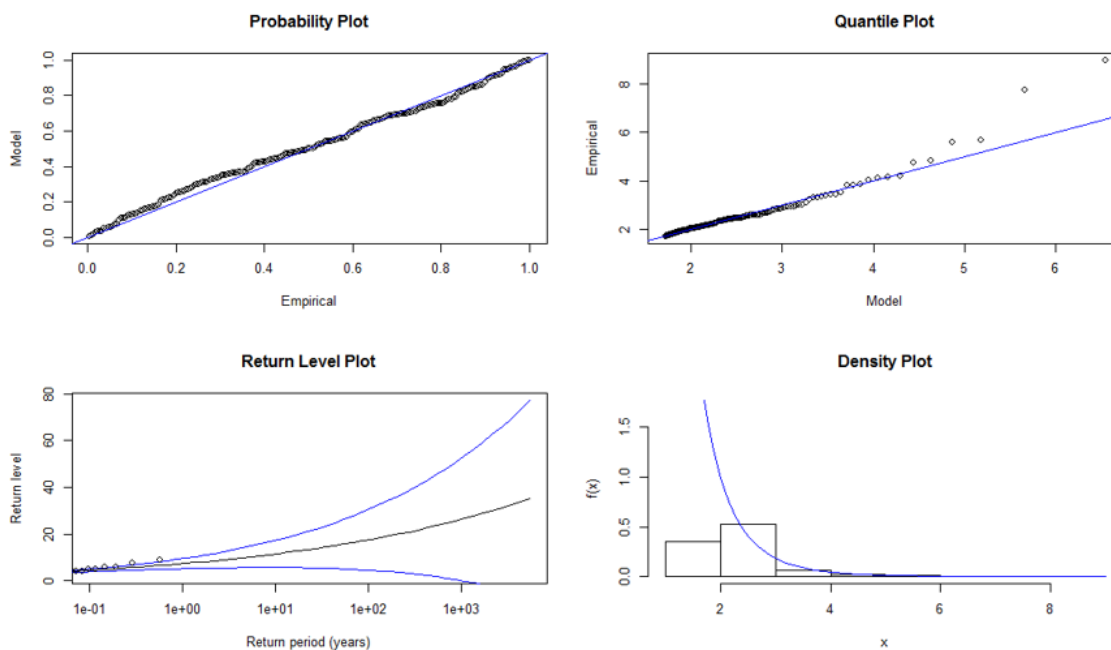


Figure 7.19: GPD Diagnostic plot of positive standardised residuals (gold)

*P-P plot (on the upper left panel), Q-Q Plot (on the upper right panel), Return level plot (on the lower left panel), Density plot (on the lower right panel)

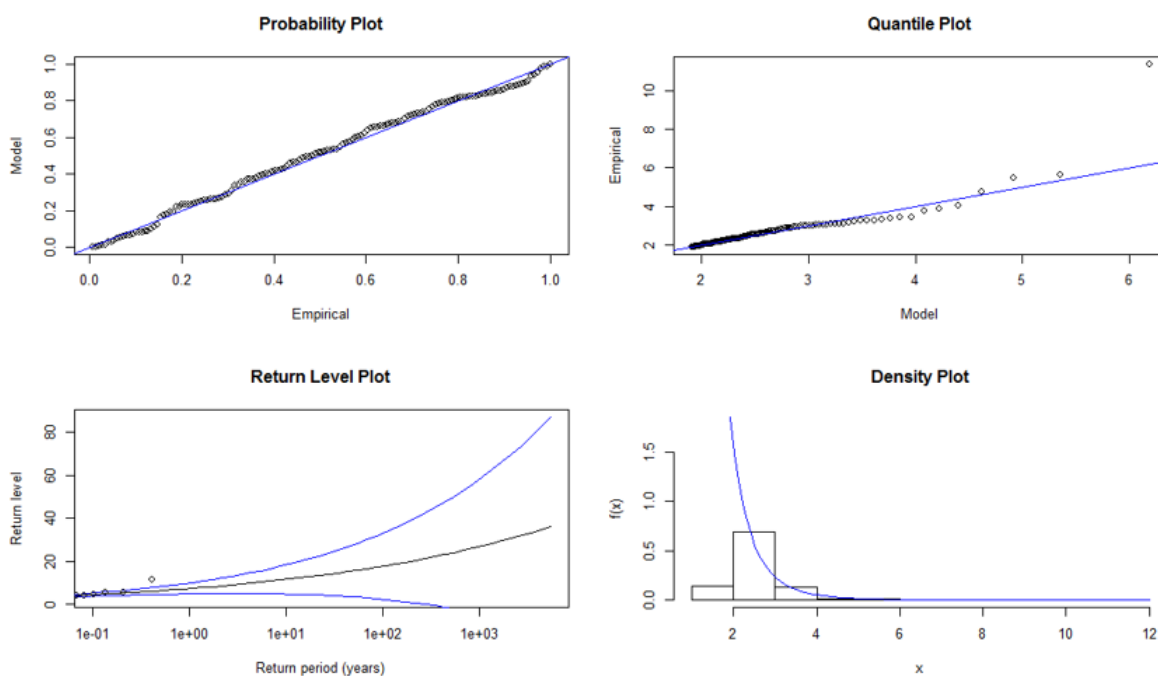


Figure 7.20: GPD Diagnostic plot of negative standardised residuals (gold)

*P-P plot (on the upper left panel), Q-Q Plot (on the upper right panel), Return level plot (on the lower left panel), Density plot (on the lower right panel)

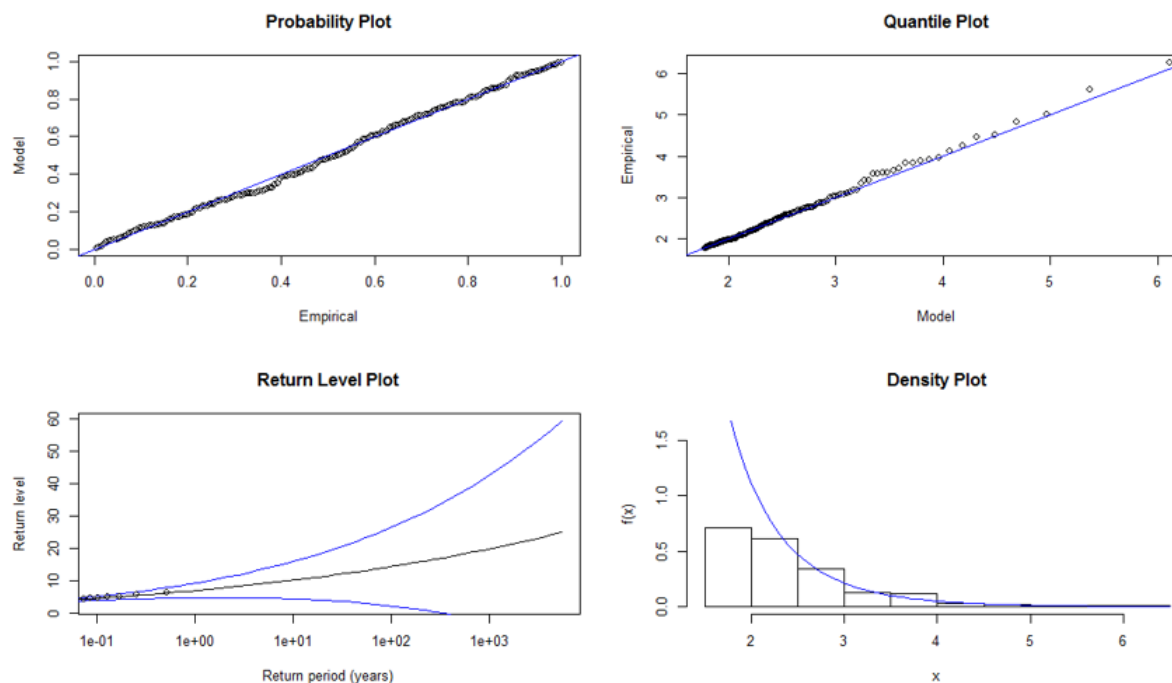


Figure 7.21: GPD Diagnostic plot of positive standardised residuals (platinum)

*P-P plot (on the upper left panel), Q-Q Plot (on the upper right panel), Return level plot (on the lower left panel), Density plot (on the lower right panel)

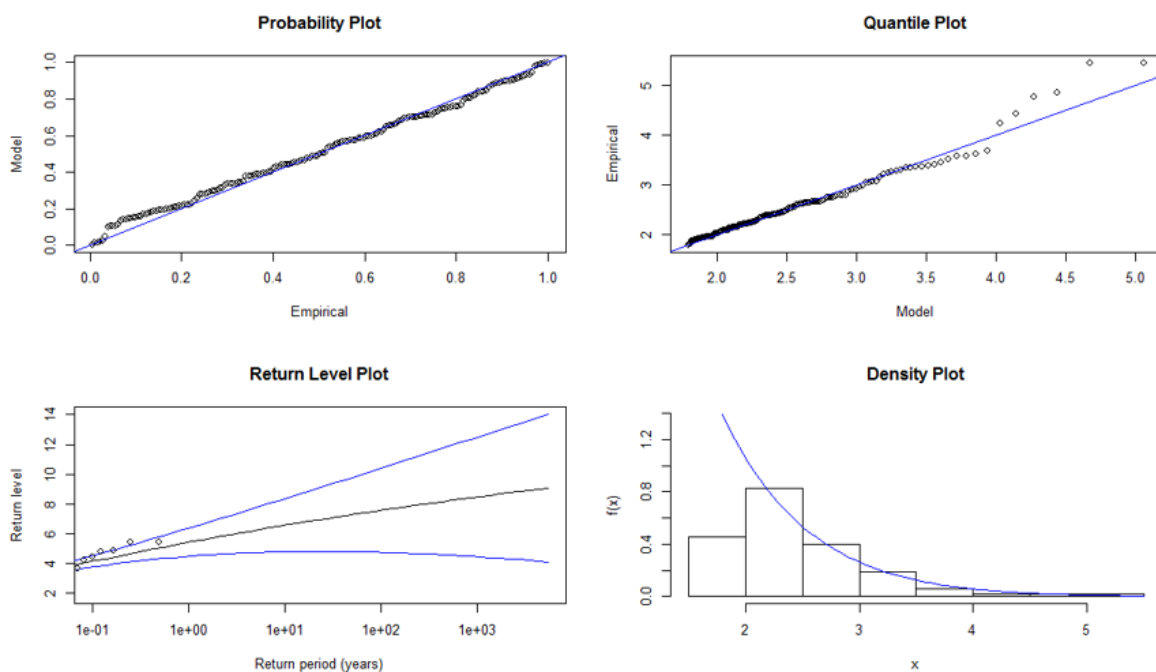


Figure 7.22: GPD Diagnostic plot of negative standardised residuals (platinum)

**P-P plot (on the upper left panel), Q-Q Plot (on the upper right panel), Return level plot (on the lower left panel), Density plot (on the lower right panel)*

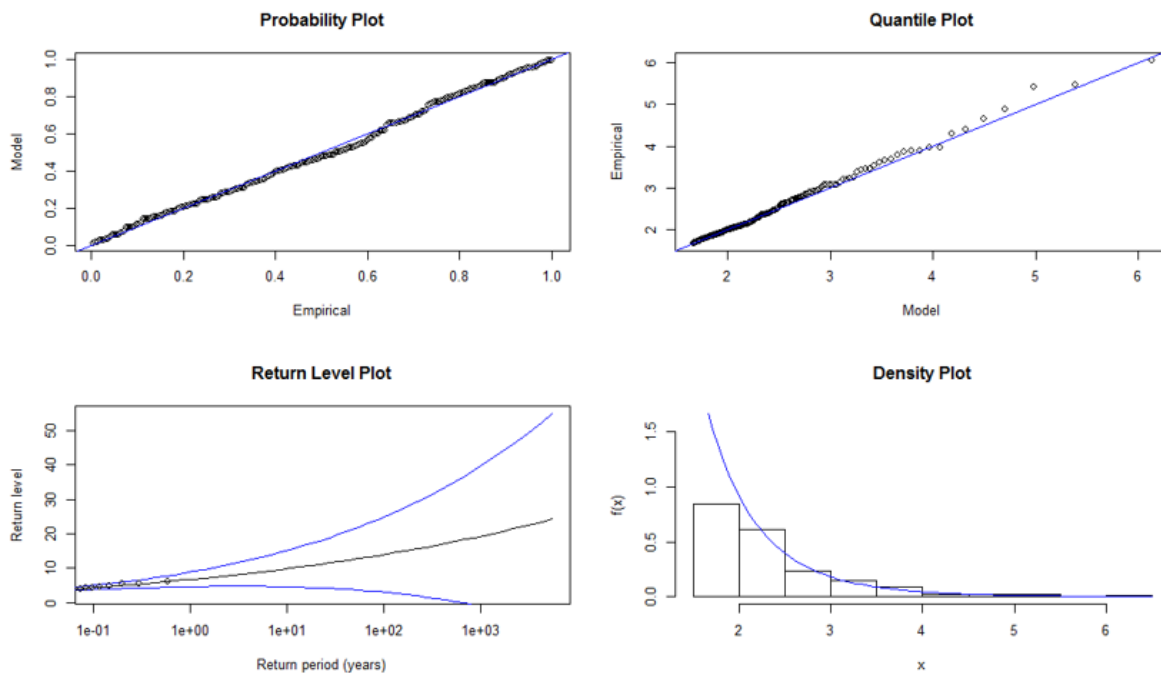


Figure 7.23: GPD Diagnostic plot of positive standardised residuals (silver)

**P-P plot (on the upper left panel), Q-Q Plot (on the upper right panel), Return level plot (on the lower left panel), Density plot (on the lower right panel)*

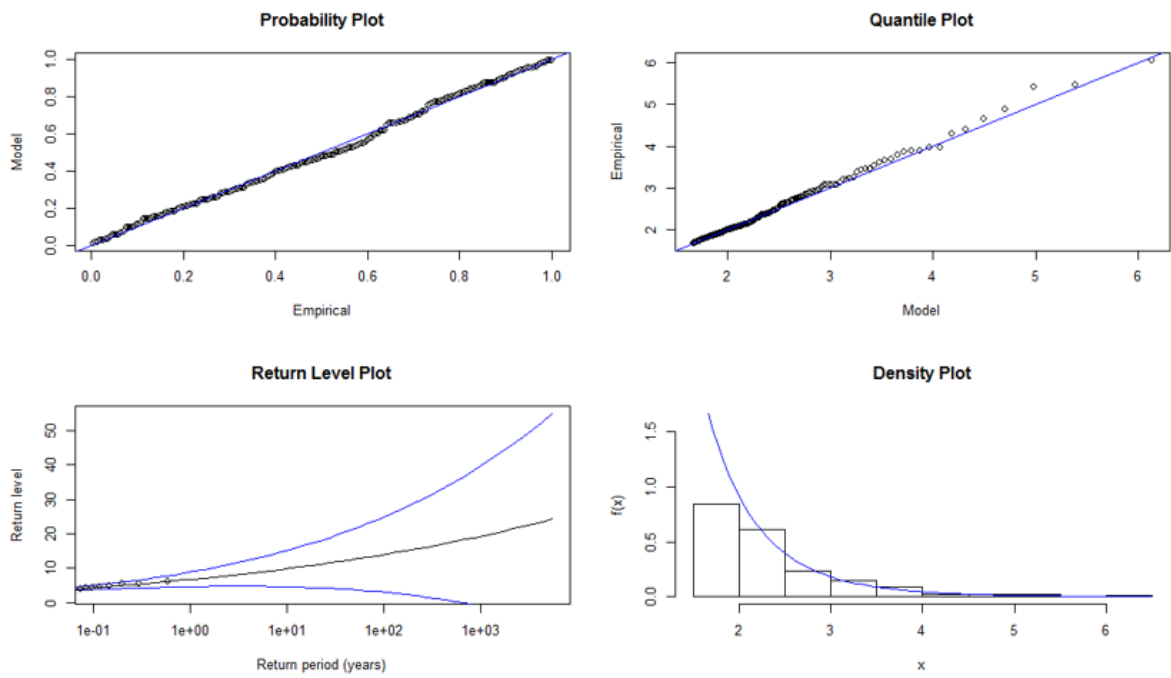


Figure 7.24: GPD Diagnostic plot of negative standardised residuals (silver)

**P-P plot (on the upper left panel), Q-Q Plot (on the upper right panel), Return level plot (on the lower left panel), Density plot (on the lower right panel)*

Chapter 8

Value-at-Risk estimation of precious metal returns: A long memory GARCH-heavy-tailed approach

8.1 Introduction

The Long memory test results in chapter 3 indicate long-range dependence in the daily conditional and volatility process for precious metals returns. In this section, we provide the theory of the long-memory GARCH models used in the study. We fit the long-memory GARCH models to the precious metal returns and provide the empirical results.

8.2 The GARCH-Type Models

This section discusses GARCH type models and their shortcomings. We shall model the metal price returns using ARFIMA-FIGARCH, ARFIMA-HYGARCH and ARFIMA-FIAPARCH processes, starting with the ARFIMA model for the mean (see section 2.9). Without loss of generality we denote the long memory parameters for the mean

and volatility models as d_m and d_v , respectively. The ARFIMA model is discussed in section 2.9.

The GARCH(p, q) model

The GARCH(p, q) framework presents some advantages over the ARCH(q) model as follows:

- It avoids overfitting.
- It is less prone to breach of non-negativity constraints than the standard ARCH(q).

The apparent persistence implied by the estimates of the conditional variance is an empirical finding common to most applied work. This is manifested by the presence of an approximate unit root in the autoregressive polynomial, that is, $1 - \alpha(L) - \beta(L)$, contains a unit root, meaning the shocks are infinitely persistent (Bollerslev et al, 1992). The GARCH(p, q) formulation considers that shocks decay at a fast exponential rate, this specification is not appropriate to describe the long memory and is only suitable for short-memory phenomena. In order to overcome this shortcoming, Engle and Bollerslev(1996) introduced the IGARCH(p, q) integrated GARCH model.

The IGARCH(p, q) Model

The IGARCH is a special type of GARCH model when $\sum_{i=1}^q \alpha_i + \sum_{j=1}^p \beta_j = 1$, and is thus suitable for capturing infinite persistence in the conditional variance. GARCH(p, q) model describes $I(0)$ type processes and IGARCH(p, q) model captures $I(1)$ type processes for the conditional variance as infinite persistence remains important for forecasts of all horizons.

Assuming that $v_t \equiv a_t^2 - \sigma_t^2(p, q)$ IGARCH(p, q) model can be written in the form of an ARMA(p, q) process as

$$[\phi(L)(1 - L)]a_t^2 = \omega + [1 - \beta(L)]v_t, \quad (8.1)$$

where, $\phi(L) = [1 - \alpha(L) - \beta(L)](1 - L)^{-1}$ and all roots of $\phi(L)$ and $[1 - \beta(L)]$ lie outside the unit root circle.

Although, the IGARCH(p, q) model is an improvement of the GARCH(p, q) model, it is not fully satisfactory when describing long memory in the volatility process because the shocks never die out in the IGARCH(p, q) process, and this is an unrealistic assumption. In an attempt to describe the long memory of time series in a realistic way, Baillie et al (1996) introduced a new class of models called the fractional integrated GARCH(p, d, q) model (FIGARCH).

The FIGARCH(p, d, q) Model

The FIGARCH(p, d, q) model allows us to model a slow decay of volatility (long memory behavior), as well as to distinguish between long memory and short memory in conditional variance.

In contrast to an $I(0)$ time series in which shocks die out at a fast exponential rate or an $I(1)$ time series where there is no mean reversion, shocks to an $I(d)$ time series with $0 < d_v < 1$ decay at a very slow hyperbolic rate (see Baillie et al, 1996 for proof).

Formally, the FIGARCH(p, d, q) model can be obtained by replacing the difference operator in equation 8.1 with a fractional differencing operator

$$[\phi(L)(1-L)^{d_v}]a_t^2 = \omega + [1 - \beta(L)]v_t, \quad (8.2)$$

and the conditional variance given by

$$\begin{aligned} \sigma_t^2 &= \omega + \beta(L)\sigma_t^2 + [1 - \beta(L)]a_t^2 - \phi(L)(1-L)^d a_t^2 \\ &= \omega + [1 - \beta(L)]^{-1} + 1 - [1 - \beta(L)]^{-1}\phi(L)(1-L)^d \\ &= \omega[1 - \beta(L)]^{-1} + \lambda(L)a_t^2, \end{aligned} \quad (8.3)$$

where (L) is the lag-operator, $\lambda(L) = \sum_{i=1}^{\infty} \lambda_i L^i$ and $0 \leq d_v \leq 1$. $\lambda(L)$ is an infinite summation which, in practice, has to be truncated. Baillie *et al.* (1996) showed that

$\lambda(L)$ should be truncated at 1000 lags, $(1 - L)^d$ is the fractional differencing operator.

It can be defined as follows:

$$\begin{aligned}
 (1 - L)^d &= \sum_{k=0}^{\infty} \frac{\Gamma(d + 1)L^k}{\Gamma(k + 1)\Gamma(d - k + 1)} \\
 &= 1 - dL - \frac{1}{2}d(1 - d)L^2 - \frac{1}{6}d(1 - d)(2 - d)L^3 \dots\dots\dots \\
 &= 1 - \sum_{k=1}^{\infty} c_k(d)L^k, \tag{8.4}
 \end{aligned}$$

where $c_1(d) = d$, $c_2(d) = (\frac{1}{2})d(1 - d)$ etc.

The main advantage of the FIGARCH(p, d, q) approach compared to the aforementioned methods is that it provides greater flexibility for modelling the conditional variance. It accommodates the covariance stationary GARCH(p, q) model when $d_v = 0$ and the IGARCH(p, q) model when $d_v = 1$, as special cases, i.e. if $d_v = 0$, the model has a short memory and reduces to GARCH(p, q) model. If $d_v = 1$, the model becomes an IGARCH(p, q) whose variance process is no longer mean-reverting.

For the FIGARCH(p, d, q) process the persistence of shocks to the conditional variance or the degree of long memory is measured by the fractional differencing parameter d_v . The advantage of this model is that for $0 < d_v < 1$, it is sufficiently flexible to allow for an intermediate range of long memory because the shocks in variance decrease at a hyperbolic rate (Brunnetti and Gilbert, 2000).

Inequality constraints for FIGARCH(p, d, q) model (Conrad and Haag, 2006)

Inequality constraints are necessary and sufficient conditions that ensure the non-negativity of the conditional variance of the FIGARCH model. The FIGARCH($1, d, 1$) model is definitely the most used specification in empirical applications. Therefore, we discuss the inequality constraints for the FIGARCH ($1, d, 1$) model. Various conditions are available in the literature but the most used conditions are the Conrad and Haag (2006) inequality constraints which use an ARCH(∞) repre-

sentation of the FIGARCH(1, d , 1) using ψ_i coefficients defined by

$$\psi_1 = d + \phi_1 - \beta_1, \quad (8.5)$$

$$\text{and } \psi_i = \beta_1 \psi_{i-1} + (f_i - \phi_1)(-g_{i-1}), \quad \forall i \geq 2 \quad (8.6)$$

and alternatively,

$$\psi_i = \beta_1^2 \psi_{i-2} + [\beta_1(f_{i-1}\phi_1) + (f_i - \phi_1)f_{i-1}](-g_{i-2}), \quad \forall i \geq 3. \quad (8.7)$$

Corollary 1

The conditional variance of the FIGARCH(1, d , 1) is nonnegative if:

Case 1: $0 < \beta_1 < 1$

Either $\psi_1 \geq 0$ and $\phi_1 \leq f_2$ or for $k > 2$ with $f_{k-1} < \phi_1 \leq f_k$, it holds that $\psi_{k-1} \geq 0$.

Case 2: $-1 < \beta_1 < 0$

Either $\psi_1 \geq 0, \psi_2 \geq 0$ and $\phi_1 \leq f_2(\beta_1 + f_3)/(\beta_1 + f_2)$ or for $k > 3$ with

$$f_{k-2}(\beta_1 + f_{k-1})/(\beta_1 + f_{k-2}) < \phi_1 \leq f_{k-1}(\beta_1 + f_k)/(\beta_1 + f_{k-1}),$$

it holds that $\psi_{k-1} \geq 0$ and $\psi_{k-2} \geq 0$,

where $F_i = f_i - \phi_i$ and $g_j = f_j g_{j-1} = \prod_{i=1}^j f_i$ and the initial conditions are

$$g_0 = 1, \quad f_1 = -d < 0, \quad f_2 = (1 - d)/2 > 0 \text{ and } f_i > 0, \quad \forall i \geq 2.$$

The sufficient constraints of Baillie *et al.* (1996) are defined by

$$0 \leq \beta_1 \leq \phi_1 + d \text{ and } 0 \leq d \leq 1 - 2\phi_1 \text{ which is equivalent to } \psi_1 \geq 0 \text{ and } F_2 \geq 0.$$

Bollerslev and Mikkelsen (1996) inequality constraints are defined by

$$\beta_1 - d \leq \phi_1 \leq \frac{2-d}{3} \text{ and } d[\phi_1 - \frac{1-d}{2}] \leq \beta_1(\phi_1 - \beta_1 + d) \text{ which is equivalent to } \psi_1, \psi_2 \geq 0 \text{ and } F_3 \geq 0.$$

Chung (1999) suggests sufficient constraints given by

$$0 \leq \phi_1 \leq \beta_1 d < 1.$$

The FIGARCH model is one of the most understood and easiest models to use when modelling fractional integration of conditional heteroscedastic models. This model has some drawbacks that are not ideal for modelling financial returns. One common drawback found in almost all applications of this model is that we must have $d \geq 0$ and the polynomial coefficients must satisfy the above mentioned constraints for the conditional variance to be positive. In the following sections, we discuss additional models which could be used to avoid this shortcoming.

The FIAPARCH Model

Tse (1998) extended the FIGARCH(p, d, q) model in order to take into account asymmetry and the long-memory feature in the process of the conditional variance. He proposed the fractional integrated asymmetric power ARCH (FIAPARCH) model which explicitly accommodates both long-memory and asymmetry effects in the conditional volatility. He introduced the function $(|a_t| - \gamma a_t)^\delta$ of the APARCH process.

The FIAPARCH(p, d, q) model can be written as follows:

$$\sigma_t^\delta = \omega[1 - \beta(L)]^{-1} + \left\{ 1 - [1 - \beta(L)]^{-1} \phi(L)(1 - L)^{d_v} \right\} (|a_t| - \gamma a_t)^\delta, \quad (8.8)$$

where $\omega > 0, \delta > 0, \beta < 1, \lambda < 1$.

The parameter γ refers to the asymmetric parameter satisfying the condition $-1 < \gamma < 1$.

The FIAPARCH process can consider some stylised facts on volatility of financial and commodity prices as follows

- If $\gamma > 0$, negative shocks will have more impact on the commodity return volatility than positive shocks of equal magnitude.
- If $0 < d_v < 1$, the FIAPARCH model captures the patterns of long memory property in the conditional variance process. I.e., volatility exhibits long memory property if $0 < d_v < 1$.

- The FIAPARCH process nests the FIGARCH process when $\gamma = 0$ and $\delta = 2$. As a result, the FIAPARCH process is superior to the FIGARCH as it takes into account asymmetry and long memory in the conditional variance behavior.
- λ is a power term in the volatility structure and should be specified by the data.
- Conrad *et al.* (2011) noted that a sufficient condition for the conditional variance of the FIAPARCH model to be positive is $\gamma > -1$ for all t .

The HYGARCH model

The HYGARCH model by Davidson (2004) is obtained by extending the conditional variance of the FIGARCH model by introducing weights in the difference operator. The conditional variance of the HYGARCH is expressed as follows:

$$\sigma_t^2 = \omega[1 - \beta(L)]^{-1} + \{1 - [1 - \beta(L)]^{-1}\phi(L)[1 + \{\tau(1 - L)^{d_v}\}]\}a_t^2, \quad (8.9)$$

where L is the lag operator, $\omega > 0$, $\delta > 0$, $\beta < 1$, $\lambda < 1$, and $0 < d_v < 1$.

Davidson (2004) shows that the HYGARCH model permits the existence of the second moment at more extreme magnitudes than the simple IGARCH and FIGARCH models do.

According to Conrad (2010), equation 8.2 can be simplified to

$$\phi(L) \left[(1 - \tau) + \tau(1 - L)^{d_v} \right] a_t^2 = \omega + \beta(L)v_t \quad (8.10)$$

by including an additional parameter $\tau \geq 0$. This results in a HYGARCH process nests the Stable GARCH and FIGARCH when $\tau = 0$ and $\tau = 1$, respectively (Conrad, 2010). According to Davidson (2004), when $d = 1$ the parameter τ becomes autoregressive root and the HYGARCH reduces to either a stationary GARCH ($\tau < 1$), an IGARCH ($\tau = 1$) or an explosive GARCH $\tau \geq 1$.

According to Conrad (2010), equation 8.10 can be written as:

$$\sigma_t^2 = \frac{\omega}{B(1)} + \psi^{HY}(L)a_t^2 = \frac{\omega}{B(1)} + \sum_{i=1}^{\infty} \psi_i^{HY} a_{t-i}^2 \quad (8.11)$$

with

$$\psi^{HY}(L) = \tau\psi^{FI}(L) + (1 - \tau)\psi^{GA}(L) \quad (8.12)$$

and

$$B(1) = 1 - \sum_{i=1}^p \beta_i. \quad (8.13)$$

From

$$\psi_i^{HY} = \tau\psi_i^{FI}(L) + (1 - \tau)\psi_i^{GA}(L), \text{ for } i = 1, 2, 3, \dots \quad (8.14)$$

According to Conrad (2010), in order to gain a better understanding of the HY-GARCH specification, equation 8.11 is re-written as

$$\sigma_t^2 = \tau\sigma_t^{2(FI)} + (1 - \tau)\sigma_t^{2(GA)}, \quad (8.15)$$

where

$$B(L)\sigma_t^{2(FI)} = [B(L) - (1 - L)^d\phi(L)]a_t^2, \quad (8.16)$$

and

$$B(L)\sigma_t^{2(GA)} = \frac{\omega}{(1 - \tau)} + [B(L) - \phi(L)]a_t^2. \quad (8.17)$$

According to Conrad (2010), equations 8.15, 8.16, and 8.17 can be interpreted as follows

- The HYGARCH conditional variance is a two-component GARCH model. One component is the GARCH-type and the other is of FIGARCH-type. Thus, the HYGARCH has a short-run component and a long-run component.
- The HYGARCH allows for more flexibility in the long-run component using the memory parameter d Conrad (2010).

We should note that the main advantage of this model is to simultaneously account for volatility clustering, long-range memory and leptokurtosis in the time series behavior. However, this model is unable to consider asymmetry in the return distribution.

Inequality constraints for HYGARCH(p, d, q) Model (Conrad, 2010)

According to Conrad (2010), the GARCH and FIGARCH model's restrictions on the parameters of the HYGARCH have to be imposed to ensure the non-negativity of the conditional variance. From equation 8.14, Conrad (2010) showed that for $0 < \tau < 1$, a restrictive sufficient condition for the non-negativity of the coefficients is the non-negativity of all the ψ_i^{FI} and ψ_i^{GA} coefficients (Conrad, 2010). A recursive representation for the ARCH(∞) is key in understanding the constraints.

Lemma 8.1 (Taken from Conrad (2010))

In the HYGARCH(p, d, q) the sequence $\psi_i^{HY}, i = 1, 2, \dots$ can be written as

$$\psi_i^{HY} = \psi_i^{HY(p)}, \quad (8.18)$$

where

$$\psi_i^{HY(r)} = \lambda_{(r)} \psi_{i-1}^{HY(r)} + \psi_i^{HY(r-1)}, \quad 1 \leq r \leq p, \quad i \geq 1. \quad (8.19)$$

The starting value $\psi_0^{HY(r)} = -1, r = 2, \dots, p$ and $\psi_i^{HY(1)}$ is given by

$$\psi_i^{HY(1)} = (-c_i + \sum_{j=1}^i \phi_j c_{i-j}) + (1 - \tau)(-\lambda_{(1)}^i + \sum_{j=1}^i \lambda_{(1)}^{i-j} \phi_j), \quad \text{for } i = 1, \dots, q \quad (8.20)$$

$$= \lambda_{(1)} \psi_{i-1}^{HY(1)} + \tau F_i(-g_{i-q}), \quad \text{for } i \geq q + 1 \quad (8.21)$$

where $c_i = \sum_{j=0}^i \lambda_{(1)}^{i-j} g_j$.

For HYGARCH($1, d, 1$) model, the recursive representation of the ARCH(∞) coefficients in Lemma 8.1 simplifies to:

$$\psi_i^{HY} = \tau d + \phi_1 - \beta_1,$$

$$\psi_i^{HY} = \beta_1 \psi_{i-1}^{HY} + \tau(f_i - \phi_1)(-g_{i-1}) \quad \text{for } i \geq 2,$$

$$\text{and } \psi_i^{HY} = \beta_1^2 \psi_{i-2}^{HY} + \tau(\beta_1(f_{i-1} - \phi_1) + (f_i - \phi_1)f_{i-1})(-g_{i-2}) \quad \text{for } i \geq 3. \quad (8.22)$$

Theorem 2. (Taken from Conrad (2010)) The conditional variance of the HYGARCH(1, d , 1) is non-negative almost surely if and only if

Case 1: $0 < \beta_1 < 1$

Either $\psi_1^{HY} \geq 0$ and $\phi_1 \leq f_2$ or for $k > 2$ with $f_{k-1} < \phi_1 \leq f_k$ it holds that $\psi_i^{HY} \geq 0$.

Case 2: $-1 < \beta_1 < 0$

Either $\psi_1^{HY}, \psi_2^{HY} \geq 0$ and $|\beta_1| \leq f_2$ or for $k > 3$ with $f_{k-2} < |\beta_1| \leq f_{k-1}$ it holds that $\psi_1^{HY}, \dots, \psi_{k-1}^{HY} \geq 0$.

These are sufficient conditions for HYGARCH(1, d , 1). Conditions of higher order HYGARCH are found in Conrad (2010).

Parameter Estimation

In this methodology, the parameters can be estimated by an approximate quasi-Maximum likelihood estimation technique as advocated by Bollerslev and Woodridge (1992).

The ARFIMA-FIGARCH model is estimated by using the quasi-maximum likelihood (QML) estimation method allowing for asymptotic Normal distribution based on the following log-likelihood function:

$$LL_T(a_t, \theta) = -\frac{1}{2}T \log(2\pi) - \frac{1}{2} \sum_{t=1}^T \left[\log(\sigma_t^2) + \frac{a_t^2}{\sigma_t^2} \right], \quad (8.23)$$

where $\theta' \equiv (\omega, d, \beta_1, \dots, \beta_p, \phi_1, \dots, \phi_q)$. In practice some initial condition are required to start up the recursions for the conditional variance function. The approach here is to maximise the likelihood function conditional on the start-up values. It follows by the central limit theorem that the QMLE obtained by maximising the above equation is both consistent and asymptotically Normally distributed (Baille *et al*, 1996).

8.3 Combining long-memory-GARCH models with heavy-tailed distributions

In this study, the following steps are used to develop new models, which are then used for calculating VaR and are backtested using the Kupiec LR test. The steps are similar to that of McNeil and Frey (2000), Bhattacharyya *et al.* (2008) and Bhattacharyya and Madhav (2012). Thus, we extend the McNeil and Frey (2000) approach based on the conditional-GPD. We extend GARCH model to fractional integrated GARCH models to take into account volatility clustering and long memory on precious metal returns. We extend conditional-GPD to conditional-SSTD, NIGD, PIVD, VGD, GLD, GEVD, SD, full GHD and conditional-GHStD to account for asymmetry and heavy-tailedness inherent in the innovations.

The combined approach may be presented in the following five steps:

- Step 1 - Fit a long-memory-GARCH model to the precious metal return by quasi-Maximum likelihood. Estimate μ_{t+1} and σ_{t+1} from the fitted model.
- Step 2 - Extract standardised residuals from the fitted model.
- Step 3 - Estimate the tail of the innovations using PIVD, NIGD, VGD, full GHD, GEVD, GLD, and SD, and check model adequacy using Anderson-Darling test. Compute the quantiles of the innovations.
- Step 4 - Construct VaR from parameters estimated in steps 1 and 3.
- Step 5 - Backtesting the new models using Kupiec likelihood ratio test.

8.4 Empirical Results

Estimating GARCH-type models

Tables 8.1 to 8.9 provide the parameter estimation results of ARFIMA-FIGARCH, ARFIMA-HYGARCH and ARFIMA-FIAPARCH models assuming Normal (N), STD

and SSTD innovation distributions for all three precious metal returns. For all models, the long range dependence parameter of the ARFIMA model ($-0.5 < d_m < 0$) is negative for silver and platinum returns, indicating anti-persistence and long memory process (Box *et al.*, 2008). This shows that the log returns of both platinum and silver are mean reverting. However, in the case of gold returns, (d_m) was statistically insignificant for all models. For volatility, the long range parameter is positive ($0 < d_v < 1$) and indicates strong long memory. This is similar to the result of Arouri *et al.* (2012) which shows high persistence in precious metals.

As shown in Tables 8.1 to 8.3, all ARFIMA-FIGARCH models under different innovation distributions are able to capture long memory phenomenon for both gold, platinum and silver returns volatilities. We used several diagnostic tests to evaluate the accuracy of model specifications. The Ljung-Box test on both standardised and squared standardised residuals show that the mean and volatility equations are adequate.

The insignificance of ARCH LM(10) and $Q^2(10)$ statistics show that no ARCH effect are observed in the residuals. All ARFIMA-HYGARCH and all ARFIMA-FIAPARCH models under different error distributions are adequate for all three precious metals as shown by diagnostics tests in Tables 8.4 to 8.9.

Finally, we employ Akaike information criterion (AIC) and Schwarz information criterion (SBI) to select the best model to describe the conditional dependence in the volatility process. The most appropriate model to describe the data is the one that minimises SBI and AIC criteria. Based on the AIC and SBI, the best model to capture the dependence in the conditional variance for gold returns is the FIGARCH model under the STD. For platinum returns, both AIC and SBI selected the ARFIMA-HYGARCH under the STD as the best model. In the case of silver, both AIC and SBI selected the ARFIMA-HYGARCH under the STD. Since ARFIMA-FIGARCH and ARFIMA-FIAPARCH were adequate for all precious metals, our results are similar to the results of Arouri *et al.* (2012) and Diaz (2016).

*ARFIMA-FIGARCH models***Table 8.1:** ARFIMA-FIGARCH parameter estimation with different error distributions and Diagnostic tests (Gold returns)

Parameters	Normal		Student-t		Skewed Student-t	
	Statistic	<i>p</i> -value	Statistic	<i>p</i> -value	Statistic	<i>p</i> -value
Cst(M)	-		-		-	
<i>d</i> -ARFIMA (d_m)	-		-		-	
AR(1)	0.9414	<0.0001	-		-	
MA(1)	-0.9482	<0.0001	-		-	
Cst(V)	-	-	0.3070	0.0031	0.3071	0.0030
<i>d</i> -FIGARCH (d_v)	0.4551	<0.0001	0.4359	<0.0001	0.4342	<0.0001
ARCH(α_1)	0.3757	<0.0001	0.2950	<0.0001	0.2948	0.0419
GARCH(β_1)	0.7144	<0.0001	0.6662	<0.0001	0.6647	0.0542
Q (10)	13.2902	0.1022	9.1882	0.5150	9.1733	0.5157
Q(15)	17.4321	0.1803	14.8394	0.4630	14.8337	0.4635
Q(20)	37.0810	0.0051	30.0215	0.0695	30.0125	0.0697
Q ² (10)	5.7269	0.6778	13.9073	0.0842	13.9726	0.0825
Q ² (15)	9.4998	0.7342	18.0398	0.1560	18.0824	0.1544
Q ² (20)	13.3652	0.7694	21.4726	0.2562	21.5023	0.2548
ARCH LM(5)	0.5151	0.7651	2.1576	0.0559	2.1737	0.0542
ARCH LM (10)	0.5591	0.8482	1.3437	0.2006	1.3503	0.1972
AIC	2.6402		2.5330		2.5330	
SBI	2.6466		2.5395		2.5407	

-Statistically insignificant parameters were dropped.

Table 8.2: ARFIMA-FIGARCH parameter estimation with different error distributions and Diagnostic tests (Platinum returns)

Parameters	Normal		Student-t		Skewed Student-t	
	Statistic	<i>p</i> -value	Statistic	<i>p</i> -value	Statistic	<i>p</i> -value
Cst(M)	-		0.0201	0.0814	0.0272	0.0122
<i>d</i> -ARFIMA (d_m)	-		-0.03268	0.0244	-0.0333	0.0221
AR(1)	-		-0.5561	0.0084	-0.5667	0.0087
MA(1)	-		0.5947	0.0030	0.6061	0.0031
Cst(V)	1.2430	0.0009	1.0931	0.0020	1.1089	<0.0001
<i>d</i> -FIGARCH (d_v)	0.4050	<0.0001	0.3823	<0.0001	0.3801	<0.0001
ARCH(α_1)	0.3378	<0.0001	0.2600	<0.0001	0.2626	0.0003
GARCH(β_1)	0.5885	<0.0001	0.5391	<0.0001	0.5365	<0.0001
Q (10)	13.6255	0.1908	11.9830	0.1520	12.1821	0.1433
Q(15)	17.3142	0.3004	16.3808	0.2292	16.5966	0.2184
Q(20)	28.6010	0.0959	29.0951	0.0472	29.4207	0.0435
Q ² (10)	7.3393	0.5005	9.6251	0.2923	9.3193	0.3161
Q ² (15)	13.8802	0.3823	18.0289	0.1564	17.7681	0.1665
Q ² (20)	16.0976	0.5857	20.3276	0.3147	20.0317	0.3310
ARCH LM(5)	0.7775	0.5658	1.1099	0.3527	1.0445	0.3895
ARCH LM (10)	0.7441	0.6833	0.9788	0.4594	0.9476	0.4878
AIC	3.2147		3.1598		3.1601	
SBI	3.2198		3.1726		3.1717	

-Statistically insignificant parameters were dropped.

Table 8.3: ARFIMA-FIGARCH parameter estimation with different error distributions and Diagnostic tests (Silver returns)

Parameters	Normal		Student-t		Skewed Student-t	
	Statistic	<i>p</i> -value	Statistic	<i>p</i> -value	Statistic	<i>p</i> -value
Cst(M)	-		-		-	
<i>d</i> -ARFIMA (d_m)	-0.062379	<0.0001	0.0642	<0.0001	-0.0639	<0.0001
AR(1)	-		-		-	
MA(1)	-		-		-	
Cst(V)	3.539744	0.0113	-		2.869921	0.0023
<i>d</i> -FIGARCH (d_v)	0.452067	<0.0001	0.491001	<0.0001	0.450248	<0.0001
ARCH(α_1)	0.349151	<0.0001	0.399324	<0.0001	0.425372	<0.0001
GARCH(β_1)	0.696679	<0.0001	0.774474	<0.0001	0.752825	<0.0001
Q (10)	31.5091	0.0004	32.1970	0.0004	31.8889	0.0004
Q(15)	36.2849	0.0017	37.5668	0.0010	36.8180	0.0013
Q(20)	42.9962	0.0021	44.5951	0.0013	43.6307	0.0017
Q ² (10)	4.4048	0.8189	8.03816	0.4298	6.5431	0.5866
Q ² (15)	5.9916	0.9465	10.0508	0.6898	8.2025	0.8302
Q ² (20)	10.1211	0.9279	14.0482	0.7259	12.5310	0.8186
ARCH LM(5)	0.6016	0.6988	1.3592	0.2365	1.0521	0.3851
ARCH LM (10)	0.4411	0.9268	0.8126	0.6166	0.6506	0.7710
AIC	3.9204		3.8390		3.8347	
SBI	3.9268		3.8466		3.8423	

-Statistically insignificant parameters were dropped.

ARFIMA-HYGARCH models**Table 8.4:** ARFIMA-HYGARCH parameter estimation with different error distributions and Diagnostic tests (Gold returns)

Parameters	Normal		Student-t		Skewed Student-t	
	Statistic	<i>p</i> -value	Statistic	<i>p</i> -value	Statistic	<i>p</i> -value
Cst(M)	-		-		-	
<i>d</i> -ARFIMA (d_m)	-		-		-	
AR(1)	-0.700426	<0.0001	-		-	
MA(1)	0.694912	<0.0001	-		-	
Cst(V)	-		-		-	
<i>d</i> -FIGARCH (d_v)	0.4245	<0.0001	0.5762	<0.0001	0.5724	<0.0001
ARCH(α_1)	0.3223	0.0186	0.2444	<0.0001	0.2448	<0.0001
GARCH(β_1)	0.6337	<0.0001	0.7631	<0.0001	0.7607	<0.0001
Q (10)	10.5705	0.2272	10.2080	0.4224	10.1961	0.4235
Q(15)	16.8240	0.2075	15.4740	0.4178	15.4682	0.4182
Q(20)	32.9035	0.0171	30.1939	0.0668	30.1897	0.0668
Q ² (10)	3.9160	0.8646	14.8211	0.0627	14.8370	0.0624
Q ² (15)	7.1238	0.8957	20.4539	0.0845	20.4292	0.0850
Q ² (20)	10.9321	0.8972	24.5492	0.1378	24.4969	0.1394
ARCH LM(5)	0.3228	0.8995	2.1800	0.0536	2.1875	0.0522
ARCH LM (10)	0.3908	0.9513	1.4199	0.1645	1.4221	0.1635
AIC	2.6332		2.5348		2.5346	
SBI	2.6409		2.5412		2.5424	

-Statistically insignificant parameters were dropped.

Table 8.5: ARFIMA-HYGARCH parameter estimation with different error distributions and Diagnostic tests (Platinum returns)

Parameters	Normal		Student-t		Skewed Student-t	
	Statistic	<i>p</i> -value	Statistic	<i>p</i> -value	Statistic	<i>p</i> -value
Cst(M)	-		-			
<i>d</i> -ARFIMA (d_m)	-0.0367	0.0553	-0.0274	0.0403	-0.02403	0.0678
AR(1)	0.0650	0.0080	-0.5845	0.0048	-0.6049	0.0054
MA(1)	-		0.6196	0.0017	0.6382	0.0021
Cst(V)	-		-			
<i>d</i> -FIGARCH (d_v)	0.4002	<0.0001	0.3737	<0.0001	0.3770	<0.0001
ARCH(α_1)	0.3059	0.0008	0.2651	<0.0001	0.2691	<0.0001
GARCH(β_1)	0.57777	<0.0001	0.5487	<0.0001	0.5520	<0.0001
Q (10)	7.3660	0.5991	11.0008	0.2017	10.4932	0.2321
Q(15)	11.0353	0.6833	15.0318	0.3054	14.5651	0.3353
Q(20)	23.3377	0.2228	26.8208	0.0824	26.0900	0.0977
Q ² (10)	6.8445	0.5535	8.7407	0.3646	8.7124	0.3671
Q ² (15)	13.2234	0.4307	16.8605	0.2058	16.9849	0.1999
Q ² (20)	15.3730	0.6362	18.8428	0.4016	19.0697	0.3875
ARCH LM(5)	0.7914	0.5557	1.0293	0.3984	0.9993	0.4165
ARCH LM (10)	0.6878	0.7369	0.8763	0.5548	0.8746	0.5564
AIC	3.2023		3.1605		3.1494	
SBI	3.2099		3.1720		3.1596	

-Statistically insignificant parameters were dropped.

Table 8.6: ARFIMA-HYGARCH parameter estimation with different error distributions and Diagnostic tests (Silver returns)

Parameters	Normal		Student-t		Skewed Student-t	
	Statistic	p-value	Statistic	p-value	Statistic	p-value
Cst(M)	-		-		-	
<i>d</i> -ARFIMA (d_m)	-		-		-	
AR(1)	-0.1038	<0.0001	-		-0.1161	<0.0001
MA(1)	-		-0.1166	<0.0001	-	
Cst(V)	-		-		-	
<i>d</i> -FIGARCH (d_v)	0.4105	<0.0001	0.4382	<0.0001	0.4386	<0.0001
ARCH(α_1)	0.3889	<0.0001	0.4611	<0.0001	0.4609	<0.0001
GARCH(β_1)	0.6997	<0.0001	0.7767	<0.0001	0.7762	<0.0001
Q (10)	14.6218	0.1019	19.3259	0.0226	16.2763	0.0613
Q(15)	20.8588	0.1053	25.6994	0.0283	22.7416	0.0646
Q(20)	26.9518	0.1058	31.6694	0.0340	28.8287	0.0687
Q ² (10)	4.4855	0.8109	6.4937	0.5921	6.5187	0.5893
Q ² (15)	6.1174	0.9418	8.2545	0.8266	8.2755	0.8252
Q ² (20)	9.9368	0.9339	11.7819	0.8583	11.7768	0.8585
ARCH LM(5)	0.5832	0.7129	1.0161	0.4063	1.0159	0.4064
ARCH LM (10)	0.4483	0.9229	0.6433	0.7776	0.6436	0.7773
AIC	3.9166		3.8294		3.8291	
SBI	3.9229		3.8383		3.8367	

-Statistically insignificant parameters were dropped.

ARFIMA-FIAPARCH models

Table 8.7: ARFIMA-FIAPARCH parameter estimation with different error distributions and Diagnostic tests (Gold returns)

Parameters	Normal		Student-t		Skewed Student-t	
	Statistic	p-value	Statistic	p-value	Statistic	p-value
Cst(V)	-		-		-	
<i>d</i> -ARFIMA (d_m)	-		-		-	
AR(1)	-		-		-	
MA(1)	-		-		-	
Cst(V)	-		-		-	
<i>d</i> -FIGARCH (d_v)	0.4609	<0.0001	0.5758	<0.0001	0.5721	<0.0001
ARCH(α_1)	0.3041	0.0090	0.2330	<0.0001	0.2336	<0.0001
GARCH(β_1)	0.6461	<0.0001	0.7456	<0.0001	0.7427	<0.0001
APARCH(γ_1)	-0.0741	0.0305	-0.1087	0.0215	-0.1118	0.0185
APARCH (δ)	2.1436	<0.0001	2.0663	<0.0001	2.0667	<0.0001
Q (10)	9.2958	0.5043	9.9909	0.4413	9.9682	0.4433
Q(15)	15.4851	0.4171	15.3839	0.4241	15.3733	0.4249
Q(20)	30.9463	0.0559	29.7761	0.0736	29.7603	0.0738
Q ² (10)	4.0528	0.8523	13.5152	0.0953	13.4541	0.09715
Q ² (15)	7.4254	0.8789	18.8831	0.1268	18.7631	0.1306
Q ² (20)	10.9112	0.8981	22.2555	0.2008	22.0963	0.2277
ARCH LM(5)	0.3009	0.9126	1.9109	0.0891	1.9039	0.0903
ARCH LM (10)	0.4049	0.9451	1.3116	0.2176	1.3066	0.2204
AIC	2.6331		2.5350		2.5349	
SBI	2.6395		2.5427		2.5440	

-Statistically insignificant parameters were dropped.

Table 8.8: ARFIMA-FIAPARCH parameter estimation with different error distributions and Diagnostic tests (Platinum returns)

Parameters	Normal		Student-t		Skewed Student-t	
	Statistic	p-value	Statistic	p-value	Statistic	p-value
Cst(M)	0.02740	0.0125	0.0294	0.0056	-	
<i>d</i> -ARFIMA (d_m)	-0.04845	0.0255	-0.0387	0.0255	-0.0272	0.0444
AR(1)	0.0766	0.0038	0.0411	0.0604	-0.5738	0.0059
MA(1)	-				0.6084	0.0022
Cst(V)	-				-	
<i>d</i> -FIGARCH (d_v)	0.3971	<0.0001	0.3818	<0.0001	0.4396	<0.0001
ARCH(α_1)	0.2900	0.0013	0.2528	0.0002	0.2509	<0.0001
GARCH(β_1)	0.5615	<0.0001	0.5397	<0.0001	0.5946	<0.0001
APARCH(γ_1)	-0.1023	0.0159	-0.1133	<0.0001	-0.1059	0.0096
APARCH (δ)	2.0876	<0.0001	2.0771	<0.0001	<0.0001	
Q (10)	9.2291	0.4164	15.6247	0.0751	11.3782	0.1812
Q(15)	13.0386	0.5235	19.5533	0.1448	15.4569	0.2797
Q(20)	26.3605	0.1205	32.4107	0.0281	27.1830	0.0756
Q ² (10)	6.1708	0.6281	8.0896	0.4248	9.5857	0.2953
Q ² (15)	12.1931	0.5119	14.8650	0.3159	15.6586	0.2681
Q ² (20)	14.1883	0.7167	16.8046	0.5366	17.5727	0.4841
ARCH LM(5)	0.6485	0.6627	0.9423	0.4522	1.2714	0.2732
ARCH LM (10)	0.6191	0.7988	0.8055	0.6235	0.9633	0.4734
AIC	3.2131		3.1608		3.1601	
SBI	3.2233		3.1723		3.1742	

-Statistically insignificant parameters were dropped.

Table 8.9: ARFIMA-FIAPARCH parameter estimation with different error distributions and Diagnostic tests (Silver returns)

Parameters	Normal		Student-t		Skewed Student-t	
	Statistic	p-value	Statistic	p-value	Statistic	p-value
Cst(M)	-		-		-	
<i>d</i> -ARFIMA (d_m)	-		-		-	
AR(1)	-0.1037	<0.0001	-0.1181	<0.0001	-0.1195	<0.0001
MA(1)	-		-		-	
Cst(V)	-		-		-	
<i>d</i> -FIGARCH (d_v)	0.4047	<0.0001	0.4334	<0.0001	0.4336	<0.0001
ARCH(α_1)	0.3715	<0.0001	0.4241	<0.0001	0.4233	<0.0001
GARCH(β_1)	0.6731	<0.0001	0.7467	<0.0001	0.7468	<0.0001
APARCH(γ_1)	-0.1117	0.0569	-0.2169	<0.0001	-0.2219	<0.0001
APARCH (δ)	2.1424	<0.0001	2.0610	<0.0001	2.0596	<0.0001
Q (10)	14.2518	0.1136	17.2202	0.0454	17.6880	0.0390
Q(15)	20.4800	0.1157	23.6739	0.0501	24.1527	0.0439
Q(20)	26.2276	0.1240	29.3005	0.0614	29.7740	0.0547
Q ² (10)	4.3861	0.8207	4.7997	0.7788	4.8727	0.7711
Q ² (15)	6.1014	0.9423	6.8469	0.9099	6.9328	0.9056
Q ² (20)	10.1379	0.9273	10.5919	0.9109	10.6802	0.9074
ARCH LM(5)	0.5613	0.7298	0.6491	0.6622	0.6616	0.6527
ARCH LM (10)	0.4387	0.9281	0.4743	0.9076	0.4815	0.9030
AIC	3.9227		3.8330		3.8328	
SBI	3.9303		3.8420		3.8431	

-Statistically insignificant parameters were dropped.

Long memory-GARCH models with heavy-tailed distribution

We extracted the standardised residuals from ARFIMA-FIGARCH, ARFIMA-HYGARCH, and ARFIMA-FIAPARCH models fitted to precious metals using the pseudo MLE procedure with the Normal distribution governing the innovations. The descriptive statistics of the standardised residuals are shown in Table 8.10. The moment coefficient excess kurtosis values indicate the leptokurtic behaviour of all standardised residuals. This implies that the empirical distribution of the standardised residuals are much heavier than the Normal distribution. Figures 8.1, 8.2 and 8.3 show the Q-Q plots of standardised residuals extracted from the ARFIMA-FIGARCH model fitted to precious metals using the pseudo MLE procedure with the Normal distribution governing the innovations. The Q-Q plots suggest a departure from Normality and this is confirmed by the Jarque-Bera test for Normality reported in Table 8.10. The standardised residuals are all skewed to the left. Therefore, we need nonlinear GARCH-type models with innovations having a PIVD, NIGD, VGD, full GHD, GLD, GEVD, GPD and SD. These models can account for asymmetry and kurtosis in the conditional distribution.

Table 8.10: Descriptive Statistics of standardised residuals of the ARFIMA-FIGARCH, ARFIMA-HYGARCH and ARFIMA-FIAPARCH models.

Model	Descriptive Statistics	Gold	Platinum	Silver
ARFIMA-FIGARCH	Moment Coefficient of Skewness	-0.1778	-0.5547	-0.5435
	Moment Coefficient of Excess Kurtosis	6.6992	9.9548	9.6066
	Jarque-Bera test (p -value)	<0.0001	<0.0001	<0.0001
ARFIMA-HYGARCH	Moment Coefficient of Skewness	-0.1778	-0.5618	-0.5997
	Moment Coefficient of Excess Kurtosis	6.6992	10.0717	9.8223
	Jarque-Bera test (p -value)	<0.0001	<0.0001	<0.0001
ARFIMA-FIAPARCH	Moment Coefficient of Skewness	-0.1862	-0.5659	-0.5995
	Moment Coefficient of Excess Kurtosis	6.7141	9.9697	9.7660
	Jarque-Bera test (p -value)	<0.0001	<0.0001	<0.0001

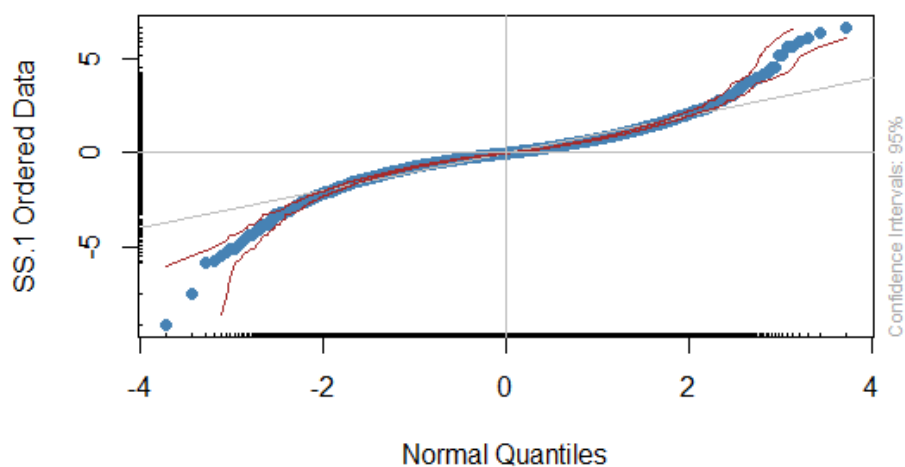


Figure 8.1: Q-Q plot of standardised residuals ARFIMA-FIGARCH model (gold returns)

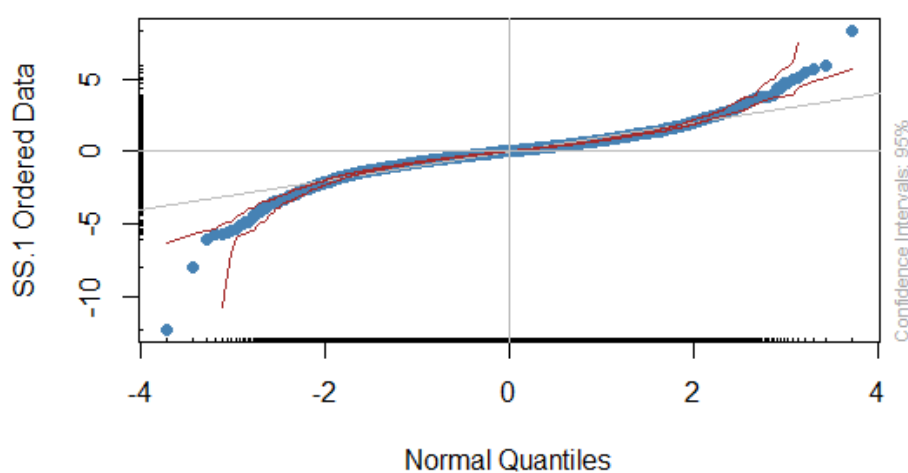


Figure 8.2: Q-Q plot of standardised residuals ARFIMA-FIGARCH model (platinum returns)

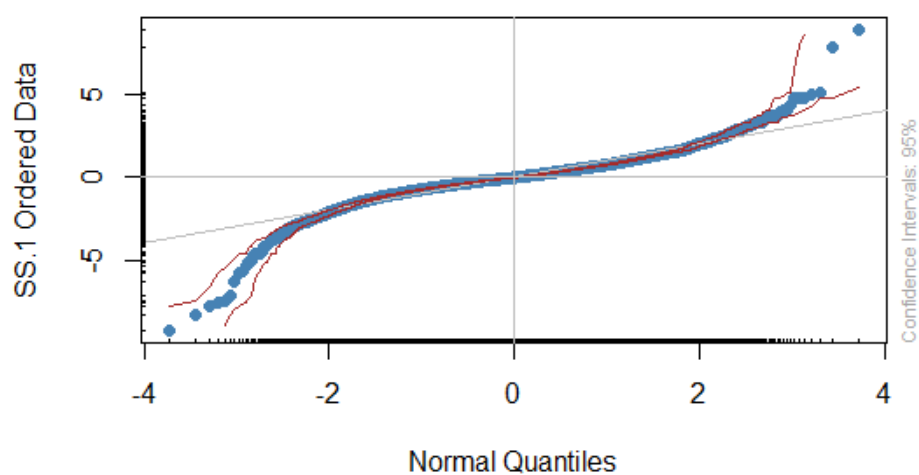


Figure 8.3: Q-Q plot of standardised residuals from ARFIMA-FIGARCH model (silver returns)

We then incorporated LM GARCH models where the innovation process follows GLD, full GHD, GEVD, GPD, SD, GHStD, VGD, NIGD and PIVD. We introduced GLD, full GHD, GEVD, GPD, SD, GHStD, VGD, NIGD and PIVD to depict the tail distribution of the standardised residual series. The PIVD distribution was fitted to the standardised residuals extracted from the ARFIMA-FIGARCH, ARFIMA-HYGARCH, ARFIMA-FIAPARCH with Normal innovations. The parameters were estimated using the method of Maximum likelihood. The MLE procedure was carried out using R package Pearson DS. Tables 8.11, 8.13 and 8.19 show the Maximum likelihood estimates of PIVD distribution fitted to the ARFIMA-FIGARCH, ARFIMA-HYGARCH, ARFIMA-FIAPARCH models with Normal innovations respectively.

From Tables 8.11, 8.13 and 8.19, the values of $\hat{m} > 0.5$ for all PIVD models, thus satisfying the condition for PIVD. The AD statistics are significant, thus the PIVD distribution is a good fit of the extracted standardised residuals from the ARFIMA-FIGARCH, ARFIMA-HYGARCH, ARFIMA-FIAPARCH models.

We fit NIGD, full GHD, GHStD and VGD to the standardised residuals extracted from the ARFIMA-FIGARCH, ARFIMA-HYGARCH, ARFIMA-FIAPARCH models. The Maximum likelihood (ML) parameter estimates are shown in Tables 8.12, 8.18 and 8.24. The AD test results suggest that the extracted standardised residuals follow the fitted distributions. The high p -values indicate that we cannot reject the null hypothesis that the standardised residuals follow NIGD, VGD, full GHD and GHStD. Table 8.12 shows that for silver returns, VGD is a good fit of the standardised residuals at 1% level of significance.

FMKL GLD, SD, GEVD and GPD are fitted to the standardised residuals extracted from the ARFIMA-FIGARCH, ARFIMA-HYGARCH, ARFIMA-FIAPARCH models. The ML estimates and AD test results of the FMKL GLD are shown in Tables 8.14, 8.20 and 8.25. The AD test results suggest that the extracted residuals follow FMKL GLD. Tables 8.15, 8.21 and 8.26 summarise the ML parameter estimates of the SD fit-

ted to the standardised residuals extracted ARFIMA-FIGARCH, ARFIMA-HYGARCH, ARFIMA-FIAPARCH models. The AD test statistics are significant for SD (except for gold returns). We fit GEVD to positive and negative standardised residuals extracted ARFIMA-FIGARCH, ARFIMA-HYGARCH, ARFIMA-FIAPARCH models and the results are summarised in Tables 8.16, 8.22 and 8.27. Based on the AD test, positive and negative standardised residuals follow GEVD in the upper tail. The shape parameter is positive for gold, platinum and silver suggesting all positive and negative standardised residuals follow a Fréchet distribution. We selected reasonable threshold for positive and negative standardised residuals using mean excess plots and Pareto quantile plot shown in Figure 8.14 to 8.21 (Appendix section at the end of this chapter). Using the selected threshold, we then fit GPD to the positive and negative standardised residual. Tables 8.17, 8.23, 8.28 summarise the ML parameter estimates of GPD for the ARFIMA-FIGARCH-GPD, ARFIMA-HYGARCH-GPD, ARFIMA-FIAPARCH-GPD models. For all positive and negative standardised residuals, the shape parameter, $\xi > 0$ implying fat tails. The diagnostic plots for GPD fit to negative and positive standardised residuals are presented in Figures 8.22 to 8.39. The P-P plots indicate that the standardised residuals follow the GPD. However, using Q-Q plots, for positive gold and negative platinum standardised residuals show some deviations from the straight line maybe suggesting a poor GPD fit.

ARFIMA-FIGARCH models

Table 8.11: ML parameter estimates of the Pearson type-IV distribution for the ARFIMA-FIGARCH-PIVD model

Returns	\hat{m}	$\hat{\nu}$	$\hat{\lambda}$	\hat{a}	AD Test	
					Statistic	p -value
Gold	1.8768	0.0118	0.0354	1.0610	2.1259	0.0784
Platinum	2.1325	0.1195	0.1156	1.6507	0.4068	0.842
Silver	2.0702	0.0131	0.0700	2.2458	0.9380	0.3915

Table 8.12: ML parameter estimates of the GHDs for the ARFIMA-FIGARCH-GHDs model

Returns	Distr	alpha	beta	delta	mu	lambda	AD Test	
							Statistic	p-value
Gold	NIG	0.6146	-0.0052	0.6938	0.03161	-0.5	0.87056	0.4328
	VG	1.2749	0.0068	0	0.0185	0.8610	0.7535	0.5158
	GHD _{full}	0.9613	0.0005	0.3619	0.0253	0.2558	0.47181	0.7757
	GHStD	0.0069	-0.0069	1.0614	0.0347	-1.3773	2.1309	0.0779
Platinum	NIG	0.5605	-0.0313	1.0731	0.0857	-0.5	0.4164	0.8324
	VG	1.0736	0.0133	0	0.0011	1.0655	3.3649	0.0179
	GHD _{full}	0.7778	-0.0184	0.9871	0.0889	-0.1435	1.3914	0.2047
	GHStD	0.0263	-0.0263	1.6538	0.0801	-1.6365	0.4002	0.8485
Silver	NIG	0.3783	-0.0071	1.4601	0.0682	-0.5	1.071	0.3221
	VG	0.7452	0.0120	0	-0.0028	1.0218	2.6452	0.0416
	GHD _{full}	0.1393	-0.0119	2.0850	0.0881	-1.3552	0.9756	0.3703
	GHStD	0.0103	-0.0103	2.2498	0.0837	-1.5744	1.0422	0.3359

Table 8.13: ML parameter estimates of the Pearson type-IV distribution for the ARFIMA-HYGARCH-PIVD model

Returns	\hat{m}	$\hat{\nu}$	$\hat{\lambda}$	\hat{a}	AD Test	
					Statistic	p-value
Gold	1.8752	0.0224	0.0403	1.0593	2.12	0.0790
Platinum	2.1372	0.1042	0.1097	1.6480	0.2676	0.9603
Silver	2.0699	0.0639	0.1073	2.2416	0.7554	0.5143

Table 8.14: ML parameter estimates of the FMKL GLD for the ARFIMA-FIGARCH-GLD model.

Returns	$\hat{\lambda}_1$	$\hat{\lambda}_2$	$\hat{\lambda}_3$	$\hat{\lambda}_4$	AD test	
					Statistic	p-value
Gold	0.0304	2.7708	-0.2499	-0.2413	1.5018	0.1761
Platinum	0.0534	1.8815	-0.2052	-0.1702	0.2841	0.9496
Silver	0.0605	1.3650	-0.2107	-0.1900	0.9586	0.3798

Table 8.15: ML parameter estimates of the Stable distribution for the ARFIMA-FIGARCH-SD model

Returns	$\hat{\alpha}$	$\hat{\beta}$	$\hat{\gamma}$	$\hat{\delta}$	AD test	
					Statistic	p-value
Gold	1.5439	0.0001	0.5268	0.0319	4.1410	0.0074
Platinum	1.6430	-0.0880	0.7417	0.0624	1.6292	0.1484
Silver	1.6284	0.0009	1.0325	0.0676	2.2101	0.0706

Table 8.16: ML parameter estimates of GEVD for the ARFIMA-FIGARCH-GEVD model.

Returns	Standardised Residuals	$\hat{\xi}$ (Se)	$\hat{\mu}$ (Se)	$\hat{\sigma}$ (Se)	AD test	
					Statistic	<i>p</i> -value
Gold	Positive	0.1387 (0.0225)	0.6542 (0.0208)	0.5965 (0.0160)	0.02940	0.9426
	Negative	0.1220 (0.0200)	0.6196 (0.0210)	0.6083 (0.0158)	1.4563	0.1872
Platinum	Positive	0.0783 (0.0185)	0.9405 (0.0268)	0.7797 (0.0196)	1.9937	0.0926
	Negative	0.1207 (0.0179)	0.8965 (0.0267)	0.7832 (0.0200)	1.0507	0.3317
Silver	Positive	0.0367 (0.1412)	1.3486 (0.0398)	1.1892 (0.0281)	2.5070	0.0491
	Negative	0.1373 (0.0180)	1.2266 (0.0372)	1.0944 (0.0280)	1.9814	0.0940

*Se means standard error

Table 8.17: ML parameter estimates of GPD for the ARFIMA-FIGARCH-GPD model.

Returns	Standardised Residuals	Threshold	No. of Exceedances	$\hat{\xi}$ (Se)	$\hat{\beta}$ (Se)
Gold	Positive	1.4235	1601	0.1670 (0.0642)	0.6626 (0.0549)
	Negative	1.4483	1422	0.1735 (0.0696)	0.7201 (0.0640)
Platinum	Positive	1.7796	1488	0.2034 (0.0676)	0.7927 (0.0670)
	Negative	1.6827	1451	0.2536 (0.0665)	0.8550 (0.0702)
Silver	Positive	2.0210	1657	0.1429 (0.0460)	1.1364 (0.0701)
	Negative	1.7592	1653	0.1198 (0.0397)	1.1592 (0.0631)

*Se means standard error

Table 8.18: ML parameter estimates of the GHDs for the ARFIMA-HYGARCH -GHDs model

Returns	Distr	alpha	beta	delta	mu	lambda	AD Test	
							Statistic	<i>p</i> -value
Gold	NIG	0.6144	-0.0080	0.6933	0.0335	-0.5	0.8846	0.4239
	VG	1.2791	0.00142	0	0.0233	0.8650	0.7603	0.5105
	GHD _{full}	0.9516	-0.0020	0.3720	0.0267	0.2336	0.5174	0.7292
	GHStD	0.0099	-0.0099	1.0582	0.0367	-1.3740	2.1115	0.0793
Platinum	NIG	0.5648	-0.0283	1.0723	0.0843	-0.5	0.2933	0.9431
	VG	1.1191	-0.0197	0	0.0661	1.1329	1.5968	0.1550
	GHD _{full}	0.1924	-0.0257	1.5223	0.0802	-1.4114	0.1950	0.9917
	GHStD	0.0245	-0.0245	1.6509	0.0806	-1.6411	0.2588	0.9656
Silver	NIG	0.3788	-0.0151	1.4567	0.0851	-0.5	0.8215	0.4658
	VG	0.7517	-0.0013	0	0.0319	1.0346	2.3783	0.0574
	GHD _{full}	0.1697	-0.0224	2.0685	0.1124	-1.3260	0.8108	0.4733
	GHStD	0.0161	-0.0161	2.2437	0.0940	-1.5722	0.7820	0.4942

Table 8.19: ML parameter estimates of the Pearson type-IV distribution for the ARFIMA-FIAPARCH-PIVD model

Returns	\hat{m}	\hat{v}	$\hat{\lambda}$	\hat{a}	AD Test	
					Statistic	<i>p</i> -value
Gold	1.8804	0.0224	0.0402	1.0634	2.0747	0.0836
Platinum	2.1452	0.1134	0.0840	1.6628	0.252	0.9693
Silver	2.0702	0.0653	0.1091	2.2506	0.8003	0.4808

ARFIMA-HYGARCH models**Table 8.20:** ML parameter estimates of the FMKL GLD for the ARFIMA-HYGARCH-GLD model.

Returns	$\hat{\lambda}_1$	$\hat{\lambda}_2$	$\hat{\lambda}_3$	$\hat{\lambda}_4$	AD test	
					Statistic	<i>p</i> -value
Gold	0.0304	2.7741	-0.2519	-0.2403	1.4984	0.1769
Platinum	0.0558	1.8864	-0.2029	-0.1707	0.1491	0.9987
Silver	0.0604	1.3674	-0.2164	-0.1842	0.6759	0.5793

Table 8.21: ML parameter estimates of the Stable distribution for the ARFIMA-HYGARCH-SD model.

Returns	$\hat{\alpha}$	$\hat{\beta}$	$\hat{\gamma}$	$\hat{\delta}$	AD test	
					Statistic	<i>p</i> -value
Gold	1.5360	<0.0001	0.5252	0.0327	4.0156	0.0086
Platinum	1.6451	<0.0001	0.7389	0.0515	1.5982	0.1547
Silver	1.6243	-0.0672	1.0307	0.07854	2.1038	0.0806

Table 8.22: ML parameter estimates of GEVD for the ARFIMA-HYGARCH-GEVD model.

Returns	Standardised Residuals	$\hat{\xi}$ (Se)	$\hat{\mu}$ (Se)	$\hat{\sigma}$ (Se)	AD test	
					Statistic	<i>p</i> -value
Gold	Positive	0.1335(0.0221)	0.6583(0.0208)	0.5974(0.0159)	0.2709	0.9583
	Negative	0.1281(0.0201)	0.6215(0.0208)	0.6043(0.0157)	1.4825	0.1807
Platinum	Positive	0.07984(0.0186)	0.9411(0.0265)	0.7762(0.0194)	1.8050	0.1179
	Negative	0.1323 (0.0189)	0.8851 (0.0262)	0.7667(0.0197)	0.8452	0.4495
Silver	Positive	0.0504 (0.0154)	1.1543(0.0278)	1.1528(0.0278)	1.7489	0.1268
	Negative	0.1478 (0.0371)	1.2269 (0.0371)	1.0891(0.0281)	1.6979	0.1356

*Se means standard error

Table 8.23: ML parameter estimates of GPD for the ARFIMA-HYGARCH-GPD model.

Returns	Standardised Residuals	Threshold	No. of Exceedances	$\hat{\xi}$ (Se)	$\hat{\beta}$ (Se)
Gold	Positive	1.3925	1651	0.1528(0.0618)	0.6794(0.0548)
	Negative	1.2406	1783	0.1368(0.0543)	0.6817(0.0489)
Platinum	Positive	1.5150	1821	0.1701 (0.0523)	0.7824 (0.0531)
	Negative	1.6082	1538	0.2729(0.06550)	0.8096 (0.0647)
Silver	Positive	1.9787	1686	0.1237(0.0441)	1.1644(0.0702)
	Negative	1.7714	1665	0.2373 (0.0493)	1.1840(0.0742)

*Se means standard error

Table 8.24: ML parameter estimates of the GHDs for the ARFIMA-FIAPARCH -GHDs model

Returns	Distr	alpha	beta	delta	mu	lambda	AD Test	
							Statistic	p-value
Gold	NIG	0.6170	-0.0078	0.6959	0.0334	-0.5	0.8581	0.441
	VG	1.2556	0.0232	0	0.0000	0.8396	1.4082	0.2000
	GHD _{full}	0.8930	-0.0039	0.4412	0.0288	0.0984	0.5218	0.7246
	GHStD	0.0093	-0.0093	1.0633	0.0364	-1.3805	2.0709	0.0840
Platinum	NIG	0.5650	-0.0302	1.0809	0.0559	-0.5	0.2864	0.948
	VG	1.1183	-0.0279	0	0.0488	1.1406	1.503	0.1758
	GHD _{full}	0.2399	-0.0287	1.5099	0.0545	-1.3534	0.1696	0.9966
	GHStD	0.0264	-0.0264	1.6668	0.0515	-1.6507	0.2445	0.9732
Silver	NIG	0.3774	-0.0154	1.4618	0.0867	-0.5	0.8421	0.4516
	VG	0.7474	-0.0003	0	0.0280	1.0309	2.3916	0.0564
	GHD _{full}	0.1504	-0.0159	2.1120	0.0789	-1.3879	1.0817	0.3171
	GHStD	0.0163	-0.0163	2.2548	0.0951	-1.5745	0.8273	0.4618

ARFIMA-FIAPARCH models

Table 8.25: ML parameter estimates of the FMKL GLD for the ARFIMA-FIAPARCH-GLD model.

Returns	$\hat{\lambda}_1$	$\hat{\lambda}_2$	$\hat{\lambda}_3$	$\hat{\lambda}_4$	AD test	
					Statistic	p-value
Gold	0.0307	2.7665	-0.2504	-0.2390	1.461	0.1861
Platinum	0.0251	1.8726	-0.2024	-0.1682	0.1378	0.9993
Silver	0.0610	1.3622	-0.2165	-0.1840	0.7102	0.5503

Table 8.26: ML parameter estimates of the Stable distribution for the ARFIMA-FIAPARCH-SD model.

Returns	$\hat{\alpha}$	$\hat{\beta}$	$\hat{\gamma}$	$\hat{\delta}$	AD test	
					Statistic	<i>p</i> -value
Gold	1.5450	<0.0001	0.5245	0.0321	4.0700	0.0081
Platinum	1.6448	<0.0001	0.7430	0.0200	1.5546	0.1639
Silver	1.6217	<0.0001	1.0333	0.0628	2.0713	0.0840

Table 8.27: ML parameter estimates of GEVD for the ARFIMA-FIAPARCH-GEVD model.

Returns	Standardised Residuals	$\hat{\xi}$ (Se)	$\hat{\mu}$ (Se)	$\hat{\sigma}$ (Se)	AD test	
					Statistic	<i>p</i> -value
Gold	Positive	0.1344 (0.0221)	0.6594(0.0208)	0.5966 (0.0159)		
	Negative	0.1293(0.0202)	0.6222 (0.0207)	0.6028(0.0157)	1.4147	0.1982
Platinum	Positive	0.0758 (0.0184)	0.9141 (0.0207)	0.7819 (0.0196)	1.8966	0.1048
	Negative	0.1345 (0.0193)	0.91772(0.0264)	0.7698(0.0200)	0.7895	0.4887
Silver	Positive	0.0494 (0.0154)	1.3391 (0.0391)	1.1579(0.0280)	1.7246	0.1309
	Negative	0.1481 (0.0187)	1.2309 (0.0307)	1.0948 (0.0285)	1.6102	0.1522

*Se means standard error

Table 8.28: ML parameter estimates of GPD for the ARFIMA-FIAPARCH-GPD model.

Returns	Standardised Residuals	Threshold	No. of Exceedances	$\hat{\xi}$ (Se)	$\hat{\beta}$ (Se)
Gold	Positive	1.6389	1336	0.1623 (0.0772)	0.7107 (0.0704)
	Negative	1.4811	1369	0.1755 (0.0709)	0.7203 (0.0652)
Platinum	Positive	1.6774	1551	0.1844 (0.0614)	0.7962 (0.0624)
	Negative	1.5371	1651	0.2310 (0.0573)	0.8496 (0.0615)
Silver	Positive	2.2514	1515	0.1571 (0.0523)	1.1218 (0.0778)
	Negative	2.4025	1272	0.1968 (0.0596)	1.4450 (0.1133)

*Se means standard error

VAR estimation and Backtesting of models

VaR is calculated at 1%, 5%, 95% and 99% for each model. The estimates are then backtested using the Kupiec LR test. The *p*-values of the Kupiec test for in-sample are summarised in Tables 8.29, 8.30 and 8.31.

ARFIMA-FIGARCH models

For gold returns, ARFIMA-FIGARCH-NIGD gives the largest p -value at 1%, 5% and 95% VaR levels. ARFIMA-FIGARCH-STD is not a suitable model at 5% and 95% VaR levels. The VaR estimates from the ARFIMA-FIGARCH-N produced the lowest p -values at most VaR levels. However, the model is adequate at 5% and 95% VaR levels. It is interesting to note that ARFIMA-FIGARCH-PIVD, ARFIMA-FIGARCH-GLD, ARFIMA-FIGARCH-GHD_{full}, ARFIMA-FIGARCH-GPD, ARFIMA-FIGARCH-GHStD, ARFIMA-FIGARCH-NIGD and ARFIMA-FIGARCH-VGD models are all suitable at all VaR levels. For silver and platinum, ARFIMA-FIGARCH with GLD, full GHD, GPD, GHStD, PIVD, NIGD, STD, SSTD innovations are adequate VaR models at 1%, 5%, 95% and 99% levels. ARFIMA-FIGARCH-GEVD is the best model for platinum returns and for silver returns, the best model is ARFIMA-FIGARCH-GLD. ARFIMA-FIGARCH-SD is not suitable at 1% and 99% VaR levels. ARFIMA-FIGARCH-GEVD is not a good VaR model at 5% and 95% levels.

ARFIMA-HYGARCH models

For gold and platinum returns, ARFIMA-HYGARCH-STD, ARFIMA-HYGARCH-SSTD, ARFIMA-HYGARCH-PIVD, ARFIMA-HYGARCH-NIGD, ARFIMA-HYGARCH-GHStD, ARFIMA-HYGARCH-GHD_{full}, ARFIMA-HYGARCH-GLD, ARFIMA-HYGARCH-GPD, ARFIMA-HYGARCH-VGD are all suitable at all VaR levels. ARFIMA-HYGARCH-SD and ARFIMA-HYGARCH-GEVD are not good VaR models for gold returns. ARFIMA-HYGARCH-NIGD is the overall best model for gold returns as it has the highest p -values at all VaR levels, except at 99% VaR level. ARFIMA-HYGARCH-GHStD, ARFIMA-HYGARCH-STD compete favourably for the overall best model for platinum returns. For silver, ARFIMA-HYGARCH-STD, ARFIMA-HYGARCH-SSTD, ARFIMA-HYGARCH-PIVD, ARFIMA-HYGARCH-NIGD, ARFIMA-HYGARCH-GLD, ARFIMA-HYGARCH-GHD_{full}, ARFIMA-HYGARCH-GHStD are suitable at all VaR levels. It is interesting to note that ARFIMA-HYGARCH-VGD is not suitable at 1%, 5% and 95% VaR levels. I.e., ARFIMA-HYGARCH-VGD did not perform well for silver returns. ARFIMA-HYGARCH-SD is not suitable at 1% and 99% VaR levels.

Table 8.29: In-Sample VaR Backtesting: ARFIMA-FIGARCH models

Returns	Model	<i>p</i> -values of Kupiec LR test			
		Long positions		Short positions	
		1%	5%	95%	99%
Gold	ARFIMA-FIGARCH-N	4.363e-9	0.1631	0.1828	8.575e-9
	ARFIMA-FIGARCH-STD	0.5783	0.0437	0.0101	0.8877
	ARFIMA-FIGARCH-SSTD	0.7797	0.0878	0.0040	0.4072
	ARFIMA-FIGARCH-PIVD	0.7769	0.2526	0.1285	0.1451
	ARFIMA-FIGARCH-NIGD	0.9998	0.7473	0.9998	0.1914
	ARFIMA-FIGARCH-VGD	0.1722	0.2166	0.1931	0.6758
	ARFIMA-FIGARCH-GEVD	0.4072	0.0018	0.0236	0.4885
	ARFIMA-FIGARCH-GPD	0.7769	0.5231	0.8976	0.7797
	ARFIMA-FIGARCH-GLD	0.8877	0.6090	0.3396	0.1914
	ARFIMA-FIGARCH-GHD _{full}	0.8884	0.2166	0.2991	0.3131
	ARFIMA-FIGARCH-GHStD	0.5683	0.3086	0.1000	0.1451
ARFIMA-FIGARCH-SD	0.0002	0.0878	0.0878	0.0001	
Platinum	ARFIMA-FIGARCH-N	0.0001	0.6988	0.5180	0.0001
	ARFIMA-FIGARCH-STD	0.2179	0.1136	0.9998	0.4885
	ARFIMA-FIGARCH-SSTD	0.8884	0.4073	0.4827	0.2179
	ARFIMA-FIGARCH-PIVD	0.5783	0.7488	0.9998	0.5684
	ARFIMA-FIGARCH-NIGD	0.6758	0.2421	0.2421	0.5684
	ARFIMA-FIGARCH-VGD	0.0434	0.2421	0.0029	0.5684
	ARFIMA-FIGARCH-GEVD	0.6758	0.9999	0.9999	0.1722
	ARFIMA-FIGARCH-GPD	0.6234	0.6055	0.6988	0.6758
	ARFIMA-FIGARCH-GLD	0.6758	0.9487	0.5609	0.8884
	ARFIMA-FIGARCH-GHD _{full}	0.0162	0.6090	0.3306	0.3350
	ARFIMA-FIGARCH-GHStD	0.6758	0.7488	0.9993	0.8884
ARFIMA-FIGARCH-SD	0.1451	0.5652	0.5231	0.0258	
Silver	ARFIMA-FIGARCH-N	0.0006	0.0064	0.0546	0.0006
	ARFIMA-FIGARCH-STD	0.3046	0.7242	0.7260	0.4489
	ARFIMA-FIGARCH-SSTD	0.0692	0.4277	0.0096	0.0276
	ARFIMA-FIGARCH-PIVD	0.6278	0.6331	0.9745	0.3522
	ARFIMA-FIGARCH-NIGD	0.7283	0.2069	0.2579	0.4328
	ARFIMA-FIGARCH-VGD	0.0276	0.1272	0.0014	0.7241
	ARFIMA-FIGARCH-GEVD	0.7283	0.3570	0.7242	0.4489
	ARFIMA-FIGARCH-GPD	0.9443	0.7242	0.7730	0.8344
	ARFIMA-FIGARCH-GLD	0.9441	0.6300	0.9745	0.6200
	ARFIMA-FIGARCH-GHD _{full}	0.8328	0.7730	0.9745	0.5224
	ARFIMA-FIGARCH-GHStD	0.9440	0.7260	0.7260	0.5224
ARFIMA-FIGARCH-SD	0.0674	0.1558	0.3262	0.0033	

Table 8.30: In-Sample VaR Backtesting: ARFIMA-HYGARCH models

Returns	Model	<i>p</i> -values of Kupiec LR test			
		Long positions		Short positions	
		1%	5%	95%	99%
Gold	ARFIMA-HYGARCH-N	0.0004	0.1931	0.1931	0.0024
	ARFIMA-HYGARCH-STD	0.3889	0.3725	0.3396	0.0554
	ARFIMA-HYGARCH-SSTD	0.2472	0.7977	0.1450	0.1914
	ARFIMA-HYGARCH-PIVD	0.6698	0.2042	0.1630	0.1451
	ARFIMA-HYGARCH-NIGD	0.9998	0.8469	0.9487	0.1451
	ARFIMA-HYGARCH-VGD	0.2179	0.3642	0.1715	0.6758
	ARFIMA-HYGARCH-GEVD	<0.0001	0.0033	0.0276	0.4885
	ARFIMA-HYGARCH-GPD	0.9998	0.9487	0.0103	0.9998
	ARFIMA-HYGARCH-GLD	0.7769	0.5652	0.3725	0.3131
	ARFIMA-HYGARCH-GHD _{full}	0.8884	0.3642	0.2991	0.3889
	ARFIMA-HYGARCH-GHStD	0.5684	0.2526	0.1000	0.1451
	ARFIMA-HYGARCH-SD	<0.0001	<0.0001	0.2526	<0.0001
Platinum	ARFIMA-HYGARCH-N	0.0009	0.3170	0.2069	0.0004
	ARFIMA-HYGARCH-STD	0.9441	0.7260	0.9264	0.4489
	ARFIMA-HYGARCH-SSTD	0.1914	0.5179	0.3725	0.2720
	ARFIMA-HYGARCH-PIVD	0.6278	0.9745	0.8225	0.8328
	ARFIMA-HYGARCH-NIGD	0.7283	0.0849	0.2069	0.9441
	ARFIMA-HYGARCH-VGD	0.0916	0.0546	0.0635	0.6278
	ARFIMA-HYGARCH-GEVD	0.7283	0.5047	0.8732	0.3046
	ARFIMA-HYGARCH-GPD	0.2814	0.9235	0.5412	0.9443
	ARFIMA-HYGARCH-GLD	0.7283	0.5848	0.5412	0.9443
	ARFIMA-HYGARCH-GHD _{full}	0.7283	0.6300	0.5848	0.8328
	ARFIMA-HYGARCH-GHStD	0.7283	0.9745	0.8728	0.9443
	ARFIMA-HYGARCH-SD	0.6200	0.1954	0.9235	0.0141
Silver	ARFIMA-HYGARCH-N	0.0002	0.0202	0.0052	0.0098
	ARFIMA-HYGARCH-STD	0.5343	0.7242	0.5848	0.9441
	ARFIMA-HYGARCH-SSTD	0.9440	0.2580	0.7742	0.5343
	ARFIMA-HYGARCH-PIVD	0.7283	0.7260	0.6331	0.3522
	ARFIMA-HYGARCH-NIGD	0.8344	0.1635	0.7242	0.4328
	ARFIMA-HYGARCH-VGD	0.0380	0.0468	0.0116	0.8328
	ARFIMA-HYGARCH-GEVD	0.8328	0.2421	0.7260	<0.0001
	ARFIMA-HYGARCH-GPD	0.0674	0.7260	0.9237	0.0049
	ARFIMA-HYGARCH-GLD	0.9441	0.6765	0.6789	0.7241
	ARFIMA-HYGARCH-GHD _{full}	0.9441	0.9745	0.4277	0.8328
	ARFIMA-HYGARCH-GHStD	0.9441	0.8233	0.4653	0.6200
	ARFIMA-HYGARCH-SD	0.0142	0.2682	0.1558	0.0090

Table 8.31: In-Sample VaR Backtesting : ARFIMA-FIAPARCH models

Returns	Model	<i>p</i> -values of Kupiec LR test			
		Long positions		Short positions	
		1%	5%	95%	99%
Gold	ARFMA-FIAPARCH-N	0.0000	0.1715	0.2696	0.0007
	ARFIMA- FIAPARCH -STD	0.9998	0.0878	0.1828	0.8877
	ARFIMA- FIAPARCH SSTD	0.6698	0.1631	0.0437	0.6758
	ARFIMA-FIAPARCH-PIVD	0.6698	0.1450	0.1136	0.1451
	ARFIMA-FIAPARCH-NIGD	0.9998	0.8469	0.9998	0.1913
	ARFIMA-FIAPARCH -VGD	0.1722	0.5179	0.0421	0.8877
	ARFIMA-FIAPARCH-GEVD	<0.0001	0.0040	0.0276	0.5783
	ARFIMA-FIAPARCH-GPD	0.6698	0.7009	0.9488	<0.0001
	ARFIMA-FIAPARCH-GLD	0.8877	0.6090	0.3396	0.1914
	ARFIMA-FIAPARCH-GHD _{full}	0.8884	0.5179	0.3997	0.3131
	ARFIMA-FIAPARCH-GHStD	0.5683	0.1828	0.1136	0.1451
	ARFIMA-FIAPARCH-SD	0.0002	0.0323	0.1136	0.0001
Platinum	ARFMA-FIAPARCH-N	0.0000	0.3725	0.1174	0.0007
	ARFIMA- FIAPARCH -STD	0.4072	0.1003	0.76667	0.6758
	ARFIMA- FIAPARCH SSTD	0.7769	0.8976	0.1003	0.0784
	ARFIMA-FIAPARCH-PIVD	0.6758	0.9488	0.8469	0.7769
	ARFIMA-FIAPARCH-NIGD	0.6758	0.0893	0.2166	0.8877
	ARFIMA-FIAPARCH -VGD	0.0434	0.0214	0.0670	0.5783
	ARFIMA-FIAPARCH-GEVD	0.9998	0.7473	0.8979	0.3350
	ARFIMA-FIAPARCH-GPD	0.1077	0.1931	0.7473	0.8884
	ARFIMA-FIAPARCH-GLD	0.6758	0.4767	0.6055	0.8884
	ARFIMA-FIAPARCH-GHD _{full}	0.6758	0.5609	0.7473	0.9993
	ARFIMA-FIAPARCH-GHStD	0.6758	0.9488	0.8469	0.8884
	ARFIMA-FIAPARCH-SD	0.5684	0.1828	0.9487	0.0170
Silver	ARFMA-FIAPARCH-N	0.0001	0.0068	0.0255	0.0114
	ARFIMA- FIAPARCH -STD	0.4884	0.6054	0.6515	0.8884
	ARFIMA- FIAPARCH SSTD	0.7797	0.2991	0.8979	0.4885
	ARFIMA-FIAPARCH-PIVD	0.6758	0.6543	0.6090	0.3031
	ARFIMA-FIAPARCH-NIGD	0.9998	0.1715	0.6515	0.3889
	ARFIMA-FIAPARCH -VGD	0.04344	0.0576	0.0055	0.8877
	ARFIMA-FIAPARCH-GEVD	0.7769	0.2526	0.7488	0.2179
	ARFIMA-FIAPARCH-GPD	0.0383	0.7488	0.8474	0.8884
	ARFIMA-FIAPARCH-GLD	0.8877	0.6988	0.7488	0.6698
	ARFIMA-FIAPARCH-GHD _{full}	0.6758	0.7009	0.3725	0.8877
	ARFIMA-FIAPARCH-GHStD	0.7769	0.7009	0.4827	0.6698
	ARFIMA-FIAPARCH-SD	0.0383	0.0505	0.4827	0.0002

ARFIMA-FIAPARCH models

For gold and platinum returns, ARFIMA-FIAPARCH-STD, ARFIMA-FIAPARCH-SSTD, ARFIMA-FIAPARCH-PIVD, ARFIMA-FIAPARCH-NIGD, ARFIMA-FIAPARCH-VGD, ARFIMA-FIAPARCH-GHD_{full}, ARFIMA-FIAPARCH-GHStD, ARFIMA-FIAPARCH-GLD are all suitable at all VaR levels. For silver, ARFIMA-FIAPARCH-STD, ARFIMA-FIAPARCH-SSTD, ARFIMA-FIAPARCH-PIVD, ARFIMA-FIAPARCH-GLD, ARFIMA-FIAPARCH-GHD_{full}, ARFIMA-FIAPARCH-GHStD, ARFIMA-FIAPARCH-GEVD, ARFIMA-FIAPARCH-GPD, ARFIMA-FIAPARCH-NIGD are suitable at all VaR levels. ARFIMA-FIAPARCH-VGD did not perform well for silver returns at 1% and 95% VaR levels. For gold, ARFIMA-FIAPARCH-NIGD produced highest p -values at 1%, 5% and 95% and is clearly the best model for gold returns. For platinum, ARFIMA-FIAPARCH-GEVD produced highest p -value at 1% and 95% VaR levels and ARFIMA-FIAPARCH-GHD_{full} at a 99% VaR level. At a 5% VaR level, ARFIMA-FIAPARCH-PIVD and ARFIMA-FIAPARCH-GHStD are the most robust models for estimating VaR for platinum returns. For silver returns, at 1% ARFIMA-FIAPARCH-NIGD produces the largest p -value. ARFIMA-FIAPARCH-GPD produced highest p -values at 5% and 95% VaR levels for silver returns.

8.5 Summary

We extended the work of Arouri *et al* (2012), Diaz (2016), Ranganai and Khubeka (2016), Youssef *et al.* (2015), Mabrouk and Saadi (2012), Cochran *et al.* (2012), McNeil and Frey (2000), Bhattacharyya *et al.* (2008) and Bhattacharyya and Madhav (2012). Our findings revealed that precious metal markets are characterised by asymmetry, heavy-tail and long-range dependence. We examined the LM GARCH models under the GHDs, the STD, SSTD, GLD, GEVD, GPD, SD and PIVD assumptions. The conditional variance and long memory in the mean and volatility were modelled by ARFIMA-FIAPARCH, ARFIMA-HYGARCH and ARFIMA-FIAPARCH models with pseudo-normal assumptions. The NIGD, VGD, full GHD, GHStD, GLD, GEVD, GPD, SD and PIVD distributions were applied to capture the heavy-tail

behavior for the extracted standardised residuals and VaR was calculated at different levels. Adequacy of the resulting VaR estimates were tested using the Kupiec LR test. Backtesting results showed that ARFIMA-FIGARCH, ARFIMA-HYGARCH and ARFIMA-FIAPARCH models with PIVD, GLD, NIGD and GHStD, full GHD governing the innovations are suitable for depicting VaR in gold, platinum and silver returns. However, ARFIMA-FIGARCH, ARFIMA-HYGARCH and ARFIMA-FIAPARCH with GEVD and SD are not good VaR models for gold returns. ARFIMA-HYGARCH-VGD, ARFIMA-HYGARCH-SD and ARFIMA-FIAPARCH-SD are not suitable VaR models for silver returns. ARFIMA-FIAPARCH-VGD is not a good VaR model for silver returns.

8.6 Statistical software packages

We used OxMetrics 7 (Doornik and Hendry, 2013) to fit the ARFIMA-FIGARCH, ARFIMA-HYGARCH and ARFIMA-FIAPARCH models to gold, platinum and silver returns. We used the R packages **evir** (Pfaff *et al.*, 2012), **evd** (Stephenson, 2002, Stephenson and Ferro, 2015), **ismev** (Heffernan *et al.*, 2012), **ghyp** (Luethi and Breyermann, 2016), **laeken** (Alfons and Templ, 2013), **PearsonDS** (Becker and KlöBner, 2017), **fGarch** (Wuertz *et al.*, 2016), **stable** (Robust Analysis Inc, 2013), **GLDEX**(Su, 2007, 2016), **rugarch** (Ghalanos,2015) to fit GEVD, GPD, PIVD, STD, SSTD, full GHD, NIGD, VGD, GHStD, SD, GLD to the extracted standardised residual. We used the AD test in the **ADGofTest** (Bellosta, 2011) R package to check for model adequacy.

8.7 Appendix

ARFIMA-FIGARCH-GPD model

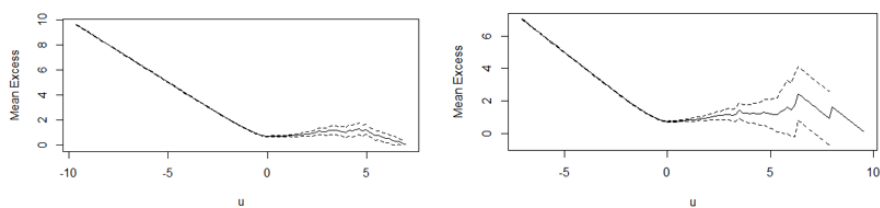


Figure 8.4: Mean excess plot of gold (a) positive (b) negative standardised residuals

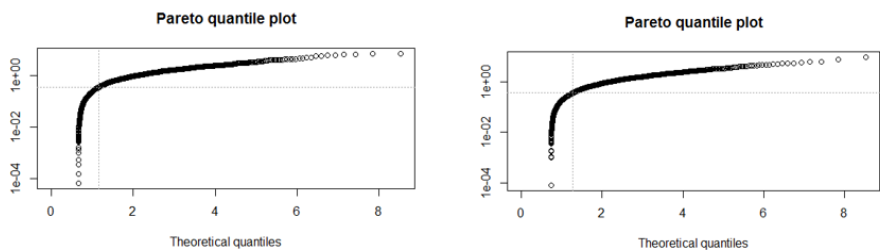


Figure 8.5: Pareto quantile plot of gold (a) positive (b) negative standardised residuals

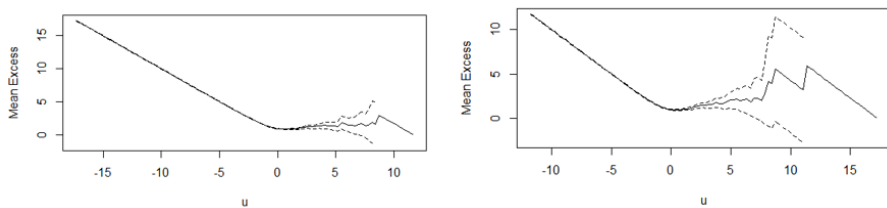


Figure 8.6: Mean excess plot of platinum (a) positive (b) negative standardised residuals

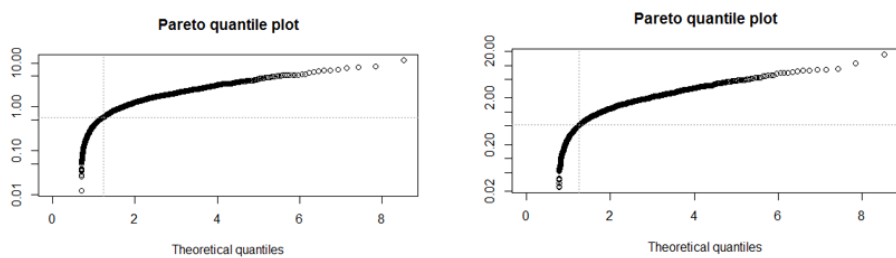


Figure 8.7: Pareto quantile plot of platinum (a) positive (b) negative standardised residuals

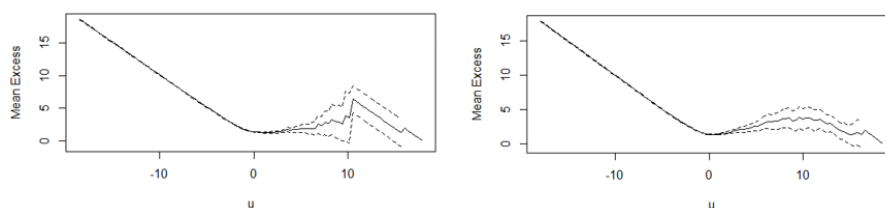


Figure 8.8: Mean excess plot of silver (a) positive (b) negative standardised residuals

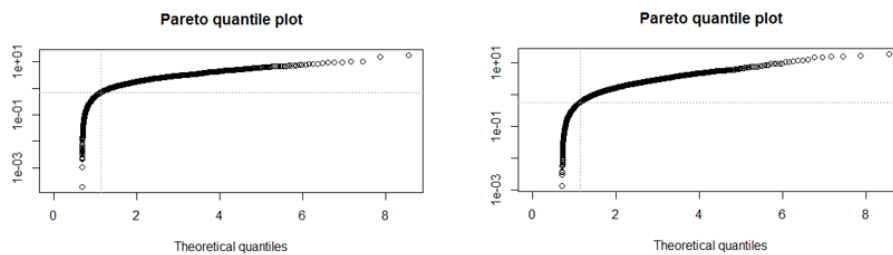


Figure 8.9: Pareto quantile plot of silver (a) positive (b) negative standardised residuals

ARFIMA-HYGARCH-GPD model

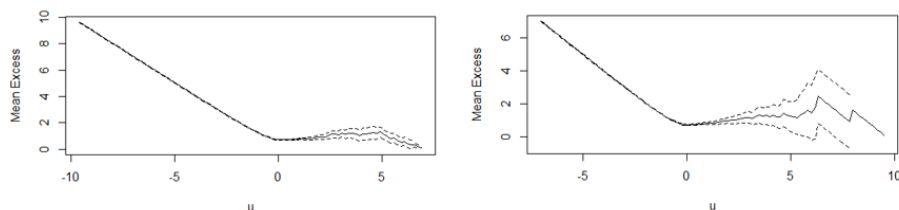


Figure 8.10: Mean excess plot of gold (a) positive (b) negative standardised residuals

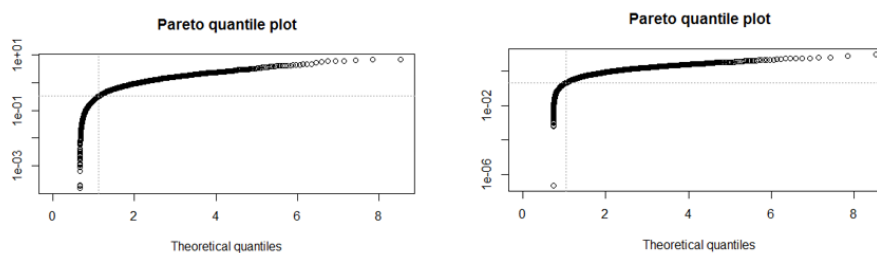


Figure 8.11: Pareto quantile plot of gold (a) positive (b) negative standardised residuals

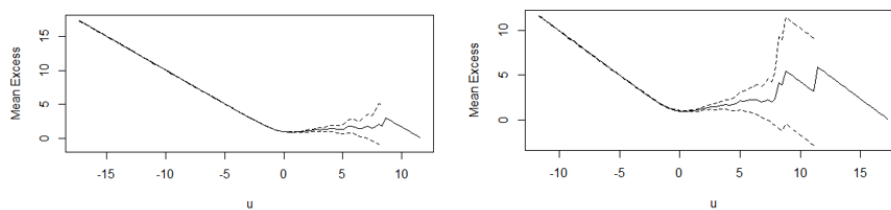


Figure 8.12: Mean excess plot of platinum (a) positive (b) negative standardised residuals

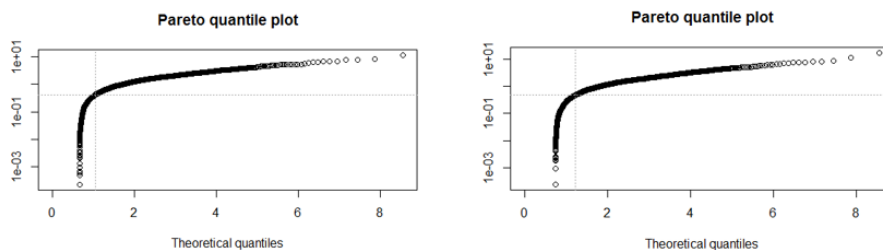


Figure 8.13: Pareto quantile plot of platinum (a) positive (b) negative standardised residuals

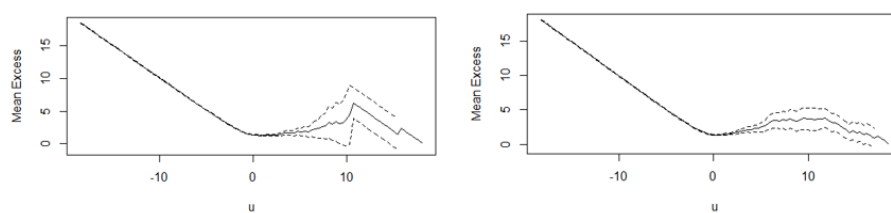


Figure 8.14: Mean excess plot of silver (a) positive (b) negative standardised residuals

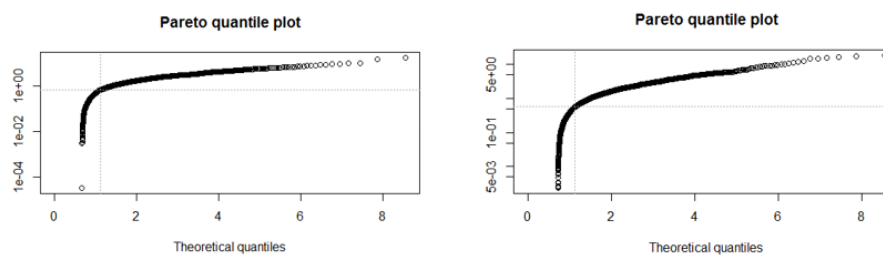


Figure 8.15: Pareto quantile plot of silver (a) positive (b) negative standardised residuals

ARFIMA-FIAPARCH-GPD model

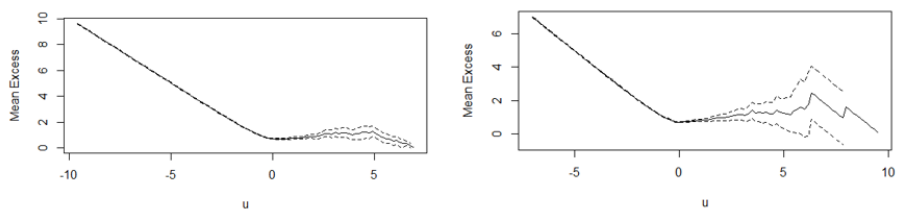


Figure 8.16: Mean excess plot of gold (a) positive (b) negative standardised residuals

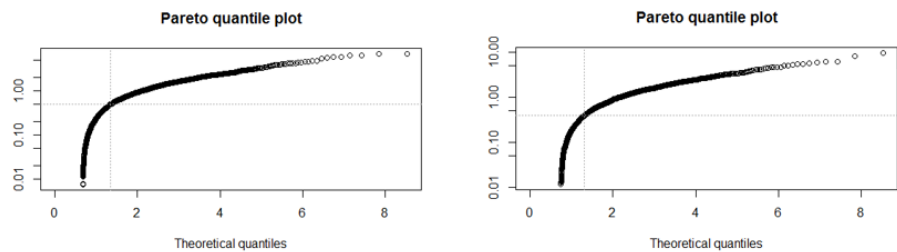


Figure 8.17: Pareto quantile plot of gold (a) positive (b) negative standardised residuals

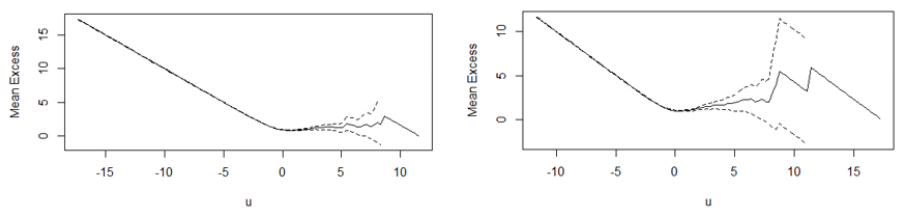


Figure 8.18: Mean excess plot of platinum (a) positive (b) negative standardised residuals

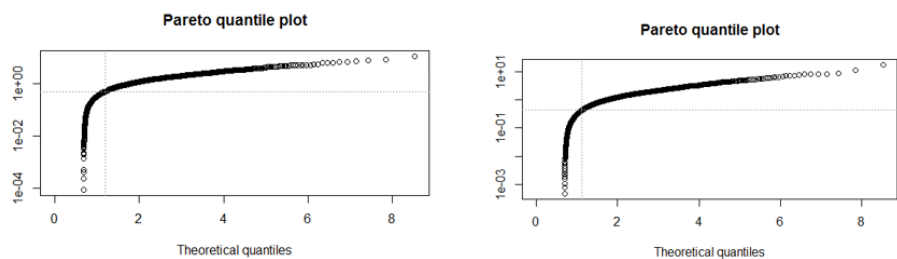


Figure 8.19: Pareto quantile plot of platinum (a) positive (b) negative standardised residuals

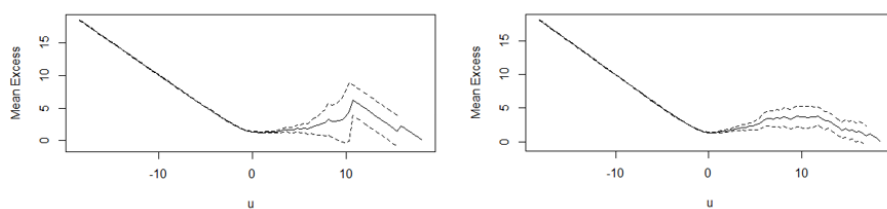


Figure 8.20: Mean excess plot of silver (a) positive (b) negative standardised residuals

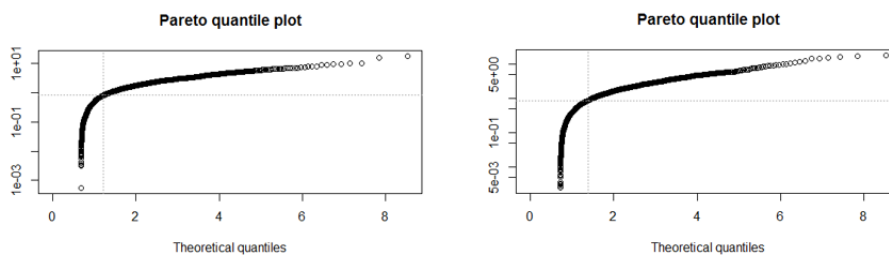


Figure 8.21: Pareto quantile plot of silver (a) positive (b) negative standardised residuals

ARFIMA-FIGARCH-GPD model

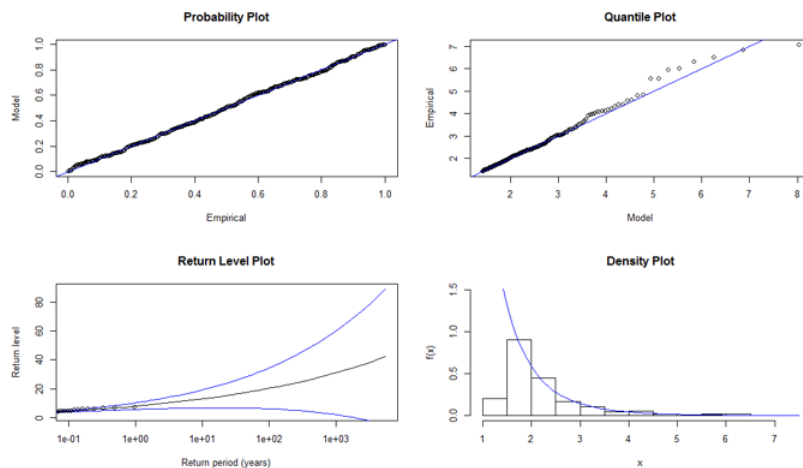


Figure 8.22: Diagnostic plots of GPD fit to positive standardised residuals (gold)

*P-P plot (on the upper left panel), Q-Q Plot (on the upper right panel), Return level plot (on the lower left panel), Density plot (on the lower right panel)

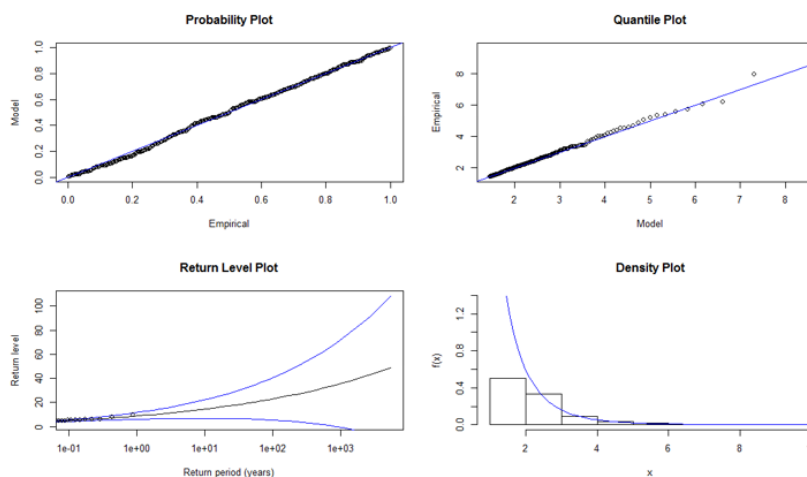


Figure 8.23: Diagnostic plots of GPD fit to negative standardised residuals (gold)

*P-P plot (on the upper left panel), Q-Q Plot (on the upper right panel), Return level plot (on the lower left panel), Density plot (on the lower right panel)

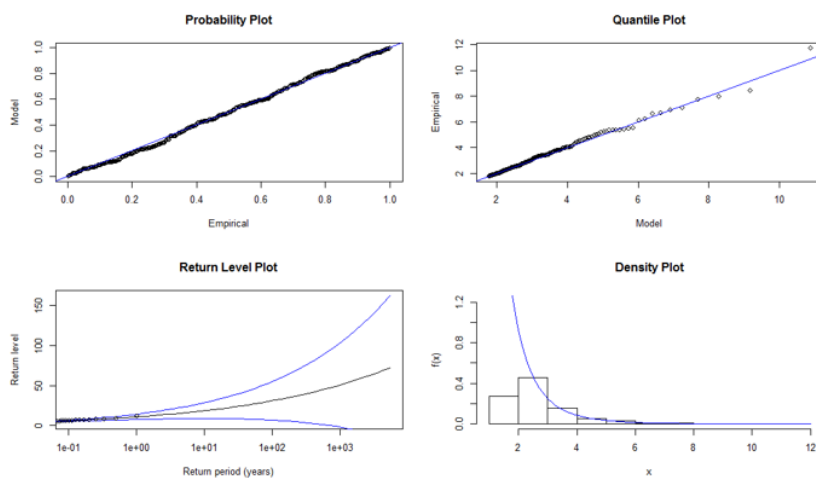


Figure 8.24: Diagnostic plots of GPD fit to positive standardised residuals (platinum)

**P-P plot (on the upper left panel), Q-Q Plot (on the upper right panel), Return level plot (on the lower left panel), Density plot (on the lower right panel)*

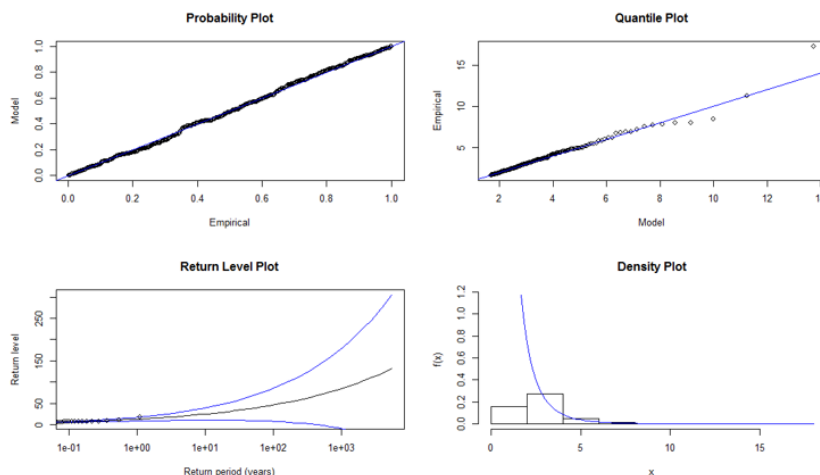


Figure 8.25: Diagnostic plots of GPD fit to negative standardised residuals (platinum)

**P-P plot (on the upper left panel), Q-Q Plot (on the upper right panel), Return level plot (on the lower left panel), Density plot (on the lower right panel)*

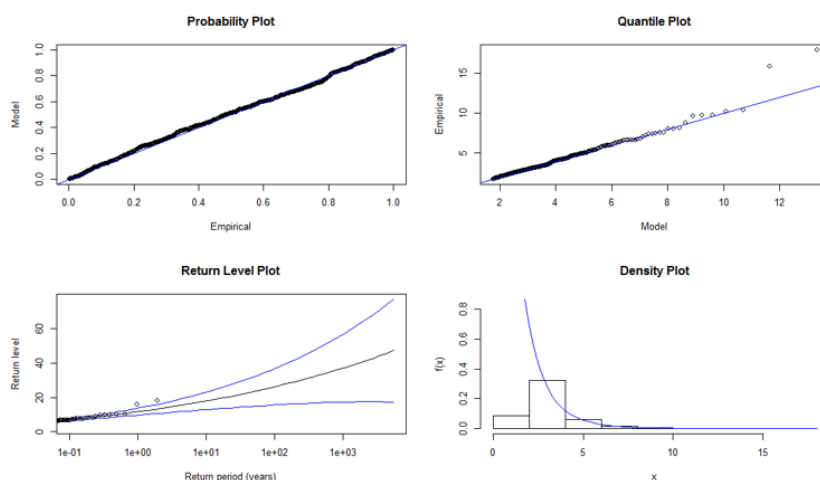


Figure 8.26: Diagnostic plots of GPD fit to positive standardised residuals (silver)

*P-P plot (on the upper left panel), Q-Q Plot (on the upper right panel), Return level plot (on the lower left panel), Density plot (on the lower right panel)

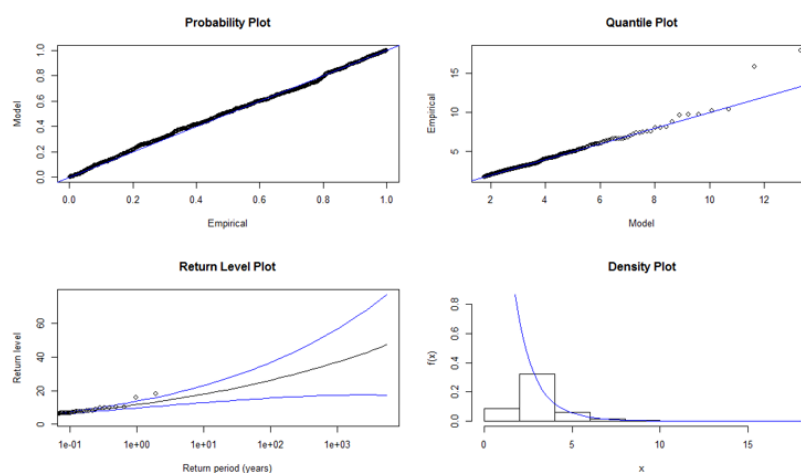


Figure 8.27: Diagnostic plots of GPD fit to negative standardised residuals (silver)

*P-P plot (on the upper left panel), Q-Q Plot (on the upper right panel), Return level plot (on the lower left panel), Density plot (on the lower right panel)

ARFIMA-HYGARCH-GPD model

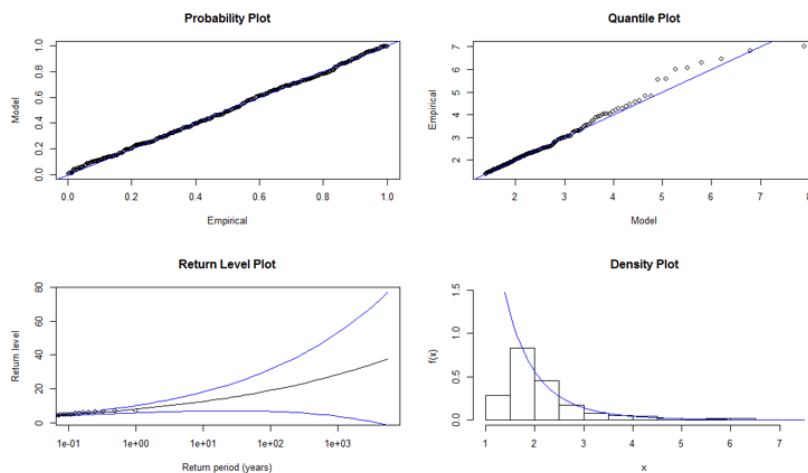


Figure 8.28: Diagnostic plots of GPD fit to positive standardised residuals (gold)

**P-P plot (on the upper left panel), Q-Q Plot (on the upper right panel), Return level plot (on the lower left panel), Density plot (on the lower right panel)*

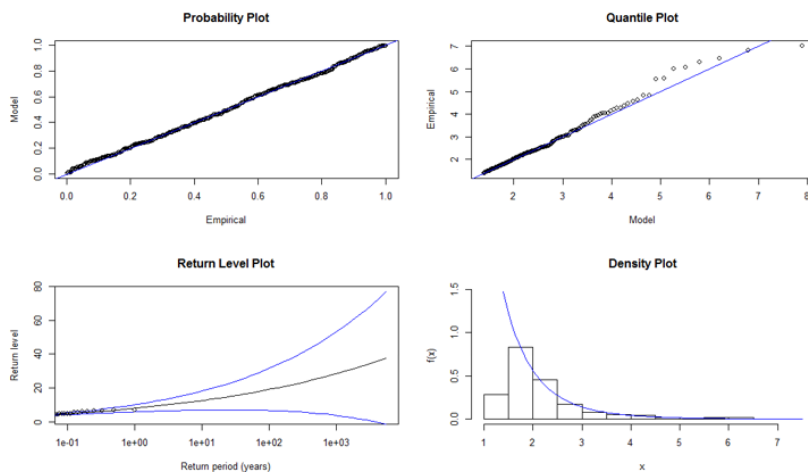


Figure 8.29: Diagnostic plots of GPD fit to negative standardised residuals (gold)

**P-P plot (on the upper left panel), Q-Q Plot (on the upper right panel), Return level plot (on the lower left panel), Density plot (on the lower right panel)*

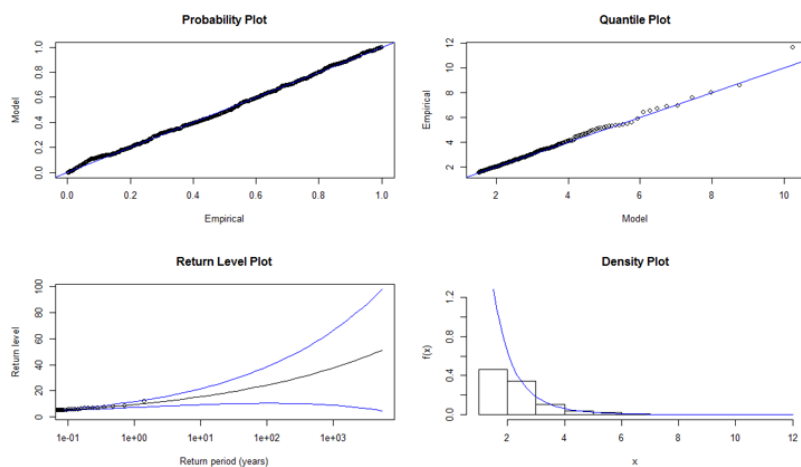


Figure 8.30: Diagnostic plots of GPD fit to positive standardised residuals (platinum)

**P-P plot (on the upper left panel), Q-Q Plot (on the upper right panel), Return level plot (on the lower left panel), Density plot (on the lower right panel)*

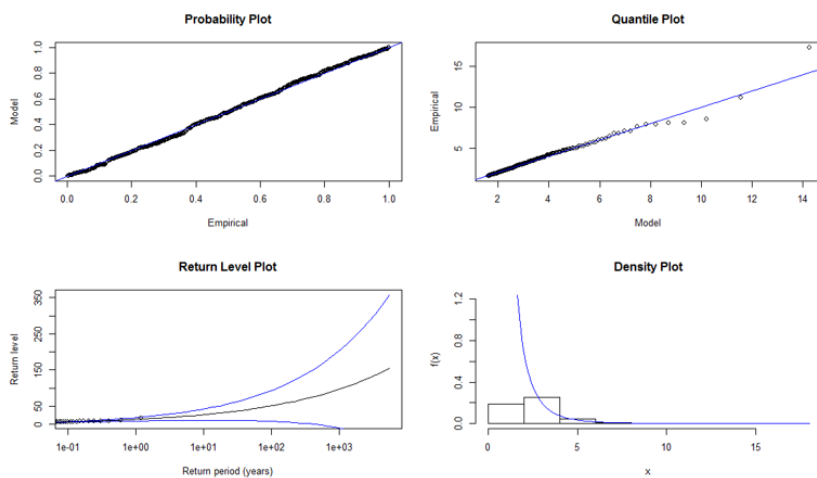


Figure 8.31: Diagnostic plots of GPD fit to negative standardised residuals (platinum)

**P-P plot (on the upper left panel), Q-Q Plot (on the upper right panel), Return level plot (on the lower left panel), Density plot (on the lower right panel)*

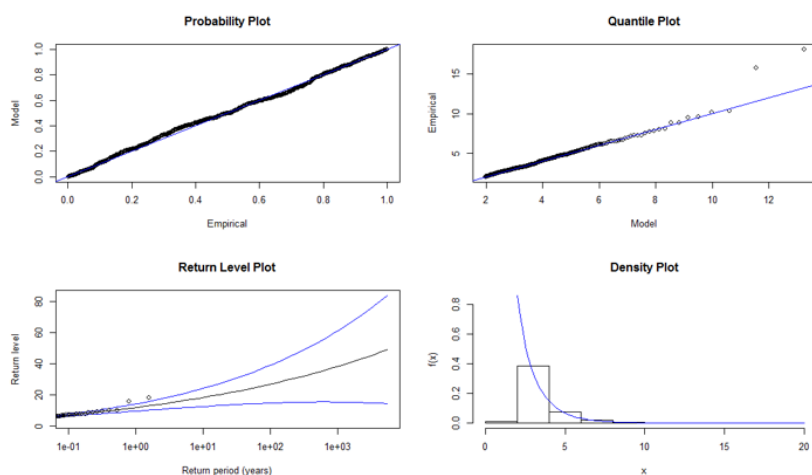


Figure 8.32: Diagnostic plots of GPD fit to positive standardised residuals (silver)

**P-P plot (on the upper left panel), Q-Q Plot (on the upper right panel), Return level plot (on the lower left panel), Density plot (on the lower right panel)*

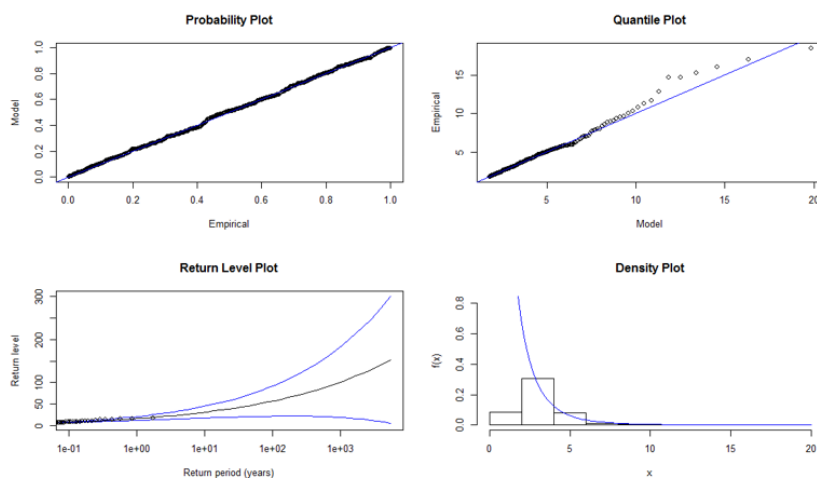


Figure 8.33: Diagnostic plots of GPD fit to negative standardised residuals (silver)

**P-P plot (on the upper left panel), Q-Q Plot (on the upper right panel), Return level plot (on the lower left panel), Density plot (on the lower right panel)*

ARFIMA-FIAPARCH-GPD model

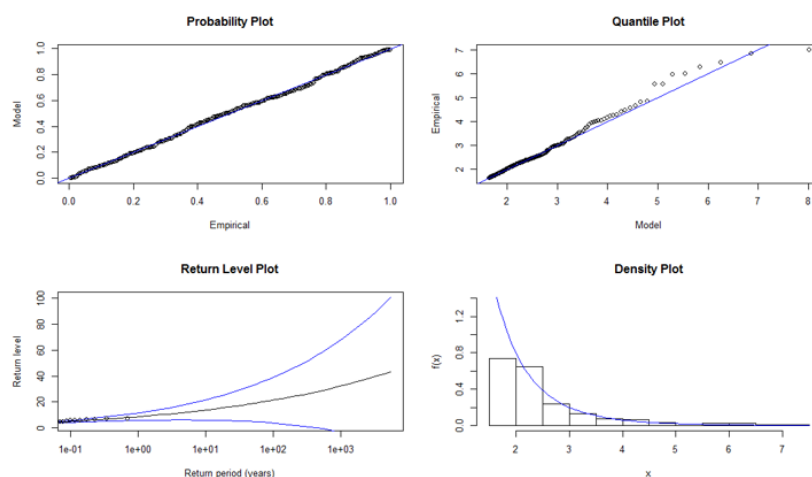


Figure 8.34: Diagnostic plots of GPD fit to positive standardised residuals (gold)

**P-P plot (on the upper left panel), Q-Q Plot (on the upper right panel), Return level plot (on the lower left panel), Density plot (on the lower right panel)*

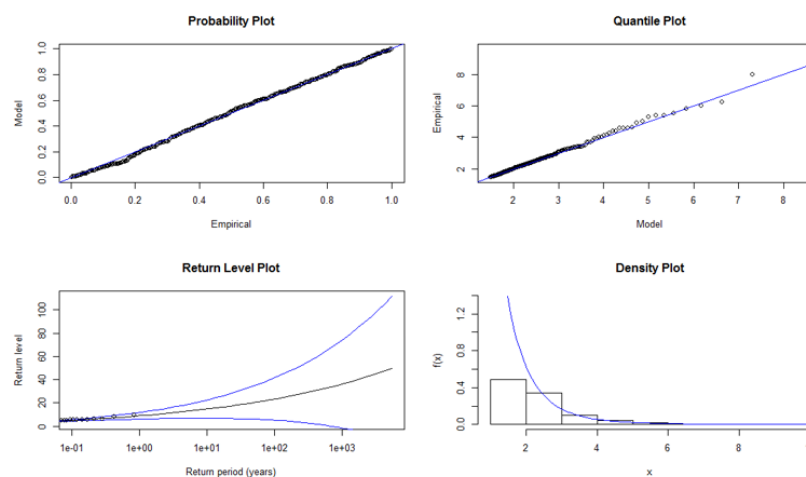


Figure 8.35: Diagnostic plots of GPD fit to negative standardised residuals (gold)

**P-P plot (on the upper left panel), Q-Q Plot (on the upper right panel), Return level plot (on the lower left panel), Density plot (on the lower right panel)*

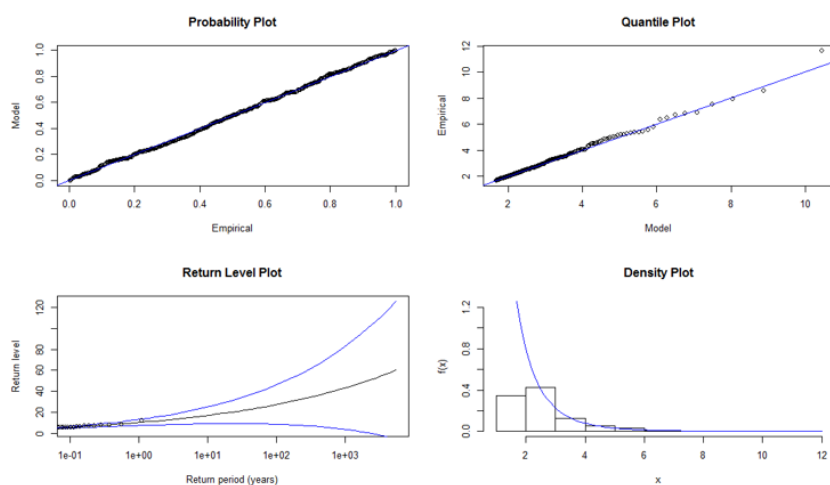


Figure 8.36: Diagnostic plots of GPD fit to positive standardised residuals (platinum)

**P-P plot (on the upper left panel), Q-Q Plot (on the upper right panel), Return level plot (on the lower left panel), Density plot (on the lower right panel)*

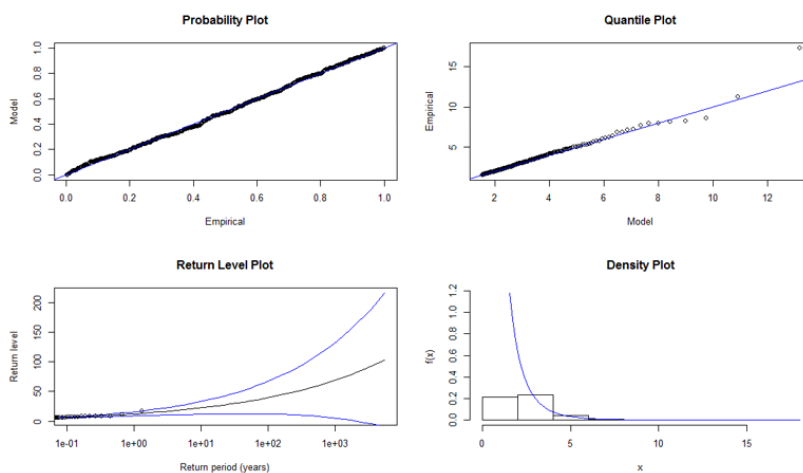


Figure 8.37: Diagnostic plots of GPD fit to negative standardised residuals (platinum)

**P-P plot (on the upper left panel), Q-Q Plot (on the upper right panel), Return level plot (on the lower left panel), Density plot (on the lower right panel)*

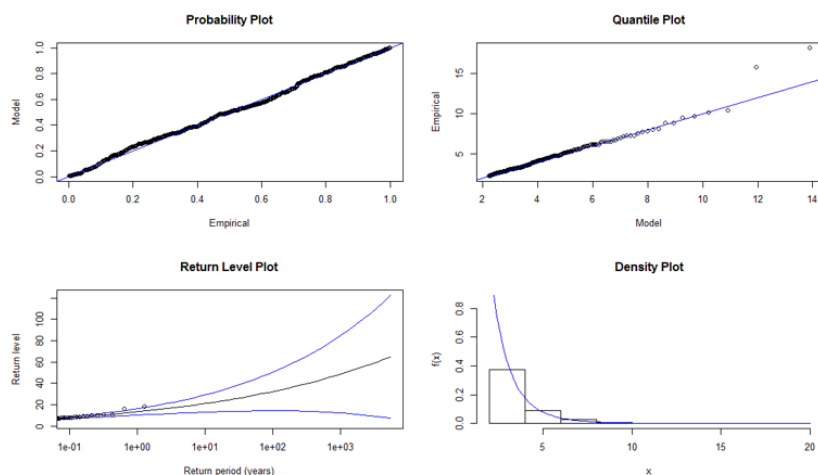


Figure 8.38: Diagnostic plots of GPD fit to positive standardised residuals (silver)

*P-P plot (on the upper left panel), Q-Q Plot (on the upper right panel), Return level plot (on the lower left panel), Density plot (on the lower right panel)

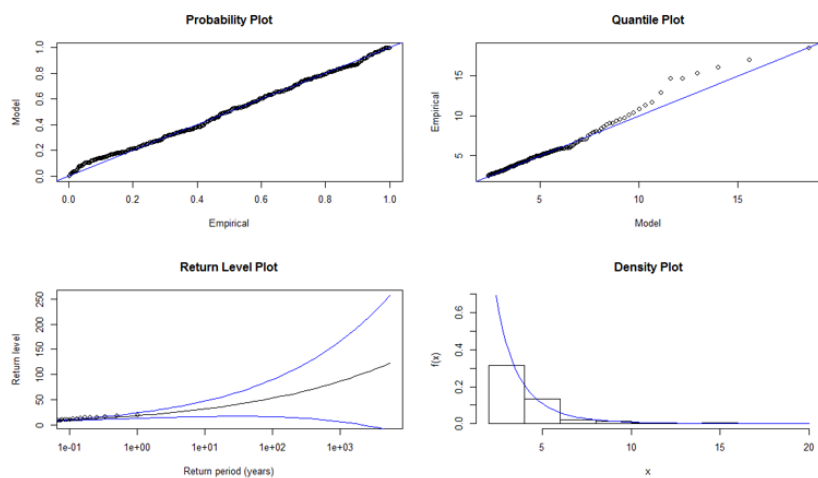


Figure 8.39: Diagnostic plots of GPD fit to negative standardised residuals (silver)

*P-P plot (on the upper left panel), Q-Q Plot (on the upper right panel), Return level plot (on the lower left panel), Density plot (on the lower right panel)

Chapter 9

Conclusion

Risk management tools, such as Value-at-Risk (VaR) and Expected shortfall (ES), are highly dependent on the underlying distributional assumptions. The development of more robust approaches in estimating VaR and ES is crucial. In this study, we investigated and proposed suitable models which are able to capture extreme tails of profit and loss distribution, and as a result improve the estimation of VaR. The models were able to capture well the features of gold, platinum and silver log-returns.

While the literature has focused on developing models that can take into account heavy tails, these stylised facts should not be considered in isolation. A realistic model for financial returns should include volatility clustering, heavy-tails, asymmetry, conditional heavy tails and long memory. The daily gold, platinum and silver log-returns that have been used in the study exhibited volatility clustering, heavy-tails, asymmetry and long-range memory. The data sets are for the period 2 April 1994 to 18 September 2014. We started by fitting heavy-tailed distributions based on two features, heavy-tails and asymmetry.

We analysed daily log-returns of precious metals (gold, platinum and silver) using nine distributions, namely: GEVD, GPD, GLD, SD, PIVD, STD, SSTD, GLD and GHDs. We then considered two other features: volatility clustering and leverage effect. We coupled the GARCH-type model with the heavy-tailed SD, PIVD, GPD,

GEVD, SSTD, STD and GHDs and the flexible GLD. We then analysed daily log-returns with the proposed models. Lastly, we considered the long memory, which was being exhibited by the daily log-returns of precious metals used in this research. We coupled long-memory GARCH models with heavy-tailed distributions. FIGARCH, FIAPARCH and HYGARCH were used to capture volatility clustering and long-range memory, and NIGD, full GHD, GHStD, GLD, GEVD, SD, VGD, and PIVD for conditional heavy tails. We analysed daily log-returns with the improved long-memory-GARCH-heavy-tailed models.

The relative adequacy and goodness-of-fit of the distributions, and models, were assessed based on the robustness of their VAR estimates. The Anderson-Darling test was used to check for model adequacy. Backtesting on the adequacy of VAR estimates is performed using Kupiec likelihood ratio test and Christoffersen conditional coverage test.

Heavy-tailed and asymmetry

Our analyses show that GPD and GLD generally outperform GEVD for the VaR estimation of negative precious metal returns. For gold, GPD stands out as the most suitable model. For platinum, it is between GPD and GLD, especially at the 1% level of significance. For silver, GLD is the most suitable at 1% level of significance, whereas GPD is the best model at 0.1% level of significance. The difference in ES estimation between the three distributions for platinum, however, is minor, with GPD being preferred for ES estimation at the 0.1% level of significance for both gold and silver. This study confirms the results by Ren and Giles (2010) that EVT is a reliable method for predicting future potential extreme losses/gains for precious metals. It also shows that GLD competes favourably with EVT for predicting future potential extreme losses/gains for precious metal results, especially for silver and platinum returns.

We evaluated the performance of Generalised Hyperbolic Distributions in characterising gold and platinum returns. In particular, we used the hyperbolic, the Normal-

Inverse Gaussian, the Variance-Gamma and GH skew Student- t distributions. The ability of these models to capture certain stylised facts, such as skewness and both symmetric and asymmetric heavy tails, provided us with a higher degree of accuracy when fitted to financial returns data. The models' performances with respect to VaR estimation and results from the Kupiec Likelihood test show that the best GHD model for VaR estimation differs at different levels, for both gold and platinum returns. We contrast these results with estimates from SD, PIVD, STD and SSTD. The performances of GHDs, SD, PIVD and SSTD are comparable in terms of VaR estimation for gold, platinum and silver price returns.

Volatility clustering (conditional heteroscedasticity), heavy-tailed and asymmetry

We evaluated the performance of ARMA-GARCH-Normal, ARMA-GARCH-Stable and ARMA-GARCH-GHDs in characterising gold log-returns. The advantage of the proposed models lies in their ability to capture conditional heteroscedasticity in the returns through the GARCH framework and at the same time model their heavy tail behaviour through the Stable Distribution, PIVD, GLD, GPD, GEVD, STD, SSTD and Generalised Hyperbolic Distributions. We also compared the VaR in-sample backtesting of the six models using the Kupiec likelihood ratio test and the Christoffersen test. An ARMA (1,1)-GARCH-Normal adequately fits gold log-returns. VaR estimates were obtained from all fitted models, both the Kupiec test and the Christoffersen test showed that an ARMA (1,1)-GARCH(1,1)-VGD model is the best model for VaR estimation at different levels for gold returns. Interestingly all models were rejected at 99% using the Christoffersen test. An ARMA (1,1)-GARCH(1,1)-NIGD is the best model for platinum returns. The overall best model for silver returns is ARMA (1,1)-GARCH(1,1)-SSTD based on the Kupiec test. In general, the performance of the models, in terms of VaR estimation is comparable at different levels.

We used the ARMA-APARCH model to take into account major stylised facts such as volatility clustering and asymmetry in gold price returns and PIVD, GLD, GEVD, STD, SSTD, SD and GHD and its subclasses, to model heavy tail behavior of stan-

standardised residuals. We computed VaR estimates for gold, platinum and silver returns using ARMA-APARCH-PIVD, ARMA-APARCH-GHD_{full}, ARMA-APARCH-NIGD, ARMA-APARCH-VGD, ARMA-APARCH-GLD, ARMA-APARCH-GEVD, ARMA-APARCH-SD, ARMA-APARCH-GHStD, ARMA-APARCH-STD, ARMA-APARCH-SSTD and ARMA-APARCH-N models. We compared the VaR in-sample backtesting of these models using the Kupiec test and Christoffersen test. The backtesting results show that ARMA-APARCH with full GHD, PIVD, SD, GLD, GEVD and GPD perform well in characterising precious metal returns. For gold returns, VaR is best modelled by an ARMA(1,1)-APARCH(1,1)-GHD_{full}. VaR is best modelled by an ARMA(1,1)-APARCH(1,1)-GPD for platinum returns. For silver returns, AR(1)-APARCH(1,1)-GHD_{full} and AR(1)-APARCH(1,1)-GHD_{full} are appropriate at all levels using the Kupiec test. However, there is no best model for the silver return series. Our findings confirm that GARCH-type models combined with filtering process such as PIVD, SD, GEVD, GLD, GPD and GHDs are important in improving risk management assessments and hedging strategies in the highly volatile metal market. GLD, GEVD, GPD, SD, PIVD and GHDs are more appropriate to describe the heavy-tails evident in metal returns. Regulators can determine capital requirements by implementing the dynamic VaR model. We thus propose full GHD, NIGD, VGD, GHStD, GLD, SD, GEVD, GPD and PIVD in conjunction with ARMA-APARCH model based on superior in-sample VaR prediction.

Volatility clustering, heavy-tails, asymmetry, conditional heavy tails and long memory

We examined the long-memory GARCH models under the Generalised Hyperbolic Distributions (GHDs), the SSTD, STD, GPD, GEVD, SD, GLD and the PIVD assumptions. The conditional variance and long range memory was modelled using nonlinear-GARCH models, ARFIMA-FIGARCH, ARFIMA-HYGARCH and ARFIMA-FIAPARCH models. GHDs, SSTD, STD, SD, GEVD, GPD, GLD and PIVD were applied to capture the heavy tail behavior for the extracted standardised residuals. The Anderson-Darling test was utilised to check for model adequacy. The Kupiec likelihood ratio test was used in this study to evaluate objectively whether the VaR model

is adequate. The backtesting results confirm that the long-memory GARCH-heavy-tailed models are adequate methods for improving risk management assessments and hedging strategies in highly volatile metal markets. Our findings can be supported by the fact that ARFIMA-FIAPARCH-PIVD, ARFIMA-HYGARCH-GLD and ARFIMA-HYGARCH-NIGD model can jointly account for salient features in financial time series: heavy tails, asymmetry, volatility clustering and long memory.

Therefore, the findings of this study show the most appropriate models in carrying out risk management or assessment of precious metals. Table 9.1 summarises the most appropriate models at different VaR levels.

Table 9.1: The most appropriate models for precious metals.

<i>VaR level</i>		<i>Gold</i>	<i>Platinum</i>	<i>Silver</i>
<i>Long Positions</i>	1%	ARFIMA-FIAPARCH-NIGD, ARFIMA-HYGARCH-NIGD, ARFIMA-HYGARCH-GPD and ARFIMA-FIAPARCH-NIGD	ARFIMA-FIAPARCH-GPD	ARFIMA-FIAPARCH-NIGD
	5%	ARFIMA-HYGARCH-GPD	ARFIMA-FIARCH-GEVD	ARFIMA-HYGARCH-GHD _{full}
<i>Short Positions</i>	95%	ARFIMA-FIARCH-NIGD and ARFIMA-FIAPARCH-NIGD	ARFIMA-FIARCH-GEVD	ARFIMA-FIARCH-PIVD, ARFIMA-FIARCH-GLD and ARFIMA-FIARCH-GHD _{full}
	99%	ARFIMA-HYGARCH-GPD	ARFIMA-FIAPARCH-GHD _{full}	ARFIMA-HYGARCH-STD

The findings reveal that daily gold, platinum and silver returns are characterised by heavy tailed distributions, volatility clustering, leverage effect behavior and long memory. Our findings confirm the importance of taking into account volatility clustering and long-range memory in the behavior of precious metals. This combined with filtering processes such as PIVD, full GHD, GHStD, NIGD, SSTD and GLD, are important in risk management assessments and hedging strategies. Our results have potential implications for portfolio managers, producers and policy makers.

Further recommendations would be:

- Comparing the results of this study with the Generalised Autoregressive Score (GAS) models.
- Comparing the results of this study with the NRIG distribution under the GARCH models and long memory GARCH models.
- Comparing the results of this study with the Exponentiated Generalised Inverse Gaussian distributions.

References

- AAS, K. AND HAFF, D. H. (2006). The generalised hyperbolic skew Student's t- distribution. *Journal of Financial Econometrics* , 4(2), 275-309.
- ABRAAMOWITZ, M. AND STEGUN, A. (1972). *Handbook of mathematical functions with formulars, graphs and mathematical tables*. 10th edition. National Bureau of Standards Applied Mathematics Series 55. Government Printing Office: Washington D.C.
- ALFONS, A. AND TEMPL, M. (2013). Estimation of social exclusion indicators from complex surveys: The R package laeken. *Journal of Statistical Software*, 54 (15), 1-25.
- ALJAZAR, A. L. (2005) Generalised Lambda Distribution and Estimation Parameters. Thesis. The Islamic University of Gaza.
- ANGABINI, A. AND WASIUZZAMAN, S. (2011). GARCH Models and the Financial Crisis-A Study of the Malaysian Stock Market. *The International Journal of Applied Economics and Finance*, 5, 226-236.
- AROURI, M.E.H., HAMMOUDEH, S., LAHIANI, A. AND NGUYEN, D.K. (2012). Long memory and structural breaks in modelling the return and volatility dynamics of precious metals. *The Quarterly Review of Economics and Finance*, 52, 207-218.
- ARTZNER, P., DELBAEN, F., EBER, J.M. AND HEATH, D. (1999). Coherent measures of risk. *Mathematical Finance*, 9(3), 203-228.

-
- AZZALINI, A. (1985). A class of distributions which includes the Normal ones. *Scandinavian Journal of Statistics*, 171-178.
- AZZALINI, A. (1996). *Statistical Inference Based On the Likelihood*. Chapman and Hall, London.
- AZZALINI, A. AND CAPITANIO, A. (1999). Statistical applications of the multivariate skew Normal distribution. *Journal of the Royal Society: Series B (Statistical Methodology)*, 61(3), 579-602.
- AZZALINI, A. AND CAPITANIO, A. (2003). Distributions generated by perturbation of symmetry with emphasis on multivariate skew t-distribution. *Journal of the Royal Society: Series B (Statistical Methodology)*, 65(3), 367-389.
- BAILLE, R.T., BOLLERSLEV, T. AND MIKKELSEN, H.O. (1996). Fractionally integrated generalised autoregressive conditional heteroscedasticity. *Journal of Econometrics*, 73, 3-20.
- BAILLE, R.T. (1996). Long memory processes and fractional integration in econometrics. *Journal of Econometrics*, 73, 5-59.
- BALAKRISHNAN, N. (ED). (1992). *Handbook of the logistic Distribution*. Marcel Dekker, Inc, New York.
- BALI, T. G. (2003). An extreme value approach to estimating volatility and value at risk. *The Journal of Business*, 76(1), 83-108.
- BALKEMA, A., AND DE HAAN, L. (1974). Residual life time at great age. *Annals of Probability*, 2, 792-804.
- BARNDORFF-NIELSEN, O.E. (1977). Exponential decreasing distributions of the logarithm of particle size. *Proceedings of the Royal Society London A*, 353,401-419.

-
- BARNDORFF-NIELSEN, O.E. (1978). Hyperbolic distributions and distributions on hyperbolae, *Scandinavian Journal of Statistics*, 5, 151-157.
- BASLE COMMITTEE (1996). Overview of the Amendment of the Capital Accord to Incorporate Market Risk. Basle Committee on Banking Supervision.
- BAUM, C.F. AND WIGGINS, V. (2000). sts16: Tests for long memory in a time series. *Stata Technical Bulletin* 57: 39-44.
- BAUM, C. F. AND ROOM, T. (2001). sts18: A test for long-range dependence in a time series. *Stata Technical Bulletin* 60: 37-39.
- BECKER, M. AND KLÖBNER, S. (2012). PearsonDS: Pearson Distribution System. R package version 1.0.
- BEENA, V. T. AND KUMARAN, M. (2010). Measuring inequality and social welfare from an arbitrary distribution. *Brazilian Journal of Probability and Statistics*, 24(1), 78-90.
- BELLOSTA, C.J.G. (2011). ADGofTest: Anderson-Darling GoF test. R package version 0.3.
- BELOV, I.A. (2005). On the computation of the probability density function of α -Stable distributions. *Mathematical Modelling and Analysis 2005. Proceedings of the 10th International Conference MMA2005 & CMAM2, Trakai c 2005 Technika. ISBN 9986-05-924-0*, 333-341.
- BENTES, S.R. (2015). Forecasting volatility in gold returns under the GARCH, IGARCH and FIGARCH frameworks: New evidence. *Physica A* , 438,355-364.
- BEKAERT, G. AND GUOJUN, W. (2000). Asymmetric Volatility and Risk in Equity Markets. *The Review of Financial Studies*, 13, 1-42.

- BENTES, S.R. (2016). Long memory volatility of gold price returns: How strong is the evidence from distinct economic cycles? *Physica A* , 443,149-160.
- BERGEVIN, R.J. (1993). An analysis of the generalised lambda distribution. Master's thesis, Air Force Institute of Technology.
- BHATTACHARYYA, M., CHAUDHARY, A. AND YADAV, G. (2008). Conditional VaR estimation using Pearson's type IV distribution. *European Journal of Empirical Operational Research*, 191, 386-397.
- BHATTACHARYYA, M. AND MADHAV, S.R. (2012). A comparison of VaR estimation procedures for leptokurtic equity index returns. *Journal of Mathematical Finance*, 2, 13-30.
- BIBBY, B.M. & SØRENSEN, M. (1996). A hyperbolic diffusion model for stock prices. *Finance and Stochastics*, 1(1), 25-41.
- BLAESILD, P. (1999) Generalised hyperbolic and generalised inverse Gaussian distributions, *Working Paper, University of Aarhus, Aarhus*.
- BOLLERSLEV, T. (1996). Generalised autoregressive conditional heteroscedasticity. *Journal of Econometrics*, 31(3), 307-327.
- BOLLERSLEV, T., CHOU, R.Y. AND KRONER, R.F. (1992). ARCH modelling in finance: A review of theory and empirical evidence. *Journal of Econometrics*, 52(1-2), 5-59.
- BOLLERSLEV, T., ENGLE, R.F. AND NELSON, D.B. (1992). ARCH models. *Handbook of Econometrics*, 4, 2959-3038.
- BOLLERSLEV, T. AND MIKKELSEN, H. O. 1996. Modeling and pricing long-memory in stock market volatility. *Journal of Econometrics* , 73, 151-184.

-
- BOLLERSLEV, T. AND WOODRIDGE, J.M. (1992). Quasi-maximum likelihood estimation of dynamics models with time varying covariances. *Econometric Review*, 5, 1-50.
- BOX, G.E.P. AND COX, D.R. (1964). An Analysis of Transformations. *Journal of the Royal Statistical Society. Series B (Methodological)*, 26, (2), 211-252.
- BOX, G.E.P., JENKINS, G.M. AND REINSEL, G.C. (2008). *Time Series Analysis Forecasting and Control*, John Wiley & Sons Inc: New Jersey.
- BRANCO, M.D. AND DEY, D.K. (2001). A general class of multivariate skew-elliptical distributions. *Journal of Multivariate Analysis*, 79(1), 99-113.
- BROOKS, C. AND PERSAUD, G. (2003). The effect of asymmetries on stock index return Value-at-Risk estimates. *Journal of Risk Finance*, 4, 29-42.
- BRUNETTI, C. AND GILBERT, C.L. (2000). Bivariate FIGARCH and fractional cointegration. *Journal of Empirical Finance*, 7, 509-530.
- BUCEVSKA, V. (2013). An Empirical Evaluation of GARCH Models in Value-at-Risk Estimation: Evidence from the Macedonian Stock Exchange. *Business Systems Research*, 4, 49-64.
- BYSTRÖM, H. N. E. (2005). Extreme value theory and extremely large electricity price changes. *International Review of Economics and Finance*, 14(1), 41-55.
- CAMPELL, J.Y. AND MANKIW, N.G. (1987). Are output fluctuations transitory? *Quarterly Journal of Economics*, 102, 857-880.
- CHAITHEP, K., SRIBOONCHITTA, S., CHAIBOONSRI, C. AND PASTPIPATKUL, P. (2012). Value at risk analysis of gold returns using extreme value theory. *The Empirical Econometrics and Quantitative Economic Letters*, 1(4), 151-168.

- CHALABI, Y., SCOTT, D AND WURTZ, D. (2010). The generalised lambda distribution as an alternative to financial returns. Working paper, Eidgenössische Technische Hochschule and University of Auckland, Zurich and Auckland.
- CHALABI, Y. (2012). New directions in statistical distributions, parametric modelling and portfolio selection. PhD Dissertation. ETH Zürich, Switzerland.
- CHAN, K-S. AND RIPLEY, B. (2012). TSA: Time Series Analysis. R package version 1.01.
- CHAN-LAU, J.A., MATHIESON, D.J. AND YAO, J.Y. (2004). Extreme contagion in equity markets. *IMF Staff papers*, 51:386-408.
- CHEN, Q., AND GILES, D. E. (2014). *Risk Analysis for Three precious Metals: An application of Extreme Value Theory*. University of Victoria. (Econometrics working paper no.EWP1405).
- CHKILI, W., HAMMOUDEH, S. AND NGUYEN, D.K. (2014). Volatility forecasting and risk management for commodity markets in the presence of asymmetry and long memory. *Energy Economics*, 41:1-18.
- CHINHAMU, K., HUANG, C-K AND CHIKOBVU, D (2015). *Evaluating Risk in Gold Prices with Generalised Hyperbolic and Stable Distributions*. Proceedings of the 57th Annual Conference of the South African Statistical Association, 30 November-2 December 2015, Pretoria, South Africa.
- CHRISTOFFERSEN, P. (1998). Evaluating interval forecasts. *International Economic Review*, 39(4): 841-862.
- CHRISTOFFERSEN, P.F., HAHN, J. AND INOUE, A. (2001). Testing and Comparing Value-at-Risk Measures. *Journal of Empirical Finance*, 8(3), 325-342.
- CHUNG, C. F. (1999). Estimating the fractionally integrated GARCH model. Taiwan:

National Taiwan University.

COCHRAN, S.J., MANSUR, I. AND ODUSAMI, B. (2012). Volatility persistence in metals returns: A FIGARCH approach. *Journal of Economics and Business*, 64, 287-305.

COLES, S (2001). *An Introduction to Statistical Modelling of Extreme Values*. Springer-Verlag, London.

CONRAD, C. (2010). Non-negativity for the hyperbolic GARCH model. *Journal of Econometrics*, 157, 441-457.

CONT, R. (2001). Empirical properties of asset returns: stylized facts and statistical issues. *Quantitative Finance*, 1: 223-236.

CONRAD, C. AND HAAG, B.R. (2006). Inequality Constraints in the Fractionally Integrated GARCH Model. *Journal of Financial Econometrics*, 4(3), 413-449.

CORLU, C.G. and CORLU, A. (2015). Modelling exchange rate returns: Which flexible distribution to use? *Quantitative Finance*, 15(11), 1851-1864.

CORLU, C.G AND METERELLIYOZ, M. (2015). Estimating the parameters of the generalised lambda distribution: Which method performs best? *Communications in Statistics - Simulation and Computation*, in press. DOI:10.1080/03610918.2014. 901355.

CORLU, C.G., METERELLIYOZ, M. AND TINI, M. (2016). Empirical distributions of daily equity index returns: A comparison. *Expert Systems with Applications*, 54, 170-192.

CORRADO, C.J. (2001). Option pricing based on the generalised lambda distribution. *Journal of Future Markets*, 21(3), 213-236.

CRYER, J.D. AND CHAN, K-S. (2010). *Time Series Analysis with Applications in R*. Springer, New York.

- DAVIDSON, J. (2004). Moment and memory properties of linear conditional heteroscedastic models, and a new model. *Journal of Business and Economic Statistics*, 22, 16-29.
- DEGIANNAKIS, S. (2004). Volatility Forecasting: Evidence from a Fractional Integrated Asymmetric Power ARCH Skewed-t Model. *Applied Financial Economics*, 14:1333-1342.
- DIAMANDIS, P.F. (2009). International stock market linkages: Evidence From Latin America. *Global Finance Journal*, 20:13-30.
- DIAZ, J.F.T. (2016). Do scarce precious metals equate to safe harbour investments? The case of platinum and palladium. *Economics Research International*, 1-7.
- DICKEY, D. AND FULLER, W. (1979). Distribution of the estimators for autoregressive time series with unit root. *Journal of American Statistical Association*, 74:427-431.
- DOORNIK, J. AND HENDRY, P. (2013). OxMetrics 7. OxMetrics Technologies.
- DOWD, K. (2005). *Model Risk, Measuring Market Risk*. John Wiley and Sons Ltd., West Sussex.
- EBERLEIN, E. (2001). Application of Generalised Levy motions to Finance : *Levy processes -Theory and Application*, Birkhauser, Boston, 319-339.
- EBERLEIN, E. AND KELLER, U. (1995). Hyperbolic distributions in finance. *Bernoulli*, 1(3): 281-299.
- EMBRECHTS, P., KLÜPPELBERG, C., AND MIKOSH, T. (1997). *Modelling Extremal Events: For Insurance and Finance*. Springer-Verlag, Berlin.
- EMBRECHTS, P., McNEIL, A.J. AND STRAUMANN, D. (2002). Correlation and dependence in risk management: properties and pitfalls. *Risk management: value at risk*

and beyond. Cambridge University Press, 176-223.

EMMER, S., KRATZ, M. AND TASCHE, D. (2015). What is the best risk measure on practice? A comparison of standard measures. *Journal of Risk*, 18(2), 31-60.

ENGLE, R.F. (1982). A general approach to Lagrange multiplier model diagnostics. *Journal of Econometrics*, 20(1), 83-104.

ENGLE, R.F. (1992). Autoregressive Conditional Heteroscedasticity with Estimates of variance of United Kingdom Inflation. *Econometrica*, 50(4), 987-1008.

ENGLE, R.F. AND BOLLERSLEV, T. (1996). Modelling Persistence of Conditional variances. *Econometric Reviews*, 5, 1-50.

ENGMANN, S. AND COUSINEAU, D. (2011). Comparing Distributions: The two-sample Anderson-Darling test as an alternative to the Kolmogorov-Smirnoff test. *Journal of Applied Quantative Methods*, 6(3):1-17.

FAMA, E.F. (1965). The behavior of stock-market prices. *Journal of Business*, 38(1), 34-105.

FREIMER, M., KOLLIA, G., MUDHOLKAR, G., AND LIN, C. (1988). A study of the generalised Tukey lambda family. *Communications in Statistics - Theory Methods*, 17(10), 3547-3567.

FULLER, W.A. (1976). *Introduction to Statistical Time Series*. Wiley: New York.

GENÇAY, R., AND SELÇUK, F. (2004). Extreme value theory and value-at-risk: Relative performance in emerging markets. *International Journal of Forecasting*, 20(2), 287-303.

GENTON, M.G., HE, L. AND LIU, X. (2001). Moments of skew-Normal random vectors and their quadratic forms. *Statistics and Probability Letters*, 51(4), 319-325.

- GENZ, A. AND BRETZ, F. (2000). Numerical computation of critical values for multiple comparison problems. *Proceedings of the Statistical Computing Section, American Statistical Association, Alexandria*, 84-87.
- GEWEKE, J., AND PORTER-HUDAK, S. (1983). The estimation and application of long memory time series models. *Journal of Time Series analysis*, 4(4), 221-238.
- GHALANOS, A. (2015). rugarch: Univariate GARCH models. R package version 1.3-6.
- GILCHILST, W.G. (2000). *Statistical Modelling and Quantile Functions*, Chapman and Hall/ CRC Press, Boca Raton, Florida.
- GILLI, M., AND KËLLEZI, E. (2006). An application of extreme value theory for measuring financial risk. *Computational Economics*, 27(2-3), 207-228.
- GIOT, P. AND LAURENT, S. (2003a). Value-at-Risk for Long and Short Trading Positions. *Journal of Applied Econometrics*, 18:641-664.
- GIOT, P. AND LAURENT, S. (2003b). Market risk in commodity markets: a VaR approach. *Energy Economics*, 25:435-457.
- GRADSYEYN, I.S. AND RYZHNIK, I.M. (1980). *Tables of integrals, series and products*, 4th ed, Academic Press, New York.
- GRANGER, C.W.J. (1980). Long memory relationships and the aggregation of dynamic models. *Journal of Econometrics*, 14, 227-238.
- GRANGER, C.W.J. AND JOYEUX, R. (1980). An introduction to long-memory time series models and fractional differencing. *Journal of Time Series analysis*, 1(1), 15-39.
- HAMMOUDEH, S., MALIK, F. AND McALEER, M. (2011). Risk management of precious metals. *The Quarterly Review of Economics and Finance*, 51(4), 435-441.

- HALULU, S. (2012). Quantifying the risk of portfolios containing stocks and commodities. Master's thesis, Bogazici University.
- HAMMOUDEH, S. AND YUAN, Y. (2008). Metal volatility in presence of oil and interest rate shocks. *Energy Economics*, 30(2), 606-620.
- HANSEN, B.E. (1994). Autoregressive Conditional Density Estimation. *International Economic Review*, 35(3), 705-730.
- HASTINGS JR, C., MOSTELLER, F., TUKEY, J.W. AND WINSTOR, C.P. (1947). Low moments for small samples: a comparative study of order statistics. *The Annals of mathematical Statistics*, 413-426.
- HEFFERNAN, J.E., STEPHENSON, A.G., GILLELAND, E. (2012). Ismev: an introduction to statistical modelling of extreme values. R package version 1.41.
- HILLER, D., DRAPER, P. AND FAFF, R. (2006). Do precious metals shine? An investment perspective. *Financial Analysts Journal*, 62(2), 98-106.
- HOECHSTOETTER, M. RACHEV, S. & FABOZZI, F.J. (2005). *Distributional Analysis of the Stocks Comprising the DAX 30*. [Online] Available: https://statistik.econ.kit.edu/download/doc_secure1/tr_distributional_analysis.pdf
- HOSKINS, J.R.M. (1981). Fractional differencing. *Biometrika*, 68(1), 165-176.
- HUANG, C.-S., HUANG, C.-K. AND CHINHAMU, K. (2014). Assessing The Relative Performance Of Heavy-Tailed Distributions: Empirical Evidence From The Johannesburg Stock Exchange. *The Journal of Applied Business Research*, 30, 1263-1286.
- HUANG, Y. C. AND LIN, B.-J. (2004). Value-at-Risk Analysis for Taiwan Stock Index Futures: Heavy Tails and Conditional Asymmetries in Return Innovations. *Review of Quantitative Finance and Accounting*, 22, 79-95.

- HURST, E. (1951). Long term storage capacity of reservoirs. *Transactions of the American Society of Civil Engineers*, 116, 770-799.
- JADHAV, D. AND RAMANATHAN, T.V. (2009). Parametric and non-parametric estimation of value-at-risk. *Journal of Risk Model Validation*, 3, 51-71.
- JARQUE, C.M. AND BERA, A.K. (1987). A test for Normality of observations and regression residuals. *International Statistical Review*, 55(2), 165-172.
- JOHNSON, N.L., KOTZ, S. AND BALAKRISHMAN, N. (1994). *Continuous univariate distributions*. Vol 1, 2nd edition. John Wiley and Sons, New Jersey.
- JOHNSON, N.L., KOTZ, S. AND BALAKRISHNAN, N. (1995). *Continuous univariate distributions*. Vol 2, 2nd edition. John Wiley & Sons: New York.
- JONES, M.C. AND FADDY, M.J. (2003). A skew extension of the t-distribution with applications. *Journal of the Royal Society: Series B (Statistical Methodology)*, 65(1), 159-174.
- KALE, M. AND BUTAR, F.B. (2010). Fractal analysis of time series and distribution properties of the hurst exponent. *Journal of Mathematical Sciences & Mathematics Education*, 5 (1), 8-19
- KARIAN, Z.A. DUDEWICZ, E.J. AND MCDONALD, P. (1996). The extended generalized lambda distribution system for fitting distributions to data: history, completion of theory, tables, applications, the "final word" on moment fits, *Communications in statistics: simulation and computation*, 25(3), 611-642.
- KARIAN, Z.A. AND DUDEWICZ, E.J. (1999). Fitting the generalised lambda to a data: A method based on percentile. *Communication in Statistics: Simulation and Computation*, 28, 793-819.
- KARIAN, Z.A. AND DUDEWICZ, E.J. (2000). Fitting Statistical Distributions: The-

Generalised Lambda Distribution and Generalised Bootstrap Methods. CRC Press.

KARIAN, Z.A. AND DUDEWICZ, E.J. (2010). *Handbook of Fitteding Statistical Distributions with R*. Chapman and Hall/ CRC Press, Boca Raton, Florida.

KARLSSON, L. (2002). GARCH-Modelling Theoretical Survey, Model Implementation and Robustness Analysis. Master degree, Royal Institute of Technology (KTH).

KARVANEN, J., ERIKSSON, J. AND KOIVUNEN, V. (2002). Adaptive sore functions for maximum likelihood ICA. *Journal of VLSI Signal Processing*, 32(1-2), 83-92.

KING, R.A.R. (1999). New distributional fitteding methods applied to the generalised λ distribution. PHD thesis, Queensland University of Technology, Queensland, Australia.

KING, A.R. AND MACGILLIVRAY, H.L. (1999). A starship estimation method for the generalized λ distributions. *Australia and New Zealand Journal Statistics*, 41(3), 353-374.

KING, R.A.R, DEAN, B. AND KLINKE, S. (2016). *gld: Estimation and Use of The Generalised (Tukey) Lambda Distribution*. R package version 2.4.1.

KUPIEC, P. (1995). Techniques for verifying the accuracy of risk measurement models. *Journal of Derivatives*, 2, 173-184.

KOUTROUVELIS, I.A. (1980). Regression - type estimation of the parameters of stable laws. *Journal of the American Statistical Association*, 75, 918-928.

KREŹŁEK, D. (2012). Non-Classical measures of investment Risk on the Market of Precious Non-Ferrous Metals. *Dynamic Economic Models*, 12:89-103.

KWIATKOWSKI, D, PHILLIPS, P.C.B, SCHMIDT, P. AND SHIN, Y. (1992). Testing the null hypothesis of stationary against the alternative of unit root. *Journal of Econo-*

metrics, 54, 154-178.

LAMPASI, D.A., DI NICOLA, F. AND PODESTA, L. (2006). Generalised lambda distribution for the expression of measurement uncertainty. *IEEE Transactions on Instrumentation and Measurement*, 55, 1281-1287.

LAURENT, S. (2003). Analytical derivatives of the APARCH model. *Computational Economics*, 24, 51-57.

LEE, P.P. (2003). The generalised lambda distribution applied to spot exchange rates. PhD dissertation, Carnegie Mellon University.

LEVY, P. (1937). *Theorie de l'addition des variables*. Gauthier-Villars, Paris.

LJUNG, G.E.P AND BOX, G.M. (1978). On the measure of lack of fitted in time series models. *Biometrika*, 65(8)

LUETHI, D. AND BREYMAN, W. (2016). ghyp: A package on Generalized Hyperbolic distributions and its Special classes. R package version 1.5.7.

MABROUK, S. AND SAADI, S. (2012). Parametric Value-at-Risk analysis: Evidence from stock indices. *The Quarterly Review of Economics and Finance*, 52, 305-321.

MACDONALD, H.M. (1899). Zeros of the Bessel functions: Proceedings of the London Mathematical Society, 30, 165-179.

MACGILLIVRAY, H.L. (1982). Skewness properties of asymmetric forms of Tukey lambda distributions. *Communications in Statistics: Theory and Methods*, 11(20), 2239-2248.

MADDALA, G.S. AND KIM, I-M. (2004). *Unit Roots, Cointegration and Structural Change*. Cambridge University Press, UK.

-
- MAROHN, F. (2005). Tail index estimation in models of generalised order statistics. *Communications in Statistics - Theory and Methods*, 34(5), 1057-1064.
- MANDEL, B. (1971). Analysis of long-run dependence in economics: the R/S technique. *Econometrica*, 39, 68-69.
- MANDELBROT, B. (1963). The variation of certain speculative prices. *Journal of Business*, 36, 394-419.
- McCULLOCH, J.H. (1997). Simple consistent estimators of stable distribution parameters, *Communication Statistics: Simulation*, 15, 1109-1136.
- McNEIL, A.J. AND FREY, R. (2000). Estimation of tail-related risk measures for heteroscedastic financial time series: an extreme value approach. *Journal of Empirical finance*, 7, 271-300.
- McNEIL, A.J., FREY, R. AND EMBRECHTS, P (2005). *Quantitative Risk Management: Concepts, Techniques, and Tools*. Princeton University Press: New Jersey.
- MITTNIK, S. AND PAOLELLA, M. S. (2000). Conditional density and value-at-risk prediction of Asian currency exchange rates. *Journal of Forecasting*, 19, 313-333.
- MITTNIK, S., PAOLELLA, M. S. AND RACHEV, S. T. (2000). Diagnosing and treating the heavy tails in financial return data. *Journal of Empirical Finance*, 7,389-416.
- MOORS, J.J.A. (1988). A quantile alternative for kurtosis. *Journal of the Royal Statistical Society, Series D (The Statistician)*, 37(1),25-32.
- NAGAHARA, Y. (1999). The PDF and CF of Pearson type IV distribution and the ML estimation of the parameters, *Statistics and Probability Letters*, 43, 251-264.
- NAGAHARA, Y. (2007). A method of calculating the downside risk by multivariate non Normal distributions. *Asian Pacific Financial Markets*, 15, 175-184.

-
- NELSON, D. (1991). Conditional heteroskedasticity in asset returns: A new approach. *Econometrica*, 59, 347-370.
- NEWKEY, W.K. AND WEST, K.D. (1987). A simple positive semi-definite, heteroscedasticity and autocorrelation consistent covariance matrix. *Econometrica*, 55, 703-708.
- NIDHIN, K. AND CHANDRAN, C. (2013). Importance of generalized logistic distribution in extreme value modelling. *Applied Mathematics*, 4, 560-573.
- NIEPPOLA, O. (2009). Backtesting Value-at-Risk models. Master Thesis. Helsinki School of Economics, Finland.
- NOLAN, J.P. (2005). *Modeling financial data with Stable distributions*, American University Department of Mathematics and Statistics.
- NOLAN, J.P. (2014). Financial modeling with heavy-tailed stable distributions. *Wiley Interdisciplinary Reviews: Computational Statistics*, 6, 45-55.
- NOLAN, J.P. (2015). *Stable Distributions: Models for Heavy-Tailed Data*. Springer: New York.
- NYSSANOV, A. (2013). An empirical study in risk management: Estimation of Value at Risk with GARCH family models. Master Thesis. Uppsala University, Sweden.
- PARZEN, E. (1979). Nonparametric statistical data modelling. *Journal of the American Statistical Association*, 74(365), 105-121.
- PETERS, J.P. (2001). Estimating and forecasting volatility of stock indices using asymmetric GARCH models and skewed student-t densities. University of Liege, Belgium.
- PFAFF, B., MCNEIL, A. AND STEPHENSON, A.G. (2012). evir: Extreme Values in R. R package version 1.7-3.

-
- PICKANDS, J. (1975). Statistical inference using extreme order statistics. *Annals of Statistics*, 3(1), 119-131.
- PFLUG, G.CH. (2000). Some remarks on the value-at-risk and the conditional value-at risk. *Probabilistic constrained optimization: Methodology and Applications*, 272-281.
- PHILLIPS, P.C.B. AND PERRON, P. (1988). Testing for a unit root in time series regression. *Biometrika*, 75, 335-346.
- PRAUSE, K. 1999. The generalised hyperbolic model: Estimation, financial derivatives and risk measures. Doctoral Thesis. University of Freiburg.
- RAMBERG, J.S. AND SCHMEISER, B.W. (1972). An approximate method of generating symmetric random variables. *Communications of the Association for Computing Machinery*, 15(11), 987-990.
- RAMBERG, J.S. AND SCHMEISER, B.W. (1974). An approximate method for generating asymmetric random variables. *Communications of Association for Computing Machinery*, 17, 78-82.
- RAMBERG, J.S., TADIKAMALLA, P.R., DUDEWICZ, E.J. AND MYKYTKA, E.F. (1979). A probability distribution and its uses in fitting data. *Technometrics*, 21(2), 201-214.
- RANGANAI, E. AND KHUBEKA, S.B. (2016). Long memory mean and volatility models of platinum and palladium price return series under heavy tailed distributions. *SpringerPlus*, 5, 2089.
- REN, F., AND GILES, D.E. (2010). Extreme value analysis of daily Canadian crude oil prices. *Applied Financial Economics*, 20(12), 941-954.
- ROBUST ANALYSIS INC. (2013). Stable. R package version 5.3.

-
- RYDERBERG, T.H. (1999) Generalised hyperbolic diffusions with application towards finance. *Mathematical Finance*, 9,183-201
- SARI, R., HAMMOUDEH,S. AND SOYTAS,U. (2010). Dynamics of oil prices, precious metal prices and exchange rate. *Energy Economics*, 32(2), 351-362.
- SCOTT, D. (2015). GeneralizedHyperbolic : The Generalized Hyperbolic Distribution. R package version 0.8-1.
- STAVROYIANNIS, S. (2016). Value-at-Risk and backtesting with the APARCH model and the standardised Pearson type IV distribution. 1-21.
- STEPHENSON, A.G. AND FERRO, C. (2015). evd: Functions for extreme value distributions. R package version 2.3-3.
- STEPHENSON, A.G. (2002). evd: Extreme Value Distributions. R news, 2(2): 31-32.
- STOYANOV, S.V., RACHEV, S.T. AND FABOZZI, F.J. (2011). Fat-tailed models for risk estimation. Karlsruhe Institut fur Technologie, Karlsruhe. (Working paper no 30).
- SU, S. (2007). Numerical maximum log likelihood estimation for the generalised lambda distribution. *Computational Statistics and Data Analysis*, 51, 3983-3998.
- SU, S.(2007). Fittedting single and mixture of generalized lambda distributions to data via discretized and maximum likelihood methods: GLDEX in R.*Journal of Statistical Software*, 21(9), 1-17.
- SU, S. (2016). GLDEX: Fittedting single and mixture of Generalized Lambda Distributions (RS and FMKL) using various methods. R package version 2.0.0.5.
- TANG, T.A. AND SHIEH,S.J. (2006). Long memory in stock index futures markets: A value at risk approach. *Physica A*, 366, 437-448.

-
- THAS, O. (2010). *Comparing Distributions*, Springer: New York.
- TRAPLETTI, A. AND HORNIK, K. (2017). tseries: Time Series Analysis and Computational Finance. R package version 0.10-41.
- TSAY, R. S. (2013). *An introduction to Analysis of Financial Data with R*. John Wiley and Sons, New Jersey.
- TSE, Y.K. (1998). The conditional heteroscedasticity of the Yen-Dollar exchange rate. *Journal of Applied Econometrics*, 13, 49-55.
- TUKEY, J.W. (1960). A survey of sampling from contaminated distributions. *Contributions to Probability and Statistics*, 2, 448-485.
- TULLEY, E. AND LUCEY, B.M. (2007). A power GARCH examination of the gold market. *Research in International Business and Finance*, 21(2), 316-325.
- VAN STADEN, P.J. (2013). Modelling of generalized families of probability distributions in the quantile statistical universe. PHD Thesis, Department of statistics, University of Pretoria, Pretoria, South Africa.
- VEE, D. N. C., GONPOT, P. N. AND SOOKIA, N. 2012. Assessing the performance of generalised autoregressive conditional heteroskedasticity-based value-at-risk models: A case of frontier markets. *Journal of Risk Model Validation*, 6(4), 95-111.
- WEI, W.W.S. (2006). *Time Series Analysis Univariate and Multivariate Methods*. Pearson Education: Boston.
- WERON, R. (2004). *Computationally intensive value at risk calculations*. *Handbook of Computational Statistics: Concepts and Methods*, eds. J.E. Gentle, W. Haerdle, Y. Mori, Springer, Berlin.
- WUERTZ, D., SETZ, T. AND CHALABI, Y. (2014). fBasics: Rmetrics - Markets and

Basic Statistics. R package version 3011.87.

WUERTZ, D., SETZ, T., CHALABI, Y., BOUDT, C., CHAUSSE, P. AND MIKLOVAC, M. (2016). fGarch: Rmetrics - Autoregressive Conditional Heteroskedastic Modelling. R package version 3042.83.

WUERTZ, D., SETZ, T. AND CHALABI, Y. (2017). fUnitRoots: Rmetrics - Modelling Trends and Unit Roots. R package version 3042.79.

YOUSSEF, M., BELKACEM, L. AND MOKNI, K. (2015). Value-at-Risk estimation of energy commodities: A long-memory GARCH-EVT approach. *Energy Economics*, 51, 99-110.

ZHUN, D. AND GALBRAITH, J.W. (2010). A generalised asymmetric Student-t distribution with application to financial econometrics. *Journal of econometrics*, 157(2), 297-305.

ZOLOTAREV, (1986). *One-dimensional Stable Distributions, Volume 65*. American Mathematical Society, Providence.